# The role of microvascular endothelial cells in the pathogenesis of emphysema

Laura Sutherland Mackay

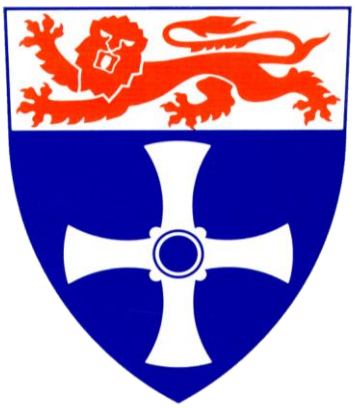

**A thesis submitted in partial fulfilment of the requirements for the degree of Doctor of Philosophy**

**Institute of Cellular Medicine**

**University of Newcastle**

**August 2015**

## *Abstract*

COPD comprising small airways disease and emphysema is a chronic, debilitating often fatal lung condition that approximately 20% of smokers develop. Current therapies mostly target inflammation and airflow obstruction caused by small airways disease however there are no current therapies which treat emphysema, the pathogenesis of which remains poorly understood. The microvascular hypothesis of COPD is a credible alternative to the classical hypothesis of inflammation and protease driven lung destruction, whereby an initial insult to the microvasculature leads to loss of alveolar structure which typifies emphysema. I planned to investigate the role of the microvasculature in the pathogenesis of COPD by isolating susceptible lung microvascular endothelial cells (LMVECs) from individuals with emphysema in an attempt to mimic *in vivo* conditions more closely. LMVECs were isolated from explanted emphysematous lungs removed at transplantation. Following successful isolation (71%) and characterisation of emphysema LMVECs, I sought to study cellular responses to cigarette smoke injury, namely apoptosis and endothelial to mesenchymal transition. Apoptosis was investigated on tissue blocks via caspase 3 immunohistochemistry and by *ex vivo* methods including flow cytometry (annexin V), TUNEL and live cell imaging for activated caspase 3. Unfortunately cigarette smoke extract caused autofluorescence of cells and as all of these techniques employed the use of fluorescence for detection, any conclusions that can be made as to whether cells underwent apoptosis are limited. Endothelial to mesenchymal transition was investigated in response to TGFβ1 and cigarette smoke extract. While there was evidence of down regulation of endothelial markers in response to cigarette smoke on confocal imaging there was no convincing evidence of upregulation of mesenchymal markers with no corresponding change in protein expression via western blotting. One explanation may be that such changes in cell structure and endothelial cell expression may be more in keeping with endothelial activation rather than a true phenotypic switch. In summary, this study presents a new model of emphysema, with attempts to gain insight into endothelial injury in the pathogenesis of COPD, highlighting the challenges and limitations of working with primary diseased cells in response to cigarette smoke injury.

# *Table of contents*

## *Acknowledgements*

I would like to thank firstly my supervisors Prof Paul Corris and Prof Andy Fisher for their guidance, unwavering support and inspiration and to Prof Tim Higgenbottam who was instrumental in setting up the collaborative work between AZ Charnwood and Newcastle University. Thanks to Dr Lee Borthwick and Dr Hannah Walden in the lab for their patient teaching and friendship. Dr Malcolm Brodlie for sharing the consent process and assisting with explanted lung retrieval. To Dr Graeme O'Boyle for teaching qPCR. Many thanks also to Ian Harvey, Susan Stamp and Dr Brian Shenton for helping with experiment planning and analysis of FACS.

At AZ Charnwood I received great help and teaching. Firstly I would like to thank Dr Kate Pinnion and Dr Martyn Foster, who guided me towards the microvasculature, and taught me about immunohistochemistry. I would also like to sincerely thank Dr Iain Dougall and his team in molecular biology, notably Dr Sara Dodd and Wendy Tomlinson who developed the methodology for isolating microvascular cells and provided support in the labs at Charnwood throughout the study. And to Alex Ingelston-Orme and Bev Isherwood in ASTL who helped facilitate the live-cell imaging work.

This work would not have been possible without the help of many people at Freeman Hospital. Notably Therese Small and Gail Johnson for help with immunocytochemistry and processing of lung tissue. Importantly I would like to thank all of the patients who donated their explanted lungs for research and to the transplant co-ordinators for their telephone calls in the middle of the night alerting me to come in and consent the patients and make all of this study possible.

I would like to thank all of my friends for their encouragement and understanding and apologise for each time I have cancelled a social engagement or left them alone at dinner so that I might attend a transplant.

To Mum, Dad and Angela, for their constant reminding, support and belief.

And to Paul and Alister for distracting me and generally making my world wonderful.

I would like to dedicate this work to Nan Sinclair, my Nana; a woman of great strength and character who sadly suffered and died with severe emphysema.

## *Abbreviations*

| | |
|---|---|
| aSMA: | Alpha smooth muscle actin |
| ADMA: | Asymmetric dimethylarginine |
| 7-AAD: | 7 -Aminoactinomycin D |
| BCA: | Bicinchoninic Acid |
| Bcl-2: | B-cell lymphoma 2 |
| BSA: | Bovine serum albumin |
| BMP: | Bone morphogenic protein |
| CD: | Cluster of differentiation |
| c-DNA: | Complementary Deoxyribonucleic acid |
| COPD: | Chronic Obstructive Pulmonary Disease |
| CSE: | Cigarette smoke extract |
| DAB: | 3, 3'-diaminobenzidine |
| DAPI: | 4',6-diamidino-2-phenylindole |
| $dH_2O$: | Deionised water |
| DMEM: | Dulbecco's Modified Eagle Medium |
| DMSO: | Dimethyl Sulfoxide |
| ECM: | Extracellular matrix |
| ELISA: | Enzyme-linked immunosorbent assay |
| EMT: | Epithelial to mesenchymal transition |

| | |
|---|---|
| EnMT: | Endothelial to mesenchymal transition |
| eNOS: | Endothelial nitric oxide synthase |
| ET1: | Endothelin-1 |
| FGF: | Fibroblast growth factor |
| FITC: | Fluorescein isothiocyanate |
| FLT1: | Fms-related tyrosine kinase 1 |
| HIF: | Hypoxia inducible factor |
| HRE: | Hypoxia responsive element |
| HRP: | Horseradish peroxidase |
| HUVECs: | Human Umbilical Vein Endothelial Cells |
| IHC: | Immunohistochemistry |
| KDR/FLK1: | Kinase insert domain receptor/ fetal liver kinase1. |
| LCMS: | Liquid chromatography-mass spectrometry |
| LMVECs: | Lung microvascular endothelial cells |
| L-NAME: | L-NG-nitroarginine methyl ester |
| MES: | 2-(*N*-morpholino)ethanesulfonic acid |
| MFI: | Median Fluorescence Intensity |
| MMP: | Matrix metalloproteinase |
| NO: | Nitric oxide |
| ODD: | Oxygen dependant degradation domain |

| | |
|---|---|
| PBS: | Phosphate buffered saline |
| PBST: | Phosphate buffered saline with 1% Triton X-100 |
| PDGF: | Platelet derived growth factor |
| PE: | Phycoerythrin |
| PECAM-1: | Platelet endothelial cell adhesion molecule-1 |
| PVDF: | Polyvinylidene difluoride |
| Q-PCR: | Quantitative real time polymerase chain reaction |
| RNA: | Ribonucleic acid |
| ROS: | Reactive oxygen species |
| RPMI: | Roswell Park Memorial Institute |
| RTK: | Receptor tyrosine kinase |
| SDS: | Sodium dodecyl sulphate |
| SDS-PAGE: | Sodium dodecyl sulphate polyacrylamide gel electrophoresis |
| TBS-T: | Tris buffered saline with 0.05% tween |
| TCA: | Trichloroacetic acid |
| TEMED: | N,N,N’,N’-tetramethylethylenediamine |
| TGF-β1: | Transforming growth factor β1 |
| TRITC: | Tetramethyl Rhodamine Iso-Thiocyanate |
| TSA: | Tyramide signal amplification |
| TUNEL: | Terminal deoxynucleotidyl transferase dUTP nick end labelling |

| | |
|---|---|
| UEA -1: | Ulex europus agglutinin-1 |
| VEGF: | Vascular endothelial growth factor |
| α1-AT: | α 1-antitrypsin |
| α-SMA: | α-smooth muscle actin |
| βME: | β Mercaptoethanol |

# *List of Figures*

# *List of Tables*

# *Chapter 1: Introduction*

## *1.1 COPD: Background*

Chronic Obstructive Pulmonary Disease (COPD) is the fourth leading cause of death worldwide and a major cause of chronic disability which costs the NHS approximately £500 million per year [1]. This burden of disease is predicted to continue to increase in coming years due to both the aging population and ongoing exposure to the major risk factor that is cigarette smoking[2]. COPD is characterised by persistent airflow limitation that occurs due to inflammation of the small airways (bronchiolitis) and lung parenchyma, with destruction of alveolar septal walls leading to permanent abnormal dilation of air spaces (emphysema) [3]. Severity of COPD has previously been determined by degree of airflow obstruction as measured by $FEV_1$, however there is marked heterogeneity among patients with COPD with poor correlation between $FEV_1$, symptoms, quality of life and functional outcomes [4]. This study however did identify that emphysema and continued smoking were the strongest predictors of disease progression. Furthermore patients with emphysema are one of the identified subgroups of COPD who have lower survival rates and have higher rates of decline in lung function (as measured by FEV1) [5]–[7]. Currently there are no medical therapies that target emphysema either by slowing the rate of septal destruction or allow alveolar regeneration. Understanding further the complex pathophysiological mechanisms which lead to septal destruction may allow the identification of novel therapeutic targets which may translate into clinical benefits for this large patient population.

Cigarette smoking is the leading cause of COPD, however only 20%[1]- 25%[8] of smokers develop this condition. An individual's cellular response to smoking injury is therefore important in the pathogenesis of emphysema, an example of the importance of interaction between the environment and an individual's genes in the development of this condition. This is further highlighted in susceptible individuals who develop COPD, in whom smoking cessation reduces the rate of loss of lung

function but often does not alter the natural history of the disease [9][10]. Research highlights that the triggered inflammatory response is amplified and persists despite smoking cessation [11], [12]. Despite awareness of the health risks associated with smoking highlighted by numerous smoking cessation campaigns, many individuals continue to smoke, making emphysema an ongoing major global health problem.

## *1.2 Normal lung structure and function*

In order to understand COPD, it is important to discuss briefly normal adult lung structure and function [13]. The lungs are formed by ten anatomically defined bronchopulmonary segments which are divided into lobes, three on the right (upper, middle and lower) and two on the left (upper and lower). The bronchial tree comprises the trachea, bronchi, bronchioles, alveolar ducts and alveolar sacs and is further subdivided into conducting airways (trachea, bronchi and bronchioles >2mm) and acinus/terminal respiratory unit (respiratory bronchioles and alveoli) which is the site of gas exchange. Alveoli comprise flattened type I pneumocytes with interspersed rounded surfactant producing type II pneumocytes. In close apposition to these specialised alveolar epithelial cells, lies the basement membrane and interstitial matrix, comprising elastin fibres. This matrix provides a supporting structure for the alveolar-capillary unit while permitting free exchange of oxygen and carbon dioxide to facilitate gas exchange.

The lungs have a dual arterial blood supply, being supplied both by the pulmonary arteries and the bronchial arteries which arise from the thoracic aorta and transport nutrients to the large airways and vessels [14]. The pulmonary arteries transport deoxygenated blood from the right heart to the capillary bed where gas exchange takes place. Blood returns to the left heart via the pulmonary veins. The pulmonary arteries branch similarly to the bronchial tree, with large capacitance vessels, muscular conducting vessels and smaller intra-acinar arterioles, which are found in close apposition to the respiratory bronchioles, to allow gas exchange. The

pulmonary capillaries are found most distally in the alveolus, and have a vast surface area (~75-250$m^2$) to allow effective transfer of oxygen and carbon dioxide[14].

## *1.3 COPD: clinical and pathological findings*

COPD was classically described as chronic bronchitis, a clinical diagnosis based upon symptoms (cough productive of sputum for 3 consecutive months over 2 successive years), and emphysema, the histopathological finding of thin, dilated alveolar septa [15]. However, chronic bronchitis has almost entirely disappeared from the COPD literature, and is now best regarded as a distinct clinical entity which can occur in the presence of normal lung function or precede or follow airflow obstruction [3]. Small airways disease (bronchiolitis) was subsequently identified as the predominant site of airflow obstruction in COPD in 1968 [16]. The mainstay treatment options of inhaled corticosteroids, β2 agonists, anti-muscarinics and mucolytics attempt to treat the airflow obstruction that occurs predominantly as a result of small airway bronchiolitis [17], however there are currently no drug therapies for emphysema. Lung volume reduction surgery, to reduce dynamic hyperinflation, and endobronchial techniques, which aim provide local volume reduction strategies, are somewhat crude attempts to treat emphysema [18].

A unique proposition would be to abandon the old theories that emphysema is simply loss of lung tissue and replace them with the more challenging theory that within severely damaged emphysematous lungs there are areas of near normality in close proximity to emphysematous areas and also regions of alveolar bed with intense attempts to repair and replace lost tissue. Regarding emphysema as a dynamic disease with active attempts at alveolar repair, rather than simply loss of lung tissue, allows speculation that these attempts at repair could be exploited and targeted to stimulate and allow reversal/ regeneration of emphysematous lung tissue.

## *1.4 Emphysema*

Emphysema, classically defined as abnormal permanent destructive dilation of airspaces distal to the terminal bronchioles [15], can be sub classified into four radiological and pathological entities [19]–[21]. Centrilobular emphysema is the commonest form observed and is that most closely associated with cigarette smoking. As the name suggests it occurs predominantly in the respiratory bronchioles in the centre of the lobule. Panacinar emphysema involves all airspaces distal to the terminal bronchioles and is found most commonly, but not exclusively, in patients with alpha-one antitrypsin deficiency who develop accelerated emphysema in association with cigarette smoking. Paraseptal emphysema (distal acinar) involves the most peripheral air spaces adjacent to the pleura. If greater than 10mm in diameter these are termed bullous. Irregular emphysema, as the term suggests, irregularly affects the respiratory acinus and is found in association with scarring. Irregular emphysema does not tend to occur in association with cigarette smoking and rather should be considered as gas trapping in association with fibrosis [21]. These phenotypes are however an oversimplification with most patients with advanced COPD displaying a combination of emphysema together with secondary traction bronchiectasis/ bronchial dilation and small airway fibrosis.

## *1.5 Bronchiolitis and small airways disease*

Persistent exposure to cigarette smoke is associated with airway inflammation and subsequent tissue remodeling, comprising goblet cell proliferation and hypertrophy, airway thickening and luminal narrowing [22]. This involves complex orchestration of epithelial cells, endothelial cells, fibroblasts, neutrophils, macrophages and T cells. Small airway pathology in COPD was examined and reported by Hogg *et al* using lung tissue from patients at risk of COPD and those diagnosed with COPD (GOLD grades 1-IV) [12]. This work demonstrated increasing luminal occlusion with increased GOLD grade, increased airways inflammatory cells with increasing GOLD grade and increased airway wall thickness with increasing GOLD grade, concluding that progression of COPD is associated with luminal narrowing by mucus infiltrates

and increasing airway inflammation and was most strongly associated with thickening of the airway wall and component parts by a repair or remodeling process.

## *1.6 Heterogeneity in COPD*

COPD encompasses a broad clinical and pathological spectrum of disease, with the majority of patients displaying a heterogeneous combination of emphysema and airways disease. While small airways disease (narrowing and loss of terminal bronchioles) has been shown to precede emphysema in COPD [23], some patients exhibit marked emphysema without evidence of airflow obstruction and limited small airways involvement, highlighting further the broad spectrum of disease.

The development and existence of these two distinct pathological processes following the same injury process (i.e. cigarette smoking) highlights the importance of regional variation in inflammatory response in determining the resulting pathology which leads to COPD in a given individual [22]. Why such disparate processes of small airway thickening and destructive emphysema occur in such close proximity poses a real challenge to researchers. Such heterogeneity presents further challenges to the study of this disease as effectively the disease witnessed within a given individual is unique to them and thus they may not respond to all therapies in a predictable manner. The acceptance of the broad heterogeneity and the attempt to phenotype patients within the COPD spectrum is thus crucial in order to understand and develop new strategies for this condition.

## *1.7 Classical hypothesis of COPD: Inflammation and Protease/ Antiprotease imbalance*

A large proportion of research into COPD has focused on the role of inflammation and imbalance between proteases which break down connective tissue elements and anti-proteases that protect against this [24], [25]. Chronic exposure to cigarette

smoking leads to recruitment of inflammatory cells into the alveolar spaces. Neutrophils and macrophages release elastolytic proteinases which cause destruction of elastin and the lung extracellular matrix [26]. This hypothesis was largely founded upon the observation of accelerated emphysema in individuals with alpha-one antitrypsin (A1AT) deficiency, who have reduced levels of the major neutrophil elastase inhibitor A1AT. Individuals with A1AT deficiency tend to, although not exclusively, develop panacinar emphysema which differs from the more common centrilobular pattern witnessed in smokers with normal levels of A1AT. However other proteases and inflammatory cells also play an important role as witnessed by the development of very severe emphysema in individuals without A1AT deficiency. A1AT replacement therapy does not altering disease progression [27] thus researchers have revisited alternative hypotheses of emphysema.

## *1.8 Alternative Hypothesis of COPD: The role of the microvasculature*

The microvascular hypothesis of COPD dates back to the 1950s when Liebow identified paucity of pulmonary capillaries in emphysema and hypothesised that reduced blood supply was important in the pathogenesis of this condition [28]. A revival of this hypothesis has been based upon an emerging literature on the importance of the pulmonary microvasculature in maintaining lung structure and function [29], [30]. Damage to endothelial cells via cigarette smoking injury, similar to that which occurs in the systemic circulation, initiates a complex injury and repair pattern that may lead to emphysema[31].

Factors which lead to loss of the microvasculature are however unclear. Cigarette smoking causes endothelial dysfunction in the systemic circulation, with imbalance of nitric oxide (NO), endothelin-1 (ET-1) and other vasoactive substances, and is implicated in the pathogenesis of ischaemic heart disease [32]–[34]. Endothelial dysfunction also occurs in the pulmonary microvasculature [14]. In response to a chronic injury such as cigarette smoking, cells may undergo necrosis, apoptosis,

senescence or a phenotypic change. In emphysema, apoptosis and a phenotype change of endothelial cells into mesenchymal cells (endothelial to mesenchymal transition) may explain both the loss of alveolar septal capillaries and alveolar septal remodelling that occurs in emphysema. I therefore planned to investigate apoptosis and EnMT in response to cigarette smoke with microvascular endothelial cells isolated from patients with emphysema.

The initial stress/injury leading to the development of emphysema is most commonly cigarette smoking, however the initiating event in emphysema remains unknown. This largely relates to poor understanding of the natural history of this condition. Some have proposed inflammation of the respiratory bronchioles (bronchiolitis)[12] whereas other have suggested a primary hit to the alveolar bed [35], with secondary inflammation. Liebow was the first to comment that the septa appeared almost avascular and further studies have confirmed that there is attenuation of the capillaries in this disease[36].

A major stumbling block to tackling emphysema is the belief that loss of alveoli is a terminal event and that neo-angiogenesis and re-alveolarisation are impossible. However alveolarisation already occurs in life, albeit in the first 2-3 years of life[37]. Understanding initial lung development may therefore assist us in understanding of how the lung repairs itself and how we may manipulate this knowledge to develop therapeutics to target the smoking related lung damage that occurs in emphysema.

## *1.9 Lung development*

Lung development in utero occurs in five overlapping stages: embryonic, pseudoglandular, canalicular, saccular and alveolar [37]–[39]. In the embryonic stage the lung primordium is formed from the foregut. Lobar airways lined with endoderm are formed within the surrounding mesenchyme. The pseudoglandular stage follows with the formation of all preacinar airways via branching of epithelial

lined primitive airways. In the canalicular stage, the most distal airways enlarge with thinned epithelial cells which eventually form type I and II pneumocytes. Surfactant is detectable from 24 weeks gestation indicating successful differentiation into type II pneumocytes. During the saccular stage the enlarged distal airways develop crests with elastin and muscle which extend to form cup shaped alveoli. Alveolarisation begins at 36 weeks gestation with the formation of secondary septa subdividing terminal saccules to form mature alveoli. This process continues until 2-4 years of age, thus highlighting the potential for alveolarisation in adult life and challenging the theory that emphysema is an irreversible process.

Furthering the link with the developing lung, alveolar enlargement similar to that in emphysema is witnessed in survivors of bronchopulmonary dysplasia (BPD), the chronic lung disease that occurs in premature infants (especially those born at less than 28 weeks, during the late canalicular or saccular stage of lung development) [40]. BPD is thought to occur due to the disruption of alveolar development that occurs with premature birth, with survivors attaining reduced maximal airway function, with the development of fewer larger alveoli with corresponding smaller surface for gas exchange in contrast to the loss of alveoli that occurs in COPD [41]. Although BPD may appear disparate from COPD, occurring at the extremes of life, understanding alveolar development may allow targeted treatments for both of these conditions [40]. Investigation of BPD has led researchers to suggest that the pulmonary vasculature actively promotes alveolar growth during development and may play a crucial role in maintenance in postnatal life, challenging the conventional hypotheses that the development of blood vessels in the lung passively follows that of airways [42][43].

## *1.10Endothelial cells and the alveolar interface*

The unique high flow, low pressure pulmonary circulation exists to effectively facilitate gas exchange between the air and lungs. This vast surface area (approximately 75-200m2) functions in healthy individuals with large reserve[14].

This reserve within capillaries allows the lungs to accept high pulmonary blood flow without compromising gas exchange. High blood flow does however not equate with high blood volume as only 10% of total blood volume is within the lungs at any time, of which only 10-15% is in the pulmonary capillary bed (less than 100ml)[14]. In time of increased demand, such as exercise, there is recruitment of pulmonary capillaries as cardiac output increases to accommodate increased flow. Other functions of the pulmonary vascular bed include acting as a filter for blood clots, vasoactive substances and as a possible area of leucocyte sequestration. Loss of this vast capillary bed as is thought to occur in emphysema has therefore many consequences.

Endothelial cells form a physical barrier to the passage of molecules contained within blood to the tissues. This is however an oversimplified view of the endothelium, which should not be regarded as a passive barrier, rather as an active interface where important metabolic processes occur which preserve vascular integrity and function[14]. The alveolar endothelium is unique in that it functions to allow gas exchange efficiently while minimising extravasation of fluid and substances into the alveolar bed. This unique property is made possible by intercellular junctions which regulate endothelial cell permeability. Four types of endothelial cell junctions are well described; tight junctions, gap junctions, adherens junctions and syndesmos[44]. Tight junctions are formed by occludins, which are a transmembrane integral proteins found between endothelial cells[45]. The frequency of tight junctions varies according to location in the vascular tree based upon the degree of permeability required, for example in large arteries they are numerous while in post capillary venules they are almost absent. Gap junctions are formed by transmembrane hydrophilic channels termed connexons which allow exchange of ions and small molecules between adjacent cells[44]. Gap junctions tend to colocalise with tight junctions and support cellular communication between both endothelial cells and their supporting cells. Adherens junctions are formed by cadherins, which are single chain transmembrane calcium proteins[46]. Endothelial cells express both specific and nonspecific cadherins. VE-cadherin is found

exclusively on intercellular junctions of all endothelial cells[47]. Cadherins only localise at intercellular adherens junctions when cells contact each other.

Platelet endothelial cell adhesion molecule (PECAM-1) also known as cluster of differentiation 31 (CD31) is a protein which belongs to the immunoglobulin family that is expressed by endothelial cells, platelets and leucocytes[48]. PECAM-1 can form homotypic bonds with PECAM-1 from neighbouring cells or can attach to glycosaminoglycans, and is widely used in histopathology as an endothelial marker. When endothelial cells are confluent, PECAM1 localises to the lateral edge of cells and appears to associate with adherens junctions, albeit with less affinity [47]. PECAM1 is important for angiogenesis, vascular injury repair and control of leucocyte extravasation with expression in influenced by the cellular milieu. For example, treatment of endothelial cells with TNFα redistributes PECAM-1 away from lateral cell surface borders with transmigration of leucocytes across the endothelium[49]. Maintenance of endothelial barrier integrity is critical to tissue health with disruption of the alveolar endothelium manifesting acutely as alveolar oedema as witnessed in pulmonary oedema and acute lung injury. Chronic insult to the endothelial barrier may lead to hyalinisation, fibrosis or necrosis/apoptosis and is the study of this thesis with reference to cigarette smoking injury.

## *1.11VEGF and the Lung*

Vascular Endothelial Growth Factor (VEGF) is a growth and permeability factor for endothelial cells [50]. It has an important role in vascular development *in utero*, underlined by the embryonic lethality of knockout models for the genes encoding VEGF and its receptors[51], however its normal biological activity in adult life is currently not fully understood. The lung has comparatively high expression of this growth factor and over the last ten years it has emerged that VEGF may play a crucial role in maintaining lung structure and function, with a number of pulmonary pathologies associated with both reduced and increased levels of VEGF [50].

In pulmonary arterial hypertension the typical angioproliferative plexiform lesions have very high levels of VEGF which suggests this growth factor may play a pivotal role in pathogenesis[52]. Increased levels of plasma VEGF have been found in patient with Acute Respiratory Distress Syndrome (ARDS)[53]and may mediate barrier dysfunction and endothelial permeability with alveolar engorgement. In emphysema, there appears to be reduced VEGF and VEGFR2[54], however there are also reports of increased VEGF within in the airways of patients with chronic bronchitis[55], thus within the same disease state regional variations in VEGF may exist and may explain the complex pathology witnessed in COPD[56].

Five family members (VEGF (a-d) and Placental Growth Factor (PlGF)) have been identified, with VEGFa (referred to as VEGF) the most biologically active member that is believed to be of greatest importance[50]. VEGF binds to 2 tyrosine kinase receptors, VEGF receptor 1 (FLT1) and VEGF receptor 2 (KDR/FLK1) [57]. These receptors are regulated by both autocrine and paracrine mechanisms. The KDR/FLK1 is the most studied which is thought to mediate most of the pro-angiogenic effects of VEGF. The FLT1 receptor is believed to play more of a modulatory role, acting as a decoy receptor to inhibit excessive proliferation. VEGF is produced by macrophages and type II pneumocytes and acts predominantly on endothelial cells and type II cells [50]. Withdrawal of VEGF leads to endothelial cell apoptosis *in vitro* and *in vivo*[57]. Endothelial cells appear more susceptible to the effects of VEGF as cultured type II pneumocytes are exposed to VEGFR blockade do not undergo cell death [50].

The gene which encodes VEGF is located on chromosome 6p21.3, with expression regulated by several factors including hypoxia, via hypoxia-inducible factor 1 (HIF-1) [58]. HIF-1 is a heterodimer composed of 2 subunits HIF-1α and HIF-1β. Both proteins are constitutively expressed, however only HIF-1α responds to changes in oxygen tension. Under normoxic conditions, the half-life of HIF-1α is less than 5 minutes due to continuous proteolysis through the ubiquitin-proteasome pathway via an oxygen-dependant degradation domain (ODD). Hypoxia slows degradation of HIF-1α via reduced proline hydroxylase, making HIF-1α resistant to degradation.

Thus in the presence of low oxygen tension, increased HIF-1 binds to a hypoxia-responsive element (HRE) on the VEGF promoter region to cause induction and stabilisation of VEGF mRNA.

VEGF has multiple effects on endothelial cells including activation of endothelial Nitric Oxide Synthase (eNOS), via c-Src and phospholipase C γ1, which mediates angiogenesis and produces NO with vasorelaxation and maintenance of endothelial function [50]. VEGF also leads to increased cellular proliferation and survival (via activation of bcl2 and inactivation of caspase 9 and Bad), prostacyclin production (via activation of prostacyclin synthase via MAPK) and increased vascular permeability [50], [59]. Thus reduced VEGF via cigarette smoking may not only cause imbalance between vasoactive substances such as NO and ET-1, but may induce apoptosis and reduce angiogenesis and may therefore be of great importance in emphysema.

## *1.12 Apoptosis*

Apoptosis was first described in by Kerr, Wyllie and Currie in 1972 as a programmed cell death, distinct from necrosis, which is a passive uncontrolled form of cell death usually precipitated by lack of cellular energy or membrane damage [60]. Apoptosis differs from necrosis in that this programmed cell death requires energy in the form of ATP and can be triggered by a number of different stimuli. The distinct morphological and cellular changes of apoptosis were described from observing the development of the nematode *caenohabditis elegans*. The deletion of cells during development of the nematode was shown to an active, energy dependant process, triggering a number of stereotyped responses that were highly conserved across the species. Apoptosis has since been shown to be an important factor in both development and in normal tissue homeostasis however has also been demonstrated to be a response to injury[61].

Apoptosis begins with cell shrinkage and pyknosis of the nuclei, as a result of chromatin condensation[61]. This can be visualised with haemotoxylin and eosin staining and light microscopy as single cells or small clusters of oval cells which appear dark due to eosinophilic cytoplasm and dense nuclear chromatin fragments. Thereafter, plasma membrane blebbing occurs with karyorrhexis and fragmentation into apoptotic bodies during a process termed budding. Apoptotic bodies are then phagocytosed by macrophages and degraded within phagolysosomes.

In response to injury, cells may undergo necrosis, apoptosis, senescence or a phenotype change. However not all cells in a population will respond in the same way to a specified stimulus. Some may undergo necrosis while others undergo apoptosis. These responses may happen independently, successively or simultaneously. Furthermore, the cellular pathways by which apoptosis may be triggered are numerous, being broadly split into the intrinsic and extrinsic pathway which merge to form a final common pathway leading to the pattern observed in programmed cell death. To further add complexity, the same stimulus may cause differing responses at different doses i.e. apoptosis at low dose and necrosis at high dose.

While clear differences exist between the active energy dependant apoptosis and passive cellular necrosis, these processes can co-exist with the balance of apoptosis/ necrosis determined by availability of apoptosis associated caspase enzymes and energy (ATP). Thus not only is cell death dependant upon stimuli, cell signaling and tissue, but rather depends crucially upon the local environment in which the injury occurs. Necrotic cells can also undergo blebbing, with membrane disruption and pyknosis and so is not a feature exclusive to apoptosis, therefore it is important to highlight other features which may differentiate these two processes[61]. In contrast with necrosis, where large numbers of cells are deleted, apoptotic cells are more likely to be found as individual cells, as the host deletes only cells which are deemed to be defective. Another important contrast with necrosis is that apoptosis does not lead to secondary inflammation, as cells do not release their toxic contents prior to being phagocytosed and digested[61]. Thus while individual

morphological changes between necrosis and apoptosis on occasions can appear similar, by studying the distribution of lesions andmicroenvironment in which these are found, one can differentiate between these two differing cell death pathways.

There are two main apoptotic pathways: the extrinsic (death receptor pathway) and the intrinsic (mitochondrial pathway). These pathways were traditionally thought to be distinct and mutually exclusive, however new evidence suggests that these pathways are linked and that molecular events in one may influence events in another[61]. In addition to the two classical pathways, there exists an additional mechanism involving T-cell mediated cytotoxicity and perforin-granzyme-dependant cell death[62]. The pathways merge to form a final common pathway with the cleavage and activation of caspase-3 with resulting DNA fragmentation, degradation of proteins and phagocytic uptake. Phagocytosis involves translocation of phosphatidylserine onto the surface of apoptotic cells which then acts as phagocytic receptors, facilitating recognition, engulfment and disposal.

The extrinsic pathway or death ligand pathway is triggered mostly by TNFα, Fas ligand and TRAIL (TNFα-related apoptosis inducing ligand). Autophosphorylation of intracellular death domains, lead to recruitment of the FADD (fas associated death domain). Upon activation of FADD, procaspase 8 and 10 are cleaved to form their active caspases, which transmit this apoptotic signal via further caspase activation to the mitochondria. The intrinsic pathway is triggered via damage to DNA such as oxidative stress and UV light. DNA damage causes activation of p53, which induces cell cycle associated genes.

## *1.13 Endothelial Apoptosis in Emphysema*

Apoptosis was first suggested to be important in the pathogenesis of COPD in the landmark study by Kasahara *et al* [63]. Chronic treatment (3 weeks) of adult Sprague dawley rats with a VEGF receptor blocker (SU5416) led to air space enlargement

associated with alveolar septal apoptosis. Lung proliferation was not inhibited. Barium gelatin angiograms from autopsy studies of these animals showed peripheral pruning of the arterial tree, with pronounced loss of the microvasculature. Treatment of rats with SU5416 and a caspase inhibitor prevented the alveolar septal apoptosis and development of air space enlargement, thus proposing that this VEGF receptor blockade model of emphysema was apoptosis dependant. A clinical study by the same group reported increased apoptotic endothelial and epithelial cells in the alveolar septa of emphysematous lung tissue when compared with tissue from non-smokers and smokers without emphysema via TUNEL staining and DNA ligation assays [54]. VEGF and VEGF receptor 2 mRNA and protein were also reduced in tissue from patients with emphysema. However SU5416 treated rats also had an 8 fold increase in isoprostane levels and 100 fold induction of cytochrome p450, both of which could catalyse the production of reactive oxygen species (ROS) in endothelial cells and contribute to apoptosis.

Apoptosis in emphysematous tissue has been investigated by other researchers with similar findings, with apoptosis rates between 1 and 2% of alveolar cells[64]–[67]. Yokohori *et al* reported increased rates of apoptosis and proliferation in alveolar septal epithelial cells in patients with emphysema compared to asymptomatic smokers and non-smokers [67]. In addition, they highlighted the dynamic nature of emphysema, with ongoing alveolar cell death and proliferation. In this study the predominant cell type undergoing apoptosis was epithelial cells and not endothelial cells. Imai *et al* demonstrated apoptosis of septal endothelial, epithelial and myofibroblasts in emphysematous tissue via cell morphology showing cytoplasmic condensation, shrinkage, condensation of nuclear chromatin of cells next to normal cells on electron microscopy [64]. These findings were confirmed via DNA fragmentation and apoptosis-related protein expression. Proliferation rates of septal cells were also increased, similar to the findings of Yokohori *et al* [67]. Furthermore, they reported a negative correlation between surface area and apoptosis, while there was no such relationship between surface area and proliferation. This finding may be crucial, as in order for tissue to be lost, apoptotic rates must exceed rate of ongoing proliferation to not support maintenance of normal tissue structure. Imai et

al also investigated the pathways via which apoptosis may be initiated [64]. The anti-apoptotic bcl2 was not found in emphysematous or normal tissue. However the pro-apoptotic Bax and Bad were. Bax expression is increased when cells die by loss of adhesion to the extracellular matrix (ECM). Thus apoptosis may be triggered by disruption of the ECM with increased caspase 3. There is also some evidence that apoptosis may be triggered by activation of cell surface death receptors via the Fas ligand [68]. Importantly, these authors highlight that increased apoptotic rates persist on smoking cessation [64].

It has also been reported that A1AT may have anti-apoptotic actions which may partly explain the accelerated emphysema witnessed in individuals homozygous for the PiZ allele. Petrache *et al* showed *in vitro* and *in vivo* in a mouse model that A1AT prevented caspase-3 activation and thus apoptosis [69], [70]. Such evidence further supports the key role apoptosis may play in the development of emphysema.

## *1.14Apoptosis and Oxidative Stress*

Tuder *et al* went on to link increased levels of oxidative stress and apoptosis in the rodent VEGF blockade model of emphysema [71]. Oxidative stress is a highly relevant stress in emphysema as cigarette smoke contains around $10^{17}$oxidants for each inhalation [72]. SU5416 treated rats had increased levels of oxidative stress compared with control animals [71]. Co-treatment of SU5416 treated rats with the manganese superoxide dismutase (MnSOD) mimetic M40419 prevented the development of air space enlargement and emphysema. In addition, M40419/SU5416 treated rats had less activated caspase 3 and TUNEL positive cells, than SU5416 treated alone. Caspase 3 was localised in the centrilobular region, the area in which most airspace enlargement occurred in SU5416 treated rats and which is the area most affected in smoking related emphysema. Co-treatment also significantly increased proliferation rates, as evidenced by the marker PCNA. SU5416 treated rats demonstrated reduced phosphorylation of the pro-survival akt, whereas higher levels were evident in co-treated animals. Apoptosis

predominated in areas of oxidative stress, which supports the hypothesis of apoptosis and oxidative stress being linked by a positive feedback mechanism.

A second animal model supports the role of oxidative stress in the development of emphysema [73]. Nrf-2 deficient mice have reduced anti-oxidant abilities due to their lack of Nrf-2 which binds to anti-oxidant response elements and leads to upregulation of anti-oxidant genes and gene products. Nrf-2 deficient mice exposed to cigarette smoke for 6 months developed emphysema, associated with increased markers of oxidative stress and increased numbers of apoptotic septal cells, compared to wild types. In keeping with the microvascular hypothesis of emphysema, endothelial cells were the predominant apoptotic cell type in this model of smoking induced emphysema.

Clinical studies also support this hypothesis linking the importance of oxidative stress and reduced VEGF on microvascular function, as a possible mechanism of emphysema. Kanazawa *et al* showed that nitrogen oxide levels were increased in sputum from patients with COPD and correlated with severity [74]. In addition, peroxynitrite stress increased with severity of COPD while VEGF levels decreased. Induced sputum also showed increased neutrophils and levels of the pro-inflammatory cytokine IL8, which in addition has been shown to induce superoxide anion release from neutrophils *in vitro*.

There are a number of possible interactions between loss of VEGF, witnessed in emphysema, and oxidative stress that results due to cigarette smoking. VEGF upregulates the anti-oxidant MnSOD and the anti-apoptotic factor bcl-2 [71]. VEGF signalling inhibition may lead to further oxidant/antioxidant imbalance via decreased eNOS and prostacylin synthase. In addition, cigarette smoke may have a direct effect on the endothelium, reducing eNOS and prostacylin synthase, with less Nitric Oxide to scavenge free radicals and block caspase activity, with reduced Prostacyclin derived glutathione [50]. Thus interruption of the feedback loop

between oxidative stress and apoptosis or free radical scavengers may represent novel targets to prevent further septal destruction.

## *1.15Senescence*

Cellular senescence, first described in 1961, is the phenomenon by which normal diploid cells cease to divide and is classically attributed to the aging process as a result of telomere shortening [75]. In addition, senescence can also be induced by DNA damage caused by reactive oxygen species (ROS) and activation of oncogenes [75]. Senescent cells are unable to replicate but remain metabolically active and frequently express pro-inflammatory ligands and stain positively for senescence associated β-galactosidase activity [76]. Thus in addition to potentially limiting tissue repair and renewal, senescent cells may further contribute to organ damage. Given that COPD is more commonly found with advancing age [3] and that emphysema (often called senile emphysema) can be found incidentally on HRCT scanning of elderly patients who have never smoked and who have normal lung function, it has been proposed that cellular senescence may play an important role in the pathogenesis of COPD. Senile emphysema does differ in that alveolar spaces are enlarged with loss of elastic recoil, however unlike true emphysema there is no destruction of alveolar walls [77], [78]. One mechanism by which senescence may play a role in emphysema is by limiting the ability of damaged alveolar cells to continue to proliferate in response to injury, thus imposing a finite number of divisions that a single cell can make. Once cellular senescence occurs, cell proliferation attempts to repopulate apoptotic alveolar cells ceases and the homeostasis between cell death and proliferation is lost, which may in part account for emphysema [79], [80]. Studies to date have furthermore shown accelerated senescence of alveolar epithelial and endothelial cells in patients with emphysema [79]. Detailed study of senescence is beyond the scope of this study but this response to cell injury should be considered when interpreting results.

## *1.16Repair and remodeling in emphysema*

Emphysema was originally defined as *"destruction of alveolar walls without fibrosis"* [15], however it is now accepted that complex tissue remodelling occurs, notably in centrilobular disease. The ability to repair a tissue after injury is an inherent property of all tissues. In addition to septal destruction, attempts at, albeit ineffective, tissue repair, are important in the pathology witnessed [24], [25], [81]–[84]. The interplay between inflammation and repair/ fibrosis may be of greater importance in centrilobular emphysema, the disease pattern witnessed in smokers, compared with the more uniform destructive pattern of panacinar emphysema seen more commonly in A1AT disease [24]. In centrilobular emphysema, while there is loss of overall tissue, thickening of the interstitium occurs, with collagen deposition in alveolar septal walls and increased interstitial fibroblasts [84]. Gosselink et al reported differential gene expression between bronchiolar and immediate surrounding lung tissue, with the balance reported to be in favour of degradation of lung tissue surrounding thickened small airways [85]. However, in both this study [85] and others [86] ECM-related genes have been shown to be upregulated in severe emphysema in support of connective tissue remodelling in severe 'end-stage' disease in humans. Vlahovic *et al* demonstrated morphometrically that while alveolar and capillary surfaces reduce with increased mean linear intercept, there was deposition of collagen and elastin in the remaining septa, in keeping with remodelling of the connective tissue matrix in alveolar walls [84]. Kononov *et al* showed in the pancreatic elastase model of emphysema that the resulting thickened elastin and collagen fibres undergo larger distortions than normal tissue [87]. Mechanical failure threshold for collagen is also reduced, such that the normal mechanics of breathing are sufficient to cause failure of the remodelled ECM that contributes to emphysema [88]. This immature collagen may be weaker and more distensible that allows distension of airspaces and breaks may cause emphysema. In keeping with the microvascular hypothesis of COPD, these changes may occur via endothelial to mesenchymal transition (EnMT) with the production of immature weak collagen and mesenchymal cells that secrete matrix metalloproteinases (MMPs) which further degrade alveolar septa and ECM.

## *1.17Endothelial to Mesenchymal Transition (EnMT)*

Endothelial to mesenchymal transition (EnMT) is a cellular response to chronic injury characterised by cytoskeletal rearrangement of cobblestone like endothelial cells into spindle shaped mesenchymal cells[89]. Cells lose endothelial markers and gain mesenchymal markers and may exhibit a proliferative and invasive phenotype, interacting with the ECM, causing deposition of collagen. EnMT was first observed in aortic endothelial cells in response to Transforming Growth Factor β1 (TGFβ1) and was proposed as a novel mechanism in atherosclerosis [89]. While this phenomenon was initially reversible, after prolonged exposure, cells lost this plasticity. Frid *et al* later demonstrated this phenomenon in mature endothelial cells from main pulmonary arteries [90]. This EnMT was inhibited by TGFβ1 neutralising anti-bodies, underlining the importance of TGFβ1 as a driver of EnMT.

Ziesberg and Kalluri went on to propose evidence of *in vivo* EnMT occurring in response to TGFβ1 in cardiac fibrosis via lineage tracing [91]. They created double transgenic mice (Tie1Cre;R26RstoplacZ), which express the lacZ gene in all cells of endothelial origin in spite of phenotypic alterations. Via this method they showed the appearance of mesenchymal cells within the areas of tissue fibrosis that were lacZ positive and thus of endothelial lineage. They presented further evidence in support via immunofluorescence with double labelling for β-galactosidase (βgal) and fibroblast specific protein 1 (FSP1 or S100A4). The use of β-galactosidase in this experiment to indicate cells of endothelial origin is confounded by the fact that β-galactosidase is commonly used as a marker of senescence [92], as it is highly expressed and accumulated is lysosomes in senescent cells. The authors do not raise this issue or discuss the potential that the endothelial cells that appear to undergo EnMT may have been senescent. This further highlights the fact that cellular senescence may be important in the pathogenesis of conditions arising from chronic inflammation (cardiac fibrosis and emphysema) and may provide the correct milieu for apoptosis and cellular plasticity such as EnMT. Importantly, in this study EnMT could be reversed by the addition of recombinant BMP7, which has a number of implications for clinical translation. EnMT was also reduced in SMAD 3 null mice,

suggesting that this TGFβ1-driven EnMT is occurring via activation of SMAD signalling pathways.

## *1.18EnMT and endothelial dysfunction*

Endothelial dysfunction occurs in response to cigarette smoke with reduction in NO and increased ET-1[34]. In addition to the important vasomotor actions of these substances, there is emerging evidence that they may play an important role in the maintenance of vascular structure and function. Change in the balance of endothelial derived relaxing and constricting factors may also contribute to the tissue remodeling witnessed in emphysema. O'Riordan *et al* have shown that NOS inhibition promotes EnMT [93]. Using human umbilical vein endothelial cells (HuVECS), they showed via phase contrast microscopy that cells treated with TGFβ1, endostatin and ADMA (an endothelial NOS inhibitor) underwent a phenotypic change becoming spindle shaped and elongated in keeping with transition to a mesenchymal phenotype. In addition, loss of endothelial markers and gain of mesenchymal markers was evidenced via western blotting. In further support of the role that NO may play in maintaining cell phenotype, Vyas-Read *et al* found that inhibition of NOS with L-NAME led to a phenotype change of alveolar epithelial cells into mesenchymal cells (epithelial to mesenchymal transition) (EMT) [94]. Exogenous NO applied to these TGFβ1 treated alveolar epithelial cells led to reduced α smooth muscle actin (αSMA) expression and reduced collagen expression, suggesting that NO may attenuate this phenotypic change. Reports in the cancer literature highlight further the role that vasoactive mediators might play in maintaining cell phenotype, with evidence of ET-1 as a driver of EMT in ovarian cancer cells [95]. Activation of ETa receptors by ET-1 leads to EMT via signaling down an integrin-linked kinase pathway with reversal of this phenotype change in the presence of ETa receptor antagonism. In the pulmonary microvasculature, cigarette smoke injury may promote EnMT via increased ET-1 and loss of protective NO, and thus agents to stabilize/restore microvascular function may prevent the loss of endothelial cells and tissue remodeling typical to emphysema.

## *1.19TGFβ1 and Emphysema*

TGFβ1 is a complex mediator of tissue repair and plays a crucial role in lung homeostasis [81]. Many different cellular responses are elicited by TGFβ1 via activation of a number of signalling pathways, including activation of MAP Kinase, PI3 kinase, Rho like GTPases and SMAD signalling, which mediate changes in target gene transcription. The signalling pathway activated and subsequent cellular response is not only determined by cell type but is also affected by the microenvironment [81]. TGFβ1 is secreted as a latent complex with activities regulated by binding to latent TGFβ binding protein (LTBP). There is evidence that reduced activation of latent TGFβ1 and defects in downstream TGFβ1 signalling leads to spontaneous lung inflammation and emphysema [25]. Homozygous mice with a mutant allele for LTBP4 (which binds only TGFβ1) develop severe emphysema with the reduced TGFβ1 and phosphorylated SMAD2 in epithelial cells [96]. Furthermore mice null for integrin αvβ6-which mediates TGFβ1 activation develop age-related emphysema [97]. These knockout mice have increased expression of MMP12, which is a matrix degrading zinc dependant protein implicated in the pathogenesis of emphysema [98]. αvβ6-integrin expression on epithelial cells may also be downregulated via toll like receptor (TLR) signalling of alveolar macrophages in response to bacterial and viral invasion [81]. Thus chronic low-grade bacterial infection, as may occur in response to altered epithelial cell function in response to smoking, may allow unopposed macrophage activation. Mice lacking this integrin develop age-related emphysema that can be prevented by transgenic expression of active TGFβ1 [97]. In further support of altered SMAD signalling, SMAD3 null mice develop age related increases in alveolar spaces associated with presence of MMP 9 and 12 in the lung, suggesting that TGFβ1 downstream signalling via SMADs may play a pivotal role in ECM metabolism [99]. However it is important to note that these increases in alveolar spaces do not fully equate with the complex tissue repair and remodelling that occurs in human emphysema and thus such animal models are an oversimplification.

TGFβ1 activation in the lung is most well described in idiopathic pulmonary fibrosis (IPF); with the presence of TGFβ1 activation associated the rapid disease

progression [81]. However it is now accepted that this factor may play an important role in other models of lung injury and repair. The pathology of septal destruction and airspace enlargement witnessed in emphysema on the surface appears far removed from the rampant fibrosis associated with IPF, however it is clear that complex tissue remodelling occurs in emphysema. Emphysematous areas express fibrosis-associated genes and proteases and it could be suggested that emphysema arises via ineffective repair and associated secondary fibrosis. [81]. In IPF the as yet unidentified injury may be relatively minor with an exaggerated fibrosis response, while in emphysema, repeated cigarette smoking may alter the microenvironment in susceptible individuals with a diminished, ineffective repair response to injury.

The levels of expression of TGFβ1 in COPD are still debated and likely reflect the heterogeneous nature of this condition. Some researchers believe there is reduced TGFβ1 and TGFβ receptor expression in COPD lung tissue, with decreased release from alveolar macrophages[100], [101], while others the report increased levels, attributing this to increased production by abundant alveolar macrophages [102]. Furthermore, the effects of cigarette smoke on TGFβ1 are also debated. There is however good evidence that alterations in redox state and increased oxidative stress, as occurs in cigarette smoking, contributes to TGFβ1 activation [81]. In addition TGFβ1 itself induces intracellular ROS, thus causing positive feedback to amplify the signal. Thus TGFβ1 likely plays as yet undetermined role in the development of emphysema, either via reduced activity, defective signalling or ineffective septal repair/ fibrosis in response to oxidative stress.

## *1.20Matrix metalloproteinases in emphysema*

Matrix metalloproteinases (MMPs) are a family of zinc and calcium dependant proteolytic enzymes that are involved in tissue remodelling and repair [98]. MMPs can degrade most components of the ECM and so are believed to play an important role in the pathogenesis of emphysema. Studies in mice have provided insights into how MMPs may contribute to this pathology. MMP1, MMP2, MMP8, MMP9 and

MMP12 have all been implicated in emphysema [98]. Mice deficient in MMP12 (macrophage elastase) exposed chronically to cigarette smoking fail to recruit macrophages to the alveolar bed and do not develop emphysema [103]. Increased expression of MMP1 (collagenase) in mice leads to airspace enlargement [104]. Cigarette smoking increases MMP9 (gelatinase B) and MMP12 expression [98]. In addition to their ECM degrading properties, MMP2, MMP7, MMP9, MMP12 are able to cleave A1AT, which inactivates this important inhibitor of neutrophil elastase, which may contribute to septal destruction via increased elastin destruction [105]. Recent studies in humans have provided further support for the role of MMPs in emphysema. MMP 8 and MMP9 are increased in bronchoalveolar lavage (BAL) fluid of subjects with COPD/emphysema compared with non-smokers [98]. There is also emerging evidence for MMP2 in emphysema. Baraldo *et al* showed upregulation of MMP2 in the lung periphery of patients with emphysema compared with non-smokers and smokers without emphysema [106]. In addition, they showed positive correlation of MMP2 with radiological severity of emphysema. MMP2 is expressed in structural cells such as endothelial cells and smooth muscle cells and macrophages. In this study, MMP2 was observed in alveolar macrophages, alveolar walls, peripheral airways and small arterioles. Interestingly, while expression was significantly increased in the alveolar walls of smokers with severe COPD, expression in smokers with mild/moderate disease had levels similar to that of smoking and non-smoking controls suggesting that MMP2 activation may be important in the development of more severe emphysematous disease. Importantly, this increase in MMP2 was unrelated to current smoking status, being related rather to the presence of COPD/emphysema. In addition to these ECM degrading properties, MMP2 may also have important immunomodulatory functions. Unrestrained expression of MMP2 may contribute to the aberrant type1 immune response that has been suggested to occur in emphysema [107].

## *1.21Apoptosis and EnMT*

A link between apoptosis and vascular smooth muscle cell growth was first reported in 2006 by Sakao *et al* [108]. Apoptosis was induced in normal human pulmonary microvascular endothelial cells via VEGF receptor blockade (SU5416). The media from these apoptotic cells was then applied to rat pulmonary artery smooth muscle cells cultured with varying degrees of sheer stress. After 24 hours incubation, cells cultured in conditioned media showed increased proliferation compared to cells cultured in non-conditioned media and serum free media. The media from apoptotic endothelial cells had increased concentrations of TGFβ1 and VEGF as assessed by RT-PCR, with the combination of high shear stress and SU5416 treatment having the highest of all gene expression. Because both TGFβ1 and VEGF were increased in the apoptotic media, they investigated the role that each might play in vascular smooth muscle proliferation via co-incubation with neutralising antibodies for each. Using this method they demonstrated that TGFβ-1 but not VEGF mediated this proliferation. Extrapolating these findings, one could propose that apoptosis of endothelial cells leads to increased TGFβ1 which may drive both EnMT and mesenchymal proliferation.

These researchers provided further evidence linking apoptosis and EnMT, as a mechanism behind the vascular remodelling witnessed in pulmonary hypertension [109]. They induced apoptosis of normal human pulmonary of microvascular endothelial cells via VEGF receptor blockade (via SU5416 treatment for 5 days) and then maintained these cultures for a further 3 to 5 passages. This treatment suppressed PGI2 gene expression but induced COX2, VEGF and TGFβ1 expression and caused transdifferentiation of mature endothelial cells (as evidenced by dil-acetylated LDL uptake, lectin and factor VIII expression) into smooth muscle like cells (expression of αsma) with some transitional cells expressing both markers. To investigate the characteristics of the cells undergoing apoptosis and transdifferentiation, cell type was investigated via magnetic cell sorting of cells for CD34 prior to SU5416 treatment. CD34 is expressed by haematopoietic progenitor cells, endothelial cells and some fibroblasts. They observed that only cells positive

for CD34 underwent this transition. They suggest that VEGF blockade causes apoptosis of susceptible endothelial cells, creating a selection pressure for CD34+ progenitor cells which, via changes in the microenvironment due to apoptotic cells, undergo EnMT. In contrast to the previous study, this transdifferentiation was not inhibited by the addition of VEGF and TGFβ-1 neutralising antibodies suggesting in this case, that these mediators do not drive this phenotype change.

## *1.22 Possible reversal of apoptosis and EnMT*

In addition to caspase inhibition and anti-oxidants such as MnSOD preventing apoptosis, prostacyclin has been shown to prevent endothelial cell apoptosis induced by cigarette smoke [110]. Treatment of normal human pulmonary microvascular endothelial cells with 0.5 and 1% cigarette smoke extract (CSE), prepared according to a standard method [111] reduced prostacyclin gene expression in a dose dependant manner with a maximal effect at 24 hours. This reduction in prostacyclin may be via acrolein, a highly toxic unsaturated aldehyde found in cigarette smoke extract, as treatment with acrolein alone also lead to a reduction in prostacyclin. Treatment of cells with 1 and 2% CSE increased apoptosis rates (assessed by annexin V staining via FACS) from 3% in control cells to 9%. Pre-treatment of these normal pulmonary microvascular cells with the prostacyclin analogue iloprost significantly reduced this apoptosis in response to CSE.

There is also evidence which suggests that simvastatin can inhibit cigarette smoking induced emphysema via reduction of inflammation and MMP-9 production [112]. In addition to anti-inflammatory actions, simvastatin may have anti-oxidant functions important to maintenance of microvascular function and prevention of emphysema. ROS in the serum of smokers can reduce eNOS expression leading to endothelial dysfunction, thus simvastatin may restore endothelial function via the removal of ROS. Removal of ROS may prevent both apoptosis and EnMT, mechanisms which may be involved in the complex tissue remodelling witnessed in emphysema.

## *1.23 Summary*

Emphysema is a common lung condition with poor survival and very limited therapeutic options. A major stumbling block to research has been the notion that emphysema simply equates with loss of lung tissue and destruction. Understanding the role that endothelial cell loss may play may lead to advances in our understanding. Furthermore the potential for realveolarisation is an attractive proposition. Thus attempts to study the fate of LMVECs in response to cigarette smoke may allow improved understanding of the pathogenesis of emphysema, and allow identification of potential new therapeutic targets.

# *Chapter 2: Hypothesis and Aims*

## *2.1 Hypothesis*

Cigarette smoke injury to human lung microvascular endothelial cells causes apoptosis and endothelial-to-mesenchymal transition with resulting emphysema in susceptible individuals.

## *2.2 Aims*

In this study I planned to use emphysematous lungs removed at the time of transplantation to create a new disease model to study emphysema with cells from individuals who had developed disease. All cell culture models have limitations including the use of cancer resection specimens (the surrounding tissue removed may have altered expression of VEGF) or normal tissue obtained from lungs not suitable for transplantation (the brain death process with subsequent inflammation). I therefore aimed to use this new model to investigate emphysema in the hope that it would provide a new way to study *ex vivo* cellular responses, as close to *in vivo* conditions as possible.

The use of severely emphysematous lungs to study the pathogenesis of emphysema with reference to endothelial cells can attract criticism with regards the relevance of studying end stage disease to the question of pathogenesis. However, research shows that in severely damaged emphysematous lungs there is ongoing evidence of repair and active inflammation and that within severely damaged lung there are some areas of near normality [86]. One may postulate that cells isolated successfully from emphysema lung tissue are likely to be a reliable model as severely damaged cells would not survive the isolation process, thus the cells isolated are likely to be susceptible yet relatively normal endothelial cells.

Isolating, purifying, cryopreserving and re-culturing microvascular endothelial cells from patients with emphysema, although challenging, may provide a way in which to study emphysema that potentially demonstrates *in vivo* cell responses in a cell culture model. In contrast to immortalised cell lines, animal models and the use of normal human primary cells, this model may allow study of the cellular response to injury (in this case, cigarette smoke) that led to the disease in cells from susceptible individuals, *ex vivo*, with the potential to improve our understanding of how cigarette smoking causes emphysema.

- I therefore investigated my hypothesis using severely emphysematous lung tissue obtained at transplantation.
- Firstly, I attempted to establish a reliable and reproducible method to isolate and fully characterise microvascular endothelial cells from the excess emphysematous tissue obtained at lung transplantation.
- Secondly, I planned to use these cells from multiple patients to investigate:
    - Whether these susceptible endothelial cells undergo apoptosis in response to cigarette smoke, in comparison with untreated cells and rates of apoptosis in cells isolated from normal individuals.
    - The characteristics of cells which were resistant to apoptosis.
    - Endothelial plasticity in response to cigarette smoking, examining cell activation and phenotype via change in cellular expression and matrix production in response to cigarette smoke extract.

I also studied the immunohistochemistry findings of severely emphysematous lungs with reference to apoptosis and endothelial to mesenchymal transition, using tissue blocks obtained from the lung tissue from which cells were obtained.

# *Chapter 3: Materials and Methods*

## *3.1 General Reagents*

### *3.1.1 Immunohistochemistry*

Phosphate buffered saline (PBS) and bovine serum albumin (BSA) were purchased from Sigma-Aldrich. Envision flex and flex plus reagents were purchased from Invitrogen. TSA kits were purchased from Perkin-Elmer.

### *3.1.2 Cell isolation*

Dulbecco's Modified Eagle medium (DMEM), Roswell Park Memorial Institute (RPMI) and PBS were purchased from Sigma-Aldrich. Type II Collagenase was purchased from Worthington (47A9338). The Dynal magnet, Dynabeads M-450 and CD31 Dynabeads were purchased from Invitrogen. The lectin UEA-1 was purchased from Sigma.

### *3.1.3 Cell Culture*

Cell culture plastics were purchased from Fisher Scientific. Cryopreserved normal human pulmonary microvascular endothelial cells were purchased from Promocell (C12281) and Lonza (CC-2527). All cells were cultured in MV2 media (C-22121, Promocell). Cells were passaged using PBS (Sigma) and cell dissociation solution (Sigma C5789).

### *3.1.4 Cigarette Exposure Experiments*

Kentucky research filterless cigarettes (Lot 4A1) were gifted from AstraZeneca R+D Charnwood and were used for all experiments. A vacuum pump was purchased Laboport (Mini pump N86 KN.18) and used in all preparation of cigarette smoke extract (CSE).

### *3.1.5 Flow cytometry*

PE conjugated Annexin V kits were purchased from BD Biosciences (556422).

### *3.1.6 Western blotting*

4-12% Bis Tris Nu-Page pre-cast Gels, MES running buffer and ‘See blue’ indicator were purchased from Invitrogen. BCA protein assay kits (#23225) and Supersignal West Pico Chemiluminescent (#34080) kits were purchased from Pierce Laboratories. PVDF membrane was purchased from Amersham biosciences (#NF1016).

### *3.1.7 Confocal microscopy*

DAPI was purchased from vectashield (H-1200).

### *3.1.8 RT-PCR*

RNA was isolated from cells using Absolutely RNA microprep kit (400805) Agilent. cDNA was then obtained using Affinity script qPCR cDNA synthesis kit (600559) Agilent.

### *3.1.9 ELISA*

Endothelin-1 ELISA kits were purchased from assay designs (#900-020A).

### *3.1.10 TUNEL*

Fluorescein In situ cell death detection kits were purchased from Roche (11684795910).

## *3.2 Antibodies: primary and secondary*

### *3.2.1 Confocal Microscopy*

For characterisation and EnMT work, CD31 (sc-53411, Santa Cruz), Ve-Cadherin (sc-6458, Santa Cruz), Vimentin (M7020, Dako), aSMA (F3777, Sigma) and fibronectin (F3648, Sigma) were used to detect cell surface expression via confocal microscopy and counterstained appropriately with either FITC (Mouse) (F2012) (Sigma) or TRITC (Rabbit) (T6778) (Sigma) with DAPI nuclear staining (H-1200, Vectashield).

### *3.2.2 Live Cell imaging*

DEVD-NucView 488 Caspase 3 substrate (Biotium Inc) was used to detect apoptosis via live cell imaging. DEVD-Nucview is a fluorogenic enzyme which can freely pass into the nucleus. Upon activation of the substrate (caspase 3) enzymatic cleavage of Nucview leads to fluorescence.

### *3.2.3 Flow Cytometry*

For cell characterisation, FITC conjugated CD31 (#555445, BD Bioscience) was used to identify endothelial cells. PE cy5 conjugated CD90 (# 555597, BD Bioscience) was used to identify fibroblast/ mesenchymal cells. APC conjugated CD62E (E-selectin) (#551144, BD Bioscience) was used to detect response to stimulation with TNFα.

Apoptosis was investigated using Annexin V (# 556422 BD Bioscience), as an early marker of apoptosis via detection of phosphatidylserine residues. Necrotic cells were detected using 7AAD (BD Bioscience), which is fluorescent and has strong affinity for DNA but requires cell membrane disruption in order for it to bind, thus labeling only dead cells and not viable cells.

### *3.2.4 Western Blotting*

Recombinant human TGFβ1 (100-21) was purchased from Peprotech. CD31 (sc-53411, Santa Cruz) and VE-Cadherin (sc-6458, Santa Cruz) were used to detect endothelial cell protein expression. Alpha smooth muscle actin (ab32575, Abcam), Vimentin (M7020, Dako), and Fibronectin (F3648, Sigma) were used to investigate cellular plasticity and endothelial to mesenchymal transition. β actin (A2228, Sigma) was used as a loading control.

### *3.2.5 PCR*

Taqman probes were purchased to detect 18s (4331182) and VEGF KDR (4465807) (Applied Biosystems).

### *3.2.6 ELISA*

Endothelin-1 ELISA kits were purchased from Assay Designs (900-020A).

## *3.3 Patients*

Ethical approval for the isolation and study of diseased cells was given by the Northumberland Local Ethics and Research Committee in January 2007 (REC reference 06/Q0902/57). All patients awaiting lung transplantation at Freeman Hospital were invited to take part in the study. Patients gave informed consent to donate their explanted lung for research purposes outlined in the study. The study was performed in accordance with ICH-GCP. Study patient information leaflet and consent form appear in Appendix 1.

Ethical approval to obtain excess normal tissue from patients undergoing lobectomy/ pneumonectomy was given by County Durham and Tees Valley 2 Research Ethics Committee in July 2009 (REC reference 09/H0908/35). Patients were identified according to the study protocol (Appendix 2) and excluded should they have evidence of emphysema/ fibrosis on radiology or pulmonary function testing. The study was performed in accordance with ICH-GCP. Study protocol, patient information leaflet and consent form appear in Appendix 2.

Clinical data such as primary diagnosis, age, body mass index, arterial oxygenation (PaO2) and pulmonary function tests were obtained from each individual who donated tissue. Smoking status and smoking history from each patient was also obtained. Those with emphysema were also categorised according to the updated GOLD criteria (2003) [113], [114]. Clinical data is summarised in Table 1. Further detail is provided in individual patient data sheets in Appendix 3.

Table 1: Patient demographics, histopathological diagnosis and clinical data

| Patient No: | Gender | Diagnosis | Age | BMI | Smoking History (Pack yrs.) | FEV1 (%) | TLC (%) | KCO (%) | GOLD stage |
|---|---|---|---|---|---|---|---|---|---|
| **1** | M | A1AT emphysema (Panacinar) | 46 | 28.7 | 15 | 18 | 133 | 15 | IV |
| **2** | F | Emphysema | 54 | 21.5 | 30 | 10 | 178 | - | IV |
| **3** | F | Emphysema (Centrilobular) | 53 | 20.9 | 30 | 22 | 131 | 32 | IV |
| **4** | F | Emphysema | 51 | 20.8 | 30 | 28 | 150 | 33 | IV |
| **5** | F | Emphysema (Centrilobular) | 46 | 20.2 | 20 | 21 | 150 | 43 | IV |
| **6** | M | Emphysema (Centrilobular) | 58 | 22.7 | 35 | 15 | 130 | 46 | IV |
| **7** | F | Emphysema (Centrilobular) | 59 | 21.8 | 25 | 34 | 155 | 38 | III |
| **8** | M | Emphysema (Centrilobular) | 44 | 23 | 15 | 14 | 138 | 69 | IV |
| **9** | F | Emphysema | 60 | 28.3 | 20 | 26 | 95 | 25 | IV |
| **10** | M | Emphysema | 45 | 21.3 | 27 | 26 | 156 | 42 | IV |
| **11** | M | Emphysema (Centrilobular) | 55 | 20.8 | 55 | 17 | 130 | 24 | IV |
| **12** | F | A1AT emphysema (Panacinar) | 40 | 26.1 | 25 | 16 | 136 | 33 | IV |
| **13** | M | Emphysema (Centrilobular) | 47 | 22.3 | 30 | 17 | 150 | 42 | IV |
| **14** | M | A1AT emphysema (Panacinar) | 52 | 21.2 | 15 | 22 | 127 | 71 | IV |
| 15 | F | Normal | 68 | - | 15 | 104 | - | - | N/A |
| 16 | F | Normal | 65 | - | 40 | 80 | - | - | N/A |
| **17** | F | IPAH | 60 | 26.4 | 0 | 83 | 107 | 109 | N/A |

## *3.4 General Methods*

### *3.4.1 Obtaining diseased lung tissue*

At the time of transplantation, the lung was inspected to confirm the macroscopic pathology was in keeping with pre-operative diagnosis and to exclude any unexpected pathology. A lobe/part of lobe was then dissected and stored at 4°C until clinical pathology assessment (which was performed within 24 hours). Following routine clinical pathology, blocks of tissue were placed in neutral buffered formalin for fixation for histology experiments. The remaining tissue (typically around 50g) was used immediately for cell isolation.

### *3.4.2 Obtaining normal tissue*

The operating surgeon performing lobectomy for suspected lung cancer identified a wedge of normal tissue within the tissue removed at surgery but discrete from the tumour resection margins. This was stapled off from the remaining tissue and tumour and placed in media. Both samples were transported to clinical pathology where the wedge sample was inspected and once confirmed to be free from disease, was used immediately for cell isolation. Tissue samples ranged from 5-30g.

### *3.4.3 Tissue preparation*

Tissue samples were fixed for 48 hours at room temperature (RT) in 10% neutral buffered formalin (Pioneer Chemicals, Surrey). The tissue was then dissected into 3mm thick blocks and processed overnight on a Leica Tissue Processor (LEICA TP 1050 fully enclosed vacuum tissue processor), an automated way in which to take tissue through graded alcohols and into paraffin. The tissue was then positioned and set into a paraffin wax block on a Leica Histoembedder. Blocks were stored at RT ready for use.

### *3.4.4Sectioning*

4µm sections were cut with a Leica Jung RM2155. Cut sections were floated on water (37°c) and transferred to Thermo Shandon Colourfrost Plus positively charged microscope slides. Positively charged slides are used to ensure that the tissue

remained adhered to the slide throughout the subsequent staining. The slides were dried overnight at 45°c and then stored at RT.

### *3.4.5Immunohistochemistry*

4µm sections were dewaxed in xylene and taken through graded alcohols to water. Antigen retrieval was determined according to each antibody and included no pre-treatment, vector unmasking fluid, microwave in low pH solution, microwave in high pH solution, boric acid at 65°C for 16 hours. Endogenous tissue peroxidase activity was quenched with pre-treatment of sections with v/v hydrogen peroxide (0.5-6%) in methanol for 10 minutes. Sections were then washed in PBS +0.05% tween (pH7.4). Non-specific binding was blocked with 20% normal goat serum in PBS with 1% BSA (pH7.4) or flex block for 20 minutes at room temperature. Sections were then incubated in primary antibody diluted in PBS 1% w/v BSA pH7.4 for 30 minutes at room temperature. Corresponding isotype controls (no primary antibody) were used in all experiments. After incubation with primary antibody, sections were washed in PBS +0.05% tween (pH7.4) before applying corresponding HRP linked secondary antibodies. HRP activity was detected using the chromagen DAB (Dako). Sections were counterstained with Gills haematoxylin, dehydrated through graded alcohols to xylene then mounted.

### *3.4.6Cell Culture*

#### *3.4.6.1 Isolation of microvascular endothelial cells from explanted lungs*

Tissue excess to pathology requirements was stored in DMEM prior to cell isolation. Alveolar macrophages were firstly removed by inflation of the tissue with PBS. The alveolar macrophage rich fluid which seeps out of the tissue was then discarded. The pleura and macroscopic vessels and airways were also dissected and discarded. The remaining tissue was finely chopped, washed in media and filtered through a 40µm filer to remove red blood cells. Tissue pieces were incubated in 0.2% type II collagenase (RPMI + 0.1% BSA) with gentle agitation at room temperature for 2 hours and then filtered, firstly through a large filter and secondly through a 100µm filter. The filtrate was centrifuged (250G for 5 minutes), supernatant removed and cell pellet resuspended. An automated cell count was

performed and cells plated onto 0.2% gelatin-coated flasks (10,000 cells/$cm^2$)in MV2 media (Promocell). Following 24 hours incubation, the flasks were washed in PBS to remove non-adherent cells and red blood cells. MV2 media was replaced and changed every 2-3 days.

#### *3.4.6.2 Passage of isolated microvascular endothelial cells*

At 70-80% confluence, cells were passaged using cell dissociation solution (Sigma). Cells were washed in PBS before incubation in cell dissociation solution for approximately 15 minutes at 37°. Detached cells were removed and remaining adherent cell attachment disrupted with gentle scraping. The detached cell suspension was centrifuged with the resulting pellet ready for cell separation.

#### *3.4.6.3 Preparation of UEA Dyna beads*

Dynabeads M-450 Tosylactivated (Invitrogen) were washed in 0.2M Sodium Tetraborate (pH 9.5) before being placed in the Dynal magnet (MPC-1, Invitrogen) for one minute. The wash was then discarded. After a further wash, the beads were resuspended in 1ml 0.2M Sodium Tetraborate (pH 9.5) containing 0.2mg/ml Ulex europaeus-1 lectin (UEA-1) (Sigma L5505) and incubated with gentle agitation at RT for 48 hours to allow coupling of the ligand to Dynabeads. After incubation, the bead-ligand mixture was washed, by adding 1ml of PBS containing 0.1% BSA, 2nM EDTA (pH 7.4) and was placed in the magnet for 1 minute. The wash was removed, and 2 further washes performed by resuspending beads in 1ml of PBS containing 0.1% BSA, 2nM EDTA (pH 7.4) and incubated on the roller for 5 minutes before removal of the wash by magnetic separation. After the final wash, beads were resuspended in 1ml of PBS containing 0.1% BSA, 2nM EDTA (pH 7.4) (bead concentration $4x10^8$ beads/ ml) and stored until use in separation experiments.

#### *3.4.6.4 Separation of cells*

UEA and commercially available CD31 Dynabeads (25 µl each) were washed in PBS containing 0.1% BSA, 2nM EDTA (pH 7.4). The cell pellet was then resuspended in 2ml of PBS containing 0.1% BSA, 2nM EDTA (pH 7.4) containing the beads. The cells/ beads suspension was incubated on a roller at 4°C (to reduce non-specific binding)for 20 minutes. Following incubation, a further 5ml of PBS containing 0.1%

BSA, 2nM EDTA (pH 7.4) was added and the beads/cells mixture placed in a magnet. The buffer containing cells unattached to beads was removed. The beads/cells mixture was washed as above a further four times with the bead-negative fraction removed each time. The bead positive cells were re-suspended in media and counted using a haemocytometer. Cells were plated onto 0.2% gelatin-coated flasks at 2000-3000 cells/cm2. The bead negative fraction, containing mostly fibroblasts, was at plated out similarly.

#### *3.4.6.5 Cryopreservation*

Once cells are a pure population, with no contaminating fibroblasts, cells were cryopreserved ($1x10^6$cells/ml) in MV2 media (Promocell) containing 1% DMSO (Sigma).

#### *3.4.6.6 Reanimation and Passage of cells*

Cryopreserved pulmonary microvascular cells isolated from patients in our centre or commercially available (Promocell and Lonza), were grown on sterile tissue culture flasks in complete MV2 media (Promocell) with supplemental antibiotic/ antimycotic (Invitrogen). When the cells reached 70-80% confluence, cells were washed with PBS and cell dissociation solution (Sigma) added to detach the cells. After 2-3 minutes incubation, the detached cells were removed and centrifuged. The number of cells in the resulting pellet was calculated using a haemocytometer and cells seeded at 2-5000 cells/$cm^2$.

#### *3.4.6.7 Harvesting Cells*

Media was removed and stored at -80°C to allow later analysis. Cells were washed in PBS to remove debris and then detached via gentle scraping. Flasks were washed in PBS, and the resulting cell suspension centrifuged (250G for 4 minutes). The supernatant was removed. The cell pellet was re-suspended in phosphosafe extraction buffer. Cells were sonicated to lyse the cells.

### *3.4.7Preparation of Cigarette smoke extract*

Cigarette smoke extract (CSE) was prepared according to the method published by Carp and Janoff [111]. This method has been widely used for over 30 years, with some researchers making their own modifications, and is highly cited in the literature. Briefly, the smoke of 1 Kentucky filterless research cigarette (Lot 4A1) was bubbled through 25ml endothelial MV2 media containing 5% FCS (Promocell), using a vacuum pump (Laboport), over approximately 6 minutes (to mimic the time to smoke a cigarette) to give a concentration of 100% CSE (Figure 3.1). Due to the precious nature of the cells, the resulting CSE was sterile filtered through a 0.2u filter. CSE was used to treat cells within 30 minutes of preparation. To standardise CSE as much as feasibly possible it was made on each occasion by the same operator (LSM) and when analysed on a spectrophotometer had the same absorbance. pH of CSE was also unaltered among CSE preparations and when compared with whole media.

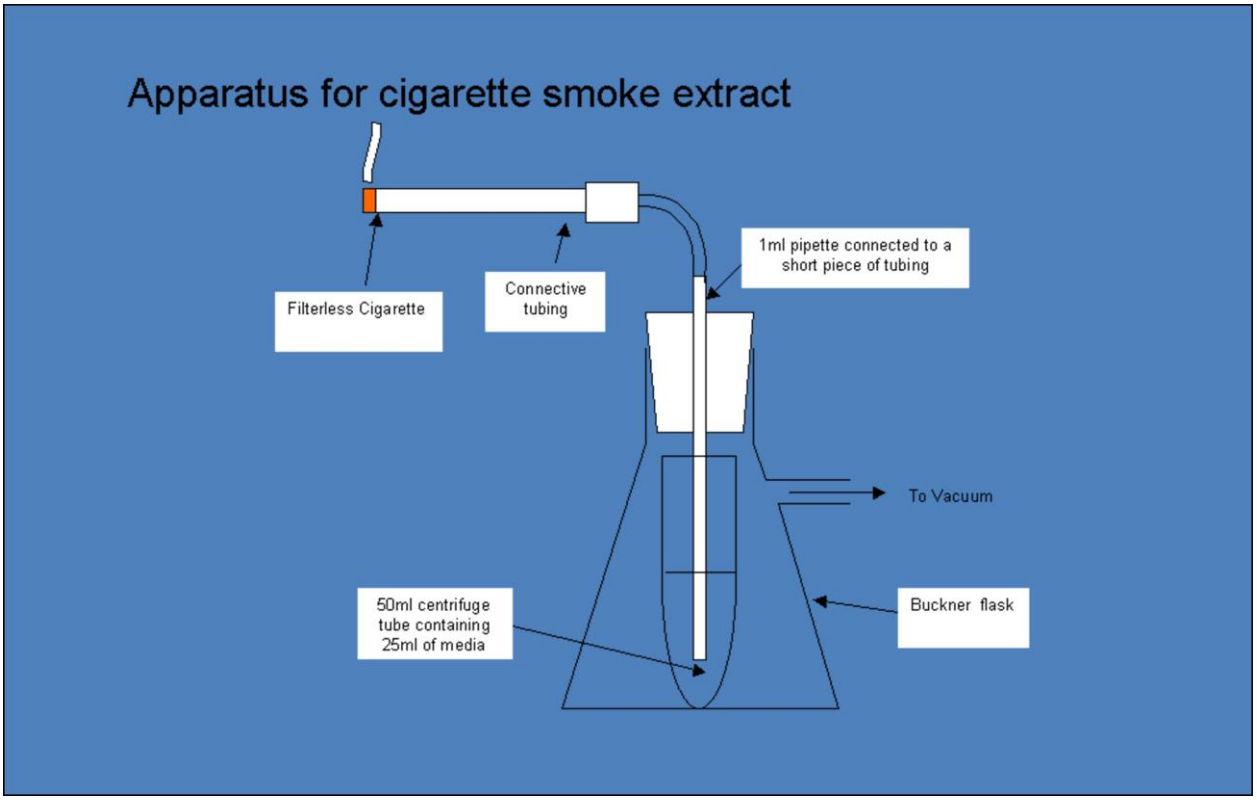


**Figure 3.1 Apparatus used to prepare cigarette smoke extract (CSE).**

### *3.4.8 Flow cytometry*

Cells were harvested using cell dissociation solution (Sigma), centrifuged and washed in PBS prior to staining. 100,000 cells/100ul were typically used for each analysis. For characterisation experiments, cells were resuspended in PBS (100ul) and volumes of cell surface markers added according to optimisation experiments. Cells and antibodies were incubated for 30 minutes at 4°C to reduce non-specific binding. Following incubation, cells were washed in 4ml PBS, centrifuged at 10,000 rpm for 5 minutes, resuspended in 200ul PBS and analysed on facs scan LSR II. For apoptosis experiments, cells were resuspended in 100ul 1x binding buffer (BD bioscience). 5ul of Annexin V and 5ul 7-AADwere added to each and incubated at RT for 15 minutes, before analysis on FACS scan. Data was analysed using Venturi software.

### *3.4.9 BCA protein assay*

A BCA protein assay was performed on all samples to ensure equal loading concentrations for western blotting. Standard dilutions of BCA (2000, 1500, 1000, 750, 500, 250 and 125ng/ml) were prepared on a 96 well plate and read on an Opsys MR microplate reader (Dynex technologies) at 570nm. A standard curve was constructed and used to determine protein concentration of unknown samples. Briefly, 80 µl of phosphosafe extraction buffer was added to 5µl of each sample. 25µl of this mixture was added in triplicate onto a 96 well plate. 200µl of BCA working reagent was added to each sample and incubated at 37°C for 30 minutes before reading at 570nm. Protein concentration was calculated according to the standard curve.

### *3.4.10 Western blotting*

Samples were prepared on ice with equal loading according to BCA protein assay. To each sample equal volume of sample buffer (laemmli buffer/ β-ME, 10%(v/v) was added to denature the protein. Samples were vortexed and heated for 5 minutes at 95°C. Samples were then loaded onto Nu-PAGE pre-cast gels (Invitrogen) together with See blue pre-stained indicator and ran in MES running buffer at 100V. Gels were transferred overnight at 20V onto PVDF membranes in 1x transfer buffer

(0.02M tris, 0.192M glycine, 10% methanol). The following day, PVDF membranes were blocked in TBS-T with 5% dried milk (marvel) for 60 minutes at room temperature. Primary antibodies were then applied in 5% marvel TBS-T overnight at 4°C. The next day, membranes were washed twice for 10 minutes in TBS-T. Corresponding secondary antibodies were applied in 5% marvel TBS-T. Following 90 minute incubation, membranes were washed three times for 10 minutes in TBS-T. Membranes were then exposed to ECL Chemiluminescence solution (50:50 concentration) (Amersham) with protein bands detected via Gel-Doc.

### *3.4.11 Confocal microscopy*

Cells were seeded onto an 18mm coverslip and treated as per each experiment. On completion of each treatment course, cells were washed in PBS and fixed with freshly prepared 4% paraformaldehyde for 30 minutes. The paraformaldehyde was removed and cells stored in PBS. For staining, the cells were quenched with 100mM glycine for 30 minutes. Cells were then permeabilised with PBS plus 1% Triton X-100 (PBST) for 30 minutes. PBST was then removed and cells washed three times in PBS. Cells were blocked with 5% BSA for 60 minutes. Primary antibodies in 5% BSA were then applied for 60 minutes at room temperature and then washed with PBS with 0.2% tween and PBS. Secondary antibodies were then applied in 5% BSA for a further 60 minutes before 3 washes in PBST and one final wash in PBS. The cells on coverslips were thereafter mounted with 4',6-diamidino-2-pheylindole (DAPI) stain and viewed on a Leica Sp2UV laser scanning confocal microscope and analysed with software from Leica (LCS 2.61).

### *3.4.12 RT-PCR*

#### *3.4.12.1 RNA isolation*

RNA was isolated using a commercially available micropreparation kit. Briefly cells were lysed a mixture of βmercaptoethanol and lysis buffer (βME0.7ul and 100ul lysis buffer per <500,000 cells). An equal volume of 70% ethanol was then added to the mixture and vortexed. DNase were then deactivated by incubating with RNase-free DNase I and DNase digestion buffer followed by a series of high and low salt buffer washes and microcentrifuge. RNA was isolated by incubation with an elution buffer

for 2 minutes at room temperature and then centrifuged. RNA concentration was determined using a nanodrop. A 2% agarose gel containing 4ul ethidium bromide was then cast and RNA samples run with loading buffer of 30% glycerol, 70% TAE (Tris-acetate-EDTA) and bromophenol blue in 1% TAE to assess quality of RNA. A trackIt (Invitrogen) DNA ladder was used to identify molecular weight. RNA was stored at -80°C until used for cDNA preparation.

#### *3.4.12.2 cDNA preparation*

cDNA was prepared from RNA using a commercially available kit. Briefly each sample was made to RNA concentration according to nanodrop, with 3ul random primers and DEPC water to a total volume of 15.7ul. This mixture was then incubated at 65°C for 5 minutes and then cooled to room temperature over approximately 10 minutes. To each sample 2ul 10X affinity script, 0.8ul dNTP mix, 0.5ul RNase block and 1ul affinity script were added. This was then incubated at 25°C for ten minutes to allow the primers to extend and then to 55°C for 60 minutes to allow the polymerase chain reaction to take place. The reaction was then terminated by increasing the temperature to 70°C for 15 minutes. cDNA was stored at -80°C until used for Q-PCR.

#### *3.4.12.3 Q-PCR*

Samples were prepared and plated onto 96 well optical plates (Applied Biosystems). Briefly, 10ul mastermix, 6.5ul RNAse free $H_2O$ and 1ul primers were added to each well. 2.5ul of cDNA (diluted according to optimisation experiments) was then added to each well. Samples were then centrifuged and ran on the PCR machine and analysed on ABI Prism 7000 SDS software. Real-time reaction products for each primer were confirmed on 2% agarose gel electrophoresis.

### *3.4.13 ELISA*

Media from control and treated cells removed at the time of harvesting was used together with commercially available ELISA kits to detect levels of Endothelin-1 (ET-1) released from treated cells. Samples and standards were added to wells pre-treated with ET-1. After incubation, samples were washed. HRP labelled monoclonal antibody to ET-1 was then added and incubated prior to further washing

to remove unbound antibody. TMB substrate solution was then added which generates a blue colour when catalysed by HRP. Stop solution (1N solution hydrochloric acid in water) was thereafter added with the resulting yellow read at 450nm. The amount of signal detected was directly proportional to the level of ET-1 and so a standard curve was constructed from which the concentration of ET-1 within the samples (unknowns) could be determined.

### *3.4.14 Statistical Analysis*

Much of the work presented in this thesis is exploratory. Statistical analysis was performed where appropriate and is reported in figures and text. Excel and Graph Pad Prism were used for all statistical analyses. Where the data was found to be parametric t-tests or ANOVA (for multiple comparisons) were performed. For non-parametric data, Mann Whitney U-tests were performed. Statistical significance was taken as $p<0.05$.

# *Chapter 4: Endothelial Cell isolation and Characterisation*

## *4.1 Abstract*

The Pulmonary microvasculature plays an important role in the maintenance of lung homeostasis via its response to injury and role in repair. Animal models, immortalised cell lines, primary cells isolated from large pulmonary arteries and human umbilical vein endothelial cells (HUVECs) have all been used to model the human microvasculature but each have limitations as to how truly they reflect *in vivo* conditions. Commercially available human pulmonary microvascular cells have overcome many of these limitations, however the ability to study disease mechanisms in cells isolated from individuals with the disease in question, whose cells have been exposed to the milieu associated with disease, may mimic *in vivo* conditions more accurately. Observing how these cells respond to injury may provide valuable insights into disease pathogenesis. I therefore attempted to isolate pulmonary microvascular endothelial cells from individuals undergoing lung transplantation for severe end stage emphysema. Cells were also isolated from excess normal tissue from patients undergoing lobectomy for cancer to act as controls.

**Methods:** Following informed consent, a lobe or part of lobe was dissected at the time of surgery. The pleura, large airways and large blood vessels were removed and contaminating macrophages and neutrophils flushed from the peripheral lung tissue before digestion with collagenase. This cell mixture was then cultured until colonies of cells were present. Endothelial cells were purified from the cell mixture via selection with CD31 and UEA-1 magnetic beads and characterised by confocal microscopy and flow cytometry.

**Results**: Successful isolation was achieved from 10 (71%) of 14 emphysematous lungs. Endothelial cells exhibited a classical cobblestone morphology with high expression of endothelial cell markers (CD31) and low expression of mesenchymal markers (CD90, αSMA and fibronectin). E-selectin (CD62E), which is reported to be absent on quiescent microvascular endothelial cells but inducible on intraacinar arterioles and venules upon stimulation, was observed in a proportion of the isolated

CD31 positive cells following stimulation with TNFα, confirming that these cells were of microvascular origin.

**Conclusions:** Susceptible human pulmonary microvascular cells from severely emphysematous lungs can be isolated with high yields. Characterisation confirms these to be of high purity. These cells provide a valuable research tool to investigate cellular mechanisms in the pulmonary microvasculature relevant to the pathogenesis of emphysema.

## *4.2 Introduction*

The pulmonary microvasculature, which comprises the luminal barrier of intra-acinar arterioles and venules and the alveolar capillary network, plays an important role in lung tissue homeostasis in health and disease [50][115]. Lung endothelial cell injury is hypothesised to be a key event in the pathogenesis of emphysema [116] and forms the increasingly credible “microvascular hypothesis” as an alternative to the classical hypothesis in which inflammatory cells are seen as the orchestrators of tissue destruction [117].

Early cellular studies exploring the pulmonary circulation tended to use large vessel endothelial cells, typically from the main pulmonary trunk, and HUVECs (human umbilical vein endothelial cells) as a surrogate for the lung microvasculature [118]. However, wide heterogeneity exists between endothelial cells isolated from different organs and between endothelial cells isolated from different vascular beds within organs [119]–[121]. The vascular bed of the lung is perhaps the best example of this heterogeneity, due to its numerous branching arteries, arterioles, capillaries and venules, which unlike the systemic circulation are exposed to low pressure and high flow. The resulting large surface area has important metabolic functions that may contribute to disease when disordered [119]. Such complexity may explain differing results found between *ex vivo* models and the difficulties when trying to translate research into clinical practice. The ability to study the disease in cells isolated from tissue from individuals in whom the disease has developed has been largely overlooked, instead relying on more readily available models and simply acknowledging the limitations of each.

Immortalised cell lines are a widely used model in cell biology. Originally derived from embryos and cancer tissue, cell lines can be used to high passage due to clonality of the cells, which escape the normal controls within the cell cycle [122]. Such a model has the advantage that they provide a stable cell population that does not have a finite lifespan, however they do not always express markers characteristic of the tissue in which they originated[123][124] and their responses *in vivo* are

unlikely to reflect the true response of cells to injury[125][126], thus limiting their use. Microvascular endothelial cells (MVECs) isolated from animals are an alternative model. MVECs have been isolated from bovine [127], ovine [128], and rodent lungs [121]. These animal cell models have the advantage that are provide an important way in which cellular response to injury and disease mechanisms can be studied, however these may not reflect the true *in vivo* response in humans. Such studies have however provided valuable insights into the responses of rat lung microvascular endothelial cells to injury and also have afforded the development of methods to effectively isolate lung microvascular cells [129][130][131][121]. The development of successful isolation techniques has then allowed these to then be applied to isolation of human LMVECs.

The emergence of commercially available primary cells in recent years has provided an alternative way in which to study cellular responses *ex vivo* [120]. While these cells are fully compliant with regulatory legislation, with information given regarding the patient age and in some cases smoking status, there exists no way in which to clarify whether the individuals from which these cells were isolated had normal pulmonary function or indeed whether they had evidence of respiratory disease. Therefore, the ability to isolate and compare cells from individuals characterised to be free from respiratory disease and from those who have developed severe disease is attractive. Furthermore, the observation that only 20% of individuals who smoke develop emphysema [1] supports the view in this disease that it is an individual's disordered cellular response to injury rather than the injury per se that leads to pathology. The study of disease in cells isolated from individuals in whom the disease has developed therefore has clear relevance. The demonstration that emphysema is not simply a disease of "loss of lung tissue" and rather a disease in which there is active response to injury and attempts at repair [25], adds further weight to the goal of isolating cells from individuals in whom the disease has developed and may provide valuable insights into the pathogenesis of emphysema. By comparing how these susceptible cells behave in contrast to cells isolated from individuals free from COPD may provide unique insights into the cellular responses to cigarette smoke which lead to COPD.

I therefore attempted to isolate human pulmonary microvascular endothelial cells (HPMVECs) from patients with severe end stage lung disease undergoing lung transplantation, obtaining clinical details such as lung function and smoking history to contextualise samples. This approach allowed both the isolation of cells from well characterised patients with advanced diseases such as emphysema and pulmonary arterial hypertension (using tissue obtained at lung transplantation). In addition, cells were isolated using the same method from healthy individuals with normal lung function without COPD (using excess tissue removed at lobectomy for lung cancer). All isolated cells were characterised and compared with normal LMVECs, using immunocytochemistry to confirm the cells were endothelial, uncontaminated by mesenchymal cells and of microvascular pedigree.

## *4.3 Subjects*

Ethical approval for the isolation and study of diseased cells was submitted and approved by the Northumberland Local Ethics and Research Committee in January 2007 (REC reference 06/Q0902/57). All patients awaiting lung transplantation at Freeman Hospital were invited to take part in the study. Patients gave informed consent to donate their explanted lung for research purposes outlined in the study. The study was performed in accordance with ICH-GCP. Study patient information leaflet and consent form appear in Appendix 1.

Ethical approval to obtain normal tissue from patients undergoing lobectomy/ pneumonectomy was given by County Durham and Tees Valley 2 Research Ethics Committee in July 2009 (REC reference 09/H0908/35). Patients were identified according to the protocol (Appendix 2) with subjects excluded should they have evidence of emphysema/ fibrosis on radiology or pulmonary function testing. The study was performed in accordance with ICH-GCP. Study protocol, patient information leaflet and consent form appear in Appendix 2.

Clinical data such as primary diagnosis, age, body mass index, arterial oxygenation (PaO2) and pulmonary function tests were obtained from each individual who donated tissue. Smoking status and smoking history from each patient was also obtained. Those with emphysema were also categorised according to the updated GOLD criteria (2003) [113], [114].

## 4.4 Methods

### 4.4.1 Obtaining diseased lung tissue

At the time of transplantation, the lung was inspected to confirm the macroscopic pathology was in keeping with pre-operative diagnosis and to exclude any unexpected pathology. A lobe/part of lobe was then dissected and stored at 4°C until clinical pathology assessment (which was performed within 24 hours). Following routine clinical pathology, blocks of tissue were placed in neutral buffered formalin for fixation for histology experiments. The remaining tissue (typically around 50g) was used immediately for cell isolation.

### 4.4.2 Obtaining normal tissue

The operating surgeon performing lobectomy for suspected lung cancer identified a wedge of normal tissue within the tissue removed at surgery but discrete from the tumour resection margins. This was stapled off from the remaining tissue and tumour and placed in media. Both samples were transported to clinical pathology where the wedge sample was inspected and once confirmed to be free from disease, was used immediately for cell isolation. Tissue samples ranged from 5-30g.

### 4.4.3 Cell isolation

Contaminating alveolar macrophages were firstly removed via repeated inflation of the tissue with sterile PBS. The pleura, visible arterioles, bronchioles and venules were then dissected to prevent overgrowth with mesothelial and epithelial cells and prevent contamination with macrovascular endothelial cells. The remaining tissue was washed in RMPI containing 10% FCS and 1% PSA and finely chopped (1-2mm$^2$ pieces). The tissue pieces were then washed through a 40µm filter to remove red blood cells before incubation with 0.2% type II collagenase (Worthington) in RPMI containing 0.1% BSA for 2 hours at room temperature. Following incubation, the suspension was filtered through a 400-500µm mesh and then a 100µm sterile filter. The filtrate was centrifuged (250*g* for 5 minutes). The supernatant was discarded and resulting cell pellet re-suspended in endothelial growth MV2 media (Promocell) containing 1% PSA. An automated cell count was performed and cells plated onto

flasks pre-coated with 0.2% gelatin (w/v in MilliQ water, coated for 30min at room temperature, excess gelatin solution was removed before cell addition) at approximately 10,000 cells/$cm^2$. Cells were cultured at 37˚C in the presence of 5% CO2. Non-adherent cells were removed after 24 hours in culture by gentle flushing with PBS over the flasks. MV2 media was replaced every 3-4 days until the cells reach confluence.

### *4.4.4 Endothelial cell purification*

When the cells reached approximately 80% confluence, they were passaged using cell dissociation solution (Sigma) and separated from any contaminating fibroblast and epithelial cells using CD31 Dynal beads (Invitrogen) and pre-prepared Ulex europaeus agglutinin-1 (UEA-1) coated Dynal beads. UEA-1 binds to the α-L-Fucosyl residues of glycoprotein present on the surface of human microvascular endothelial cells, thus in conjugation with magnetic beads allows the selection of endothelial cells from a mixed cell suspension [132]. The cells were re-suspended in PBS containing 0.1% BSA and 2mM EDTA (Dynal Buffer) and 25ul each of CD31 Dynal beads and UEA-1 coated beads were added. The cells/beads mixture was incubated on a rocker at 4˚C for 20 minutes, to minimise non-specific binding. The beads were then washed in Dynal buffer and placed in a Dynal magnet. The bead negative fluid was discarded. After repeated washing and magnetic separation, the bead positive cells were counted and plated on 0.2% gelatin coated tissue culture flasks at approximately 3,000 cells/$cm^2$ and incubated at 37˚C in the presence of 5% $CO_2$. Bead separation was performed over 3-5 passages of the cells until pure cobblestone cultures were obtained.

### *4.4.5 Cryopreservation of cells*

When cultures appeared free from contaminating cells, cells were cryopreserved in MV2 media (Promocell) containing 1% DMSO (Sigma). All emphysema cultures were cryopreserved and then later reanimated for characterisation and explorative experiments.

### *4.4.6 Commercial Human Pulmonary Microvascular Endothelial cells*

Commercial HLMVECs were purchased from Promocell (C12281) and cultured after reanimation at 37 ˚C with 5% $CO_2$ using endothelial growth MV2 media (Promocell) supplemented with 1% PSA (as used with cells isolated from patients).

### *4.4.7 Mycoplasma testing*

All isolated cells and commercial cells were routinely tested for mycoplasma infection using Myco Alert kits (LT07-218, Lonza). Testing was carried out on all isolated cells prior to experimentation and on commercial cells on a monthly basis. The cells showed no evidence of mycoplasma infection.

### *4.4.8 Phase contrast Microscopy*

Cells were grown to confluence and images taken on canon image shot.

### *4.4.9 Confocal microscopy*

Cells were cultured on 18mm glass coverslips in 12 well plates. At confluence, cells were washed in PBS and fixed in freshly prepared paraformaldehyde (4%). Following fixation, cells were quenched in 100mM glycine for 30 minutes, before permeabilisation in PBS Triton X-100 (1%v/v) for 20 minutes. Following permeabilisation, cells were washed with PBS containing 0.2% tween (0.2% PBST) and PBS. After blocking with 5% BSA for 60 minutes, coverslips were incubatedwith primary antibodies (CD31 (Sc53411, Santa Cruz) Fibronectin (F3648, Sigma), αSMA, (F3777, Sigma) in 0.5% BSA overnight at 4˚C. Cells were then washed as before with 0.2% PBST and PBS. Fluorochrome pre-conjugated secondary antibodies (FITC: Mouse (F2012) and TRITC: Rabbit (T6778), Sigma) were then applied (0.5% BSA) for 60 minutes and then washed in 0.2% PBST and PBS. The cells were then mounted with DAPI mounting medium (H-1200, Vector Labs) and viewed on a Leica Sp2UV laser scanning confocal microscope and analysed with software from Leica (LCS 2.61).

### *4.4.10 Flow cytometry*

Initial experiments to determine optimal concentrations of antibodies were conducted using microvascular endothelial cells purchased from Promocell. Each cell population was stained using the same conditions.

#### *CD31/CD90 characterisation*

Cells at 70-80% confluence were used in all characterisation experiments. Cells were harvested using cell dissociation solution (Sigma) with approximately 100,000 cells per 100ul used for each stain. Cells were washed and re-suspended in 100ul PBS and incubated with FITC conjugated CD31 (#555445 BD Bioscience) and PE cy5 conjugated CD90 (# 555597 BD Bioscience) for 30 minutes at 4°C, to reduce non-specific binding. Cells were then washed in PBS, centrifuged at 250*g* for 4 minutes, re-suspended in 200ul PBS and analysed on FACS Scan (Becton Dickinson).

#### *CD62E characterisation*

Cells were grown in 6 well plates and at 70-80% confluence were treated with TNFα (1ng/ml). Following treatment cells were harvested using cell dissociation solution with approximately 100,000 cells per 100ul used for each stain. Cells were washed and re-suspended in 100ul PBS and incubated with APC conjugated CD62E (E-selectin) (#551144 BD Bioscience) for 30 minutes at 4°C, to reduce non-specific binding. Cells were then washed in PBS, centrifuged at 250g for 4 minutes, re-suspended in 200ul PBS and analysed on FACS Scan.

## *4.5 Results*

Cell isolation was attempted from 17 patients (11 emphysema, 3 alpha-one anti-trypsin related emphysema, 2 normal, 1 pulmonary arterial hypertension) and was successful from10 (71%) of 14 emphysematous lungs. Table 3 shows the baseline characteristics and clinical data from the 17 individuals in whom cell isolation was attempted. In addition to diagnosis, smoking history, PaO2 and spirometry measures were included where available. Those patients with emphysema was categorised according to disease severity based upon the GOLD classification[3]. Cell yield from successful cultures is documented.

## Table 2: Patient demographics and cell yield

| Patient No: | Gender | Diagnosis | Age | BMI | Smoking History (Pack yrs.) | FEV1 (%) | TLC (%) | KCO (%) | GOLD stage | Cell Yield (passage number at cryopreservation) |
|---|---|---|---|---|---|---|---|---|---|---|
| **1** | M | A1AT emphysema | 46 | 28.7 | 15 | 18 | 133 | 15 | IV | 1.9 x$10^6$ cells (passage 4) |
| **2** | F | Emphysema | 54 | 21.5 | 30 | 10 | 178 | - | IV | 2.5 x$10^6$ cells (passage 4) |
| **3** | F | Emphysema | 53 | 20.9 | 30 | 22 | 131 | 32 | IV | 9.4 x$10^6$ cells (passage 5)<br>5.4 x$10^6$ cells (passage 4) |
| **4** | F | Emphysema | 51 | 20.8 | 30 | 28 | 150 | 33 | IV | 5.6 x$10^6$ cells (passage 4)<br>28.8x$10^6$ cells (passage 5) |
| **5** | F | Emphysema | 46 | 20.2 | 20 | 21 | 150 | 43 | IV | Unsuccessful |
| **6** | M | Emphysema | 58 | 22.7 | 35 | 15 | 130 | 46 | IV | Unsuccessful |
| **7** | F | Emphysema | 59 | 21.8 | 25 | 34 | 155 | 38 | III | 12x$10^6$ cells (passage 4) |
| **8** | M | Emphysema | 44 | 23 | 15 | 14 | 138 | 69 | IV | 3.2 x$10^6$ cells (passage 4)<br>21.5x$10^6$ cells (passage 6) |
| **9** | F | Emphysema | 60 | 28.3 | 20 | 26 | 95 | 25 | IV | 5.2x$10^6$ cells (passage 6) |
| **10** | M | Emphysema | 45 | 21.3 | 27 | 26 | 156 | 42 | IV | 5.4x$10^6$ cells (passage 4) |
| **11** | M | Emphysema | 55 | 20.8 | 55 | 17 | 130 | 24 | IV | Unsuccessful |
| **12** | F | A1AT emphysema | 40 | 26.1 | 25 | 16 | 136 | 33 | IV | 18.2x$10^6$ cells (passage 6) |
| **13** | M | Emphysema | 47 | 22.3 | 30 | 17 | 150 | 42 | IV | 13.9x$10^6$ cells (passage 4) |
| **14** | M | A1AT emphysema | 52 | 21.2 | 15 | 22 | 127 | 71 | IV | Unsuccessful |
| **15** | F | Normal | 68 | - | 15 | 104 | - | - | N/A | 1x$10^6$ cells (passage 3) |
| **16** | F | Normal | 65 | - | 40 | 80 | - | - | N/A | Unsuccessful |
| **17** | F | IPAH | 60 | 26.4 | 0 | 83 | 107 | 109 | N/A | 10x106 cells (passage 3) |

### *4.5.1 Phase contrast microscopy*

Prior to the first passage, cells in culture were a mixed population of elongated cells and cobblestone cells together with red blood cells. Following the initial bead separation, at the first passage, the bead positive fraction of cells displayed cobblestone morphology and grew in a monolayer in colonies (Figure 4.1A). Small beads could also be seen attached to many of the cobblestone cells. In contrast, the bead negative fraction (Figure 4.1B) consisted of elongated spindle cells which grew in sheets, becoming confluent more quickly. At the first passage there were areas in which a mixed population of cells was still present (Figure 4.1C) with some elongated cells growing together with cobblestone cells. For this reason, repeated bead separation was performed until cultures contained only cobblestone cells.

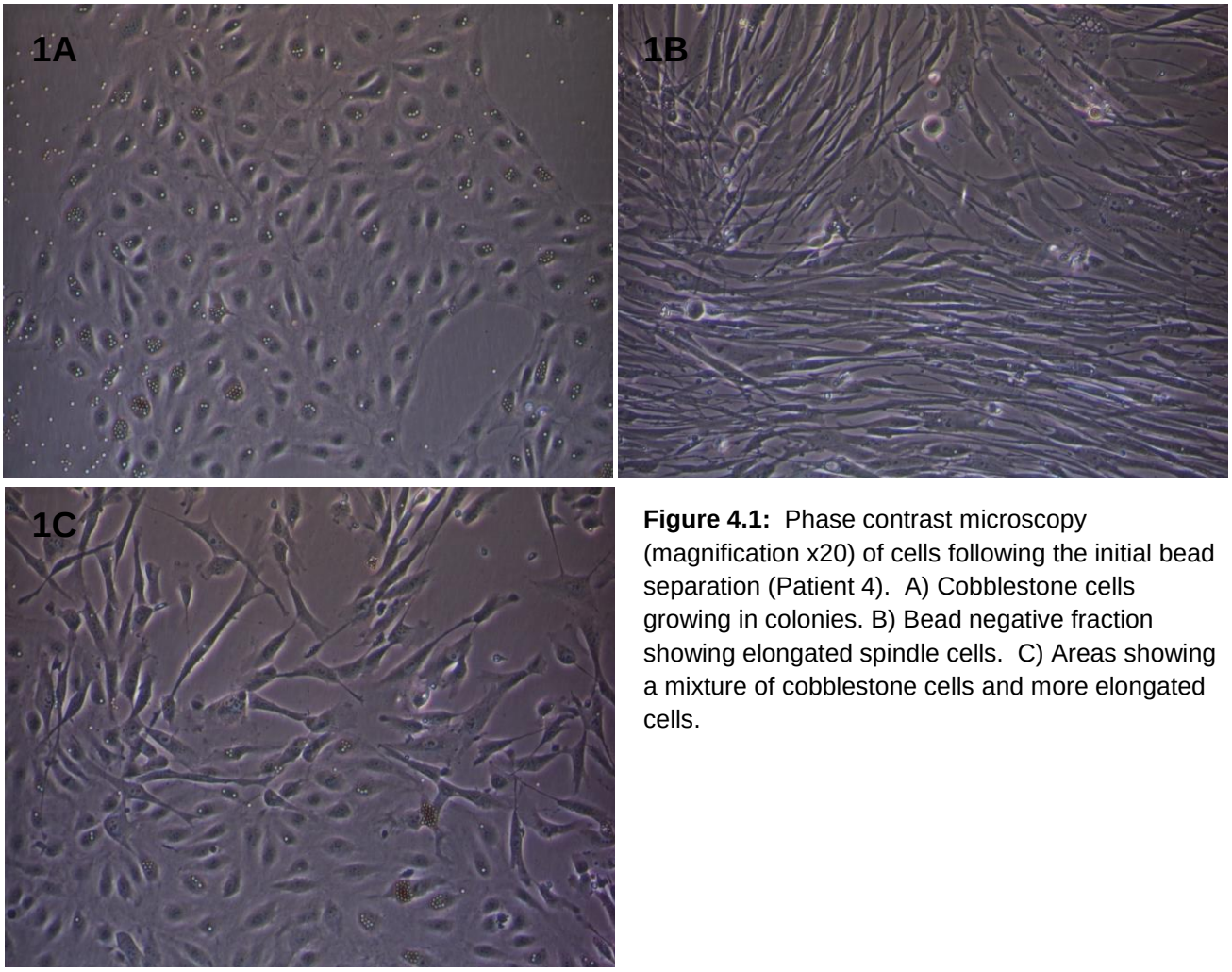


**Figure 4.1:** Phase contrast microscopy (magnification x20) of cells following the initial bead separation (Patient 4). A) Cobblestone cells growing in colonies. B) Bead negative fraction showing elongated spindle cells. C) Areas showing a mixture of cobblestone cells and more elongated cells.

### *4.5.2 Characterisation of cells via confocal microscopy*

Around passages 4-6, when cultures appeared free from contaminating spindle cells on phase contrast microscopy, cells were plated onto glass coverslips and immunocytochemistry performed with images taken via confocal microscopy. Figure 4.2 shows representative images for (a) commercially available LMVECs (Promocell), the standard to which we controlled our isolated cells, b) LMVECs isolated from a patient with emphysema (patient 8), (c) LMVECs isolated from excess normal tissue (patient 15) and contrasted with (d) the bead negative fraction from excess normal tissue (patient 15). Cells stained positively for the endothelial cell surface marker CD31 (FITC green) (Figure 4.2 a-c). Cells displayed contact inhibition with the formation of a lattice of tight junctions. The bead negative cells showed no CD31 staining (Figure 4.2d). The mesenchymal marker alpha smooth muscle actin (αSMA) (TRITC red) was absent on CD31 positive cells (Figure 4.2 a-c) but was present on the CD31 negative fraction (Figure 4.2d) in an elongated spindle shaped pattern (red). CD31 positive cells (Figure 4.2 a-c) also had very low levels of the intracellular matrix protein fibronectin, in contrast to CD31 negative cells (Figure 4.2d) which demonstrated high staining (red) in sheet like form.

## *Figure 4.2: Confocal Microscopy characterisation of cells*

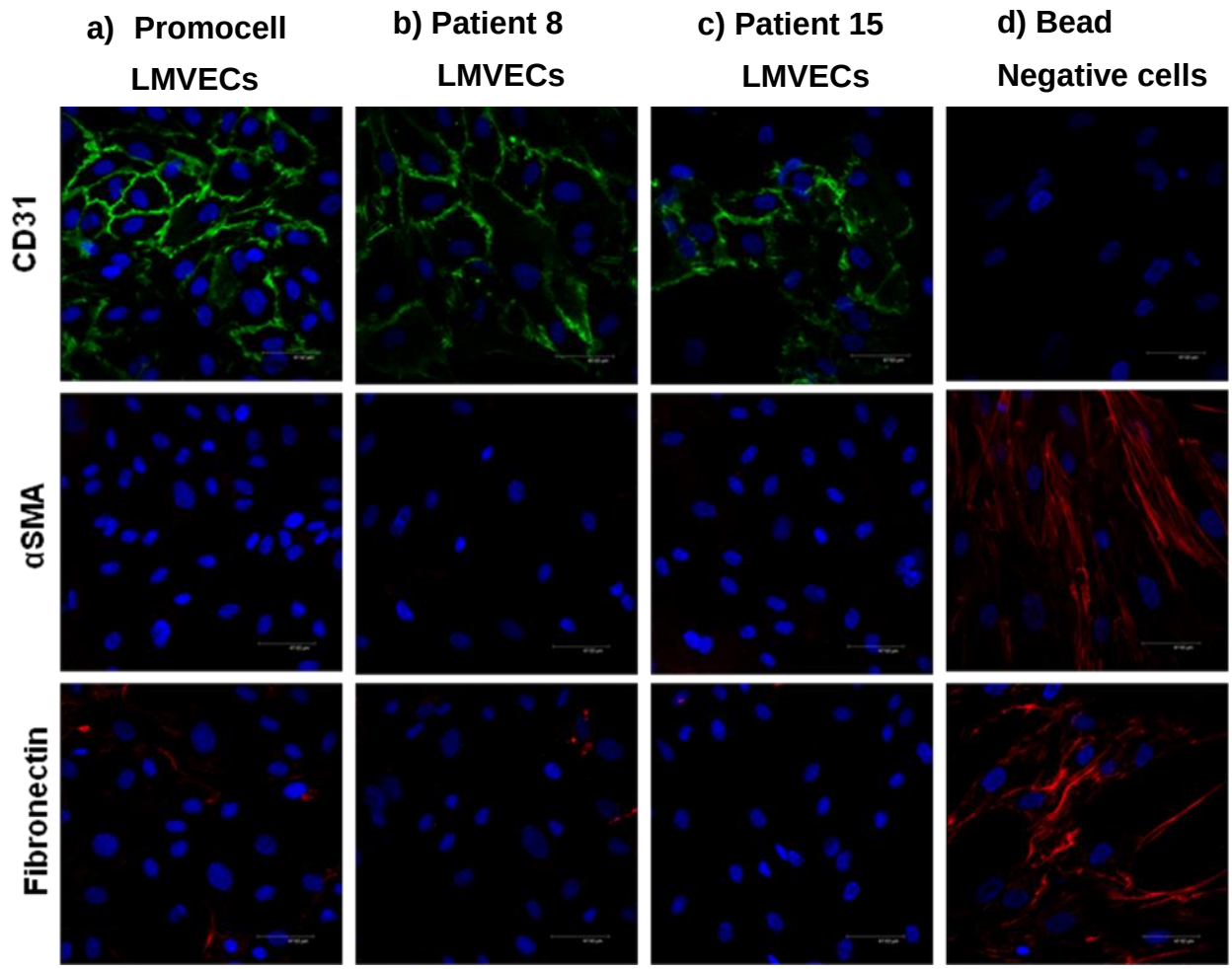


**Figure 4.2:** Detection of immunocytochemical markers via confocal microscopy (CD31: FITC green, aSMA: TRITC red, DAPI: blue). (a) LMVECs (Promocell) were compared to (b) LMVECs isolated from patient 8 with emphysema and (c) _LMVECs isolated from excess normal tissue (patient 15). Cellular expression on these cells was compared with that of the (d) bead negative fraction from excess normal tissue. All images were taken at X 63 magnification.

### *4.5.3 Flow cytometry*

LMVECs (Promocell) and dermal fibroblasts (gifted by ICM, Newcastle) were used to determine the optimal concentrations of each antibody (CD90 and CD31) required for flow cytometry characterisation experiments (Figure 4.3a-e). Once concentrations for each antibody alone were determined, a second set of experiments were conducted to determine the optimal concentration of CD31 (1ul) and CD90 (0.5ul) to separate a mixed population of HLMVECs and fibroblasts (Figure 4.3f). Following these preliminary experiments, cells from 5 patients with emphysema and a normal donor were characterised using the established protocol. The cell populations isolated from all donors were characterised by high expression of CD31 and low expression of CD90 (Figure 4.4). Cells from the normal donor (patient 15) were characterised at passage 2, as evidenced by the slightly lower number of CD31 positive cells (78%).

CD62E (E-Selectin) expression on isolated CD31 positive cells at baseline and after stimulation with TNFα was also investigated. CD62E is a cell surface adhesion molecule involved in leukocyte trafficking that is absent on microvascular endothelial cells but is inducible upon cytokine stimulation [133]. Capillaries do not express CD62E at baseline or upon activation. I therefore hypothesised that the isolated CD31 positive cells would be CD62E negative at baseline and that a proportion representing microvascular cells excluding capillaries would become CD62E positive upon stimulation while a second subpopulation representing the capillaries would remain CD62E negative. LMVECs (Promocell) were first investigated to determine the concentration of TNFα, CD62 antibody and appropriate time course required. Approximately 40-50% cells stained positively for CD62E at a low concentration of TNFα (1ng/ml) after 1 hour and 24 hours, across a range of antibody concentration (2.5ul-10ul) (Figure 4.5). A similar percentage of cells were positive for CD62E with higher concentrations of TNFα(2-8ng/ml) (figure 4.6). CD31 positive cells from 3 patients with emphysema were selected at random and thereafter stimulated with 1ng/ml TNFα for 1 hour and stained for CD62E to investigate whether these cells were microvascular in origin. The emphysema cells demonstrated minimal baseline

CD62E expression (<5%) with a rightward shift in response to TNFα stimulation at 1 hour with approximately 30% cells staining positively for CD62E (Figure 4.7). Cells from one emphysema donor (patient 8) were used to further investigate CD62E expression on these isolated cells at further time points (2, 4 and 8 hours) (Figure 4.8). There was similar induction of CD62E expression that became maximal at 8 hours and then fell at 24 hours to levels similar to previous experiments. Due to the precious nature of these cells, this time course was not repeated in multiple donors, as having demonstrated that the CD31 positive cells isolated were negative at baseline for CD62E but inducible in a proportion of cells, I had confirmed these to be of microvascular origin.

.

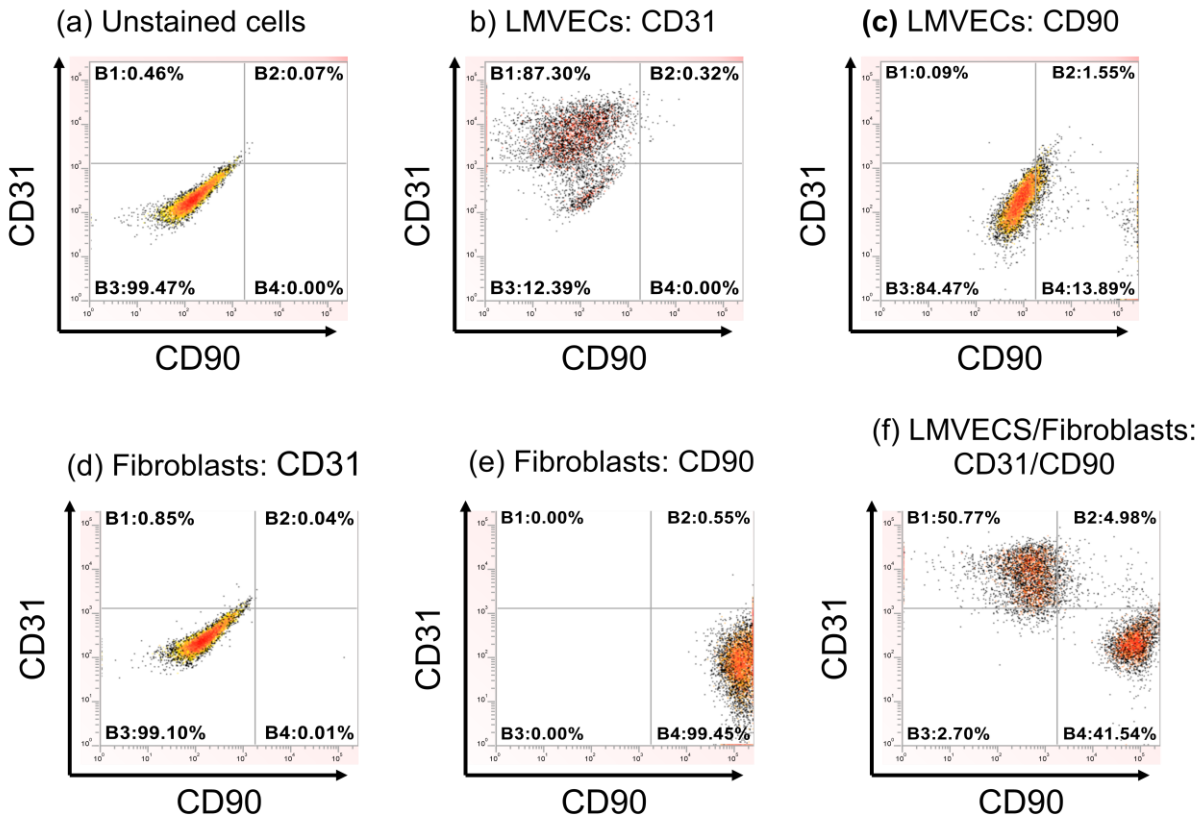


**Figure 4.3:** Representative flow cytometry scatter plots showing CD31 (FITC) and CD90 (PE cy5). Figure 4.3(a) shows scatter plot of unstained mixed cell population, LMVECs (Promocell) and fibroblasts. Figure 4.3(b) Endothelial cells stain positively for CD31 and 4.3(c) negatively for CD90. Figure 4.3(d) Fibroblasts stain negatively for CD31 but (e) strongly positive for CD90. Figure 4.3(f) Mixed Endothelial cells and fibroblasts show separation of the cell populations.

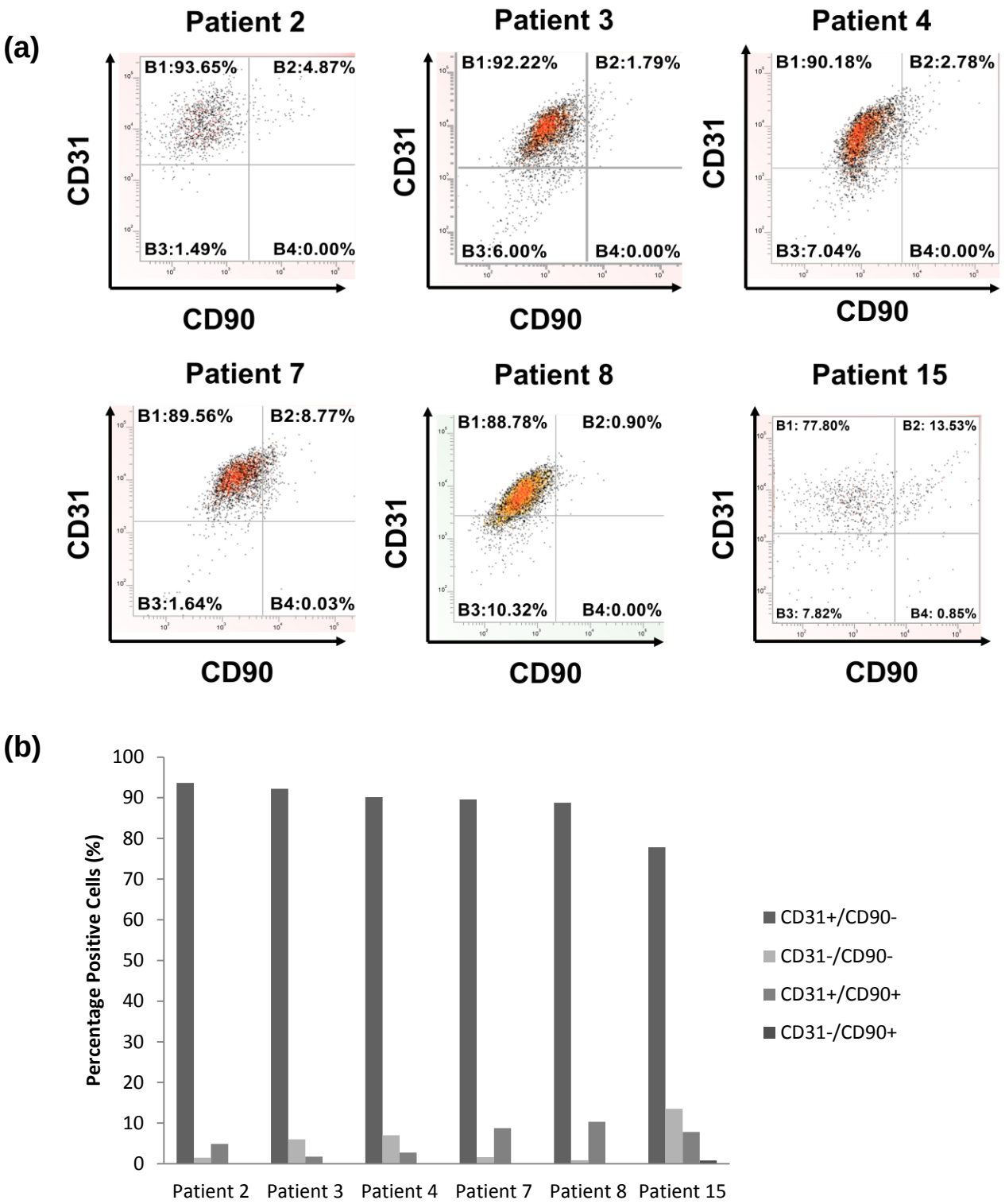


**Figure 4.4:** (a) Representative scatter plots depicting CD31 (FITC):CD90 (PEcy5) characterisation of cells isolated from patients 2,3,4,7 and 8 with emphysema and patient 15 (normal) via flow cytometry. Scatter plots show a single cell population positive for CD31 and negative for CD90 confirming these to be of endothelial origin. (b) Summary chart showing high percentage of CD31+/CD90- cells, with small number of cells negative for both markers (CD31-/CD90-). There was also a small percentage positive for both markers (CD31+/CD90+)using the gating of forward scatter and side scatter, however there were no cells which were significantly CD90+ when compared with staining on fibroblasts (Figure 4.3(e)).

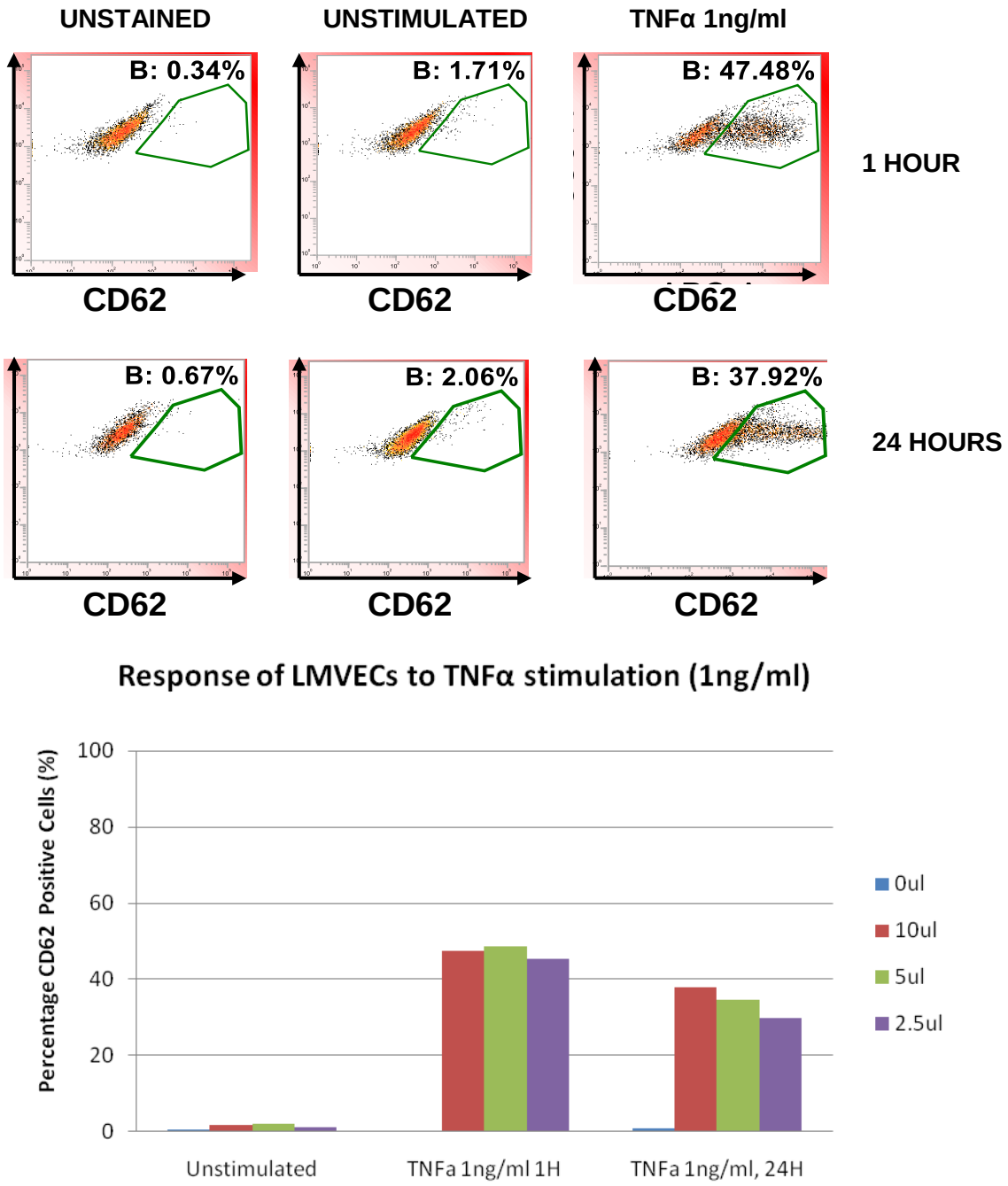


**Figure 4.5:** Representative flow cytometry scatter plots showing the response of LMVECs (Promocell) to TNFα (1ng/ml) stimulation at 1 and 24 hours as detected by differing concentration of CD62E antibody (2.5-10ul). Approximately 40-50% cells stained positively for CD62E at a low concentration of TNFα (1ng/ml) for 1 hour and 24 hours, across a range of antibody concentration (2.5ul-10ul). Due to the precious nature of these cells the data represented reflects n=1.

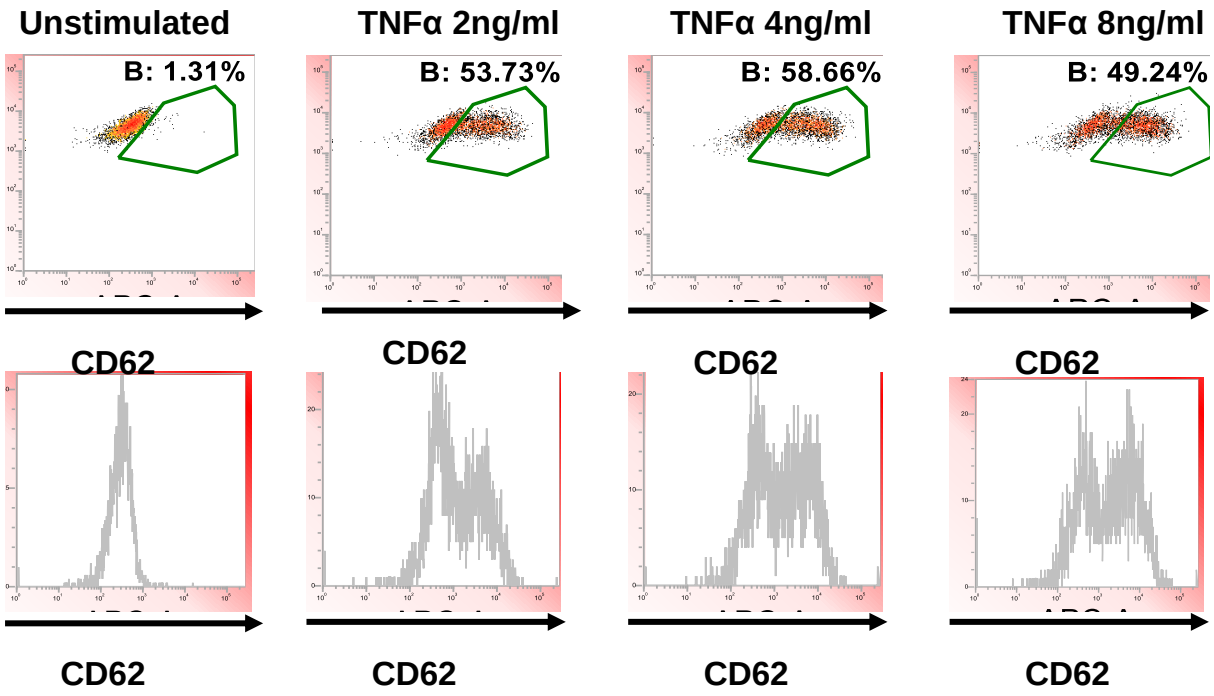


**Figure 4.6:** Representative scatter plots and histograms for LMVECs (Promocell) in response to stimulation with increasing concentration of TNFα (0-8ng/ml). A similar percentage of cells (~50%) were positive for CD62E following stimulation with higher concentrations of TNFα (2-8ng/ml).

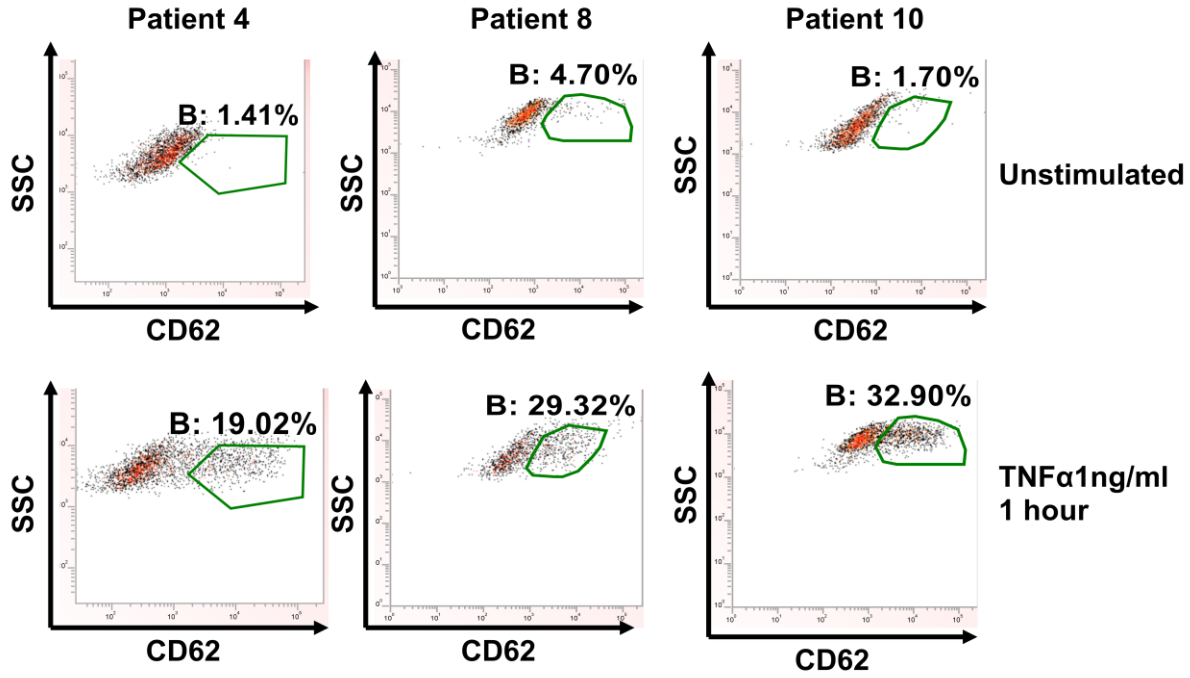


**Figure 4.7:** Representative scatter plots showing the response of microvascular endothelial cells from patients 4, 8, 10 with emphysema to TNFα (1ng/ml) stimulation for 1 hour as measured via CD62E immunostaining via flow cytometry. The emphysema cells demonstrated minimal baseline CD62E expression (<5%) with a rightward shift in response to TNFα stimulation at 1 hour with approximately 30% cells staining positively for CD62E

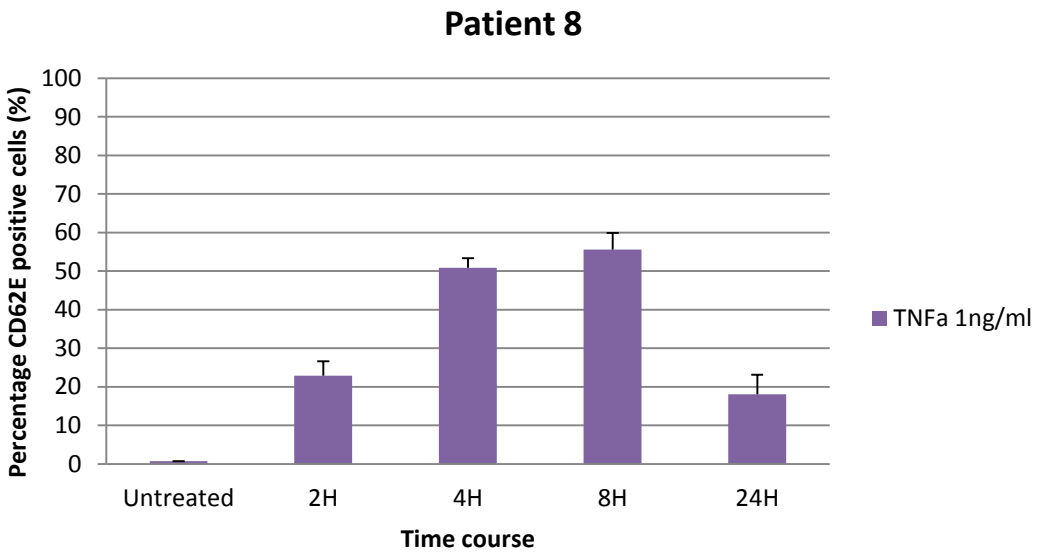


**Figure 4.8:** Percentage CD62E positive cells (patient 8) determined via flow cytometry (Mean +/- SD; n=3) following treatment with TNFα (1ng/ml). Untreated cells did not express CD62E. The percentage of treated cells that expressed CD62E was maximal at 8 hours before falling at 24 hours. The profile observed is most likely the result of TNFα induced transcriptional induction at early time points and cleavage of CD62E from the cell surface at 24 hours.

## *4.6 Discussion*

Microvascular endothelial cells have been isolated previously from a variety of tissues including human lung, however this is the first report of the ability to isolate these cells from emphysema lung tissue. This method allows *ex vivo* study of a cell population which may be key in the pathogenesis of emphysema. Importantly, this method allows the isolation and culture of large numbers of human LMVECs (Table 1) with a high success rate (71%). The isolated cells were successfully expanded following purification prior to cryopreservation and later re-animated for use in studies. All cells used in these experiments had been cryopreserved and later reanimated apart from cells from patient 15 (normal) which were used at passage 2 and had not been cryopreserved. The data presented include cells between passage 2 and 7, thus confirming that cells showed stability of phenotype.

Certain steps were critical to the success of this method. The tissue could be stored for up to 24 hours from the time of transplant until histopathological processing, however once processing began, cell isolation had to follow immediately otherwise it was unsuccessful. Careful dissection of the large vessels and removal of pleura to prevent overgrowth by contaminating mesothelial cells was also vital. Daily observation of cell numbers and doubling time was also required in order to determine the optimal time for bead separation as time between each passage differed between donors and did not appear related to passage number or disease severity.

Endothelial cell extraction employed bead separation with magnetic dynal beads for CD31 (endothelial cell surface marker) and UEA-1 (an endothelial based lectin). Other researchers have previously reported difficulties when using CD31 dynal beads, hypothesising that disruption of cell surface CD31 by beads inhibited the cell to cell interactions required for successful growth in culture [133]. I did not encounter such problems, although doubling time immediately post bead separation was more prolonged.

By passage 3-5, cells appeared free from contaminating spindle shaped cells (mesenchymal cells and fibroblasts) and were characterised according to a standard protocol developed using commercially available cells. The commercially available cells were used both to set a standard against which the cells isolated could be characterised and to ensure the precious isolated cells were not used for preliminary optimisation of dose and time characterisation experiments. Comparing the cells isolated from patients with emphysema to those isolated from lung resection operations and commercially available cells provided a further control.

The immunocytochemical detection of cell surface markers via confocal microscopy confirmed the isolated cells were endothelial, staining positively for the endothelial marker CD31 with weak/absent staining for mesenchymal markers. This was further confirmed by flow cytometry, with cells staining positively for the endothelial cell marker CD31 and negatively for the fibroblast marker CD90. These approaches proved very cell efficient, requiring only small numbers of cells for full characterisation (~$1x10^6$), thus preserving large numbers of cells for use in future studies.

Plant derived lectins have previously been employed to differentiate between microvascular and macrovascular endothelial cells [119]. I encountered difficulties with non-specific binding of the lectins *Griffonia (Bandeiraea) simplicifolia* and *Helix pomatia* previously used to differentiate between microvascular and macrovascular endothelial cells respectively both on single cells and on paraffin embedded tissue. As a result, I investigated E-selectin (CD62E) expression as an alternative method to differentiate between microvascular and macrovascular endothelial cells. E-Selectin (CD62E) and P-Selectin (CD62P) are receptor molecules for monocytes and neutrophils that are expressed on activated endothelial cells [134]. CD62E, in contrast to CD62P which is stored in Weibel-Palade bodies in endothelial cells, is transcriptionally induced on microvascular endothelial cells in response to cytokine stimulation [133]. Capillaries are not thought to express CD62E [135], [136]. Thus quiescent microvascular cells do not express CD62E but following activation intraacinar arterioles and venules express CD62E, while capillaries remain negative

for CD62E. In this study, the isolated CD31 positive cells showed very low (<5%) staining for CD62E at baseline. In response to stimulation with TNFα, there was inducible staining in around 30-50% of the isolated cells at 1 hour. Inducible CD62E in response to TNFα suggests these endothelial cells are microvascular. Furthermore, the presence of a subpopulation that was endothelial (i.e. positive for CD31) but did not up-regulate CD62E in response to TNFα suggests that the cells in this subpopulation are pulmonary capillary endothelial cells. Importantly this subpopulation was greater in the cells isolated from patients with emphysema compared with commercially available cells from Promocell used in the optimisation experiments. These pulmonary microvascular endothelial cells may therefore provide a more appropriate model than the current commercially available cells.

Infection is undoubtedly the major challenge to successful isolation and investigation of human pulmonary microvascular endothelial cells. Due to the inherent risks of introducing infection whilst culturing the cells, the lobe of lung was placed in DMEM containing 0.1% penicillin streptomycin and amphotericin (PSA) prior to processing. 0.1% PSA was included in all MV2 media used in cell culture, the risk of infection being deemed greater than any adverse effect on growth kinetics the antimicrobials may have. In spite of this, a number of cell cultures were lost to infection, mostly around P5-P6. With cell aging, growth kinetics reduced, with greater time to confluence. Thus cells spent longer time in culture at each passage, increasing the likelihood of infection. Amphotericin was included as we encountered more fungal infections than bacterial infections.

As with all *ex vivo* cell culture systems, inherent limitations are associated. Cells were passaged 3-5 times prior to obtaining pure cobblestone cultures which were characterized as endothelial. Cells therefore have a protracted culture period, with possible associated increased senescence and change in cell characteristic. Cells were grown in MV2 media (Promocell) which included 5% fetal calf serum supplementation and other survival factors such as hydrocortisone (0.2ug/ml), recombinant human epidermal growth factor (5ng/ml) fibroblast growth factor (10ng/ml) vascular endothelial growth factor (0.5ng/ml) and insulin like growth factor

(Long R3) (20ng/ml). The addition of hydrocortisone to cell culture media has been a contentious matter due to concerns over increased cell stress and how this may change cellular physiology. The concentration of hydrocortisone in MV2 media (Promocell) is considerably lower than in other types of microvascular endothelial cell media and its omission led to cell death.

Isolation of cells from patients with the disease in question, namely emphysema, was initially time consuming, requiring ethical approval and significant commitment in order to obtain fresh tissue at the time of transplantation. Furthermore, full characterisation of these cells to confirm their pedigree once again was more laborious than the use of an immortalised cell line or indeed the use of commercially available cells. However, following the initial outlay of work, one obtains a valuable resource that has been isolated and characterised via a standard methodology, with corresponding clinical data to further characterise the cells. This cell isolation method can also be applied to other respiratory diseases in which the pulmonary microvasculature may be pivotal such as pulmonary arterial hypertension and idiopathic pulmonary fibrosis. Indeed large numbers of cells from IPAH were obtained at lower passage and with higher yield than the emphysema model.

# *Chapter 5: Endothelial cell apoptosis in emphysema*

## *5.1 Abstract*

Apoptosis has been suggested to be important in the pathogenesis of emphysema and is linked to loss of the microvasculature. A number of researchers have shown in animal models that loss of VEGF leads to apoptosis and may lead to emphysema like changes. Studies of human pathology have further confirmed apoptosis of alveolar cells however the predominant cell type is still debated. It is also unclear, although a relatively simple scientific question that is sometimes alluded to as being a known fact, whether microvascular endothelial cells undergo apoptosis in response to CSE. I therefore investigated apoptosis in response to CSE using the susceptible HLMVECs isolated from patients with severe emphysema. In addition VEGFR2 gene expression was also investigated.

**Methods:** LMVECs (Promocell) were used for viability studies via flow cytometry. These studies were then repeated with cells isolated from individuals with emphysema and apoptosis detected via flow cytometry using Annexin V as a marker of apoptosis. Cells were also TUNEL stained as a second method to detect apoptosis. Due to inherent difficulties of ascertaining the most appropriate time point and concentration of CSE at which to look for apoptosis, fluorescent live cell imaging was employed to detect fluorescence generated upon activation of caspase 3 using DEVD Nucview-488. q-PCR for VEGFR2 was thereafter investigated to examine gene expression in response to CSE.

**Results:** Cell viability studies confirmed cells were resistant up to 10% CSE and that the isolated emphysema cells were less viable at baseline and more susceptible to injury. Fluorescence live cell imaging showed both short and prolonged low dose CSE treatment caused an increase in fluorescence counts in both LMVECs (Promocell) and in cells isolated from a patient with emphysema. CSE treatment alone however caused autofluorescence of the cells and although control experiments were performed in attempt to quantify this, it was therefore not possible to determine whether these cells undergo apoptosis. q-PCR for VEGFR2 was

unchanged in normal HLVECs (Promocell) in response to CSE while HLMVECs isolated from emphysema tissue show a reduction in VEGFR2 in response to CSE at 48 hours compared with untreated isolated cells. The influence of the cell isolation procedure on apoptosis and VEFR2 was not determinable.

**Conclusions:** Apoptosis in response to CSE was studied in both commercial LMVECs (Promocell) and LMVECs isolated from patients with emphysema using a number of techniques including Annexin V, TUNEL and detection of caspase 3 activation. Unfortunately all of these techniques employed the use of fluorescence and as CSE itself causes autofluorescence, despite attempts to control for this, it was not possible to state whether cells undergo apoptosis in response to this injury. qPCR suggests that LMVECs down regulate VEGFR2 in response to CSE, in contrast to normal LMVECs (commercial primary cells) which may suggest a maladaptive response to CSE injury in cells from susceptible individuals. Unfortunately due to the number of cells isolated in the same manner from normal patients free from disease it was not possible to repeat this experiment in these cells thus limiting the conclusions that can be drawn from comparing commercial primary LMVECs with the emphysema LMVECs.

## *5.2 Introduction*

Apoptosis is an energy dependant programmed cell death for the deletion of unwanted individual cells that is important in morphogenesis and is also thought to be crucial for ongoing tissue homeostasis [61]. Apoptosis has long been recognised to play an important role in tumour biology[137] and more recently has been implicated in emphysema[138]. Rats treated with a VEGF receptor blocker (SU5416) develop airspace enlargement and loss of the microvasculature similar to emphysema that can be prevented by the addition of a caspase-3 inhibitor [63]. Clinical studies support this animal model with increased apoptotic endothelial and epithelial cells in the alveolar septa of emphysematous lung tissue when compared with tissue from non-smokers and smokers without emphysema [54]. VEGF and VEGF receptor 2 mRNA and protein are also reduced in emphysema tissue [54]. A1AT has also been reported to have anti-apoptotic actions [6],[7], accounting for the accelerated emphysema witnessed in individuals homozygous for the PiZ allele and further supports the key role apoptosis may play in the development of emphysema. These studies led other researchers to investigate apoptosis rates in emphysematous tissue with similar findings, with Yokohori and Imai also highlighting the dynamic nature of emphysema; the balance between co-existent alveolar cell death and proliferation determining the complex pathology witnessed[17,20].

The response of endothelial cells to cigarette smoking *ex vivo* is however less well studied. Tuder et al presented an abstract entitled “Cigarette smoke extract decreases the expression of vascular endothelial growth factor by cultured cells and triggers apoptosis of pulmonary endothelial cells” [139] at a meeting in 2000 however while this data is noteworthy it has since not been published. U937 (monocyte cell line), HepG2 (hepatocellular carcinoma) and A549 (alveolar epithelial cell line) cells were treated with 10% CSE for 24 hours and reduced VEGF protein and mRNA was observed on western blotting and ribonuclease protection assays [139]. CSE treatment was also reported to induce a two fold increase in NO production in all cell lines studied [139]. They then investigated apoptosis in these cells lines and bovine pulmonary artery endothelial cells in response to treatment

with 10% CSE for 24 hours. They reported “apoptosis and complete detachment from the culture dish of bovine pulmonary artery endothelial cell, while minimal detachment and apoptosis were seen with the U937, HepG2 and A549 cells”. Importantly they did not specify how apoptosis was measured and did not quantify relative rates of apoptosis. Other researchers have published studies examining apoptosis in response to cigarette smoke extract but have not focused on endothelial cells, in contrast reporting apoptosis in alveolar macrophages[140], human lung fibroblasts[141] and in A549 cells, the alveolar type II cell derived line[142]. Michaud et al reported impairment of HIF-1alpha/VEGF in response to cigarette smoke extract on HUVECs but reported no toxicity up to 10%CSE and detected no apoptosis via TUNEL [143]. Later studies reported the ability of alpha-one antitrypsin [144] and prostacyclin [110] to attenuate apoptosis in cell culture models. Interestingly, these authors allude to apoptosis in response to cigarette smoke being a published and accepted finding and report simply the ability to reverse this. One of these reports used pulmonary artery endothelial cells isolated from the main pulmonary arteries of 6 month old pigs, thus has the major limitations of species specific differences and that fact that these cells are PAECs and not LMVECs. The cigarette smoke used in these experiments was also different to the standard method developed by Carp and Janoff [111]. Rates of apoptosis were surprisingly high also, with approximately 50% of cells undergoing apoptosis [144]. For these reasons, further investigative work was conducted to investigate the response of human pulmonary microvascular cells to cigarette smoke extract.

Smoking a single cigarette exposes an individual to around 6000 compounds, a large number of which are toxic [72]. Developing a model to study the effects of cigarette smoking is therefore complicated by the sheer number of compounds which can be studied and also the variability in how an individual smokes (number of inhalations, volume of inhalation etc.). Not withstanding these factors, a number of models of cigarette smoking have been developed to study the effects of smoking *ex vivo* [111][145], [146]. One of the most widely accepted methods is that developed by Carp and Janoff more than 30 years ago [111]. It involves entraining smoke and bubbling this through an aqueous solution, to produce a cigarette smoke extract.

This method has the major disadvantage that CSE is in the liquid as opposed to gaseous phase and some volatile and rapidly reactive compounds are lost. It may also be less physiological, as endothelial cells are not directly exposed to cigarette smoke *in vivo*. Other models have been developed which involve cells being exposed to cigarettes via a smoking chamber [146], which may be more physiological, however adding such complexity without large scale machinery such as a smoking robot can make the stress more variable and less reproducible. Some researchers have also developed models using individual toxins such as acrolein [147], however this model does not reflect the likelihood that smoke related injury arises via compound effects rather than the sum of multiple independent toxicities. Rejecting a model because it does not perfectly reproduce some aspect of human smoking has been correctly stated as unscientific and likely to hamper advances in our understanding [72]. Instead, it is widely accepted that a model must act as a reasonable surrogate in which investigation of a hypothesis may be conducted. In this thesis I have used the method developed by Carp and Janoff [111] due to its simplicity, highly published rate and relative reproducibility.

There are a number of methods via which apoptosis may be studied. Two of the commonest methods are the detection of phospholipid phosphatidylserine (PS) and activated caspase 3. A key step in apoptosis is the changes in plasma membrane structure, with translocation of PS from the inner to the outer leaflet of the plasma membrane[148]. On the outer leaflet of the plasma membrane PS acts as a signal for phagocytic cells in the apoptosis cascade. Annexin V is a 36kDa calcium dependant phospholipid binding protein with high affinity for PS[149]. This affinity has been exploited as a method for detecting apoptosis, with conjugation of Annexin V to a number of fluorochromes that can be detected via fluorescence, commonly via flow cytometry and confocal microscopy. In these studies I have used flow cytometry to identify apoptosis via FITC Annexin V, together with 7-Amino-Actinomycin. 7-AAD labels cells without an intact membrane, thus does not differentiate between cells which have died via necrosis and cells which have undergone apoptosis per se, as in the late stages of apoptosis cell membrane integrity is lost and cells appear indistinguishable from necrotic cells.

Detection of activated caspase 3 is another method which is frequently employed to investigate apoptosis[150]. Caspases (cysteine aspartase) are cysteine proteases which exist in their inactive pro-form in living cells. The apoptosis pathways lead to cleavage of a number of pro-caspases to caspases, with the acquisition of their protease activity, which allows transmission of apoptotic signals to the nucleus/mitochondria. Activated caspase 3 is therefore a useful marker of apoptosis. Activated caspase 3 can be detected on cell lysates via western blotting or ELISA and on tissue via immunohistochemistry. In these studies I have examined activated caspase-3 expression on emphysema tissue from which the cells were isolated in order to determine apoptosis in severe end stage emphysema.

DNA fragmentation and degradation occurs late in apoptosis and can be detected via TUNEL (TdT-mediated X-dUTP nick end labelling)[151]. TUNEL uses the nicks that appear in DNA in apoptosis as a marker that can be detected. Terminal deoxynucleotidyl transferase (tdt) identifies these nicks in DNA and catalyses the addition of dUTPs to these. dUTPs are labelled with a marker, that can be detected, most commonly via fluorescence, thereby allowing apoptosis to be quantified. In this study I have examined TUNEL staining both on cells exposed to CSE and on the tissue from which these cells were isolated.

When studying apoptosis it is important to take into account cell type, time course, dose in addition to the dynamic nature of apoptosis. Thus one could postulate that between commercially available lung microvascular cells and primary cells isolated from differing patients with emphysema, cells may undergo apoptosis at differing rates at differing time points. In addition the dose of cigarette smoke extract that may trigger apoptosis may differ. The ability therefore to image cells in real time via live cell imaging, over a wide variety of concentrations is attractive. The emergence of fluorogenic enzyme substrates that are highly cell permeable have been exploited in order to capture apoptosis via live cell imaging. DEVD-Nucview488 is a fluorogenic caspase 3 substrate that can be used for this purpose [152]. Ac-DEVD is

a highly negatively charged caspase-3 recognition site that is linked to Nucview488, a positively charged DNA binding dye. In its stable state, DEVD-Nucview488 is highly bound and does not stain the nucleus, however due to its cell permeability can pass freely into the cell where it remains. Apoptosis, with activation of caspase-3 cleaves Ac-DEVD from Nucview488, which allows the positively charged Nucview488 to migrate to the nucleus and bind to DNA, causing excitation at 488nm that can be detected via fluorescence microscopy. This method was therefore used in these studies, as it allows cell efficient investigation of apoptosis in precious primary cells in real time.

I hypothesised that pulmonary microvascular endothelial cells undergo apoptosis in response to cigarette smoke extract and will investigate this using the above techniques. Apoptosis was firstly investigated in the tissue from which microvascular endothelial cells were isolated via immunohistochemistry for activated caspase-3 and TUNEL. The receptor (KDR/FLK1) for the pro-endothelial survival factor, VEGF, was also assessed via immunohistochemistry. The *ex vivo* work began with viability studies using LMVECs (Promocell) in response to CSE to identify a concentration which would stress cells but not cause mass cell death. Apoptosis was then investigated via flow cytometry for Annexin V and 7-AAD. Following these preliminary studies, viability studies were repeated on the primary cells isolated from emphysema tissue followed by investigation of apoptosis via Annexin V. TUNEL staining on cells post CSE exposure was also investigated. DEVD-Nucview488 was used to detect apoptosis in real time via live cell imaging in both commercially available normal cells and in emphysema cells isolated from patients. Finally, VEGF-KDR mRNA expression in response to CSE was also investigated via qPCR and is reported in this chapter.

## *5.3 Materials and Methods*

### *5.3.1 Immunohistochemistry*

Immunohistochemistry for Activated caspase-3 (AF835 R+D 2.5ug/ml) and FLK1 (Santa Cruz) were performed on 4um paraffin embedded tissue sections from emphysema and control tissue. The Envision Flex system was used with reaction of the primary antibody, after blocking agent, with Flex HRP. Immunoreactants were visualised using diaminobenzidine (DAB) substrate solution. Isotype controls were included in each experiment to assess quality of staining.

### *5.3.2 TUNEL*

TUNEL was performed on paraffin embedded tissue and cells isolated from emphysema tissue using commercially available kits from Roche (11684795910). Tissue was dewaxed through xylene to graded alcohol prior to antigen retrieval via low pH microwave treatment. Endogenous tissue peroxidase was quenched with 6% H2O2. Cells were fixed in freshly prepared 4% paraformaldehyde and permeabilised on ice with 0.1% TritonX-100 in 0.1% sodium citrate. A positive control was included for experiments on tissue and cells, by pre-treatment with DNase. After washes, TUNEL reaction mixture containing TdT and fluorescein-dUTP was added and incubated at 37˚C in the dark. Incubation with TdT catalyses the addition of fluorescein-dUTP to free 3'-OH groups (DNA breaks/nicks), thus allowing detection of apoptosis. After washing, incorporated d-UTP was visualised by fluorescence microscopy. Tissue sections had high background autofluorescence, and so converted via POD to HRP/DAB for visualisation by light microscopy.

### *5.3.3 Cell culture*

Commercially available human pulmonary microvascular endothelial cells (Promocell) and cells isolated from emphysematous human lung were grown in complete MV2 media (Promocell) containing supplements and 5% FCS. Cells were grown in 25cm$^2$ flasks (qPCR), on 6 well plastic plates coated with gelatin (cell viability and apoptosis via flow cytometry), on 18mm coverslips (TUNEL) and on 96 well gelatin coated plates for live cell imaging.

### *5.3.4 CSE preparation*

Cigarette smoke extract was prepared according to the method by Carp and Janoff [111]. As outlined in figure 3.1, one Kentucky filterless research cigarette was attached via tubing to a vacuum pump and the smoke from this cigarette gently bubbled through 25ml endothelial cell culture media (containing 5% FCS), over approximately 6 minutes. The resulting media was tar stained and final concentration stated as 100% CSE. CSE was made on each occasion by the same operator (LSM) and when analysed on a spectrophotometer had the same absorbance. pH of CSE was also unaltered compared with whole media. Due to the precious nature of the cells, CSE was filtered through a 0.2um filter and then used within 30 minutes of preparation.

### *5.3.5 Flow cytometry*

Initial cell viability studies were conducted using propidium iodide. Apoptosis was investigated using Annexin V/7AAD kits purchased from BD Bioscience. (#559763 BD Bioscience). After stimulation, cells were harvested using cell dissociation solution (Sigma). Cells were resuspended in 100ul 1x binding buffer (BD Bioscience). 5ul of Annexin V and 7-AAD were added to each tube and incubated at RT for 15 minutes, before analysis on FACS scan. Flow cytometer settings were controlled using unstained cells, cells stained with Annexin V alone and 7AAD alone prior to each experiment. Data was analysed using Venturi software.

### *5.3.6 Live cell imaging via DEVD-Nucview488*

DEVD-Nucview 488 (stock concentration 1mM) was purchased from Biotium (10400). Cells were grown on 96 well gelatin coated costar plates. CSE treatments were applied in whole media, together with Nucview added (1ul stock per ml of media) and 100ul of media with DEVD-Nucview488 (final concentration 1uM) added to each well. Cells were then placed in an incubator at 37˚C with 5% $CO_2$ and observed with a fluorescence microscope in real time and analysed via Incucyte software.

### *5.3.7 VEGF-KDR qPCR*

RNA was isolated from cells using the Absolutely RNA microprep kit (400805) Agilent. RNA yield and purity was determined via UV absorbance using a NanodropSpectrophotometer (ND-1000). All RNA used had a ratio of absorbance at 260 nm and 280 nm ($A_{260/280}$) of 2.0 or above. Quality of RNA was further assessed via running samples on a 2% agarose gel containing 4ul ethidium bromide with loading buffer of 30% glycerol, 70% TAE (Tris-acetate-EDTA) and bromophenol blue in 1% TAE. A trackIt (Invitrogen) DNA ladder was used to identify molecular weight. cDNA was thereafter prepared from RNA using an Affinity Script Multiple temperature cDNA synthesis kit according to RNA concentration. cDNA was stored at -80°C until used for q-PCR.

Samples for qPCR were prepared on 96 optical well plates (Applied Biosystems) by adding 10ul mastermix, 6.5ul RNAse free H2O and 1ul primers (18s and KDR) to each well. 2.5ul of cDNA was then added to each well. Samples were ran on ABI PRISM 7000 Taqman real-time PCR machine (Applied Biosystems) and analysed on ABI Prism 7000 SDS software. Real-time reaction products for each primer were confirmed on 2% agarose gel electrophoresis.

## *5.4 Results*

TUNEL staining was firstly employed to investigate apoptosis as this has been widely reported in the emphysema literature[64][54]. The commercial kit (Roche 11684795910) recommended optimisation for each tissue with differing pre-treatment protocols. Pre-treatments including proteinase K, triton x100, low pH microwave and no pre-treatment were all assessed. High autofluorescence in peripheral lung caused by elastin made the signal uninterpretable and so the signal was converted to peroxidise/DAB using the POD converter contained within the kit. The staining with TUNEL HRP-DAB was very variable with large areas of tissue showing high staining while some areas showed no staining. A review of the literature supports this and highlights that TUNEL in archived paraffin-embedded tissue has at best 50% sensitivity[153]. The TUNEL technique relies on being able to detect breaks in DNA. Fixation of tissue in paraffin-embedded archived blocks tends to be variable across the block being greater in the centre of the block and less in the periphery, thus explaining some of the variability observed in the stain. Secondly pre-treatments (antigen retrieval) such as proteinase K and microwave low pH can in themselves lead to breaks thus leading to false positives. The use of frozen tissue sections may prove more reliable with TUNEL staining, but as with most tissues banked for research, all samples in this study were paraffin embedded. Some researchers have tried to optimise TUNEL staining in paraffin-embedded tissue, reporting sensitivity up to ~80%, however I rejected this method as such false positive and false negative staining could make the apoptosis work in vivo uninterpretable, as emphysema is a disease in which there are areas of relative normality next to areas of severe disease. Activated caspase-3 immunohistochemistry was therefore employed to investigate apoptosis in vivo.

### *5.4.1 Apoptosis of endothelial cells in emphysema in vivo*

Both (a) control and (b) emphysema tissue show DAB positive cells indicating the presence of apoptotic cells (activated caspase-3 positive cells) in health and disease and thus validate the immunostain. Isotype controls also confirmed this staining to be specific (Appendix). Activated caspase-3 positive cells were more frequent in alveolar septa of (d) emphysema tissue than (c) control tissue indicating increased apoptosis in keeping with other researcher's findings.

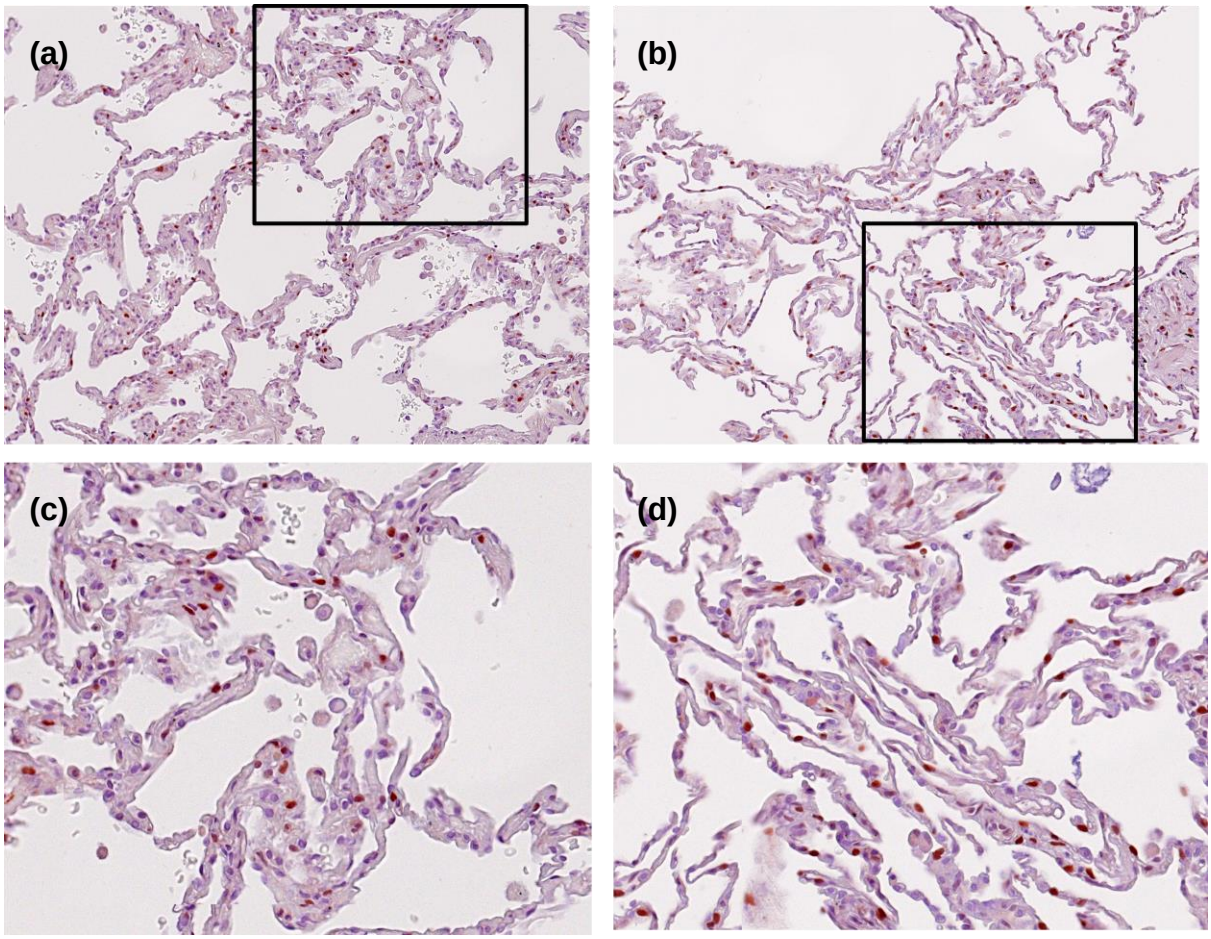


**Figure 5.1:** Immunocytochemistry images for a) control lung tissue and b) emphysema lung tissue (Image taken at x20 magnification). Activated caspase 3 (DAB positive cells) indicate the presence of apoptotic cells in both (a) control and (b) emphysema tissue. Further magnification (boxes) of the (c) control and (d) emphysema tissue shows that the positive (activated caspase 3) cells were a more frequent finding in alveolar septa of (d) emphysema tissue than (c) control tissue in agreement with the findings of other researchers of increased apoptosis in emphysema tissue.

### *5.4.2 Cell viability studies in response to cigarette smoke extract*

Human Lung Microvascular endothelial cells (LMVECs) (Promocell) at passage 3 were grown to 70% confluence and then treated (n=3) with varying concentrations (0-100%) of cigarette smoke extract (CSE). Cell viability was measured via flow cytometry using propidium iodide (PI) as a marker of cell death. The results are shown in figure 5.2. After one hour, cells showed no significant cell death up to 10% CSE, (Viable cells (mean ± sem): Control 76.18±3.12 vs 10% CSE 76.12 ±4.62, p=0.99) (Figure 6.3a). Exposure to 100% CSE for 1 hour led to significant cell death with only 55.36% ± 1.47 remaining viable (p=0.004). At 24 hours, there was no significant cell death up to 10% CSE (Control 79.26% ±3.47 vs 10% CSE 78.46 ±1.52, p=0.843) (Figure 5.3b). However, exposure for 24hours to 100% CSE led to mass cell death with only 15.61% ±2.69 cells remaining viable (p=0.000).

In order to verify this result and investigate cell viability at higher passage, LMVECs (Promocell) (n=3) at passage 5 were treated with the same varying concentrations of CSE as before (0-100%) (Figure 5.4). Similar results were found with no change in cell viability up 10% after 1 hour (Control 75.26±3.12 vs 10% CSE 67.30±4.62, p=0.075) and 24 hours treatment (Control 73.10±3.47 vs 10% CSE 70.54±1.54, p=0.308). Reduced cell viability was again observed with 100% CSE for 1 hour (57.83±1.47, p=0.001) and mass cell death at 24 hours (23.5±2.70, p=0.000).

From these preliminary studies I chose 3% CSE as a stress stimulus for cells in initial apoptosis studies in Promocell LMVECs.

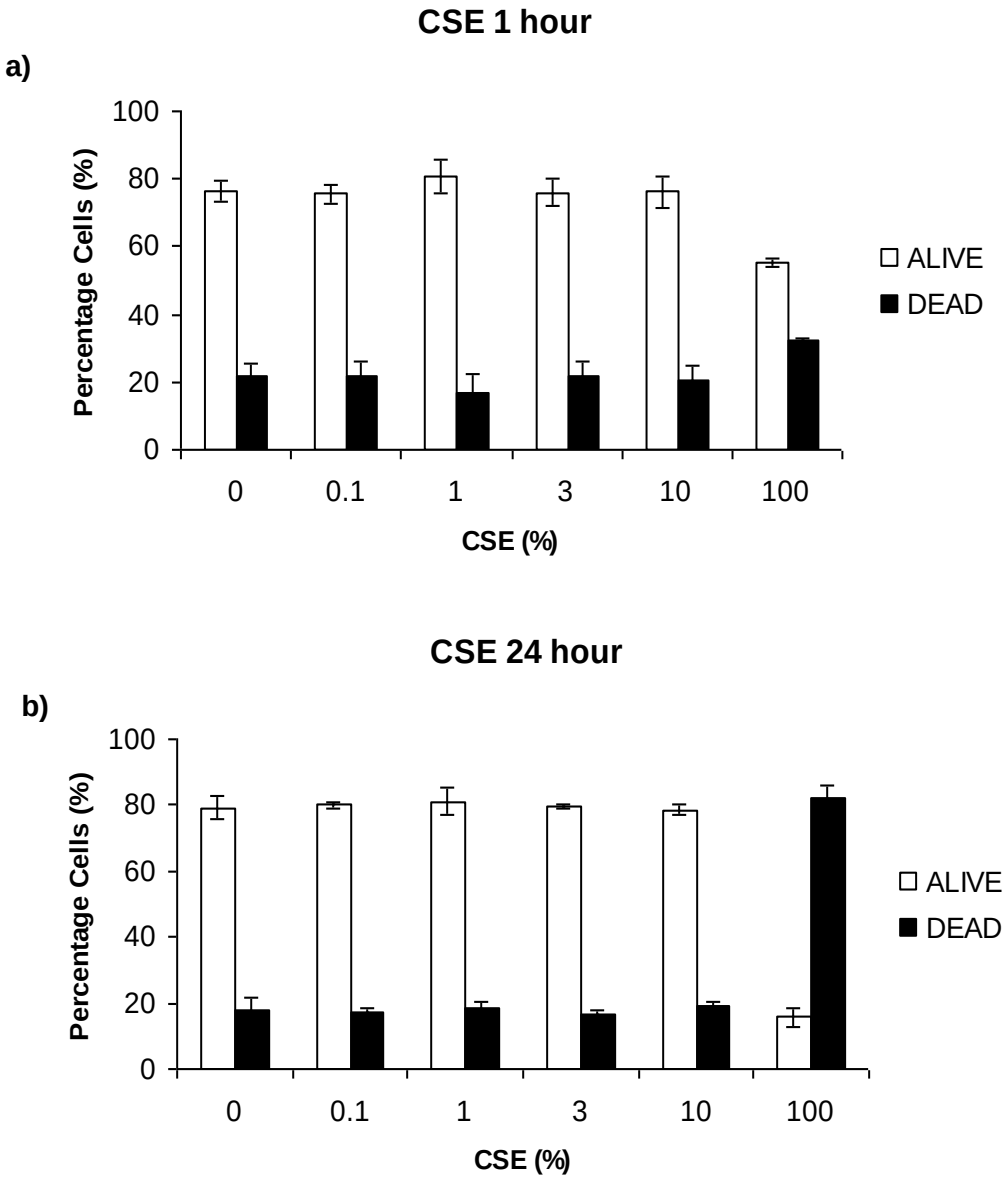


**Figure 5.2:** Flow cytometry data for LMVECs at passage 3 (Promocell) treated with 0-100% CSE and stained for propidium iodide. After one hour CSE exposure, cells showed no significant cell death up to 10% (Viable cells (mean±sem): Control 76.18±3.12 vs 10% CSE 76.12 ±4.62, p=0.99) (Figure 5.3a). Exposure to 100% CSE for 1 hour led to significant cell death with only 55.36% ± 1.47 remaining viable (p=0.004). At 24 hours, there was no significant cell death up to 10% (Control 79.26% ±3.47 vs 10% CSE 78.46 ±1.52, p=0.843) (Figure 5.3b). However, exposure for 24hours to 100% CSE led to mass cell death with only 15.61% ±2.69 cells remaining viable (p=0.000). All data points represents n=3.

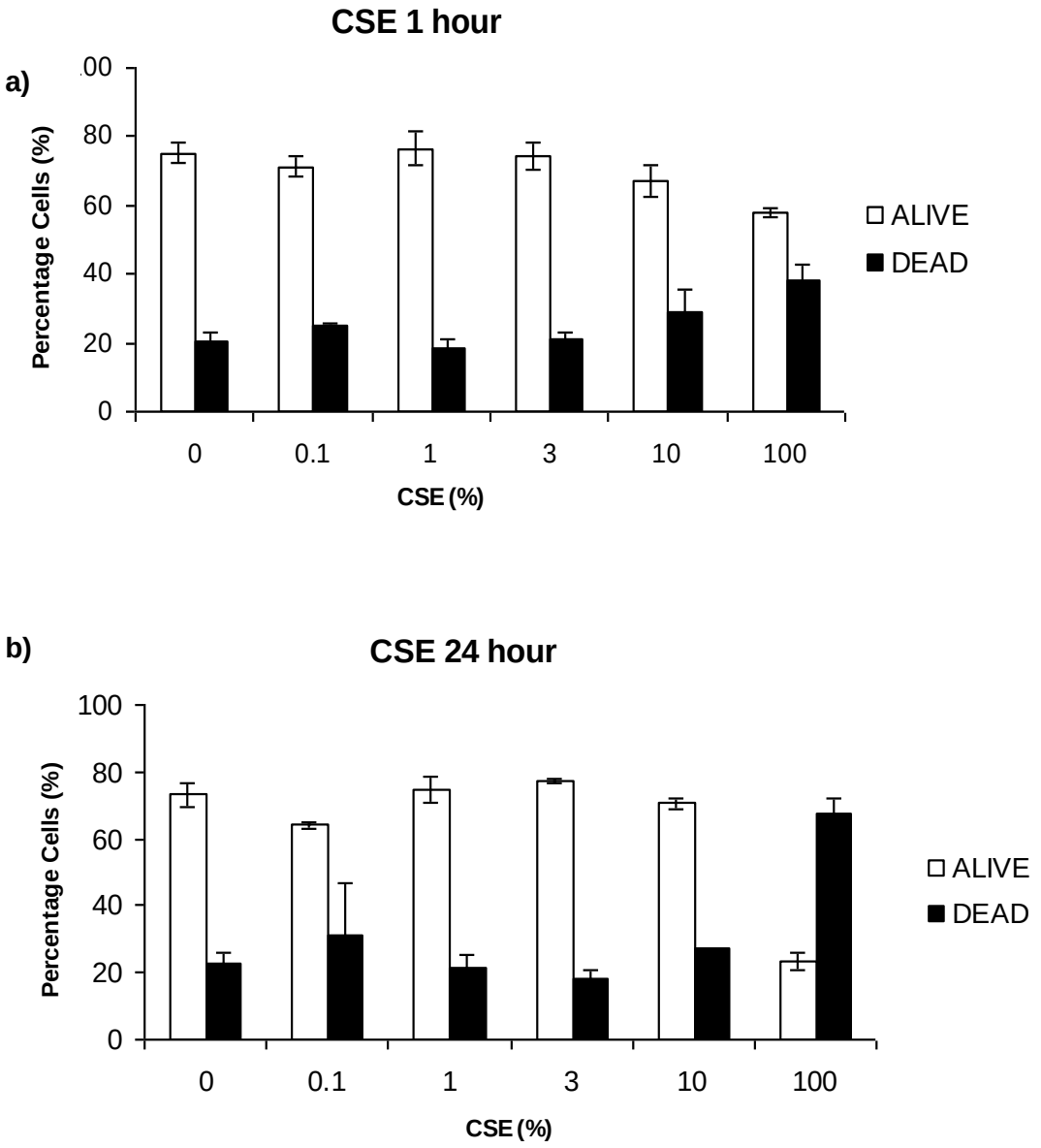


**Figure 5.3:** Flow cytometry data for LMVECs passage 5 (Promocell) treated with 0-100% CSE and stained with propidium iodide. After 1 hour treatment with CSE, there was no change in cell viability up 10% (Control 75.26%±3.12 vs 10% CSE 67.30% ±4.62, p=0.075) (Figure 5.4a). There was also no effect on cell viability with up to 10% CSE treatment at 24 hours (Control 73.10% ±3.47 vs 10% CSE 70.54% ±1.54, p=0.308) (Figure 5.4b). Following 100% CSE for 1 hour there was significant cell death with only 57.83 ±1.47 remaining viable (p=0.001) and mass cell death at 24 hours with only 23.5%±2.70 remaining viable (p=0.000). All data points represents n=3.

### *5.4.3 Apoptosis in commercially available normal cells in response to cigarette smoke extract*

LMVECs (Promocell) at were grown to 70% confluence and then treated with 3% cigarette smoke extract (CSE). Apoptosis was then investigated via flow cytometry via FITC conjugated annexin V with non-viable cells detected via 7-AAD (Figure 5.4).There was no significant change in cell viability (P=0.23) among cells, untreated vs treated with 3% CSE for up to 72H. There was no significant apoptosis detected in response to 3% CSE (P=0.39) across all time points. Of the non-viable cells (necrotic/late apoptotic) there was a trend towards increased cell death after exposure to 3% CSE for 1 hour as compared with untreated/control cells and cells treated for 24,48 and 72 hours (P=0.087) although this did not reach significance.

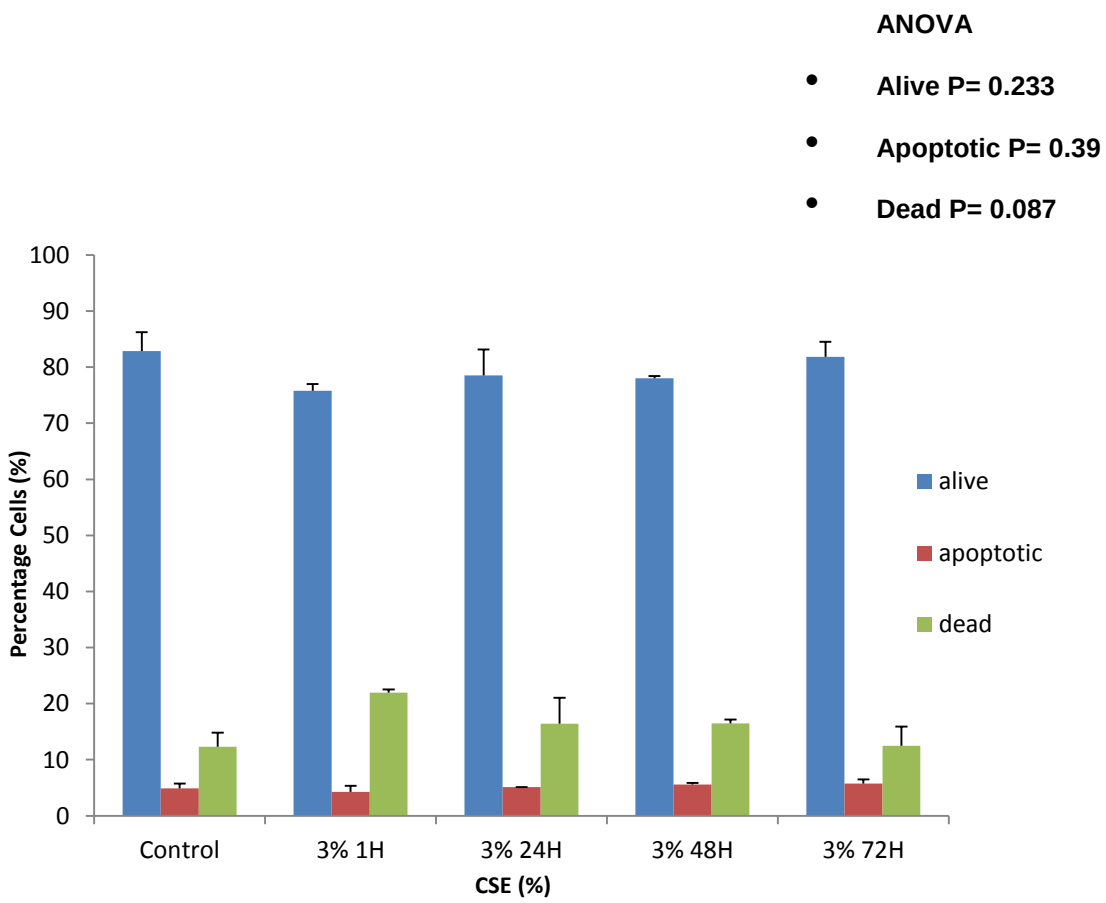


**Figure 5.4:** Flow cytometry data for LMVECs (Promocell) treated with 3% CSE and stained for annexin V to detect apoptosis and 7-AAD to detect non-viable cells. There was no significant change in viability (P=0.23) among cells treated with 3% CSE for up to 72H. There was no significant apoptosis detected in response to 3% CSE (P=0.39). Of the non-viable cells (necrotic/late apoptotic) there was a trend towards increased cell death after exposure to 3% CSE for 1 hour as compared with untreated/control cells and cells treated for 24,48 and 72 hours (P=0.087) but this did not reach significance.

### *5.4.4 Isolated Cells: Viability studies in response to cigarette smoke extract*

Cell viability and apoptosis was then investigated in LMVECs isolated from emphysema lung tissue (patient 10) at passage 5 (figure 5.5). Cells were grown to 70% confluence and then treated with varying concentrations (guided by previous viability studies conducted earlier in commercial LMVECs) of CSE. Cells were treated (n=2) with 0-30% CSE for 24 hours and viability assessed via 7-AAD. Annexin V was also added to gain insights into apoptosis. In this experiment, cell viability was generally lower with only 55.6% control cells viable. In response to CSE there was no significant change in cell viability up to 10% CSE (p=0.065) however treatment with 30% CSE led to a large reduction in cell viability, with only 14.89% ±4.32 viable at 24 hours (p=0.011). Due to low baseline cell viability and relatively wide standard errors, it is not possible to comment on any trends that may be apparent in cells undergoing apoptosis, however these emphysema cells with lower baseline viability may be more susceptible to cell death, including apoptosis.

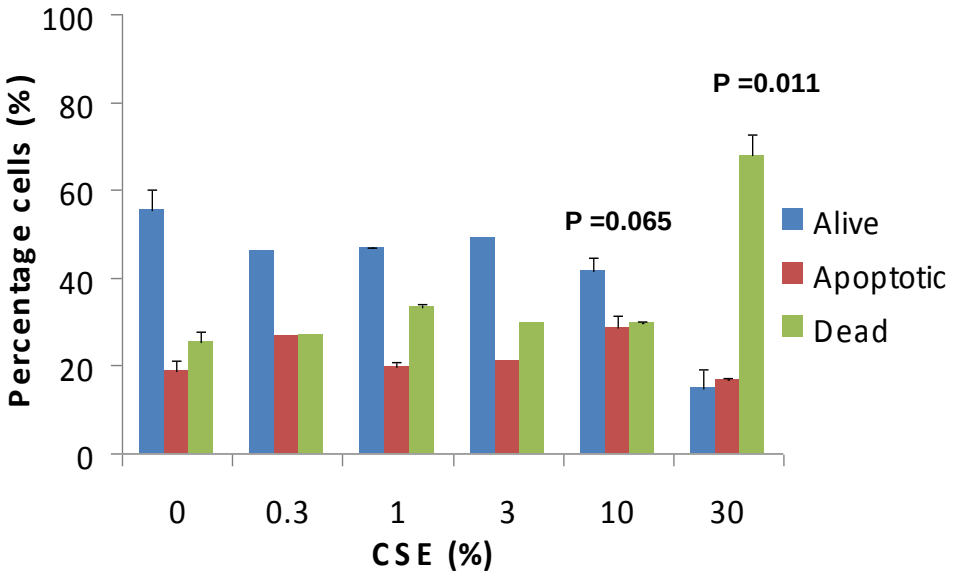


**Figure 5.5:** Flow cytometry data for emphysema cells (patient 10) (n=2) with varying concentrations of CSE (0-30%) for 24 hours and stained for 7-AAD to detect non-viable cells (and annexin V to detect apoptosis). Cell viability was generally low with only 55.6% control/untreated cells viable at the time of analysis. In response to CSE there was no significant change in cell viability up to 10% CSE (p=0.065). 30% CSE led to a large drop in cell viability, with only 14.89% ±4.32 viable at 24 hours (p=0.011).

To examine viability of cells at later passage and at 48 hours, cells at passage 7 (patient 10) were treated (n=2) with 0-12% CSE for 48 hours and viability assessed via 7-AAD (annexin V was added to gain insights into apoptosis) (figure 5.6). The concentrations of CSE investigated in this 48 hour exposure were reduced in anticipation that a more prolonged exposure to CSE was likely to further reduce cell viability. This assumption was made in order to try to investigate cells as efficiently as possible, gaining as much information from each experiment in a cell efficient manner, maximising the precious nature of these cells and time taken to grow cells sufficient for each experiment.

Cell viability was again lower than in the commercially available normal LMVECs, with 68.6% control cells viable. In response to CSE there was a stepwise decrease in cell viability in response to CSE compared with controls (Control 68.6%, 1% 64.9%, 3% 57.38%, 6% 57.6%) ($p=0.005$). 12% CSE led to a large drop in cell viability, with only 27.9% ±2.9 remaining viable after 48 hours treatment ($p=0.003$). In this experiment, there appeared to be a stepwise increase in apoptosis however as this experiment was not designed to investigate apoptosis, further analysis was not performed.

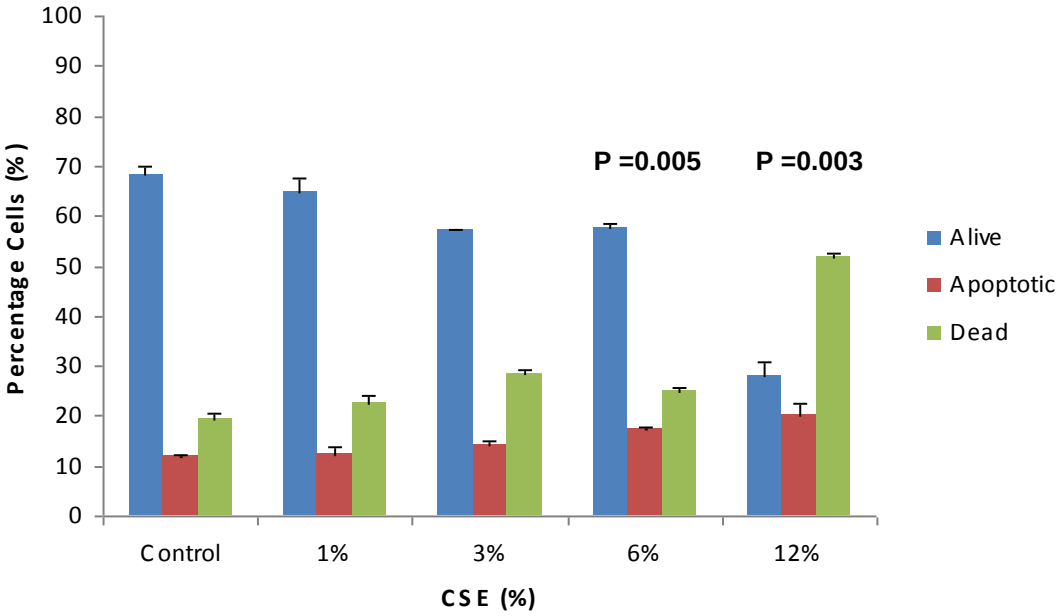


**Figure 5.6:** Flow cytometry data for emphysema cells (patient 10) at passage 7 treated (n=2) with varying concentrations of CSE (0-12%) for 48 hours and stained for 7-AAD to detect non-viable cells. Annexin V was added to detect apoptosis. Cell viability was 68.6% in control/untreated cells. In response to CSE, there was a stepwise decrease in cell viability in response to CSE (Control 68.6%, 1% 64.9%, 3% 57.38%, 6% 57.6%) (p=0.005). 12% CSE led to a large drop in cell viability, with only 27.9% ±2.9 remaining viable after 48 hours treatment (p=0.003).

In order to study apoptosis over a time course, I investigated cell viability in control (untreated) cells (Patient 10) with media having been changed 24, 48, and 72 hours before FACS analysis, to investigate whether separate controls were required for each experiment or whether controls (n=3) for cells treated for 72 hours without media change could be used as controls for cells treated for only 24 hours. This experiment was important as it would further help cell efficiency if there was no difference. Figure 5.7 shows no change in cell viability in control cells (24 hours 87.22%, 48 hours 82.5%, 72 hours 87.68%). This experiment suggests that there was no difference in control cells for a 72 hour experiment with control cells for a 24 hour exposure.

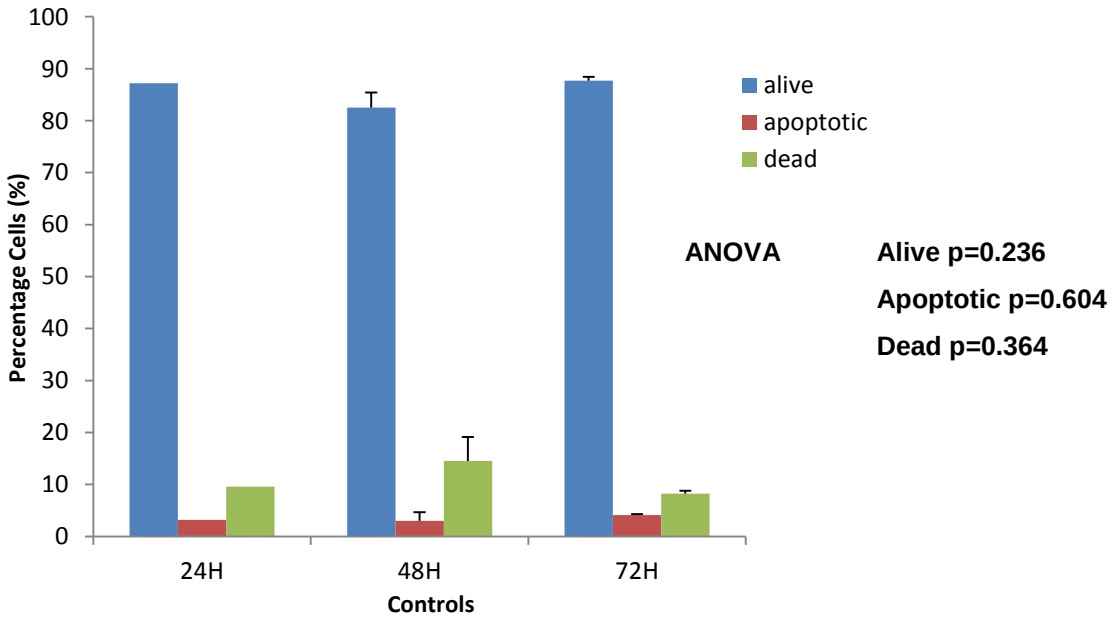


**Figure 5.7:** Patient 10 cells (n=2) untreated with simple media change at 24, 48, and 72 hours prior to experiment. 7-AAD was used to detect non-viable cells (annexin V to detect apoptosis). Cell viability was unaffected by media changes and not significantly different across time points, (24 hours, 87.22%; 48 hours, 82.5%; 72 hours, 87.68%, p=0.236).

### *5.4.5 Apoptosis in cells isolated from patients with emphysema in response to cigarette smoke extract*

From cell viability studies, 3% CSE was used in these experiments an injury sufficient to stress cells without causing non-physiological mass cell necrosis. Cells from patients 4, 8 and 10 were treated with freshly prepared 3% CSE in triplicate for 72, 48, 24 and 1 hour prior to harvesting and labelling with annexin V and 7-AAD.

Figure 5.8 confirms difference in baseline cell viability between donors with unstimulated cells from patient 10 and patient 8 approximately 70% viable, whereas only 55% of unstimulated cells were viable in cells from patient 4. In patient 10 there was a significant change detected in apoptosis (ANOVA p=0.003) but this was of less apoptosis compared with controls after 3% CSE for 1 hour. In patient 8 there was no significant apoptosis detected in response to 3% CSE (ANOVA, p=0.61) (Figure 5.8b). In patient 4 there was also significant apoptosis detected (p=0.017) with an increase in apoptosis in cells treated for 48 hours compared with untreated cells (Figure 5.8c). Figure 5.9d shows a representative scatter plot from flow cytometry with annexin V on the y axis and 7-AAD on the x axis, with four distinct populations of alive, apoptotic and dead cells (in G1 and G0). In view of the difference in low baseline cell viability and conflicting results, I attempted to repeat this experiment in patient 4 in order to investigate whether low cell viability impacted upon susceptibility to apoptosis. This was however not possible due to poor cell growth leading to insufficient number of cells and infection and so apoptosis was investigated further by more cell efficient methods.

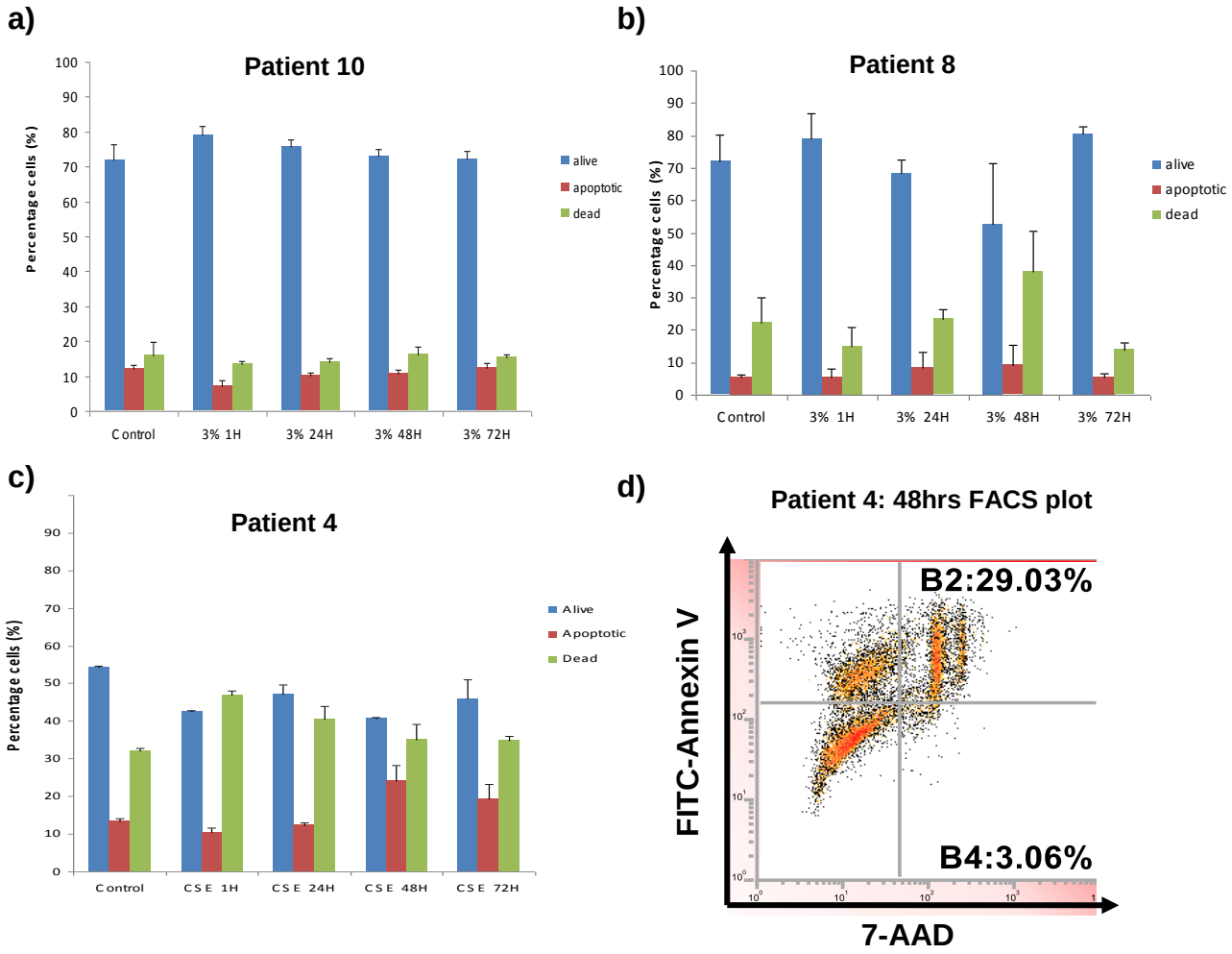


**Figure 5.8:** Apoptosis in cells isolated from three emphysema donors (Patient 10 (5.8a) Patient 8 (5.8b) Patient 4 (5.8c) treated (n=3) with 3% CSE for 1, 24, 48 and 72 hours). A difference in baseline cell viability was observed between donors with control cells from patient 10 and patient 8 approximately 70% viable, whereas only 55% of control cells were viable in cells from patient 4. In patient 10 there was a significant change detected in apoptosis (ANOVA p=0.003) but this was of less apoptosis after 3% CSE for 1 hour compared with controls (5.8a). In patient 8 there was no significant apoptosis detected in response to 3% CSE (ANOVA, p=0.61) (5.8b). In patient 4 there was also significant apoptosis detected (p=0.017) with an increase in apoptosis in cells treated for 48 hours compared with control cells (5.8c). Figure 5.9d shows a representative scatter plot from flow cytometry with annexin V on the y axis and 7-AAD on the x axis, with four distinct populations of alive, apoptotic and dead cells (in G1 and G0).

### *5.4.6TUNEL to detect apoptosis in cells isolated from patients with emphysema in response to CSE*

From flow cytometry experiments, 48 hours was chosen as a time point for which to stress cells and examine for apoptosis via TUNEL. Cells were grown on 11mm coverslips in 12 well plates and at around 70% confluence were treated with freshly prepared CSE (0-9%) for 48 hours, before fixation in 4% paraformaldehyde and TUNEL staining. DNAse was used as a positive control in order to induce DNA breaks that could be detected and a negative control (without enzyme) was also included to ensure quality of staining. Figure 5.9 summarises the data. There was no apoptosis detected in response to CSE (0-9%) compared with controls. Positive and negative controls validated the staining.

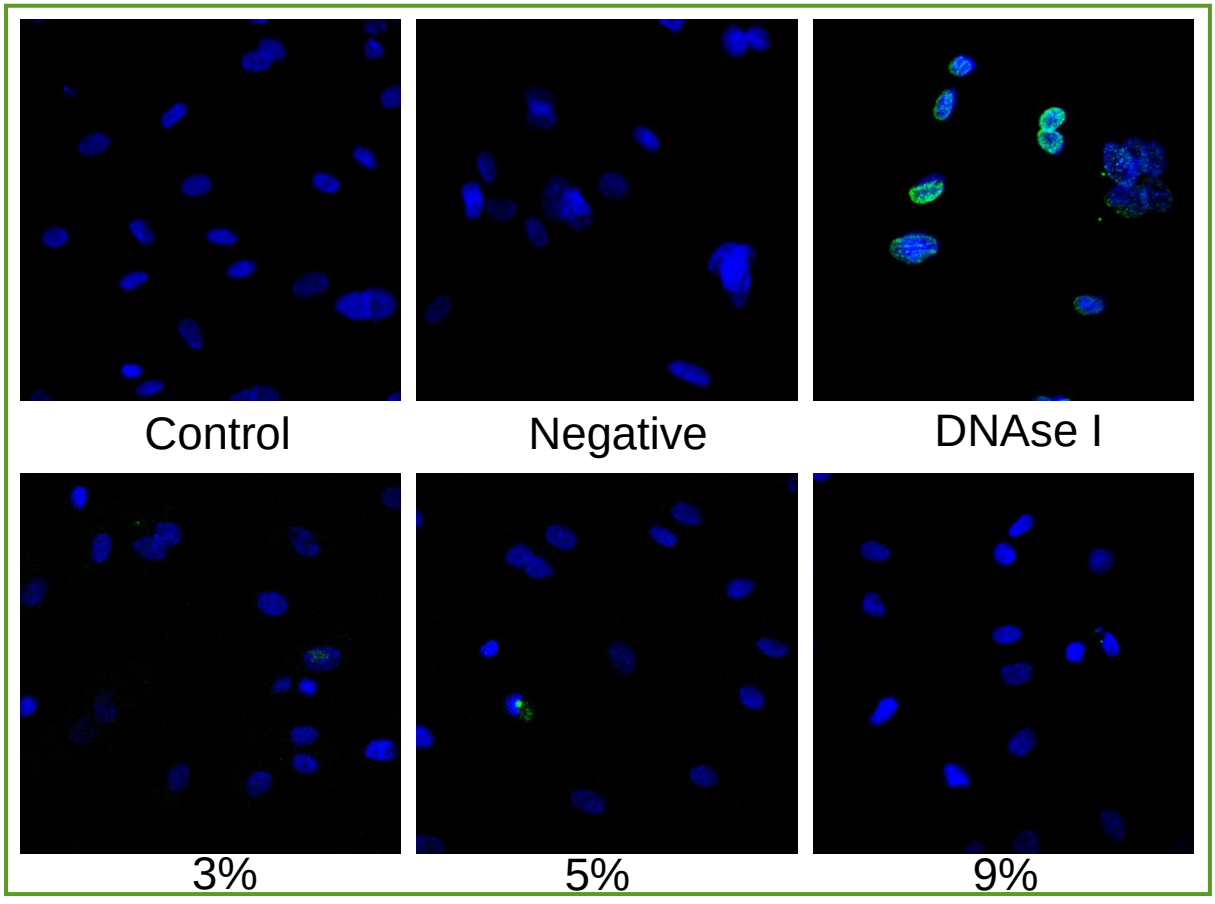


**Figure 5.9:** TUNEL staining to detect apoptosis in cells isolated from a patient with emphysema (patient 3) following treatment with 3% CSE for 48 hours. There was no apoptosis detected in response to CSE (0-9%) compared with controls. Positive (treatment with DNAse to induce DNA breaks) and negative (no enzyme) controls prove staining.

### *5.4.7Live cell imaging and DEVD-Nucview488 to detect apoptosis*

Such inconsistent results and difficulty in defining the concentration with which to stress cells and at which time point to examine for apoptosis, led to the use of live cell imaging with a caspase 3 substrate (DEVD-Nucview 488) [152] to allow investigation of apoptosis over time in emphysema patients with multiple concentrations of CSE in a cell efficient manner.

Emphysema cells were grown in 96 well plates at 10,000 cells per well (100ul) and investigated (n=3) over multiple concentrations (0-12%) of CSE across a time course (0-72 hours) via live cell fluorescence imaging. Preliminary experiments using prolonged CSE exposure to LMVECs (Promocell, and patient 7 and 8) showed a dose dependant increase in fluorescence object counts over time, suggesting increased apoptosis (Figures 5.10-5.12). However concerns over the level of fluorescence raised the issue as to whether this was simply a dose dependant increase in autofluorescence caused by increasing concentration of CSE. The experiments were therefore repeated, examining fluorescence object counts when cells were treated with increasing concentration of CSE (0-12%) in the absence of DEVD-Nucview 488 i.e. measuring cellular autofluorescence induced by CSE. Cells were treated for either the entire 72 hours (prolonged exposure), as the previous experiment, or with a short one hour exposure. In the prolonged exposure experiment, cells demonstrated autofluorescence that increased proportionally with increasing concentration of CSE (Figure 5.13). This became more marked at concentrations of 4% CSE and above. In the short exposure experiment, cells treated with CSE for one hour only prior to detection of fluorescence counts, there was initially dose dependant increase in autofluorescence but was low level (less than 20 fluorescent object counts) across all concentrations of CSE studied (Figure 5.14).

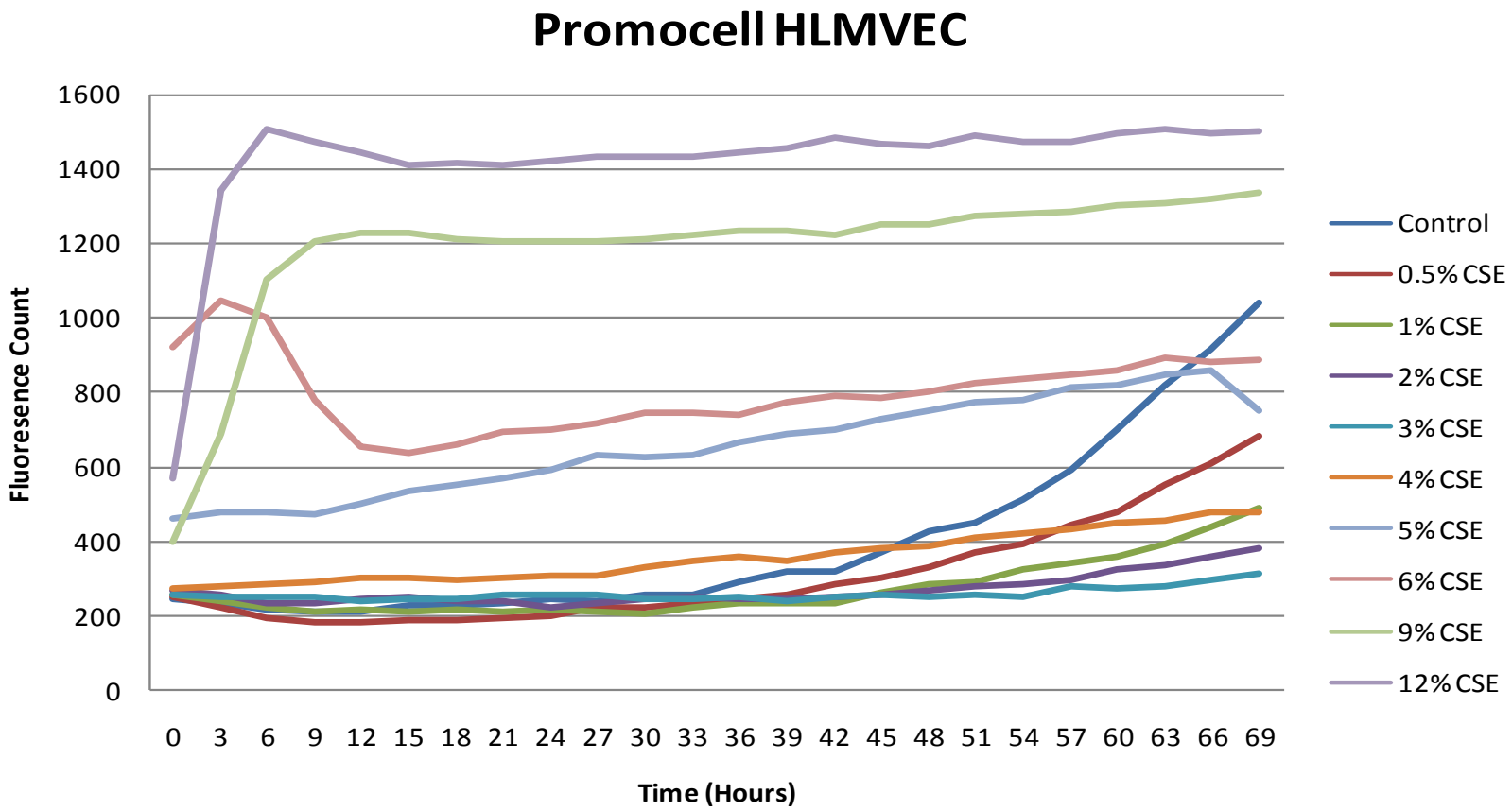


**Figure 5.10:** Apoptosis as detected via live cell imaging Nuc-view Fluorescence counts over 72 hour time course in Promocell LMVECs. High counts were observed at the higher concentrations of CSE (5-12%). At lower concentrations of CSE (1-4%) the same dose dependant rise was not observed, with control cells and cells treated with 0.5% CSE showing higher fluorescence than low dose CSE 1-4% treated cells.

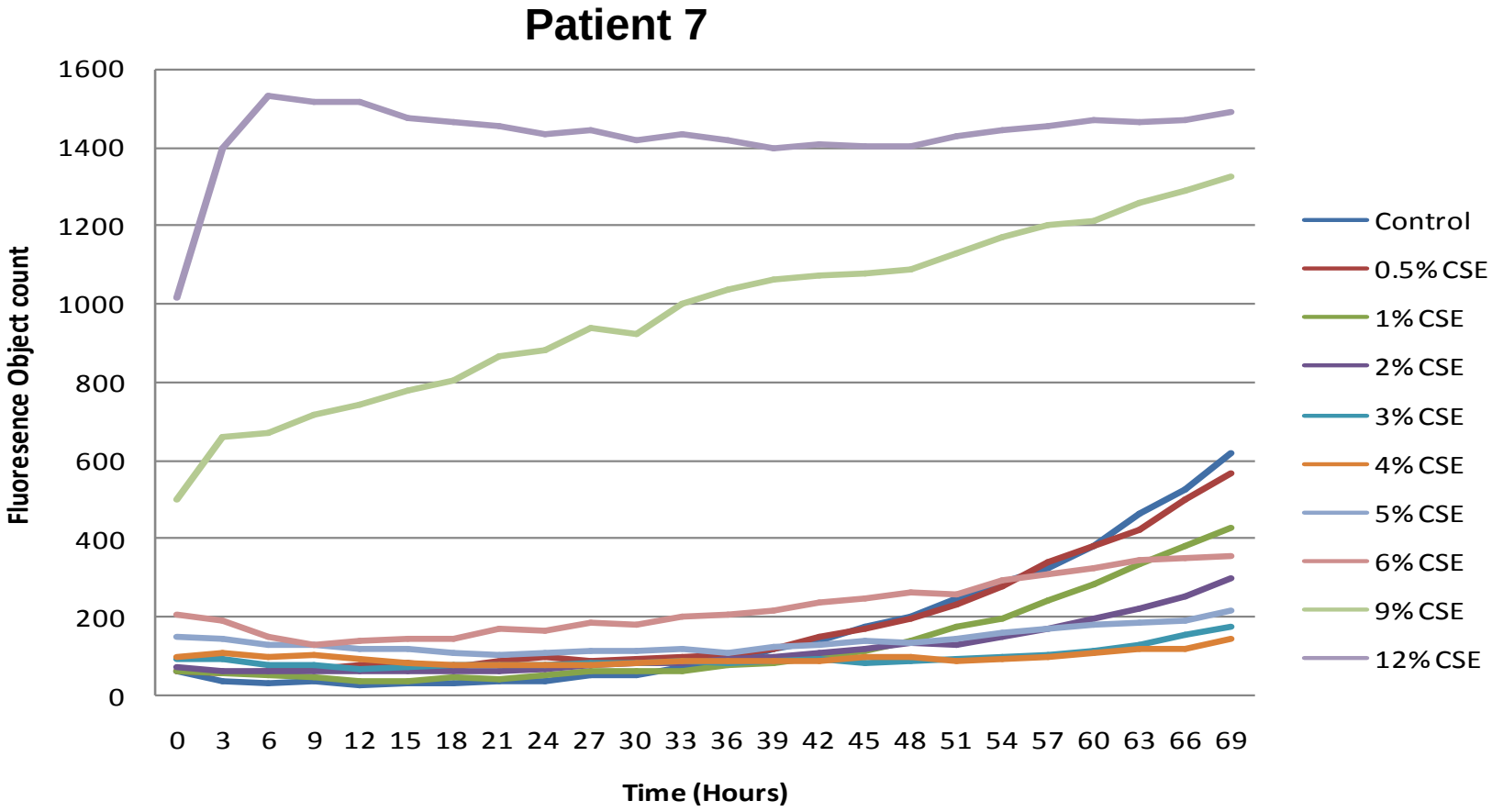


**Figure 5.11:** Apoptosis as detected via live cell imaging Nuc-view fluorescence counts over 72 hour time course in cells from patient 7 with emphysema (Patient 7). Similar to the previous experiment using LMVECs (Promocell), high counts were observed at the highest concentrations of CSE (9-12%). On these isolated emphysema cells, 5 and 6& CSE caused a slightly higher fluorescence count initially suggesting higher apoptosis. At lower concentrations of CSE (1-4%) similar to the Promocell experiment fluorescence was generally stable throughout while untreated and 05% treated cells showed increasing fluorescence over time.

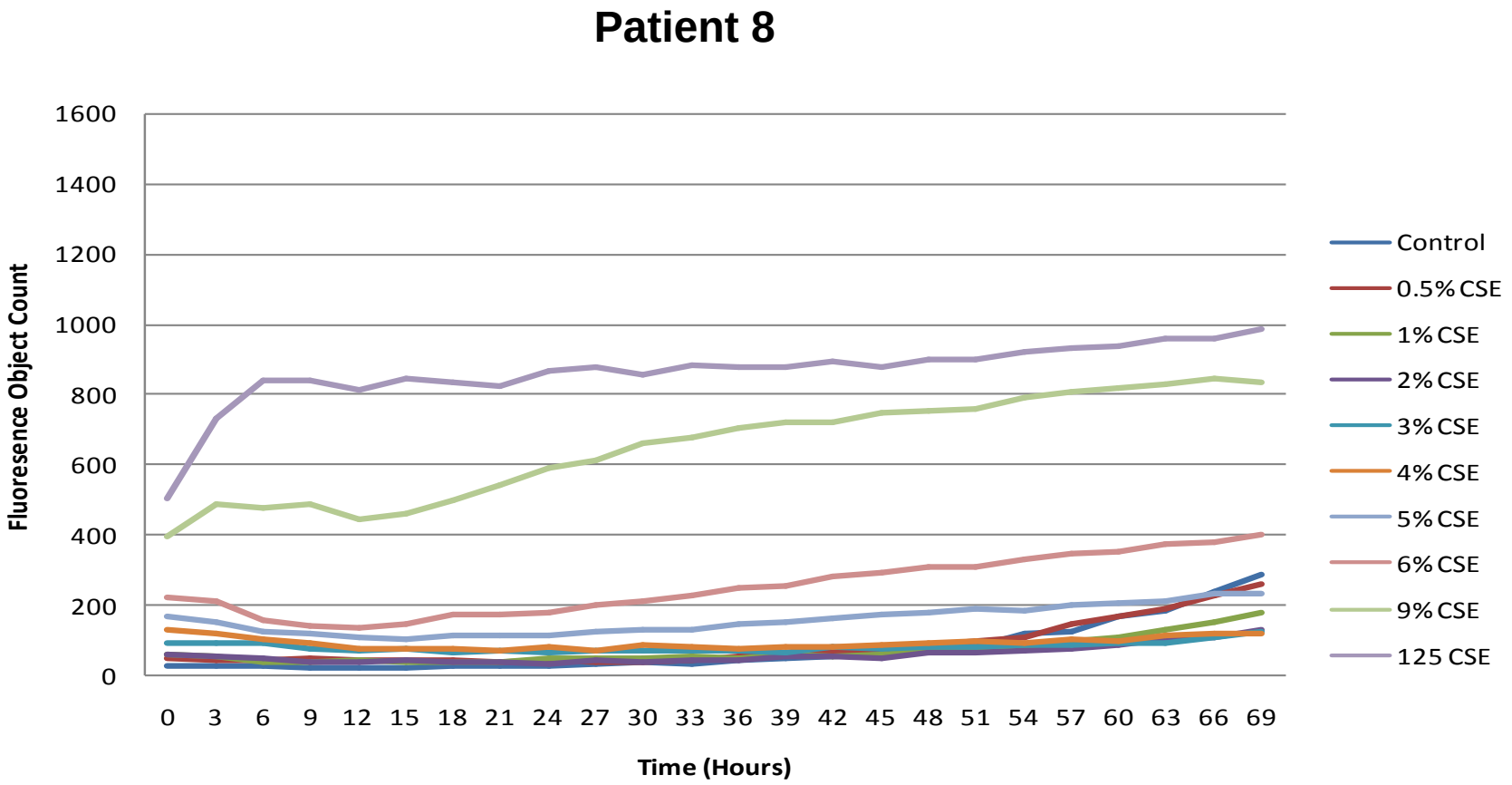


**Figure 5.12:** Apoptosis as detected via live cell imaging Nuc-view fluorescence counts over 72 hour time course in cells from patient 8 with emphysema. High fluorescence counts were observed at the highest concentrations of CSE (9-12%) with 5 and 6% also showing higher fluorescence counts in this experiment. Lower concentrations of CSE (1-4%) similar to the Promocell experiment fluorescence was generally stable throughout while untreated and 05% treated cells showed increasing fluorescence over time.

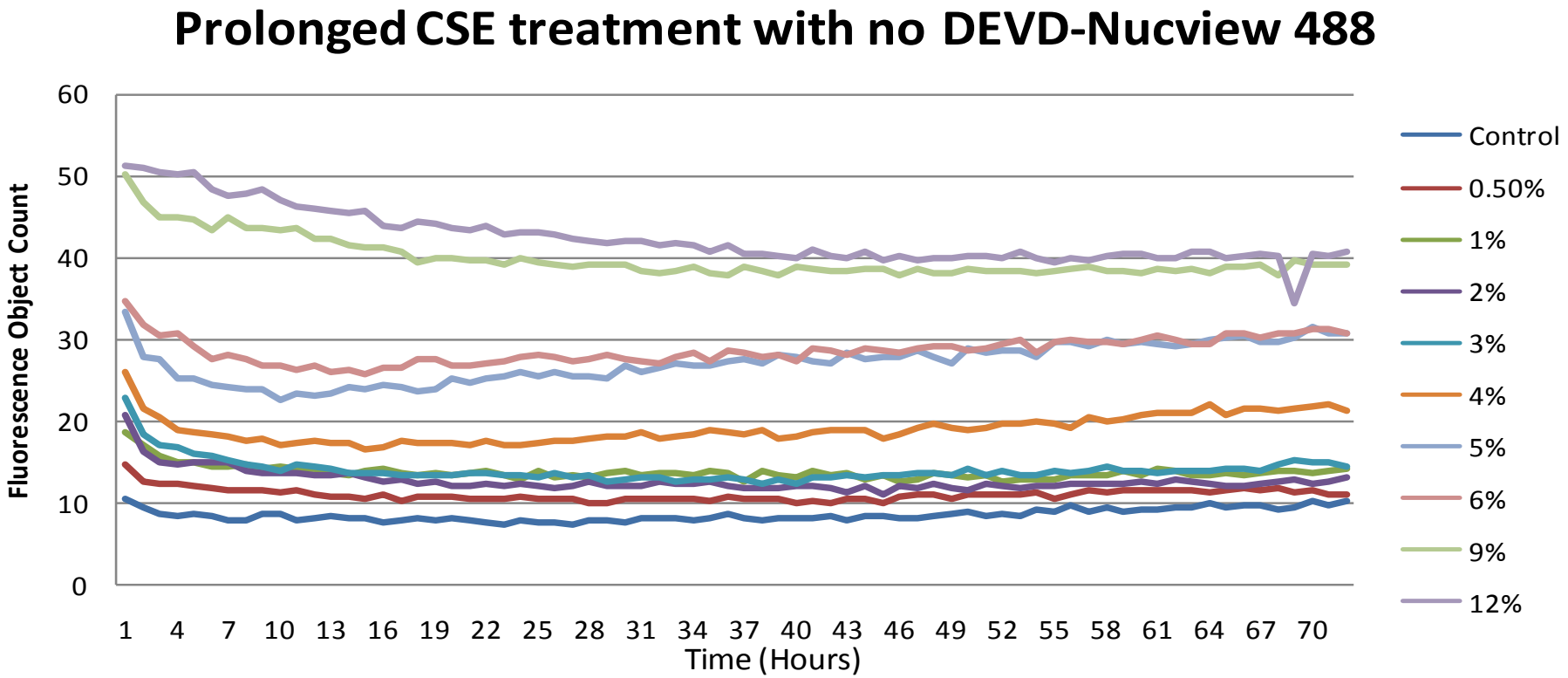


**Figure 5.13:** Mean autofluorescence of normal cells (Promocell) treated with varying concentrations of CSE (0-12%) as detected by fluorescence counts captured via live cell imaging over 72 hours. In this experiment, there was a stepwise increase in autofluorescence with increasing concentration of CSE. The highest fluorescence counts were observed at the highest concentrations of CSE (9-12%). At concentrations of 3% CSE or less, although greater than in control cells, autofluorescence was generally low.

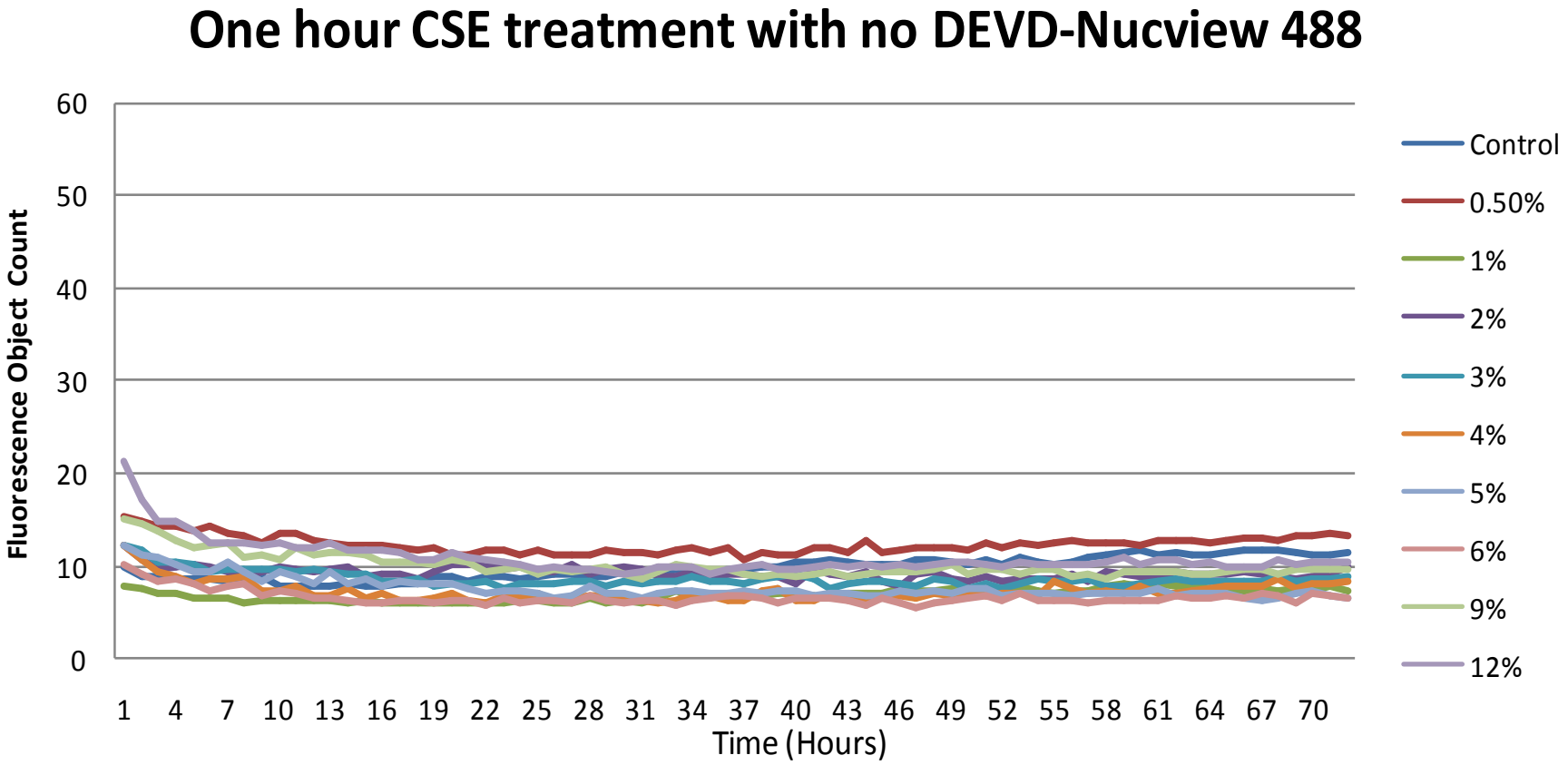


**Figure 5.14:** Mean autofluorescence of normal cells (Promocell) treated with varying concentrations of CSE (0-12%) for one hour and then followed for 72 hours. In this experiment, there was very low background autofluorescence with no difference between cells treated with 0.05% or 12% CSE.

In an attempt to model cigarette smoking closely, very short (fifteen minutes) CSE treatments to promocell cells and cells from 4 donors were conducted with the results shown below. Patients 2, 4 and 8 showed no response/ change in fluoresence counts and therefore no apoptosis over 90 hours (Figure 5.15). Promocell LMVECs showed no change in fluoresence counts initially with a late rise (after 48 hours) in fluoresence counts that was not dose dependant and actually was greatest for the control (untreated cells) (Figure 5.16a). Similarly patient 7 treated for fifteen minutes showed initially no change in fluoresence counts but a late rise (after 48 hours) with again the control cells and low concentration treated cells showing higher fluoresence counts than the cells treated with higher concentrations (Figure 5.16b). These experiments suggest that such a short CSE treatment was not sufficient to stress cells, with some donors showing no treatment response and in others the control cells had more cell death than the treated cells. This supports data which shows the effect of smoking a single cigarette persists for much longer than the time taken to smoke the cigarette. Therefore the short exposure (1 hour) and prolonged exposure experiments were therefore repeated and cellular responses further investigated.

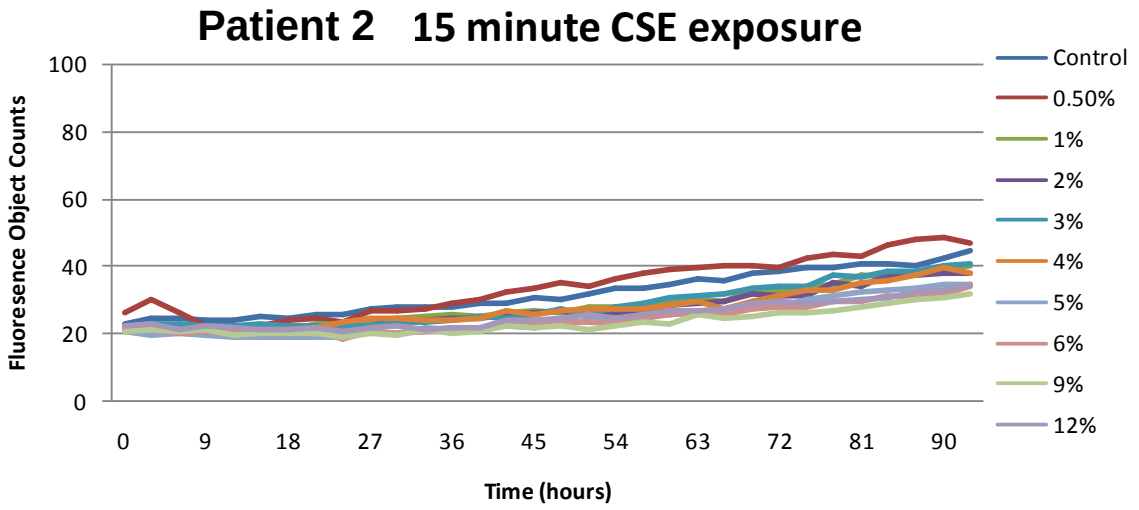


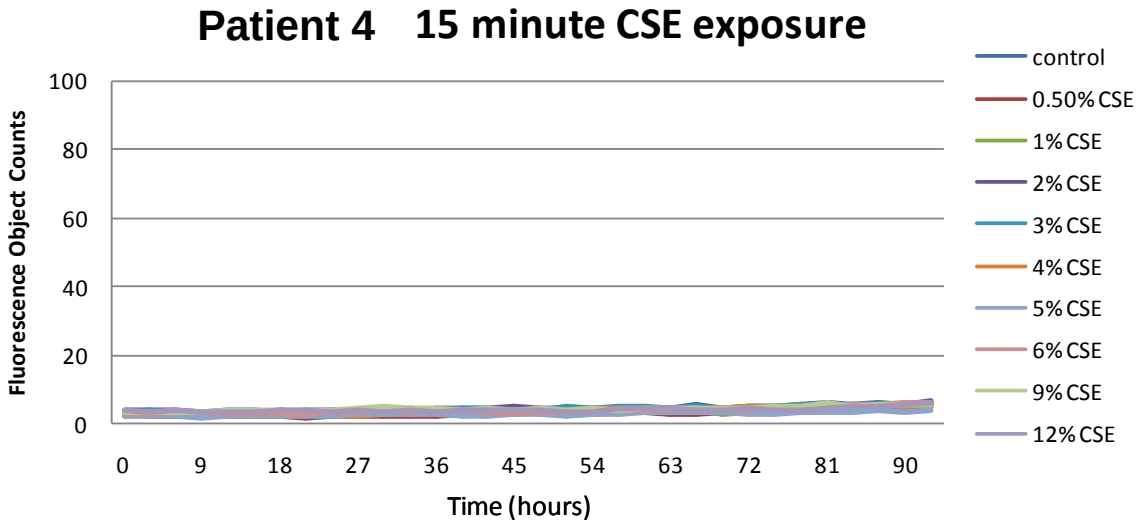


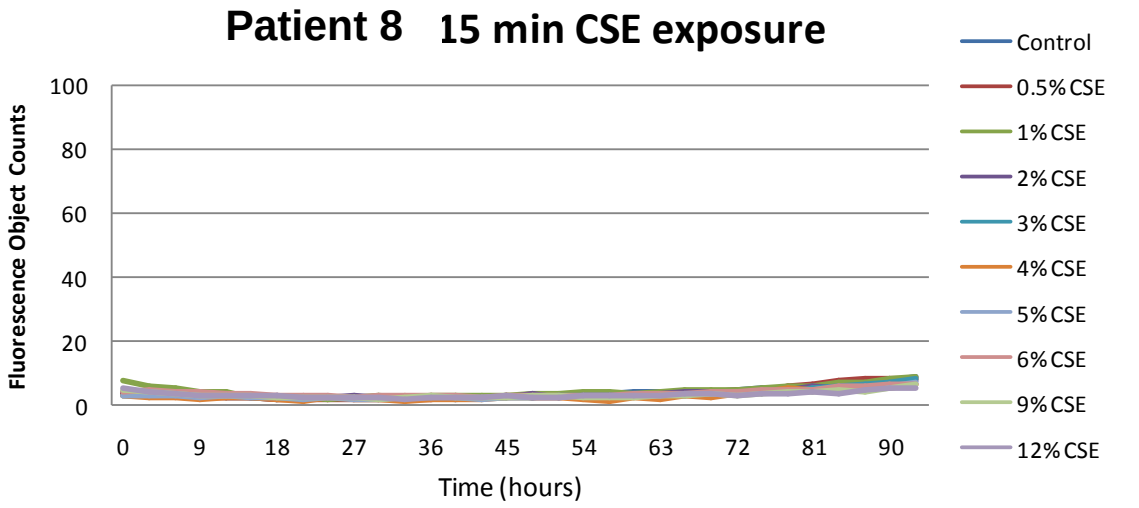


**Figure 5.15:** Cells from patients 2,4, and 8 treated with varying concentration of CSE (0-12%) for fifteen minutes and then apoptosis detected via DEVD Nucview-488 fluorescence counts via live cell imaging over 96 hours. There was no treatment effect observed in these cells in response to the very short fifteen minute treatment.

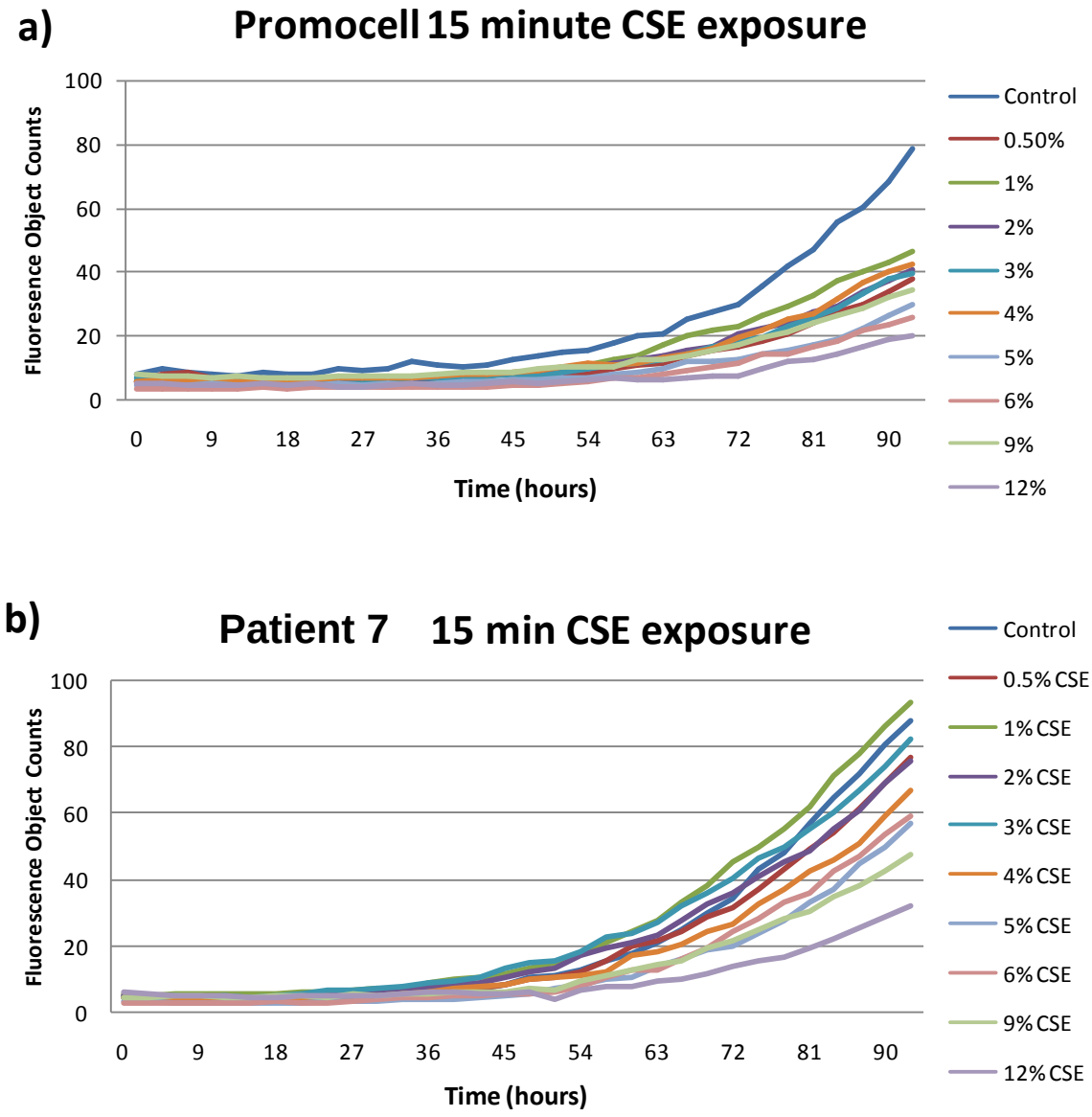


**Figure 5.16:** Promocell cells and cells from patient 7 treated with varying concentration of CSE (0-12%) for fifteen minutes with apoptosis thereafter detected via DEVD Nucview-488 fluorescence counts via live cell imaging over 96 hours. Promocell cells showed no change in fluoresence counts initially until a late increase (after 48 hours) in fluoresence counts that was not dose dependant and notably was greatest for the control (untreated cells) (Figure 5.17a). Similarly patient 7 treated for fifteen minutes showed initially no change in fluoresence counts. After 48 hours, once again there was an increase in fluoresence counts that was most evident among the untreated (control) cells and cells treated at low concentration (Figure 5.17b).

LMVECs (Promocell) and from patient 7 were grown to confluence on 96 well plates and treated (n=3) for either 1 hour (short exposure) or a prolonged expsoure with CSE and imaged for 64 hours. Although intitial experiments suggested that autofluorescence of cells was only encountered with the prolonged CSE exposure experiments (figure 5.13), all experiments included cells treated without DEVD Nucview-488 (n=3) to act as an internal control to assess autofluorescence in each individual experiment.

Promocell LMVECs treated with 0-12% CSE for one hour prior to cell imaging demonstrated high fluoresence counts (1 hour post treatment) above 6% CSE with lower fluorescence counts in cells treated with 5% CSE and lower (Figure 5.17a). This is likely to represent CSE induced autofluorescence of cells and is confirmed by Figure 5.17b which shows stepwise autofluorescence of cells treated with CSE in the absence of DEVD Nucview-488. Cells treated with concentrations of 4%CSE and above produced notable autofluorescence. In cells treated with 6-12% this was maximal at the start of imaging and fell over time. In 4% and 5% CSE treated cells this became maximal at 2 hours and then fell over time. Thus higher concentrations (>4% CSE) were therefore excluded from the analysis. The data for this experiment for concentrations up to 3% is presented in Figure 5.17c. When examining cells treated with up to 3% CSE compared with untreated (control) cells, there is no significant difference in fluoresence object counts at the start of imaging, however at 24 hours, the lines have become divergent, with statistically significant more fluoresencent object counts at 24 hours in the 3% CSE treated cells compared with control cells (P=0.05). To further investigate thisthe autofluorescence data obtained during this experiment (figure 5.17b) was subtracted from the data in figure 5.17c to examine whether this divergence at 24 hours between control and CSE treated cells persisted (Figure 5.17d). Figure 5.17d which shows divergence of lines at 24 hours with similar fluorescence counts for 1-3% treated CSE cells, however this failed to reach statistical significance and so did not confirm apoptsis.

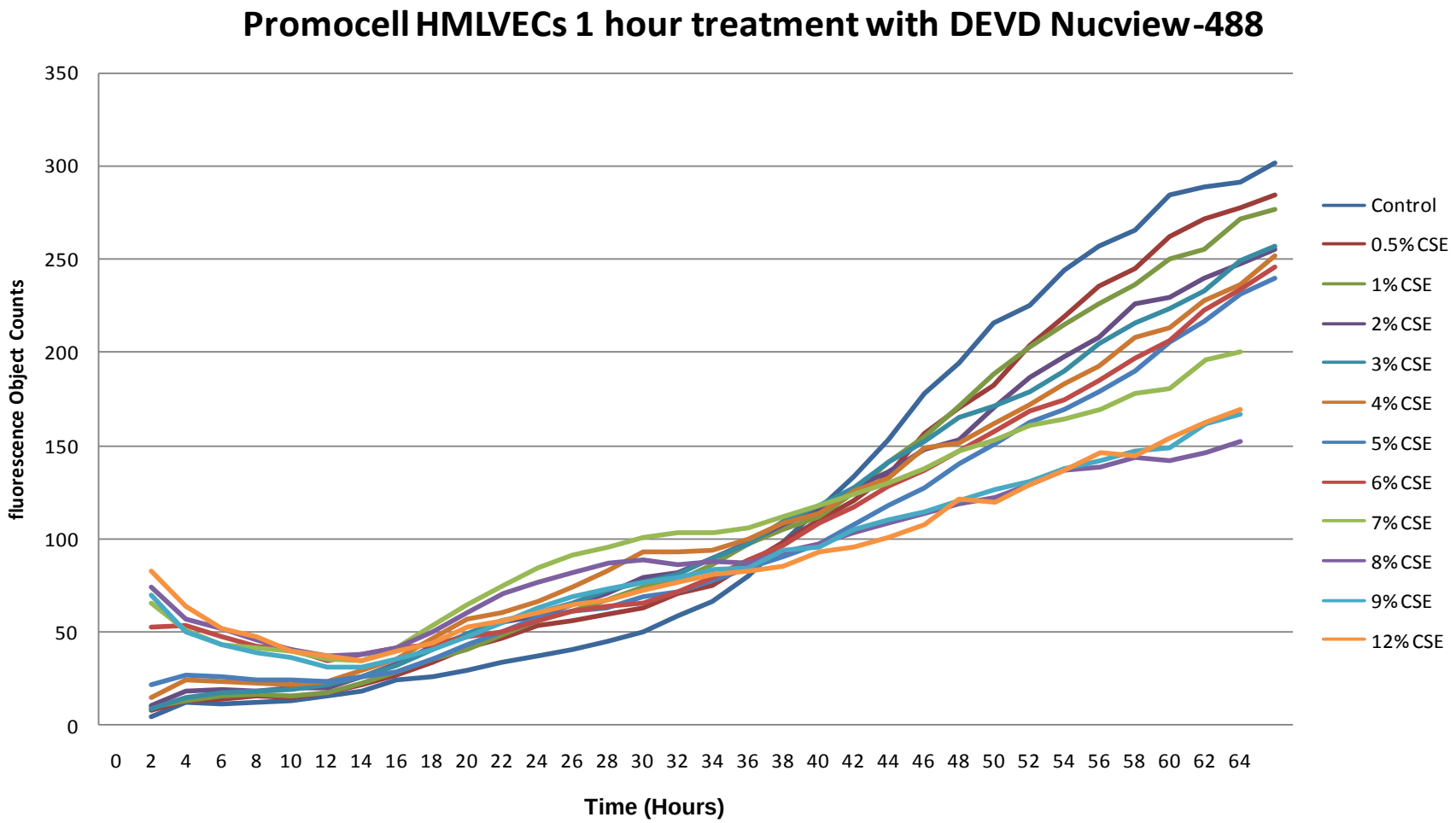


**Figure 5.17a:** Fluorescence counts of cells (Promocell) treated with varying concentrations of CSE (0-12%) for one hour and then imaged for 64 hours.

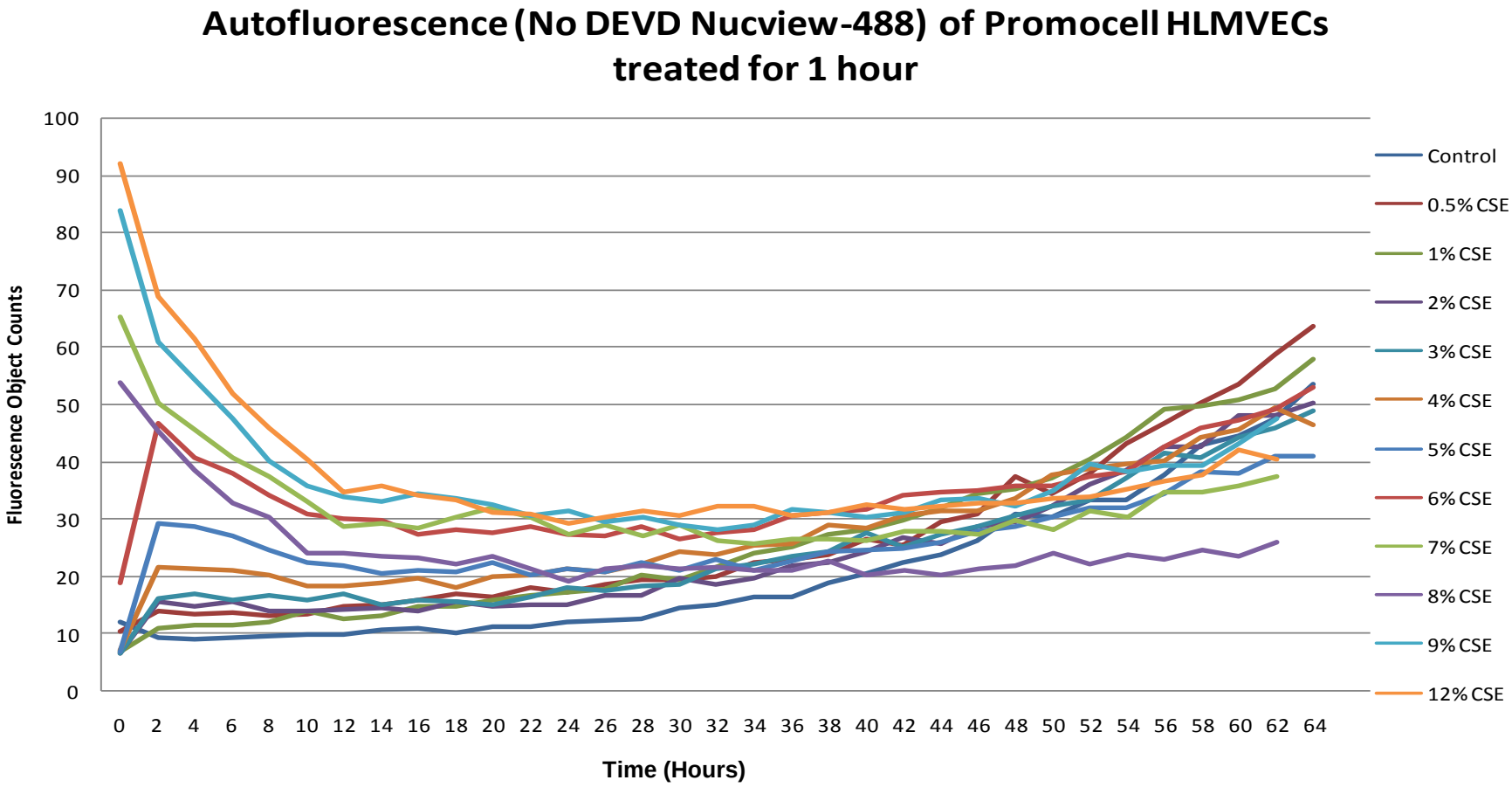


**Figure 5.17b:** Autofluorescence of CSE treated cells (Promocell) (0-12%) for one hour and then imaged for 64 hours. Increasing autofluorescence was seen with increasing concentration of CSE. This was apparent from concentrations greater than 3%.

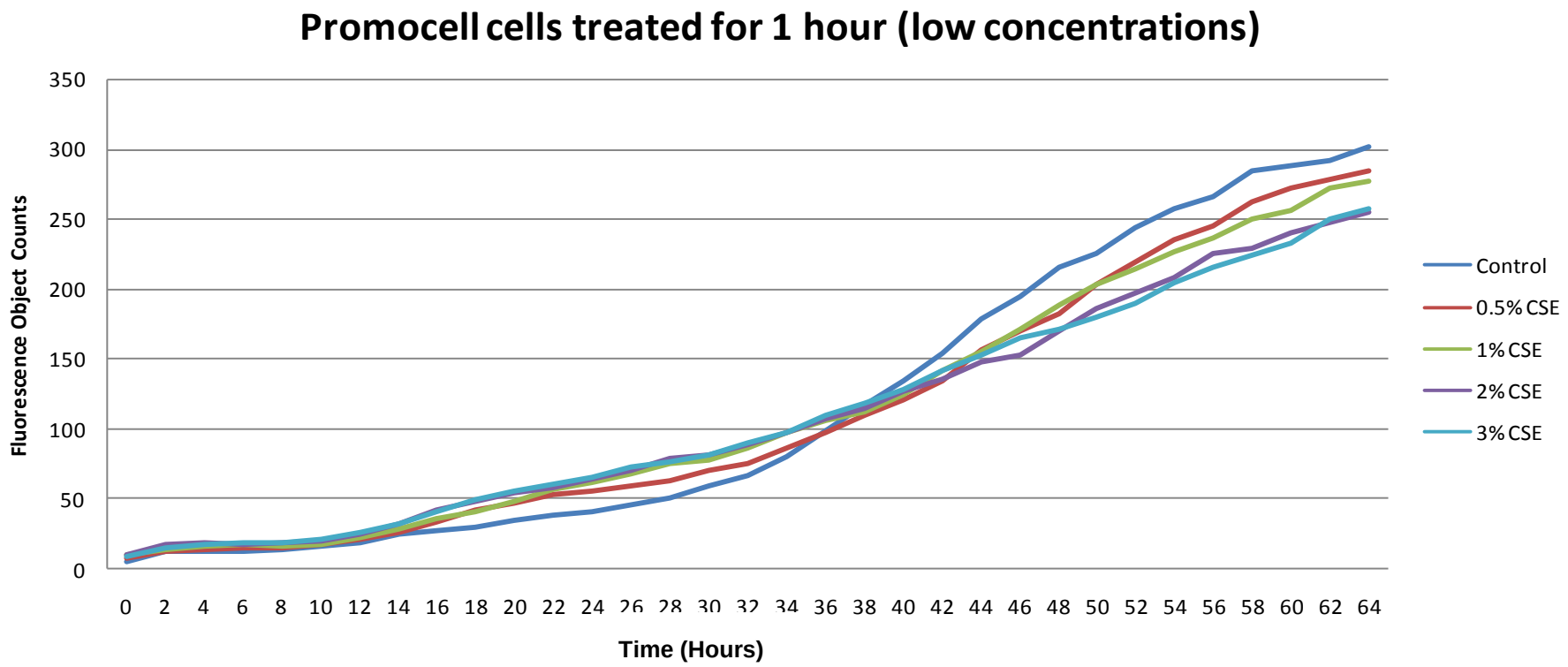


**Figure 5.17c:** Promocell HLMVECs treated with low dose (0-3%) CSE and followed for 64 hours.

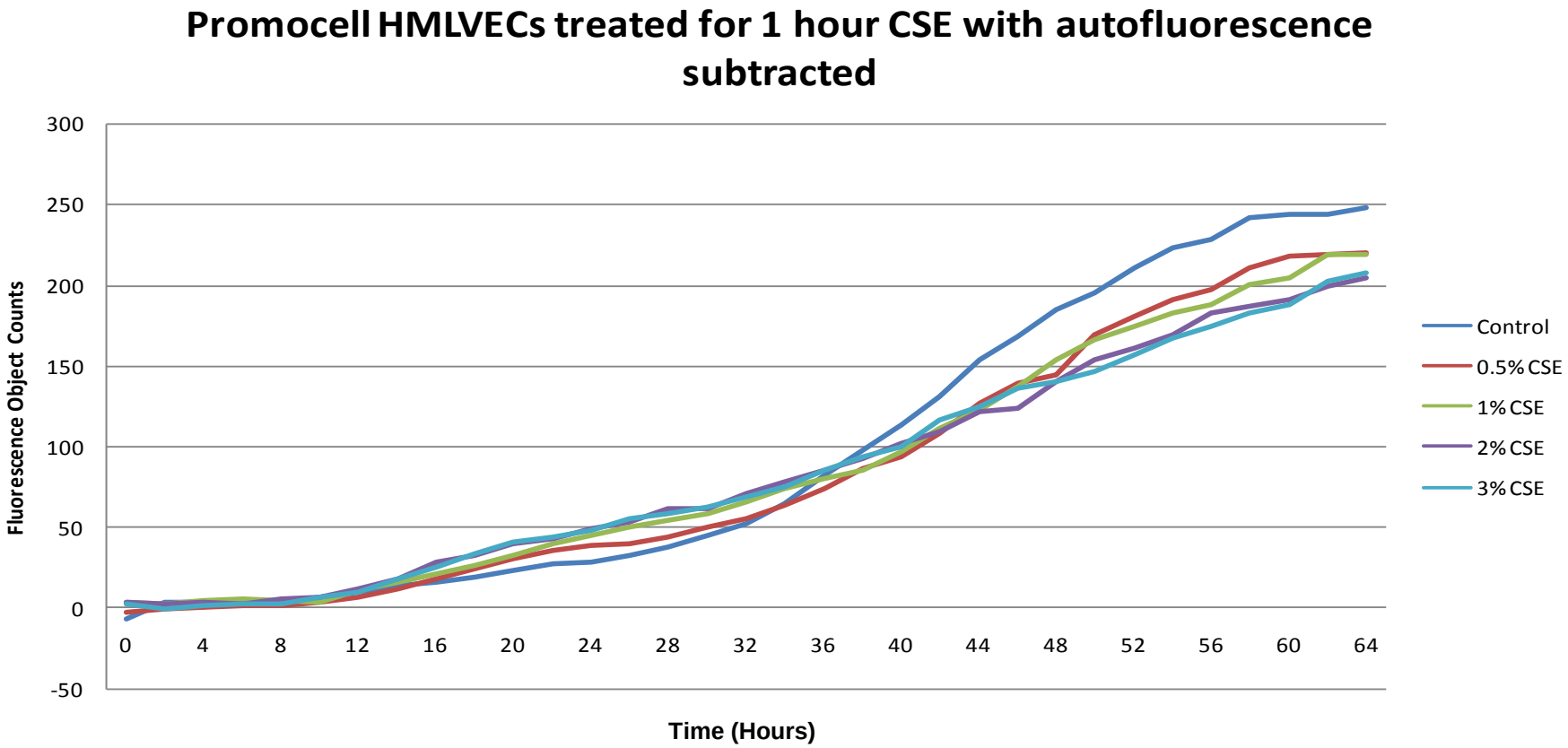


**Figure 5.17d:** Promocell HLMVECs treated with low dose (0-3%) CSE and followed for 64 hours. Data shown here includes subtraction of autofluorescence from all data points.

LMVECs (Promocell) were treated with a prolonged exposure to CSE (concentration 0-3%) and followed for 64 hours via live cell imaging to detect apoptosis via DEVD Nucview-488 Fluorescence counts. At the start of imaging higher fluorescence counts were observed in the CSE treated than control cells (Figure 5.18a). However this quickly became similar in all groups, including control (untreated cells). At 24 hours, there was divergence of the lines between the treated and untreated cells with greater fluorescence counts in the CSE treated cells. By 36 hours fluorescence counts started to increase in the control (untreated) cells to such an extent that by 64 hours there was an inverse relationship between CSE treatment and fluorescence counts. Autofluorescence was investigated as before in tandem with this experiment with all concentrations examined in triplicate for fluorescent counts with increasing concentration of CSE in the absence of DEVD Nucview-488. Control and 0.5% CSE treated cells had very low autofluorescence at baseline (Figure 5.18b). Over time this increased. Cells treated with 1 and 2% CSE had initial high autofluorescence that fell, remained stable and then demonstrated a late rise. In this experiment, cells treated with 3% CSE had surprisingly low autofluorescence at baseline that then increased and remained high. This result in not keeping with the previous however was similar across all values (n=3). The autofluorescence observed in the experiment with 3% CSE treated cells cannot be easily explained. To examine the effect of autofluorescence in this experiment, fluorescence counts observed in sham treated cells were subtracted from the fluorescence counts observed with the DEVD Nucview-488 cells as before (Figure 5.17c). Control cells had no fluorescent counts at baseline but began to rise at 24 hours and became highest at 64 hours. 0.5, 1 and 2% CSE treated cells had initially higher fluorescence counts that fell and then gradually rose with divergence from control cells at 24 hours, which may support CSE induced apoptosis. As previous, the results observed for the 3% CSE treated cells in this experiment are difficult to interpret but are presented for completeness.

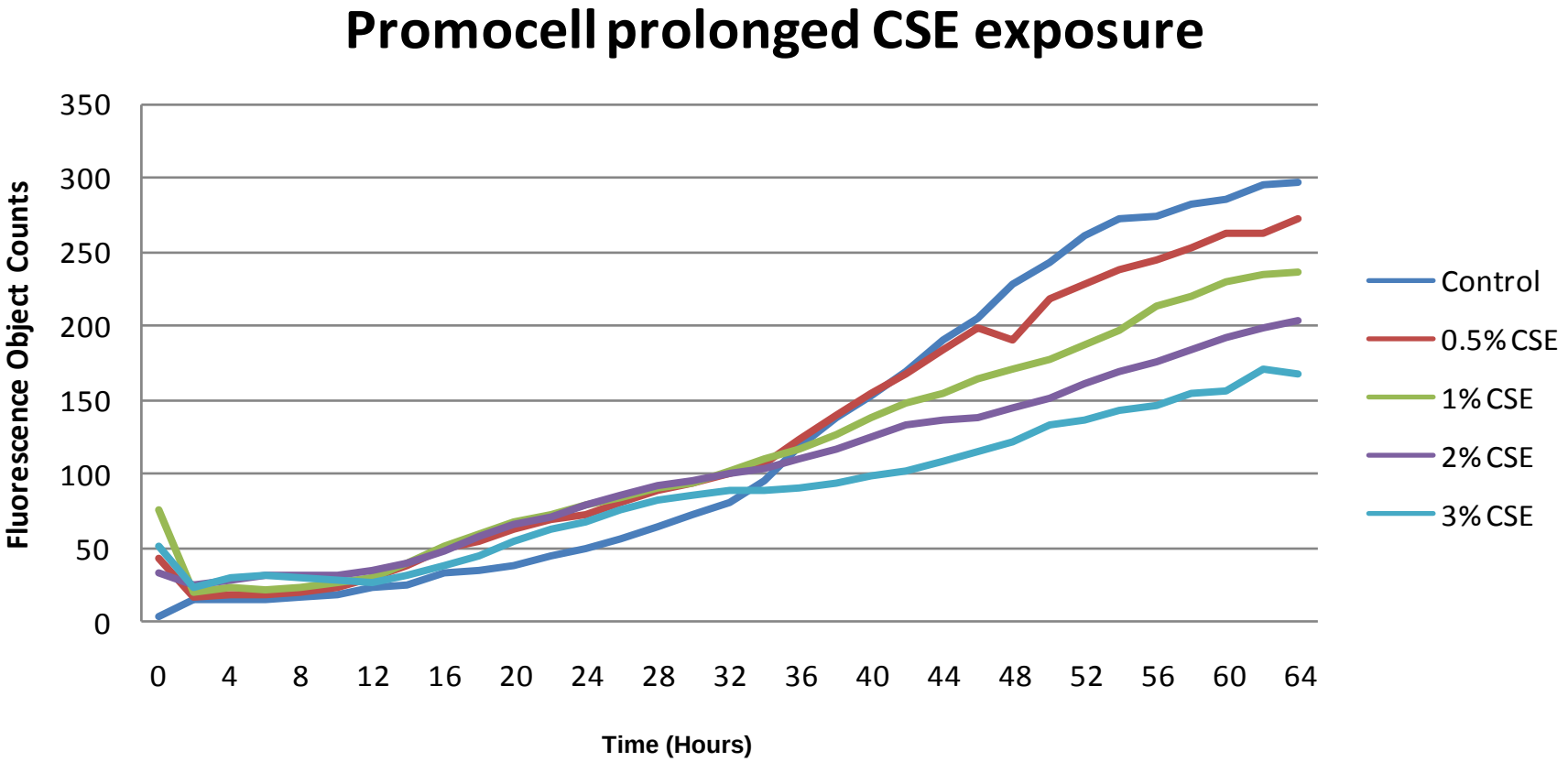


**Figure 5.18a:** Promocell LMVECs treated with low dose (0-3%) CSE and followed for 64 hours via live cell imaging to detect apoptosis via DEVD Nucview-488 Fluorescence counts. Immediately after treatment at the start of imaging there was higher counts in the CSE treated than control cells. However this quickly became similar in all groups. At 24 hours there was divergence of the lines between the treated and untreated cells with greater fluorescence counts in the CSE treated cells. At 36 hours fluorescence counts started to increase in the control (untreated) cells to such an extent that by 64 hours there was an inverse relationship between CSE treatment and fluorescence counts.

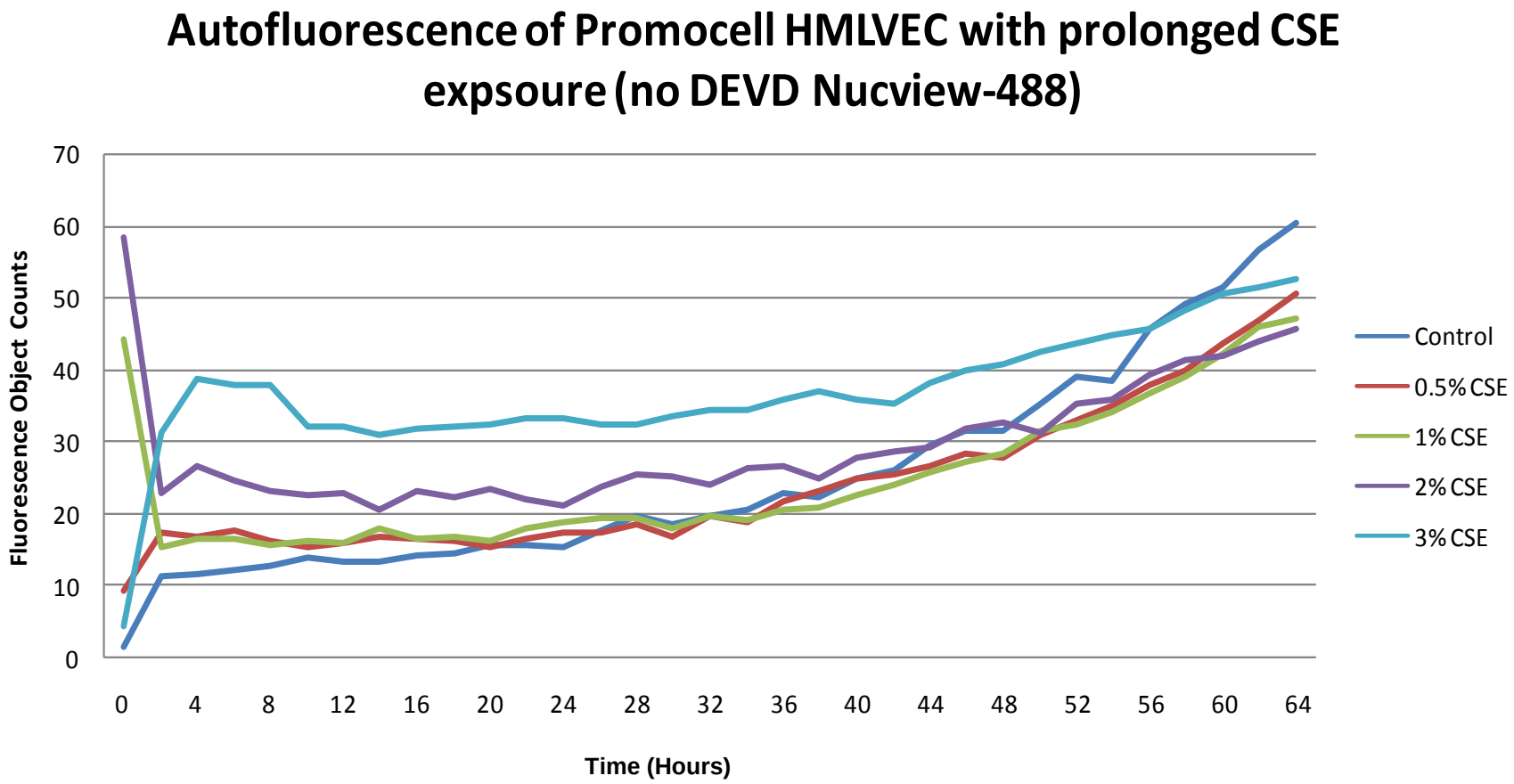


**Figure 5.18b:** Promocell HLMVECs treated with low dose (0-3%) CSE and followed for 64 hours via live cell imaging with no DEVD Nucview-488 added to detect background autofluorescence due to CSE. Control cells at baseline had very low autofluorescence. Similarly cells treated with 0.5% CSE had similar low autofluorescence at baseline and then increased with time. Cells treated with 1 and 2% CSE had initial high autofluorescence that fell, remained stable and then demonstrated a late rise. In this experiment, cells treated with 3% CSE had surprisingly low autofluorescence at baseline that then increased and remained high. This result in not keeping with the previous however was similar across all values (n=3).

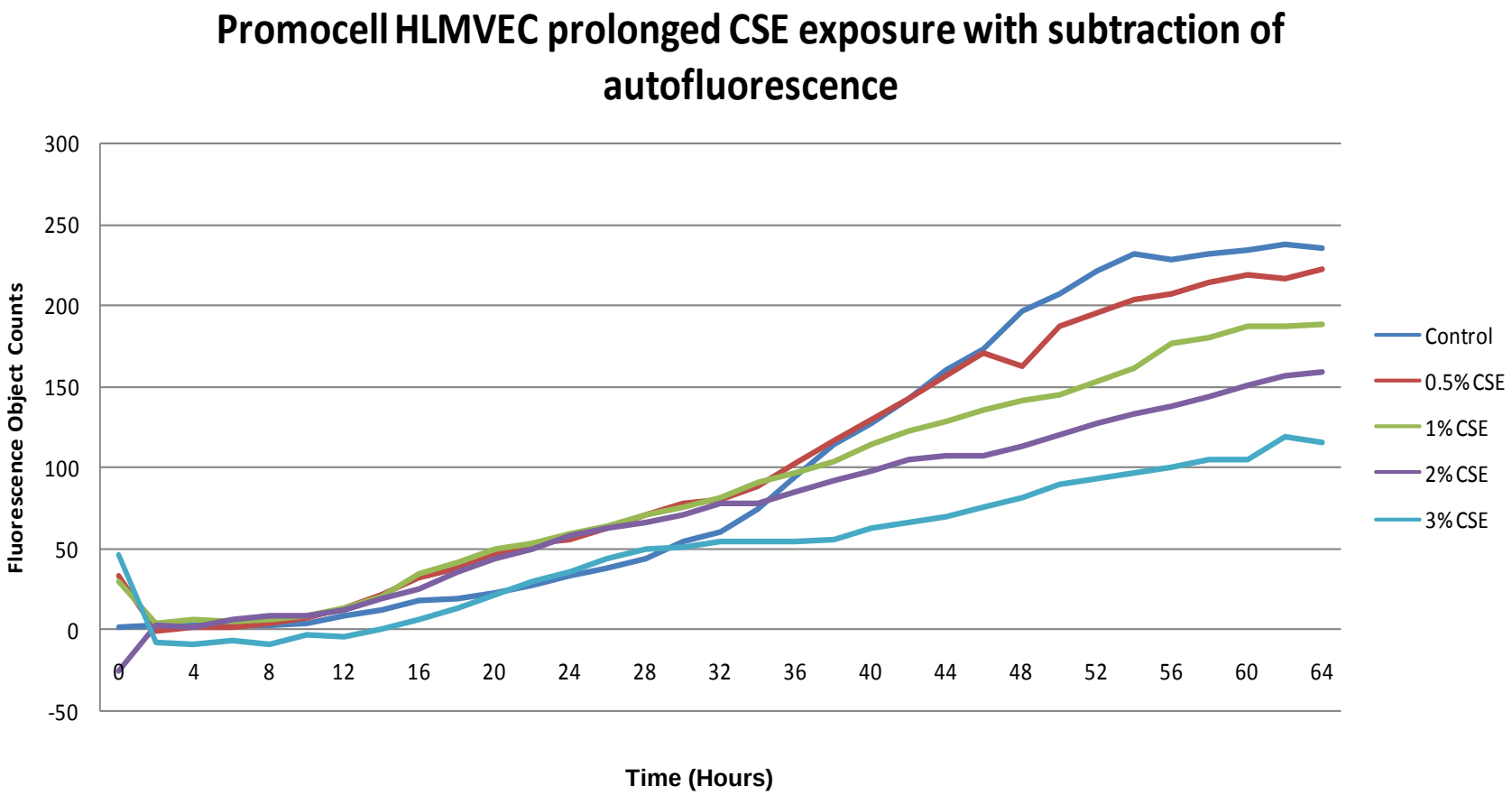


**Figure 5.18c:** Promocell HLMVECs treated with low dose (0-3%) CSE and followed for 64 hours via live cell imaging to detect apoptosis via DEVD Nucview-488 fluorescence counts with autofluorescence subtracted. Control cells had no fluorescent counts at baseline but began to rise at 24 hours and became highest at 64 hours. 0.5, 1 and 2% CSE treated cells had initially higher fluorescence counts that fell and then gradually rose with divergence from control cells at 24 hours. As previous, the results observed for the 3% CSE treated cells in this experiment are difficult to interpret but are presented for completeness.

LMVECs from patient 7were also treated with CSE for short 1 hour exposure and a prolonged exposure and analysed as previously. LMVECs isolated from patient 7 and thentreated with 0-12% CSE for one hour prior to cell imaging demonstrated high fluoresence counts (1 hour post treatment) above 5% CSE (Figure 5.19a) similar to the promocell cells (Figure 5.18a). This CSE induced autofluorescence of cells is confirmed by Figure 5.19b which shows stepwise autofluorescence of cells treated with CSE in the absence of DEVD Nucview-488, most notably for the cells treated with 9 and 12% CSE. Cells treated with concentrations of 5%CSE and above produced most autofluorescence and were therefore excluded from the analysis. The data for this experiment for concentrations up to 4% is presented in Figure 5.19c. Cells treated with up to 4% CSE compared with untreated (control) cells show no difference in fluoresence object counts at the start of imaging, however at 24 hours, the lines have become divergent, with statistically significant more fluoresencent object counts at 24 hours in the 1% CSE treated cells compared with control cells (P=0.048).This result was similar to that observed in Promocell LMVECs, but occurred at lower concentration of CSE in the emphysema cells (patient 7). Tofurther investigate this,the autofluorescence data obtained during this experiment (figure 5.19b) was subtracted from the data in figure 5.19c to examine whether this divergence at 24 hours between control and CSE treated cells persisted (Figure 5.19d). Figure 5.19d which shows divergence of lines between 24 and 48 hours most notably for the lowest dose of CSE treatment (0.5% and 1% CSE) but this failed to reach statistical significance and so did not comfirm apoptosis.

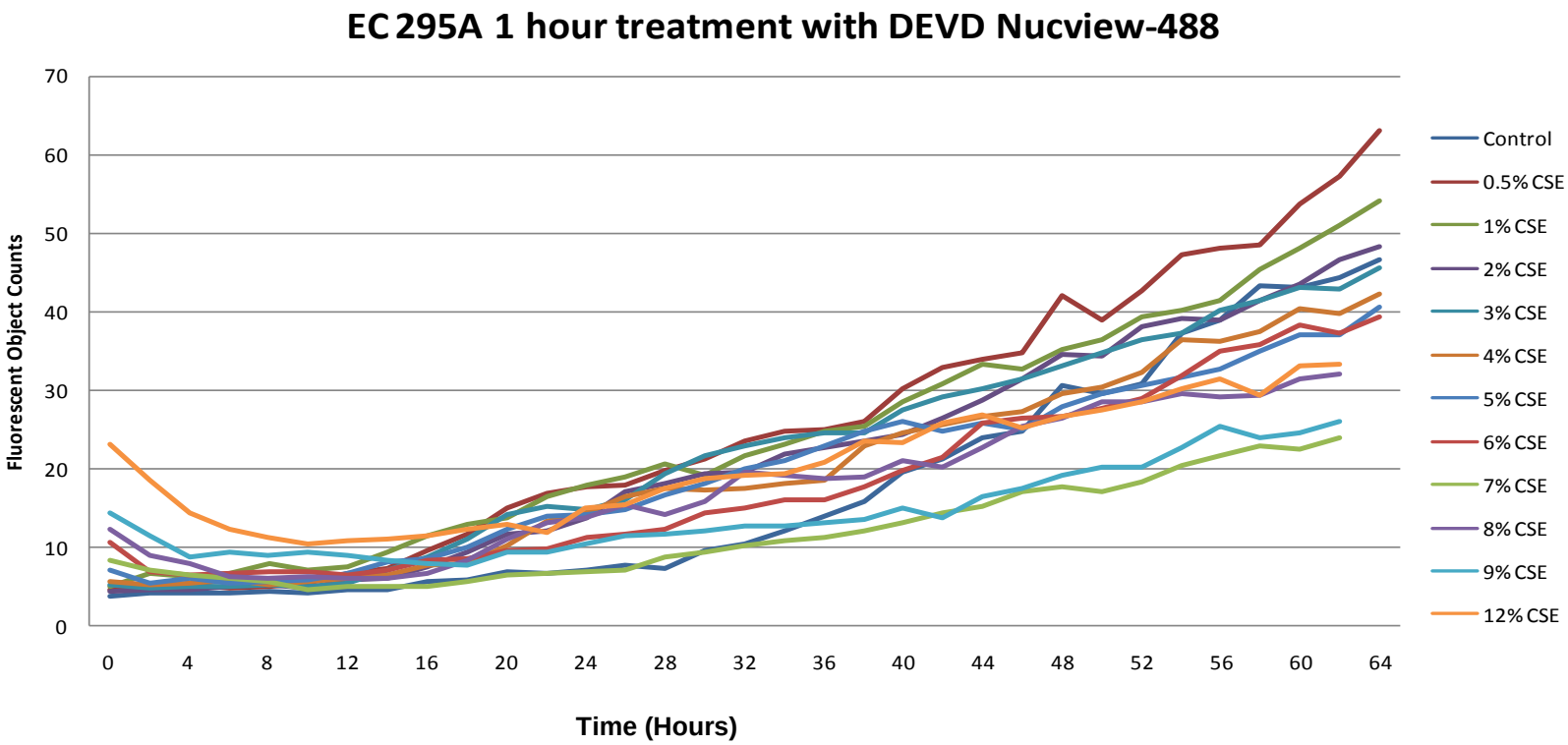


**Figure 5.19a:** Fluorescence counts of emphysema primary LMVECs (patient 7, EC295A) treated with varying concentrations of CSE (0-12%) for one hour and then imaged for 64 hours.

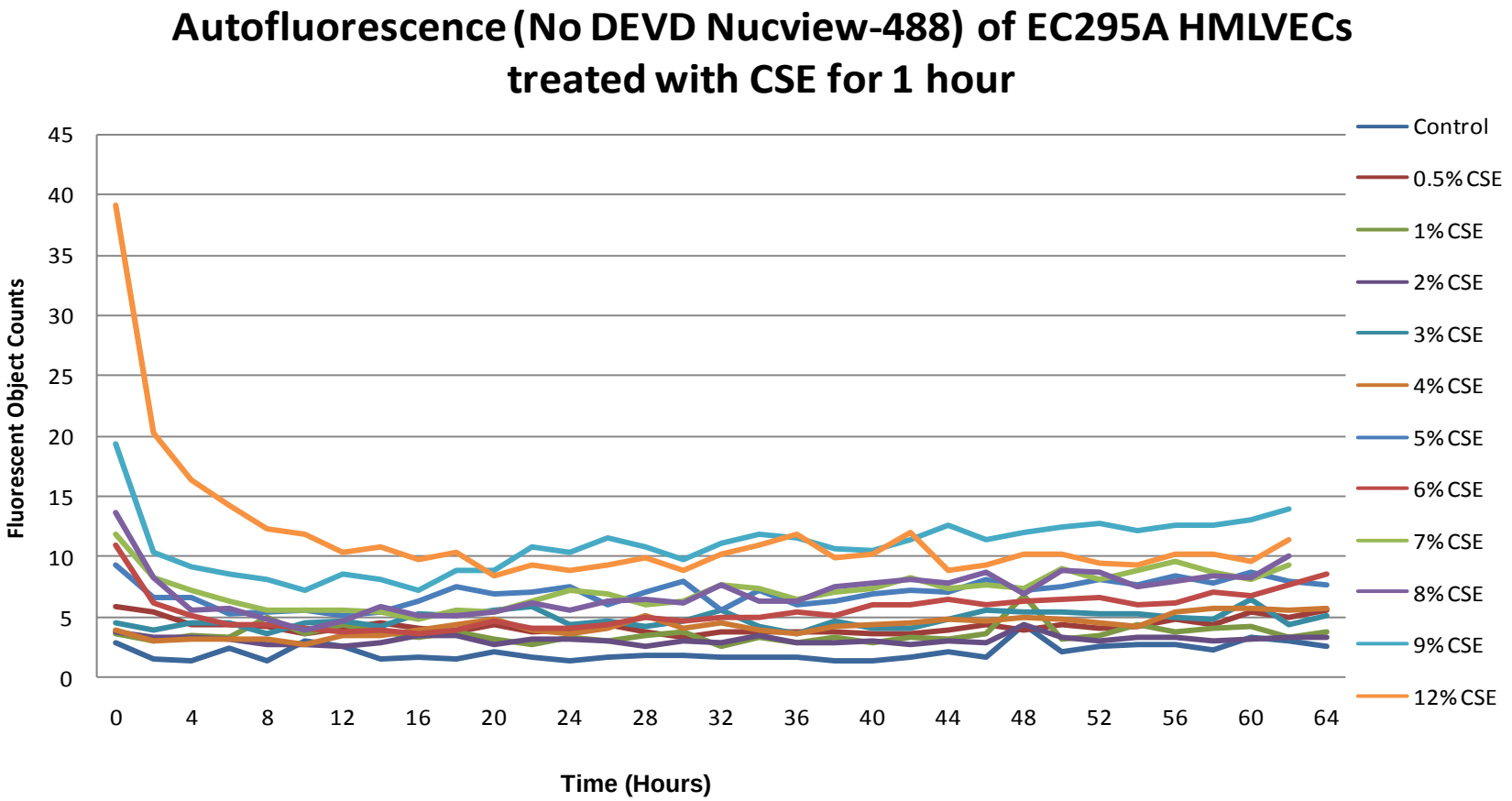


**Figure 5.19b:** Autofluorescence of patient 7 cells (EC295A) (0-12%) for one hour and then imaged for 64 hours. Increasing autofluorescence was seen with increasing concentration of CSE.

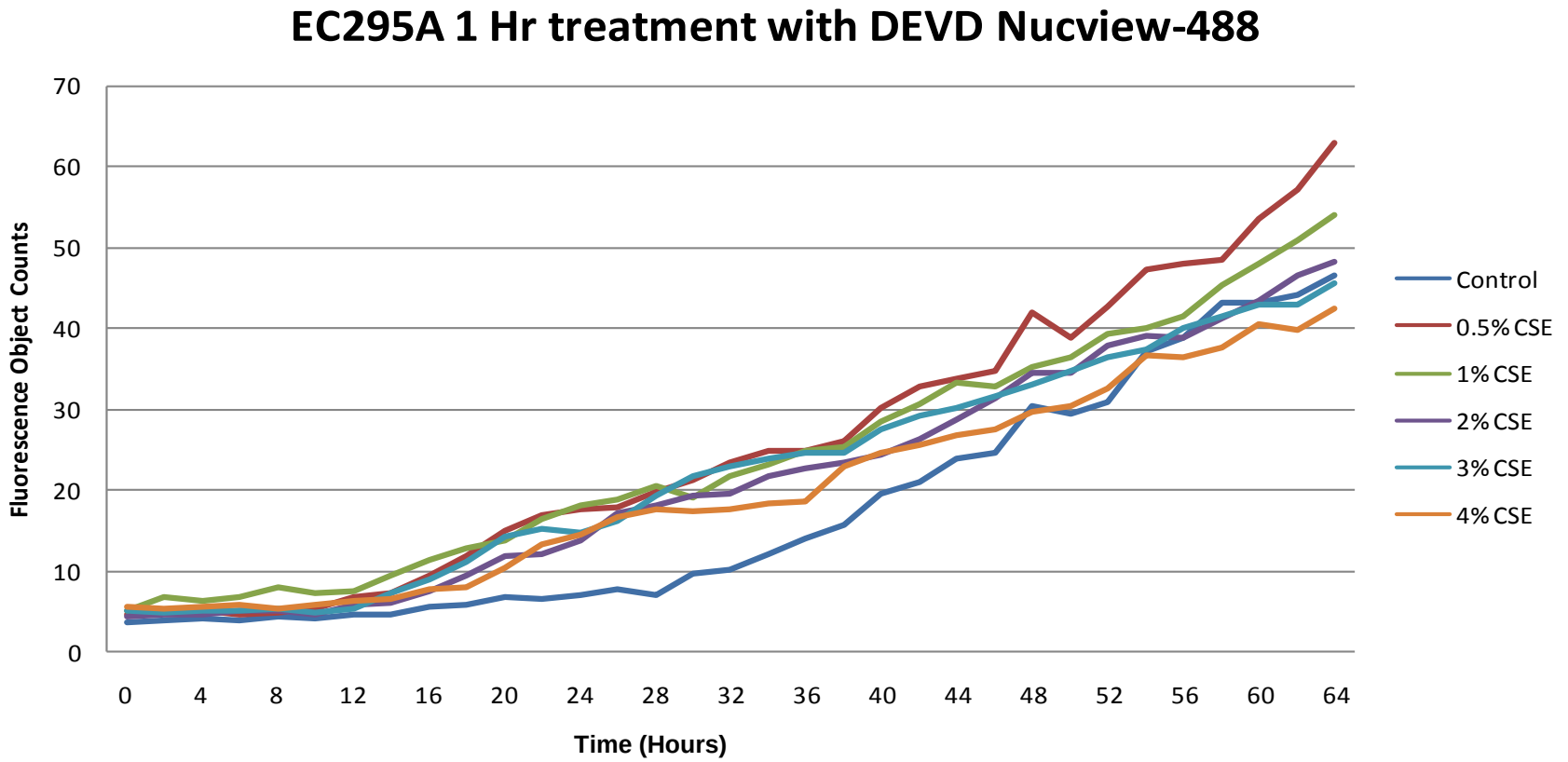


**Figure 5.19c:** HLMVECs isolated from patient 7 (EC295A) treated with low dose (0-3%) CSE and followed for 64 hours via DEVD Nucview-488 live cell fluorescence imaging.

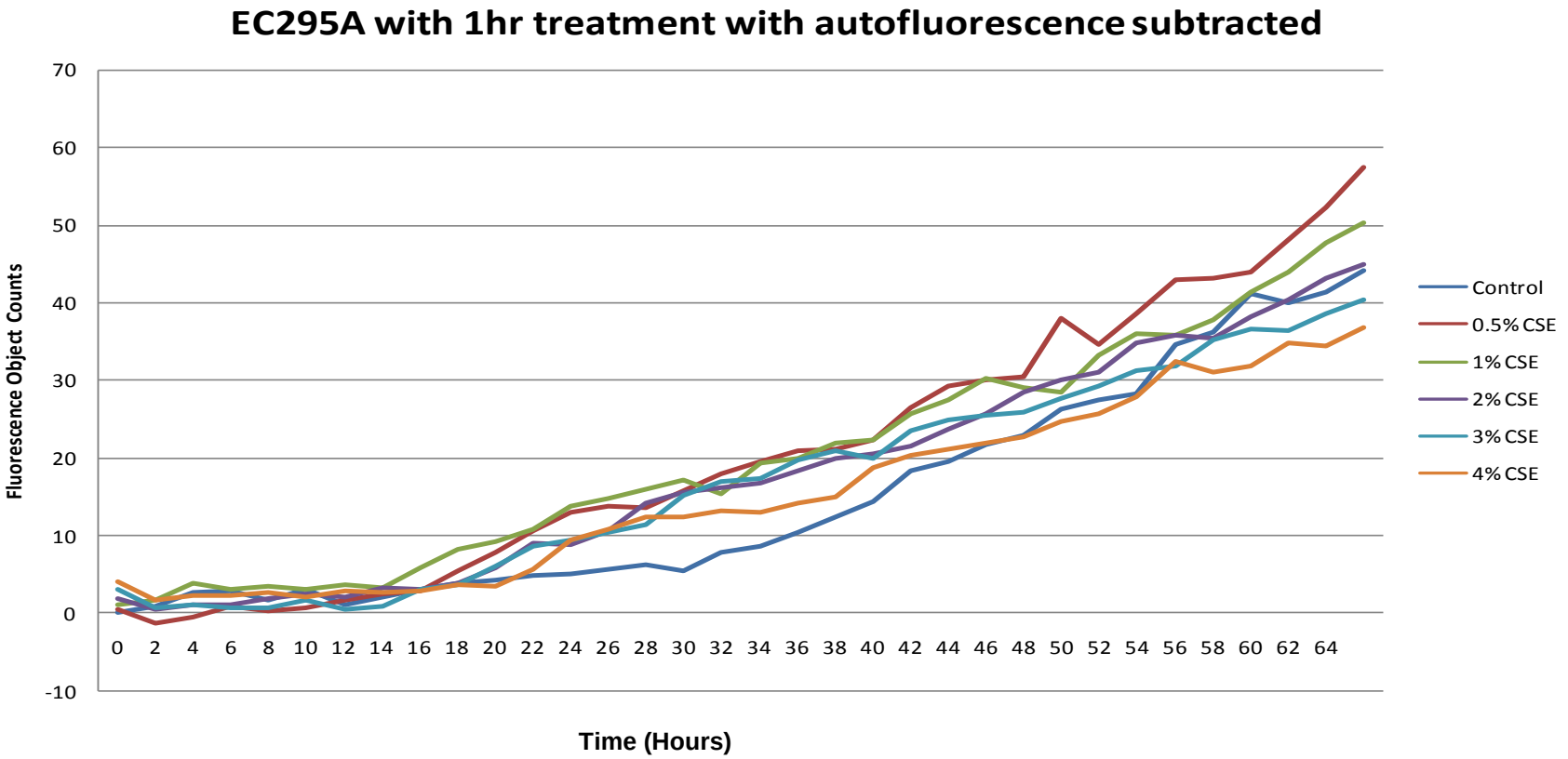


**Figure 5.19d:** HLMVECs isolated from patient 7 (EC295A) treated with low dose (0-3%) CSE and followed for 64 hours via DEVD Nucview-488 live cell fluorescence imaging with autofluorescence subtracted.

Emphysema LMVECs (patient 7) were treated with a prolonged exposure to low dose CSE (concentration 0-3%) and followed for 64 hours via live cell imaging to detect apoptosis via DEVD Nucview-488 Fluorescence counts. All cells treated had similar fluorescence object counts for the first 12 hours (Figure 5.20a). Thereafter there was divergence of fluorescence counts with CSE treated cells (notably the lowest doses 0.5-1% CSE) showing greater counts than the control cells. By 48 hours fluorescence counts had begun to converge again, although the low dose CSE treated cells continued to be divergent. Autofluorescence was investigated as before in tandem with this experiment with all concentrations examined in triplicate with increasing concentration of CSE in the absence of DEVD Nucview-488. Control and 0.5% CSE treated cells had very low autofluorescence (Figure 5.20b) and unlike the Promocell experiment this remained largely unchanged over time. Cells treated with 1-3% CSE demonstrated a stepwise increase in autofluorescence. All cells including control cells showed a transient increase in fluorescence counts at 48 hours. This is likely to represent a technical signaling error of the equipment and should not be interpreted as a real effect as was seen in all cells. Autofluorescence (Figure 5.20b) was subtracted as before from original data (Figure 5.20a) to give fluorescence count data taking into account autofluorescence (Figure 5.20c). There was no difference in fluorescence in the first 12 hours. After 12 hours, cells treated with very low dose (0.5-1% CSE) had more fluorescence counts observed than control cells, suggesting apoptosis in response to CSE. As in previous experiments, the results observed for 2-3% CSE treated cells in are difficult to interpret due to the high autofluorescence but are presented for completeness.

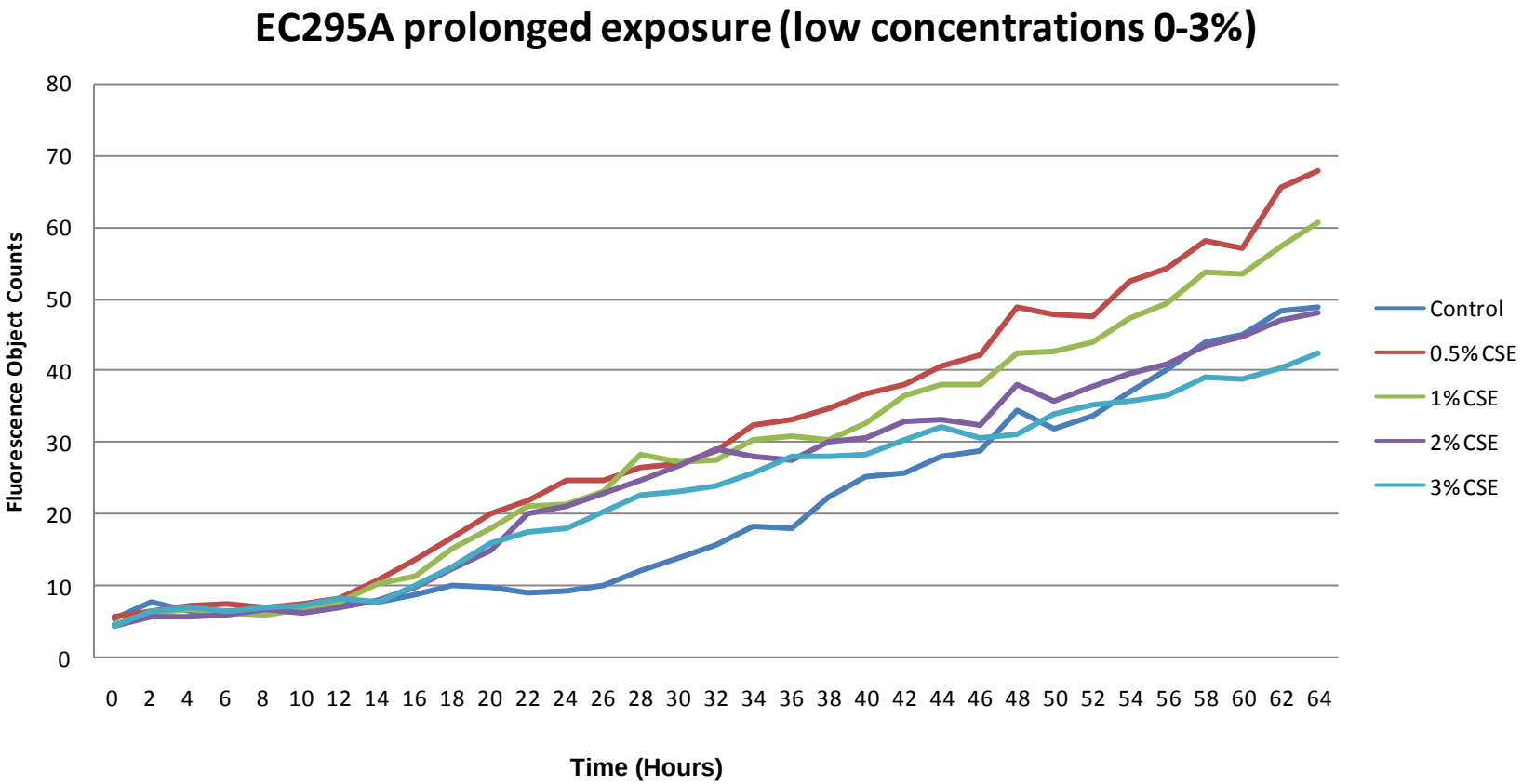


**Figure 5.20a:** HLMVECs isolated from patient 7 (EC295A) treated with low dose (0-3%) CSE and followed for 64 hours via DEVD Nucview-488 live cell imaging.

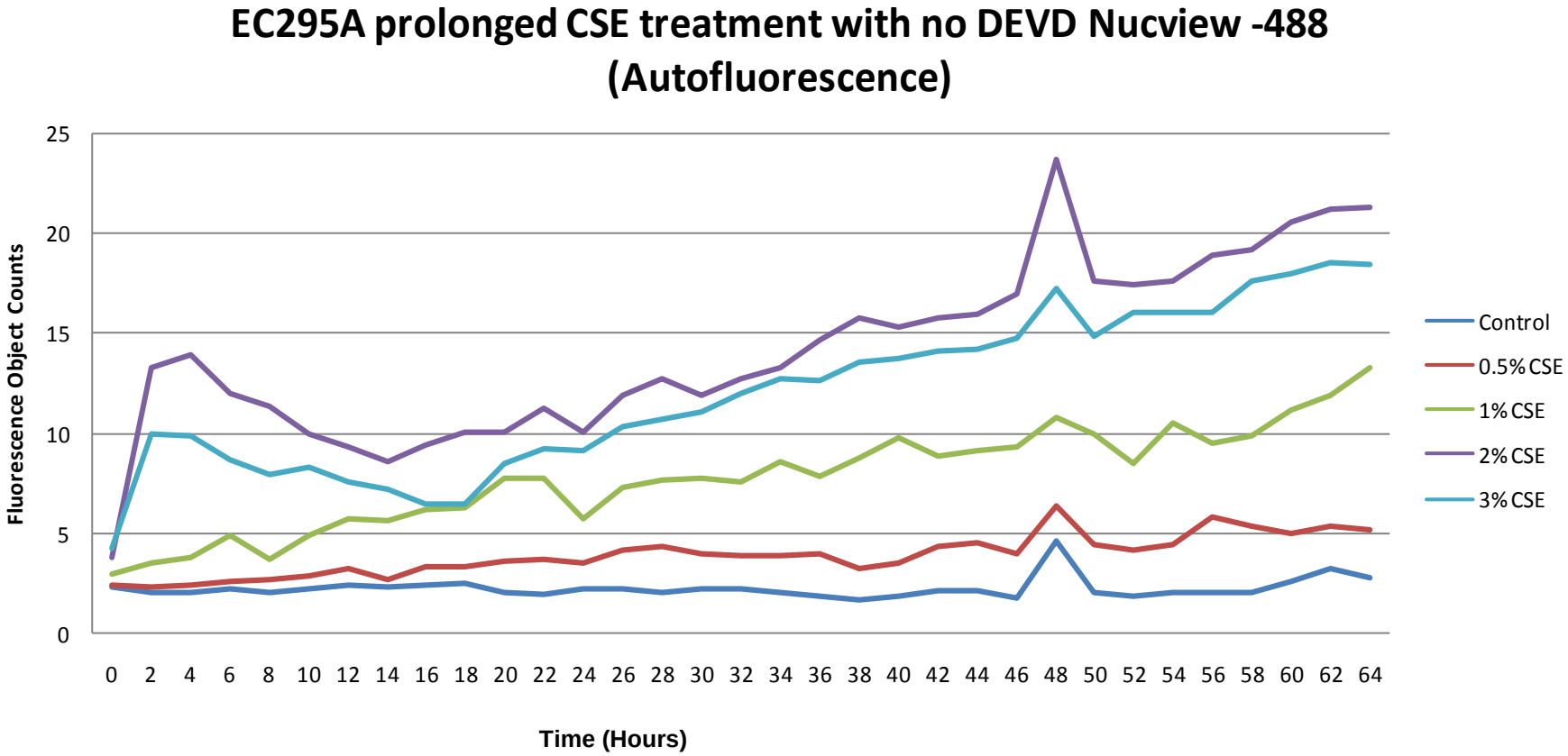


**Figure 5.20b:** HLMVECs isolated from patient 7 with emphysema (EC295A) treated with low dose (0-3%) CSE and followed for 64 hours via fluorescence live cell imaging. No DEVD Nucview-488 was added to allow detection of autofluorescence. There was a stepwise increase in autofluorescence with increasing concentration of CSE, although in this experiment autofluorescence for the 2% CSE treated cells was greater than the 3% CSE treated cells.

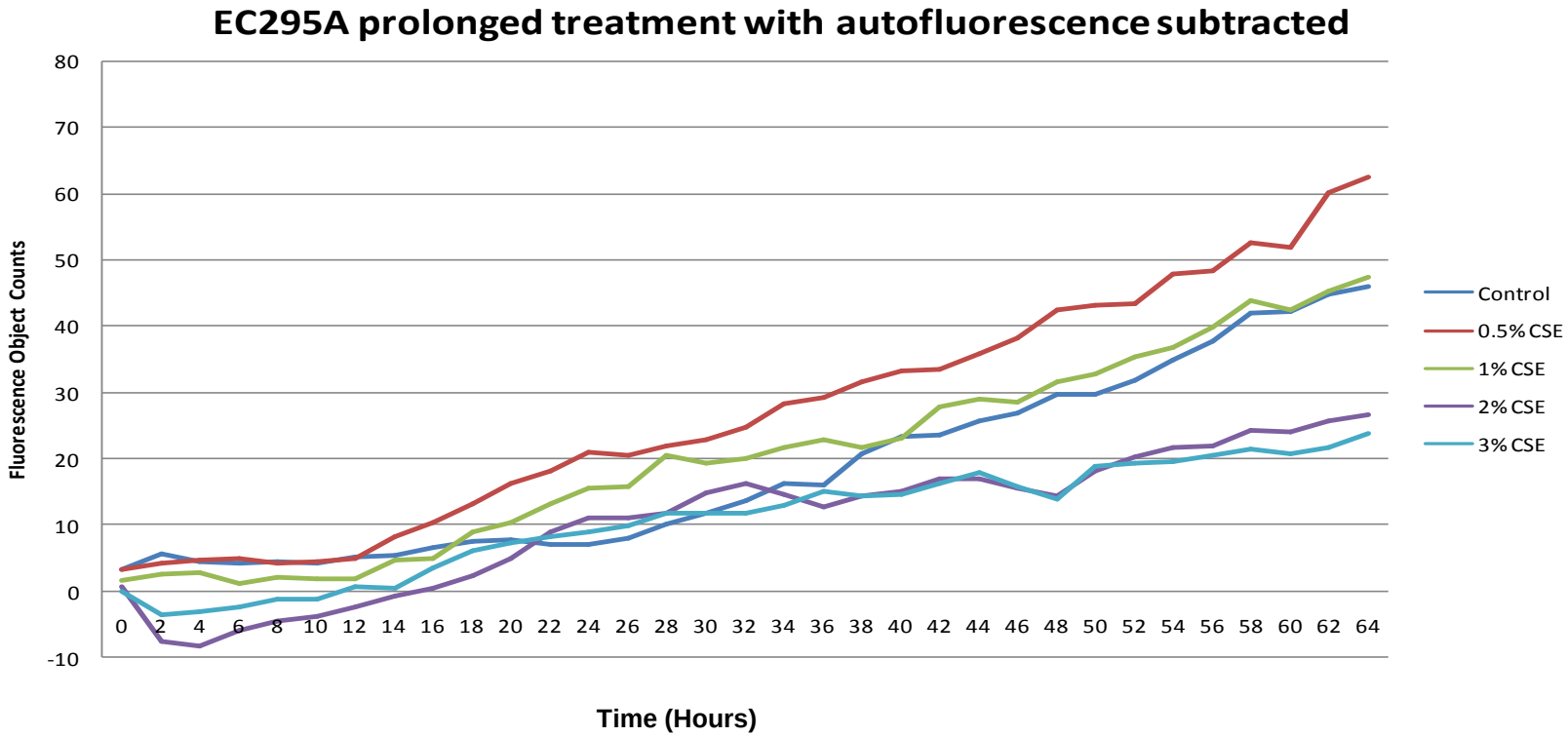


**Figure 5.20c:** HLMVECs isolated from patient 7 with emphysema (EC295A) treated with low dose (0-3%) CSE and followed for 64 hours via fluorescence live cell imaging. Autofluorescence was subtracted from each time point from the corresponding repeat experiment without DEVD Nucview-488 added. Cells treated with 2 and 3% CSE appeared to be influenced by autofluorescence, with lower fluorescent object counts than control cells, after subtracting autofluorescence. Both 0.5% and 1% CSE treatments in this experiment seemed to lead to more apoptosis as detected by fluorescence counts than control treated cells. This was most apparent at 24 hours but persisted for the 0.5% CSE treated cells.

In summary, I attempted to systematically assess apoptosis in real time in a number of patients with emphysema employing DEVD Nucview-488 to detect caspase activation and thus apoptosis. Unfortunately this technique employs fluorescence and unfortunately throughout this experiment it became apparent that CSE treatment of cells causes cells to autofluoresce thus limiting the use of this technique and limiting any conclusions that can be drawn from this data. The data suggests, while taking into account the effect of CSE induced autofluorescence of cells treated with both short (1 hour) and prolonged treatments, with careful controls, that low dose CSE may cause an increase in apoptosis. This was witnessed in both normal HLMVECs (Promocell) (Figure 5.17, Figure 5.18) and in cells isolated from a patient with emphysema (patient 7) (Figure 5.19, Figure 5.20) over both a short exposure (1 hour) and prolonged exposure. The effect was generally maximal at 24 hours and was witnessed with low dose CSE. Interestingly, the dose of CSE required to achieve this was lower in the emphysema cells than the Promocell, in keeping with my hypothesis that these cells are more susceptible. However due to the autofluorescence of cells no firm conclusions can however be drawn.

### *5.4.8qPCR for VEGF KDR*

The VEGF KDR/FLK1 receptor may play a key role in the pathogenesis of emphysema in relation to apoptosis of the microvasculature[26]. VEGF KDR cellular expression on normal and emphysema cells in response to CSE was therefore investigated via qPCR.

Initial qPCR validation experiments were performed using untreated commercial HLMVECs (Promocell). RNA was isolated as described and UV absorbance via spectrophotometry plotted with the ratio of absorbance at 260 nm and 280 nm ($A_{260/280}$) found to be 2.12 confirming purity (Figure 5.21). RNA quality was further assessed on 2% agarose gel electrophoresis with DNA ladder to investigate contamination with DNA (Figure 5.22). Two discrete ribosomal bands corresponding to 28S and 18S were visualised in an approximate 2:1 ratio with little degradation. cDNA was thereafter prepared from RNA as described.

Before using the comparative CT (ΔΔCT) method for relative gene quantification, validation experiments were performed to investigate the efficiencies of the gene of interest (VEGF KDR) and housekeeping gene (18S). Initially, the probe for gene of interest (VEGF KDR) and housekeeping gene (18S) were used with undiluted cDNA to determine at which cycle a signal appeared (Figure 5.24). A 96 well optical plate was loaded with probes alone (no template control), template plus probe and RNA plus probe for both VEGF and 18S to confirm detection of PCR product (Figure 5.23). Negative controls (probe alone) and RNA plus probe were included to ensure there was no genomic DNA contamination with which probes reacted. In this initial experiment 2 amplification plots were identified with 18S being relatively more abundant than VEGFR2 as evidenced by the earlier CT. No other products amplified confirming no reaction with the negative control and RNA plus probe.

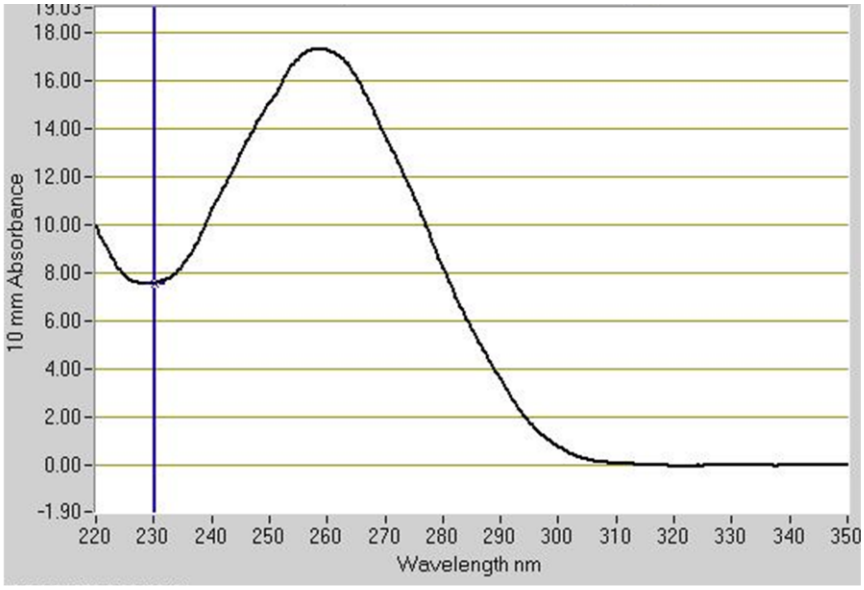


**Figure 5.21:**Representative spectrophotometry plot via which RNA yield and purity were determined. The ratio of absorbance at 260 nm and 280 nm ($A_{260/280}$)was used to assess RNA purity. An $A_{260/280}$ value of 2.0 or greater was accepted as pure. All RNA samples used for cDNA synthesis had a ratio of absorbance at 260 nm and 280 nm ($A_{260/280}$)of 2.0 or above.

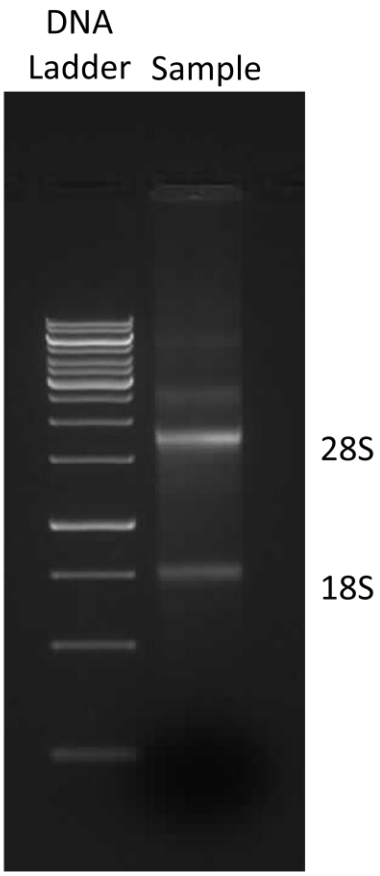


**Figure 5.22:** Electrophoresis of RNA isolated from HLMVECs (Promocell) ran on 2% agarose gel with DNA Trackit ladder shows 2 discrete ribosomal bands corresponding to 28S and 18S in an approximate 2:1 ratio with little degradation.

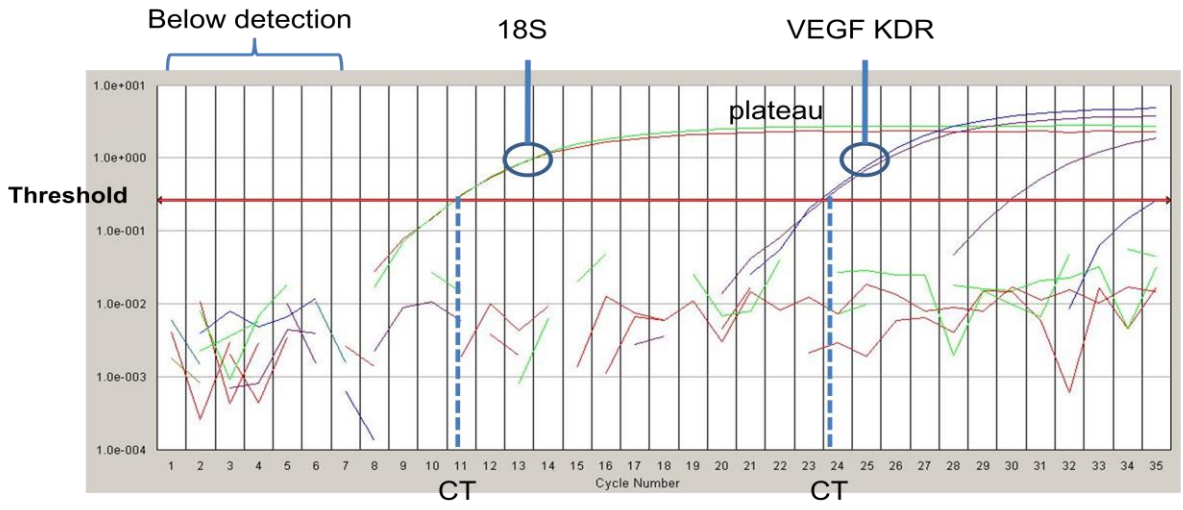


**Figure 5.23:** RT-PCR HLMVECs (Promocell) with 18S probe and VEGF KDR probe confirms 2 amplification plots. Cycles 1-7 are below detection. The exponential phase of amplification is shown both for 18S and VEGFR2, which is most reliable for quantifying PCR, is shown prior to plateau. Cycle threshold (CT) occurs earlier for 18S than VEGFR2 implying greater abundance.

qPCR can be used to determine gene quantity via an absolute or relative method. Calculation of the number of gene copies can be determined from a standard curve if absolute quantification is required. Change in gene expression in response to a treatment with reference to a standard housekeeping gene which does not change in response to this treatment i.e. relative quantification, is also a sensitive validated method[154] and was used in this study to determine the response of VEGFR2 (KDR/FLK1) in response to CSE using 18S as a housekeeping gene, which has been reported to be unaffected by apoptosis [155]. Relative quantification requires construction of a dilution series from which ΔCT (difference between CT between GOI and housekeeping gene) can be determined. This then allows the use of the ΔΔCT method which is a sensitive method to detect change that has been validated. A dilution series was performed, with cycle threshold (CT) plotted against $\log^{10}$ dilution of primers with gradient and line of best fit ($r^2$) calculated (Figure 5.24). The ideal PCR increases one CT with each dilution, thus giving slope y=-log10= -3.3. The results obtained in the dilution series for 18S and VEGFR2 are in good agreement ($r^2$=0.99) with gradient of slope validating the dilution series and thus the use of the comparative CT method.

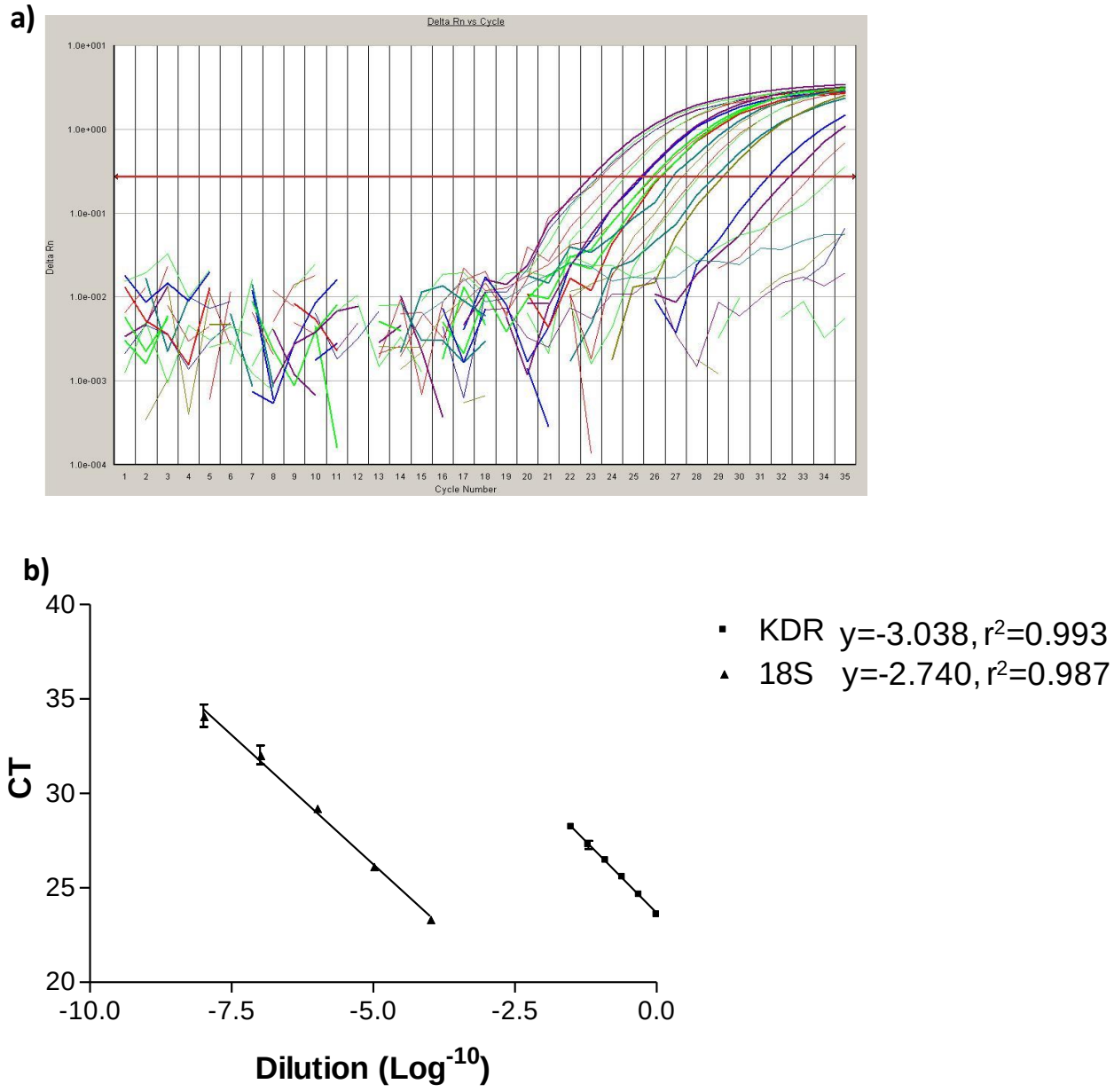


**Figure 5.24:** Results from the dilution series to validate the comparative CT method. A) Amplification plot showing CT for 18S and KDR multiple dilutions. B) CT determined from amplification plot plotted against dilution ($Log^{-10}$). The 'perfect PCR' amplification increases one CT upon dilution ($y=log^{-10}= -3.3$) thus the gradient of slope of both 18S and KDR is within acceptable limits with good correlation ($r^2=0.99$) and so validates the use of the comparative CT method.

The comparative ΔΔCT method was then used to investigate relative change in VEGFR2 gene expression in response to 3% CSE at 0 (control), 24, 48 and 72 hours. Promocell cells were first investigated. There was no significant change in CT across treatments in VEGFR2 expression (n=3) when controlled for 18S and expressed as a fold change (Figure 5.25a). Cells isolated from four emphysema patients (Patient 2 (EC208A), Patient 7 (EC295A), Patient 8 (EC300C), Patient 10 (EC326C)) were similarly investigated following a validation dilution series experiment as before. Emphysema cells (n=3 for each donor) showed biological variation in their response that is common to experimentation with primary cells. There was however a trend towards a reduction in VEGFR2 in response to 3% CSE treatment that was significant at 48 hours ($P<0.05$). Thus VEGFR2 gene expression is unchanged in normal cells (Promocell) in response to CSE (with a possible trend towards upregulation), while emphysema cells show a reduction in VEGFR2 in response to CSE at 48 hours. This supports my hypothesis of a maladaptive response to injury in cells from a susceptible individual.

a)

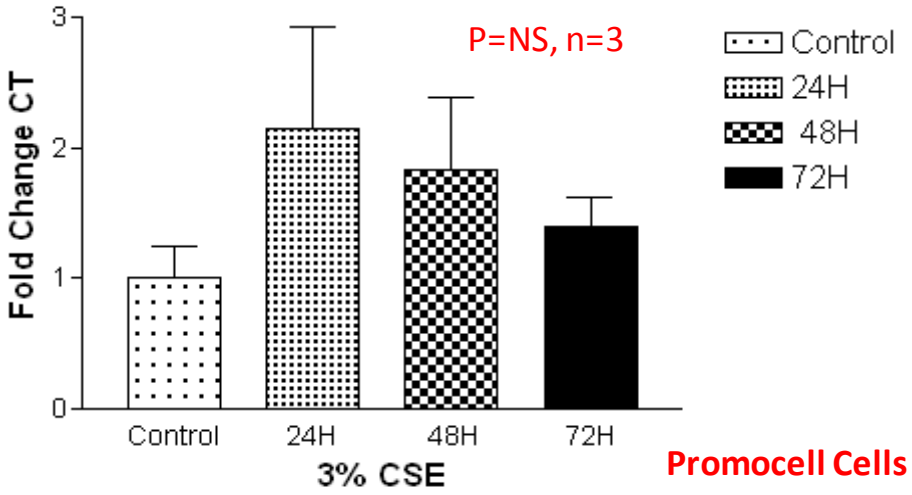


b)

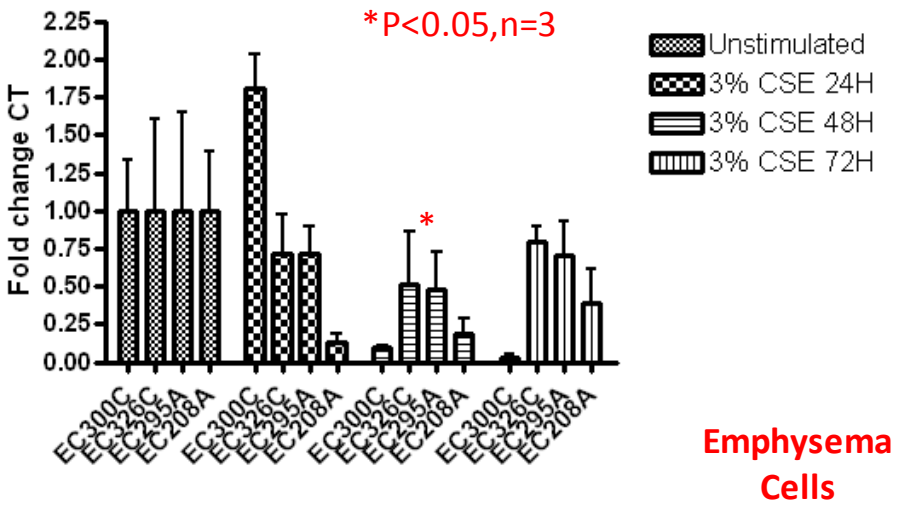


**Figure 5.25:** HLMVECs (Promocell (a) and isolated from patients with emphysema (b)) treated with 3% CSE for 0 (control), 24, 48 and 72 hours. Cells were harvested and RNA and cDNA isolated as before. Q-PCR was performed using 18S as a calibrator/ housekeeping gene. Fold change CT fold change relative to housekeeping gene is presented for each of the treatments for (a) Promocell and (b) cells isolated from patients with emphysema. In Promocell cells there was no significant change in VEGFR2 gene expression in response to CSE across the treatments (P=NS). In the Emphysema cells, 4 patients were examined. Patient 2 (EC208A), Patient 7 (EC295A), Patient 8 (EC300C), Patient 10 (EC326C). While there was variation between the donors, there was a trend towards reduction in VEGFR2 in response to CSE that was significant at 48 hours (P<0.05).

## *5.5 Discussion*

In this chapter I attempted to investigate apoptosis *in vivo* and *ex vivo*. Immunocytochemical detection of the apoptosis marker caspase 3 in emphysema lung tissue was more frequent in the alveolar bed compared with normal lung tissue in keeping with the findings of other studies which report increased apoptosis in emphysema. I then went on to study apoptosis in vivo using the cells isolated from emphysema lung tissue. Initially I hoped to study responses in diseased emphysematous tissue and normal control tissue, isolating the cells using the same method. Unfortunately due to the time constraints of the study and the time taken to isolate emphysema cells, similar time could not be devoted to isolating enough normal cells from excess lung tissue for the same experiments to be conducted. Commercially available primary LMVECs (Promocell) which were also relatively slow growing, precious cells that were prone to infection and a greater challenge than a conventional cell line, were therefore used in initial viability and pilot studies and unfortunately were also used as to represent normal cells in more detailed later experiments. This is a major limitation of this study. There was however an internal control (untreated cells) in all experiments to allow assessment of response to treatment.

Initial viability studies confirmed that normal LMVECs (Promocell) were viable up to and including 10% CSE at 24 hours. However in view of the possibility that cells isolated from patients with emphysema would be more susceptible to cell injury, viability studies were also performed on these diseased cells. These additional experiments confirmed that indeed the cells were more susceptible with lower baseline viability of these cells including the untreated controls. The lower cell viability of isolated cells and death response to CSE at lower concentration and earlier time course suggests these cells are indeed more susceptible to injury and may explain the differences observed between these and normal LMVECs (Promocell).

Investigation of apoptosis in multiple emphysema donors with the chosen (3% CSE) stimulus/injury via flow cytometry yielded rather inconsistent results. There was no clear apoptosis of cells that was measurable by flow cytometry or via TUNEL. This was perhaps not unsurprising given the limitations of the model. In essence, trying to stress primary cells with CSE, while not overtly killing them via necrosis with high concentrations of CSE, and assess this at a limited number (24,48,72 hours) of time points may explain the lack of results. The dynamic nature of apoptosis and also the variation from one donor make this difficult to study. Live cell imaging was therefore employed to overcome these difficulties.

Investigating in triplicate the response in real time of cells to multiple concentrations of CSE via live cell imaging yielded more encouraging results. There was a step wise increase in fluorescence counts with increasing concentration of CSE. This led me to question whether CSE caused autofluorescence of cells. Further experiments were therefore conducted as negative controls with no active Nucview-488 added i.e. any fluorescence counts above baseline were therefore autofluorescence of cells and not caused by cleavage of caspase3 and thus not indicative of apoptosis. This experiment confirmed significant autofluorescence of cells in response to CSE and has highlighted a major challenge for researchers when studying the effect of cigarette smoking that has to my knowledge not been reported before. Autofluorescence of LMVECs in response to CSE suggests changes in cell structure which is fascinating from an endothelial biology perspective but from a practical point of view makes analysis of results obtained via fluorescence very difficult to interpret. The results presented in this chapter from the live cell imaging are presented in such a way to attempt to tease out whether there is an important signal i.e. apoptosis of cells in response to CSE. Multiple experiments via live cell imaging show with careful controls and allowance for autofluorescence may suggest low dose CSE (0-3%) may cause an increase in apoptosis. This was witnessed in both normal LMVECs (Promocell) and in cells isolated from a patient with emphysema over both a short exposure (1 hour) and prolonged exposure. The effect was generally maximal at 24 hours and was witnessed with low dose CSE. Interestingly, the dose of CSE required to achieve this was lower in the emphysema cells than the

Promocell, in keeping with my hypothesis that these cells are more susceptible injury. Unfortunately due to autofluorescence it is not possible to state conclusively that this increase in fluorescence count (after controlling for autofluorescence) is directly attributable to apoptosis and further experiments to detect apoptosis via live cell imaging that do not rely upon the use of fluorescence imaging is now required.

Trying to link the apoptosis witnessed in response to low dose CSE with the seminal *in vivo* and *ex vivo* studies which showed emphysema arising due to loss of VEGFR2[63][54] led me to investigate VEGFR2 gene expression via Q-PCR in response to CSE. After initial validation experiments, RNA and cDNA were prepared from emphysema cells treated with 3% CSE for 24, 48 and 72 hours and compared with untreated control cells. This was repeated in emphysema cells isolated from 4 donors and in Promocell (normal) cells. In response to CSE there was no significant change in VEGFR2 in Promocell (normal) cells. In 4 emphysema donors there was however a fold reduction in VEGFR2 that was significant at 48 hours. Further work is required to investigate this preliminary signal.

# *Chapter 6: Alveolar septal remodelling in emphysema: the role of endothelial cell plasticity and mesenchymal transition.*

## *6.1 Abstract*

Classically, thin sparsely cellular septa are seen in emphysematous lungs, but in addition remodelling of the alveolar bed also occurs, with matrix deposition and increased collagen content and turnover. Expansion of alveolar matrix may arise via proliferation of resident fibroblasts or recruitment of circulating bone marrow derived fibrocytes to the lung. A further novel mechanism which may link matrix deposition with endothelial loss is endothelial to mesenchymal transition (EnMT). EnMT has a well-documented role in embryogenesis, however the potential of mature cells to undergo this process has now also been demonstrated in epithelial cells and larger endothelial cells. I therefore investigated plasticity of human lung microvascular endothelial cells in response to cigarette smoke extract and other inflammatory mediators, to investigate EnMT in emphysema.

**Methods:** LMVECs (commercially available cells and cells isolated from patients with emphysema undergoing lung transplantation) were stimulated with TGFβ, and CSE. Endothelial plasticity was investigated on phase contrast microscopy, confocal microscopy and western blotting. Change in cell function was also investigated via examination of matrix deposition from the cells and production of matrix metalloproteinases. Paraffin embedded lung tissue was dual stained for an endothelial marker (CD34) and mesenchymal marker (aSMA) and co-localisation of markers investigated.

**Results**: Morphological changes in cell structure were detected following treatment with TGFβ1 and CSE when compared with untreated control cells. In addition, cells appeared to downregulate the endothelial cell surface marker CD31 on confocal immunofluorescence. Co-localisation of markers was also investigated but did not show evidence of dual staining of endothelial and mesenchymal markers. Flow cytometry evaluation of CD31/CD90 suggested there was down regulation of CD31, no upregulation of CD90. Furthermore there was no change in protein concentration

detected via western blotting across all treatments. EnMT was also investigated *in vivo* via immunohistochemistry however there was no clear evidence of dual stained transitional cells in emphysema.

**Conclusions:** Endothelial cells change morphology in response to TGFβ1 and CSE and appear to down regulate endothelial cell surface markers. This may however reflect endothelial activation with internalisation of cell surface markers as opposed to a true mesenchymal transition. Immunohistochemistry for CD34/aSMA in emphysema show evidence of endothelial loss with associated sclerotic casts and increased mesenchymal markers. Further work is required to determine whether these are transitional cells or whether this is simply a response of an endothelial cell to injury.

## *6.2 Introduction*

Complex changes occur in the alveolar wall of patients with emphysema. In addition to well documented thin alveolar walls with sparse capillaries [25], thickening of the alveolar interstitium occurs in some regions, with collagen deposition and increased interstitial fibroblasts [87]. Although somewhat at odds with the classical description of emphysema as *"destruction of alveolar walls without fibrosis"* [15], emphysematous areas express several fibrosis associated matrix genes and proteases [82], with the balance of these factors dictating the direction in which damage proceeds, either towards fibrosis or septal destruction. The relationship between endothelial loss and fibrosis has been studied in chronic heart and kidney disease with some researchers hypothesising that that immature fibrosis may originate from injured endothelial cells acquiring mesenchymal cell characteristics and potential [91][93]. This endothelial to mesenchymal transition (EnMT) has been reported by other researchers to be one of many cellular responses to chronic injury. Cytoskeletal rearrangements of cobblestone endothelial cells into spindle shaped mesenchymal cells have been described and put forward as evidence of EnMT [89]. In addition to morphological changes, cells have been shown to down regulate endothelial markers and acquire mesenchymal markers. Functionally, transitional cells may also demonstrate proliferative, invasive and secretory characteristics, not displayed by native endothelial cells [156]. This chapter aims to investigate the fate of lost endothelial cells in emphysema, in particular whether regional endothelial plasticity/ EnMT may contribute to endothelial loss and septal fibrosis witnessed in emphysema.

EnMT is less well studied than epithelial to mesenchymal transition (EMT), of which there are over 3000 citations in the literature. EMT is implicated as an important mechanism in cancer biology, kidney fibrosis, post lung transplant obliterative bronchiolitis and idiopathic pulmonary fibrosis [157]. The plasticity witnessed in EMT/EnMT is also a key event *in utero* during embryogenesis [39]. In recent years there has been controversy surrounding the origin of myofibroblasts in chronic inflammatory diseases [158]. A number of researchers report expansion of resident

tissue myofibroblasts, while others report phenotype transition (EMT/EnMT) or recruitment of circulating bone marrow derived progenitor cells. Any one or combination of these mechanisms may give rise to myofibroblasts and may be dictated by the tissue in which the injury occurs [159]. In emphysema, there is disruption of the vasculature with endothelial loss, thus making it theoretically difficult for circulating bone marrow derived progenitor cells to reach the site of injury. Furthermore, resident myofibroblasts may be in low numbers in the delicate alveolar structures of the adult lung. Therefore cellular plasticity may be an important source of myofibroblasts in emphysema linking microvascular injury and repair.

EnMT was first described in aortic endothelial cells in response to Transforming Growth Factor β1 (TGFβ1) as a novel mechanism in atherosclerosis [89]. This plasticity was initially reversible but became irreversible with time. The importance of TGFβ1 as a driver of this response to injury has been highlighted by many more studies [90], [157], [160], [161]. TGFβ1 driven EnMT has been reported *in vivo* in a mouse model of cardiac fibrosis via lineage tracing [91]. This could be reversed by the addition of recombinant BMP7 and was attenuated in SMAD 3 null mice, providing insights into the cell signalling pathways which support this plasticity.

TGFβ1 is expressed in most tissues and is secreted by many cell types including epithelial, endothelial, smooth muscle cells, fibroblasts and also most immune system cells [162]. Levels of TGFβ1 in emphysema are still debated, with some researchers reporting reduced TGFβ1 and TGFβ receptor expression in COPD lung tissue [100], [101] while others report increased levels [102]. The effect cigarette smoking may have on TGFβ1 is also debated. Alterations in redox state with increased oxidative stress that occurs in cigarette smoking is reported to contribute to TGFβ1 activation [81]. In addition, TGFβ1 itself induces intracellular ROS[163], thus causing positive feedback to amplify the signal. Thus TGFβ1 may play a role in the pathogenesis of emphysema, via reduced activity, defective signalling or inappropriate septal fibrosis as an example of dysregulated repair in response to oxidative stress in the areas that remain. Both TGFβ1 and CSE were used to stress cells in these experiments and investigated systematically.

EnMT/EMT has been defined in many ways with some researchers reporting morphological change and down regulation of endothelial cell surface markers with acquisition of mesenchymal markers as sufficient evidence of a phenotypic change [161]. Others have sought greater evidence such as change in protein expression of cell surface markers and functional change such as deposition of collagen and release of matrix metalloproteinases [156]. Due to the exploratory nature of this work, using diseased human primary cells, cell morphology and cell surface marker expression in response to treatment with TGFβ1 was initially assessed, progressing later to look for evidence of change in protein expression and function. More detailed examination of the signalling pathways behind such EnMT was also planned.

The time between injury and observation of phenotype change varies between cell type and between the various methods reported by investigators. Arciniegas *et al*[89] isolated and characterised adult bovine endothelial cells and used these in experiments between passage 11 and 30. Cells were treated at ~20% confluence with control media or media containing 1ng/ml of TGFβ1. The cultures were incubated for up to 20 days changing the media every 2-3 days. After 3 days incubation, the TGFβ1 treated cells were enlarged compared with controls and displayed a ragged morphology, with only 50-60% cells staining positively for endothelial markers. By 5 days, only 30-40% cells stained positively for endothelial markers while 40-60% stained positively for αsma. Plasticity was further suggested by dual immunofluorescence with the endothelial marker factor VIII and αsma after 5 days incubation. Withdrawal of TGFβ1 after 10 days incubation caused cells to revert to their original polygonal morphology with positive endothelial markers with absent αsma, however this reversibility was not apparent following withdrawal of TGFβ1 at 20 days. Frid et al reported the appearance of mesenchymal cells spontaneously over time (44% by passage 2) in endothelial cells isolated from adult bovine aortas and main pulmonary arteries [90]. This was only apparent in arterial cells purified on day one post isolation via FACs for Dil-Acetylated-LDL. Cells which were left for more than 5 days prior to sorting did not give rise to mesenchymal cells.

These methods to investigate EnMT differ significantly in that Arciniegas reports plasticity in cells between passage 11 and 30, at a much higher passage than primary cells are normally used. Frid in contrast reports this phenomenon was only seen in cells sorted on day one post isolation i.e. prior to the first passage. From the morphological description of Arciniegas, the cells they observed may have become senescent (enlarged raggy morphology) with age related reduction in cell surface markers rather than showing a true phenotypic switch. The description by Frid *et al* suggests they may have been witnessing appearance and rapid growth of small numbers of contaminating mesenchymal cells.

Zhu *et al* isolated cells from porcine small arteries and examined evidence for EnMT following 1 day and 7 days hypoxia [161]. They reported morphological and cell surface expression change as evidence of EnMT at 7 days. Zeisberg *et al*, in addition to lineage tracing in their mouse model, cultured coronary endothelial cells and between passages 3 and 5 treated cells with TGFβ1 (10ng/ml) or control media for 6 days [91]. They demonstrated change in morphology and immunofluorescence via confocal microscopy in the TGFβ1 treated cells compared with control cells. Zeisberg also demonstrated that the cell culture media from TGFβ1 treated cells contained more collagen I and fibronectin on ELISA. Cell viability, investigated via MTT assay, was reduced not increased. O'Riordan *et al* used HUVECs as a model of chronic kidney disease to examine endothelial plasticity in response to inhibition of nitric oxide for up to 72 hours [93]. Collagen XVIII expression was increased via western blotting and qPCR following treatment of HUVECs with the eNOS inhibitors ADMA and L-NAME when compared with untreated cells. In addition the endothelial marker Tie-2 reduced and αsma increased when detected via immunofluorescence after treatment with ADMA. Borthwick *et al* using primary bronchial epithelial cells obtained from patients with bronchiolitis obliterans observed change in cell surface markers, protein expression and function in cells treated with TGFβ1 and TNFα for 72 hours [156]. Although this work was conducted in bronchial epithelial cells and not lung microvascular endothelial cells, this is the most similar model to date as it uses primary cells isolated from individuals who have developed the disease of study. From these published experiments, cells were treated with TGFβ1 5ng/ml

and 10ng/ml and CSE 3% (based upon viability studies) for 1 hour and 24 hours initially with EnMT examined at 5 days and 7 days. Later I examined plasticity in response to 3% CSE stimulation for 24, 48, and 72 hours.

In addition to investigating EnMT in cell culture models using primary cells from patients with emphysema, I also investigated the relationship between endothelial loss and mesenchymal deposition/repair *in vivo* using immunohistochemical staining on paraffin embedded lung sections from the tissue from which cells were isolated. In addition I utilised dual staining to investigate the presence of cells staining positive for both endothelial and mesenchymal markers. Such dual stained cells would investigate *in vivo* evidence of this phenomenon, with examination of the environment in which dual stained cells were found highlighting the biological relevance of this mechanism and giving important clues as to the pathogenesis.

## 6.3 Materials and Methods

### 6.3.1 Immunohistochemistry

Immunohistochemistry for CD31, CD34 and aSMA was performed on 4um paraffin embedded tissue sections from emphysema and control tissue. Immunoreactants were visualised using diaminobenzidine (DAB) substrate solution and vector red substrate. Isotype controls were included in each experiment to assess quality of staining.

### 6.3.2 Cell culture

Commercially available human pulmonary microvascular endothelial cells (Promocell) and cells isolated from emphysematous human lung and excess normal tissue were grown in complete MV2 media (Promocell) containing supplements and 5% FCS. Cells were grown on 6 well plastic plates coated with gelatin (cell viability), in 75cm$^2$ flasks (western blotting) and on 18mm coverslips (Confocal microscopy).

### 6.3.3 CSE preparation

Cigarette smoke extract was prepared according to the method by Carp and Janoff [111] as outlined previously and used within 30 minutes of preparation.

### 6.3.4 Phase Contrast Microscopy

Images were taken on a cannon image shot.

### 6.3.5 Cell Viability

Cell viability studies were performed via flow cytometry using 7-AAD to detect non-viable cells, with FITC annexin V to detect early apoptotic cells. All experiments were conducted in triplicate.

### *6.3.6 Confocal Microscopy*

Cells were fixed in 4% (w/v) paraformaldehyde as before, permeabilised, blocked in BSA and incubated with primary antibodies and detected using an appropriate fluorochrome-linked secondary antibody. DAPI was used as a nuclear counter stain. Images acquired using a LSM 510 laser scanning confocal microscope.

### *6.3.7 Western blotting*

Cell lysates (5–20 µg determined via BCA protein assay) were separated via gel electrophoresis (4–12% bis-Tris gels, Invitrogen, Paisley, UK) and then transferred overnight onto PVDF membranes. Membranes were then blocked prior to incubation with primary antibodies and detected with horseradish peroxidase (HRP)-labelled IgG conjugates (Abcam, Cambridge, UK). Antibody complexes were visualised using the SuperSignal West Pico chemiluminescent kit (Perbio Science). β-actin and β-tubulin loading controls were detected for each experiment.

## *6.4 Results*

### *6.4.1 Cell Viability in response to TGFβ1 and CSE at 24 hours*

Initial cell viability results were conducted using LMVECs (Promocell) prior to replication of work in the emphysema LMVECs. Cells were treated with complete MV2 media containing TGFβ1 10ng/ml, CSE 3% or control. Cells treated with CSE were exposed for 1 hour and 24 hours before replacement with complete media. Cells were harvested at 24 hours and viability examined via annexin V and 7AAD staining via flow cytometry. Results (mean± sem, n=3) are shown in figure 6.1. There was no significant cell death in cells exposed to TGFβ1, or 3% CSE for 1 hour or 24 hours compared with controls (p=0.338).

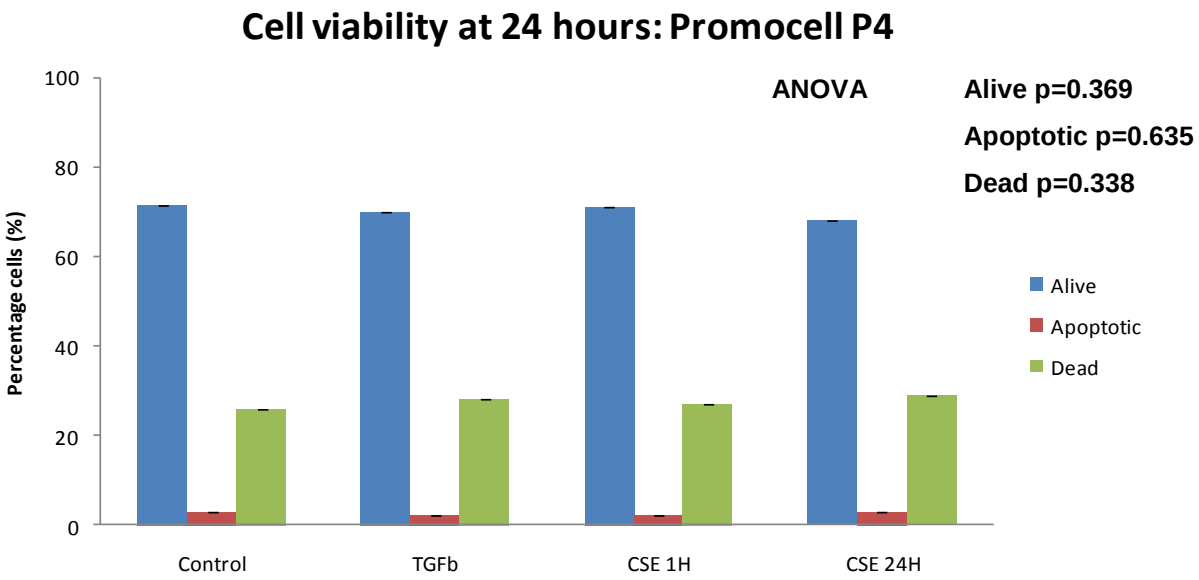


**Figure 6.1:** Human pulmonary microvascular endothelial cells (HLMVECs) were treated in triplicate with complete MV2 media containing TGFβ1 10ng/ml, CSE 3% for 1 hour or 24 hours or control. Cells were harvested at 24 hours and viability investigated via annexin V and 7AAD staining via flow cytometry. There was no significant cell death in cells exposed to TGFβ1, or 3% CSE for 1 hour or 24 hours compared with controls (p=0.338).

### *Cell Viability in response to TGFβ1 and CSE at 7 days*

From the 24 hour viability experiment, I concluded that cell viability remained unchanged across the treatments. I therefore examined cell viability after 7 days exposure to TGFβ1 and 7 days from treatment with 3% CSE for 1 hour and 24 hours. Cells were treated at time zero with complete MV2 media containing TGFβ1 1ng/ml, TGFβ1 10ng/ml, CSE 3% or control. Cells treated with CSE were exposed for 1 hour and 24 hours before replacement with complete media. Cells were harvested at 7 days and viability examined investigated via annexin V and 7AAD staining via flow cytometry. Results (mean± sem, n=3) are shown in figure 7.2. Cell viability was much lower (approximately 40-45% viable) than at 24 hours with an apparent increase in apoptosis ($p=0.001$). There was however no significant cell death in cells exposed to TGFβ1, or 3% CSE for 1 hour or 24 hours compared with controls ($p=0.321$).

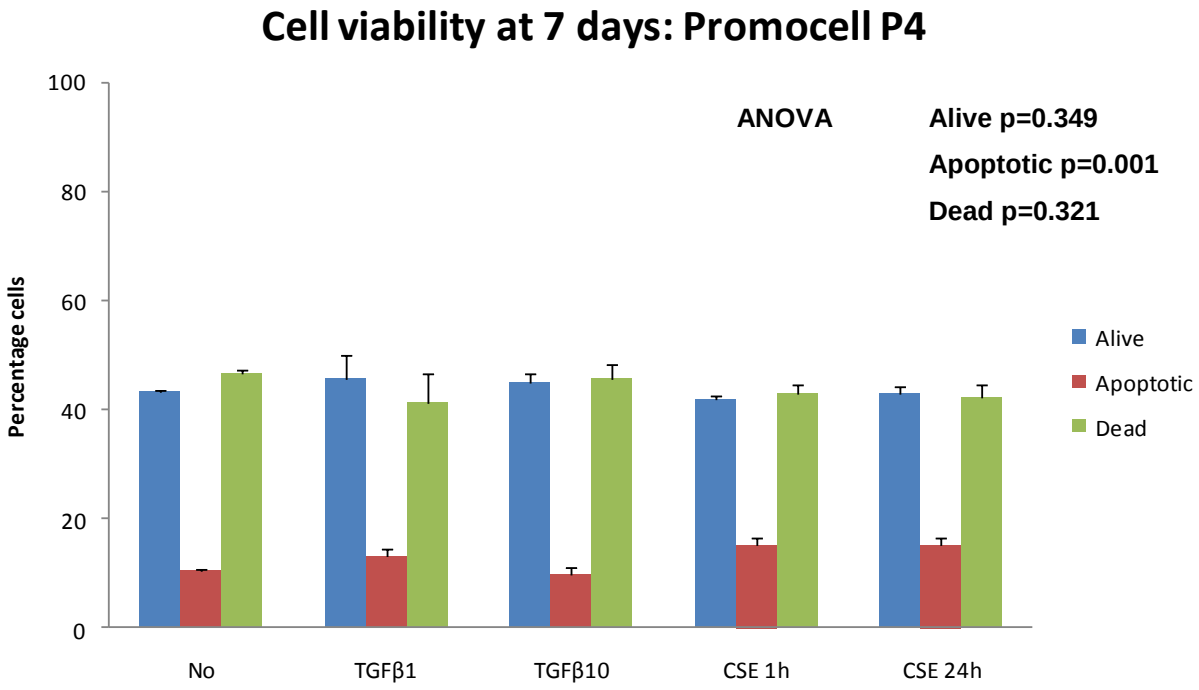


**Figure 6.2:** Human pulmonary microvascular endothelial cells (HLMVECs) were treated in triplicate with complete MV2 media containing TGFβ1 1ng/ml, TGFβ1 10ng/ml and CSE 3% for 1 hour or 24 hours or control. Cells were harvested at 7 days post treatment and viability investigated via annexin V and 7AAD staining via flow cytometry. There was no significant difference in cell death in cells exposed to TGFβ1 or 3% CSE for 1 hour or 24 hours compared with controls (p=0.321). Cell viability was however much lower with only approximately 40-45% viable compared with approximately 70% at 24 hours (figure 6.1) and may account for apparent increase in apoptosis observed (p=0.001).

Cell viability studies (Promocell LMVECs and cells isolated from emphysema patients) in response to CSE treatment for 1, 24, 48 and 72 hours was shown in chapter 5. There was no significant cell death among cells treated with up to 3% CSE for 1, 24, 48 and 72 hours. Control cells (untreated) with media change at 24, 48 and 72 hours also showed no significant difference in viability. Due the the precious nature of these cells, these experiments were not repeated and the data used to guide CSE treatment dose for investigation of EnMT.

### *6.4.2 Cell Morphology*

Examination of cell morphology 7 days post TGFβ1 10ng/ml (Figure 6.3b), 3% CSE for 1 hour on day one (Figure 6.3c) and 3% CSE for 24 hours on day one (Figure 6.3d), revealed elongated spindle cells compared with untreated control cells (Figure 6.3a). TGFβ1 and CSE treated cells appeared less dense than control cells, but as evidenced in Figure 6.2, cell viability was unchanged despite these treatments. In view of these morphological changes on phase contrast microscopy, cell surface marker expression was investigated similarly at 7 days via confocal microscopy.

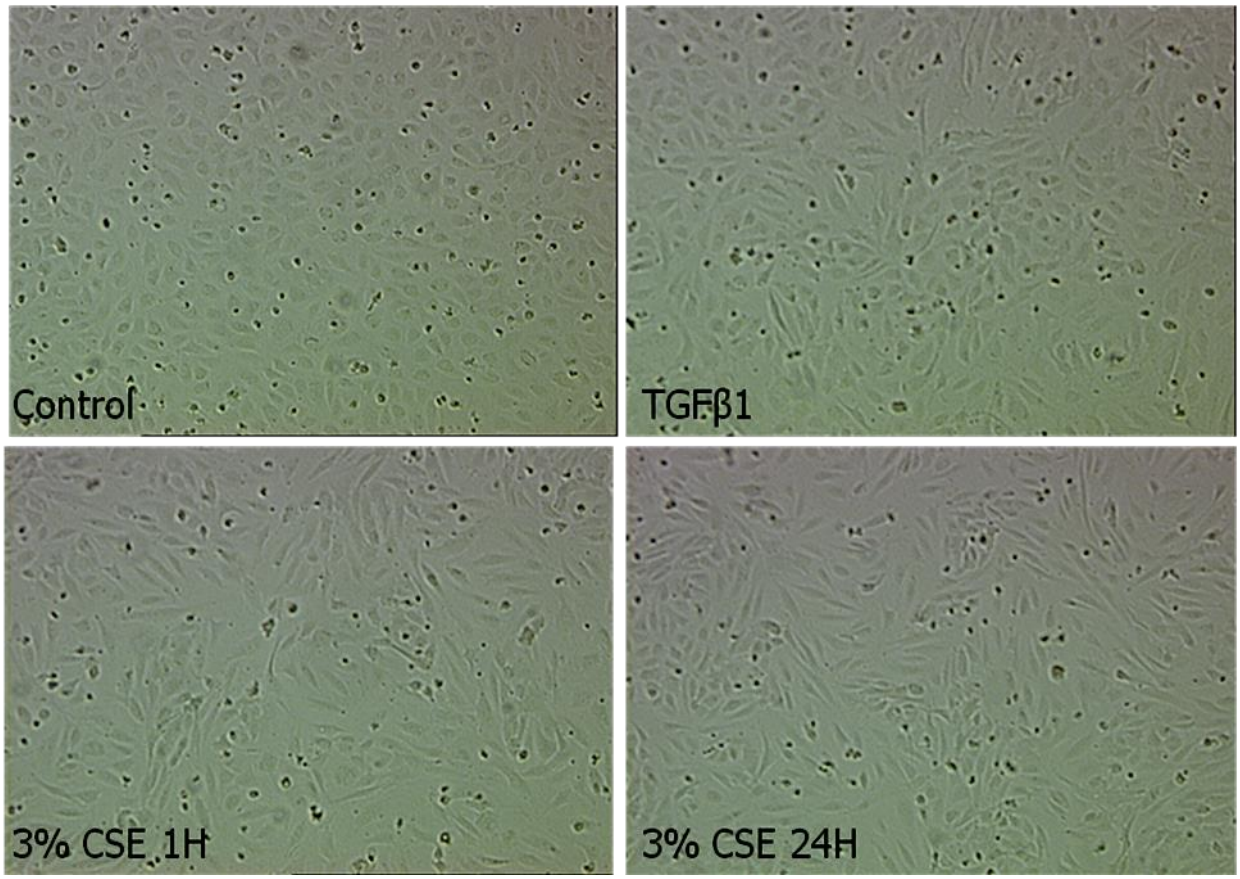


**Figure 6.3:** Cell morphology 7 days post TGFβ1 10ng/ml, 3% CSE for 1 hour on day 1 and 3% CSE for 24 hours on day 1 was examined and compared with untreated cells (controls). Phase contrast microscopy images demonstrated untreated control endothelial cells maintained their cobblestone morphology at 7 days. TGFβ1 treated cells were a mixture of elongated spindle cells and some cobblestone cells. Similarly the 3% CSE treated cells that were elongated compared with untreated cells.

### *6.4.3 Cell surface marker expression of human pulmonary microvascular endothelial cells (HLMVECs) in response to TGFβ1 and control HLMVECs and fibroblasts*

Cells treated with TGFβ1 10ng/ml for 7 days and untreated cells (controls) were fixed and stained for the endothelial markers VE-Cadherin and PECAM-1 and the mesenchymal markers vimentin and fibronectin with FITC (green, mouse secondary) and TRITC (red, rabbit secondary) secondary antibodies. DAPI was used to counter stain nuclei. Isotype controls with secondary antibody alone were included for all experiments to exclude nonspecific staining (figure 6.4).

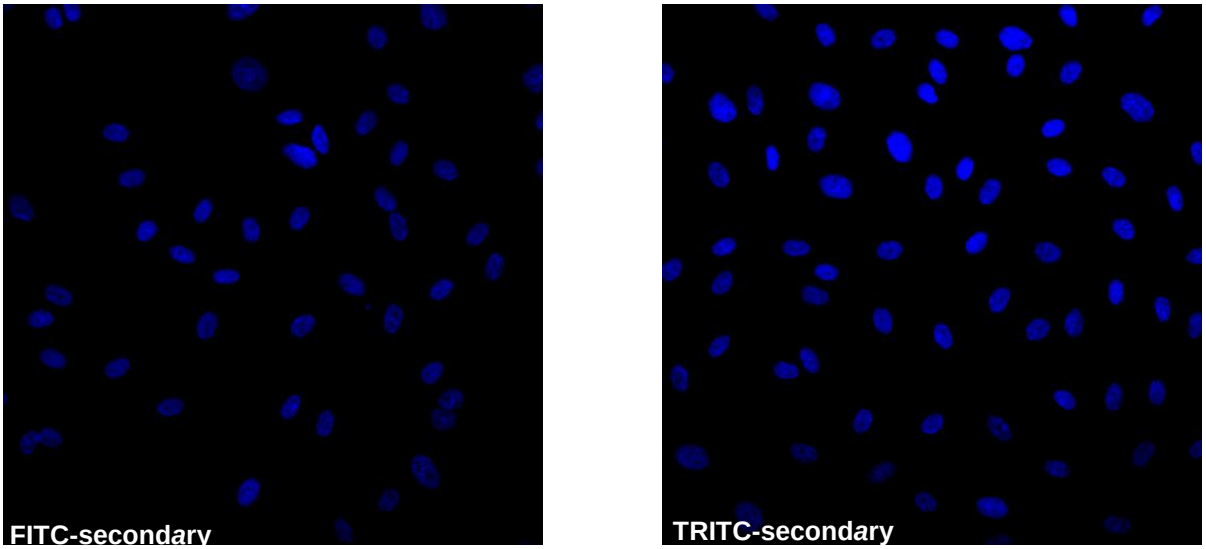


**Figure 6.4:** Example of secondary antibody only for FITC mouse secondary antibody and TRITC rabbit secondary antibody, counterstained with DAPI to stain nuclei blue. As demonstrated in both images there is no non-specific secondary antibody signal.

Control HLMVECs were cobblestone shaped and stained positively for the endothelial cell surface markers VE-Cadherin (Figure 6.5a (i)) and PECAM-1 (Figure 6.5a (ii)). Control cells also stained positively for vimentin (Figure 6.5a (iii)). Vimentin is a cytoskeletal protein which maintains cell structure and form and facilitates endothelial cells' ability to change shape during its many cellular tasks. There was also minimal fibronectin staining in control cells (Figure 6.5a (iv)). In response to TGFβ 10ng/ml, HLMVECs appear to down regulate VE-Cadherin (Figure 6.5b (i)). PECAM-1 staining was also altered being relocated from the cell surface to within the cytoplasm (Figure 6.5b (ii)). Cells elongated (vimentin staining) (Figure 6.5b (iii)) with apparent increased fibronectin staining (Figure 6.5b (iv)). In contrast and to act as an internal control to assess the quality of staining, fibroblasts were negative for the endothelial markers VE-Cadherin (Figure 6.5c (i)) and PECAM-1 (Figure 6.5c (ii)). Fibroblasts stained with vimentin showing dense spindle cells with bright cytoplasmic staining (Figure 6.5c (iii)) while there was dense deposition of fibronectin (Figure 6.5c (iv)).

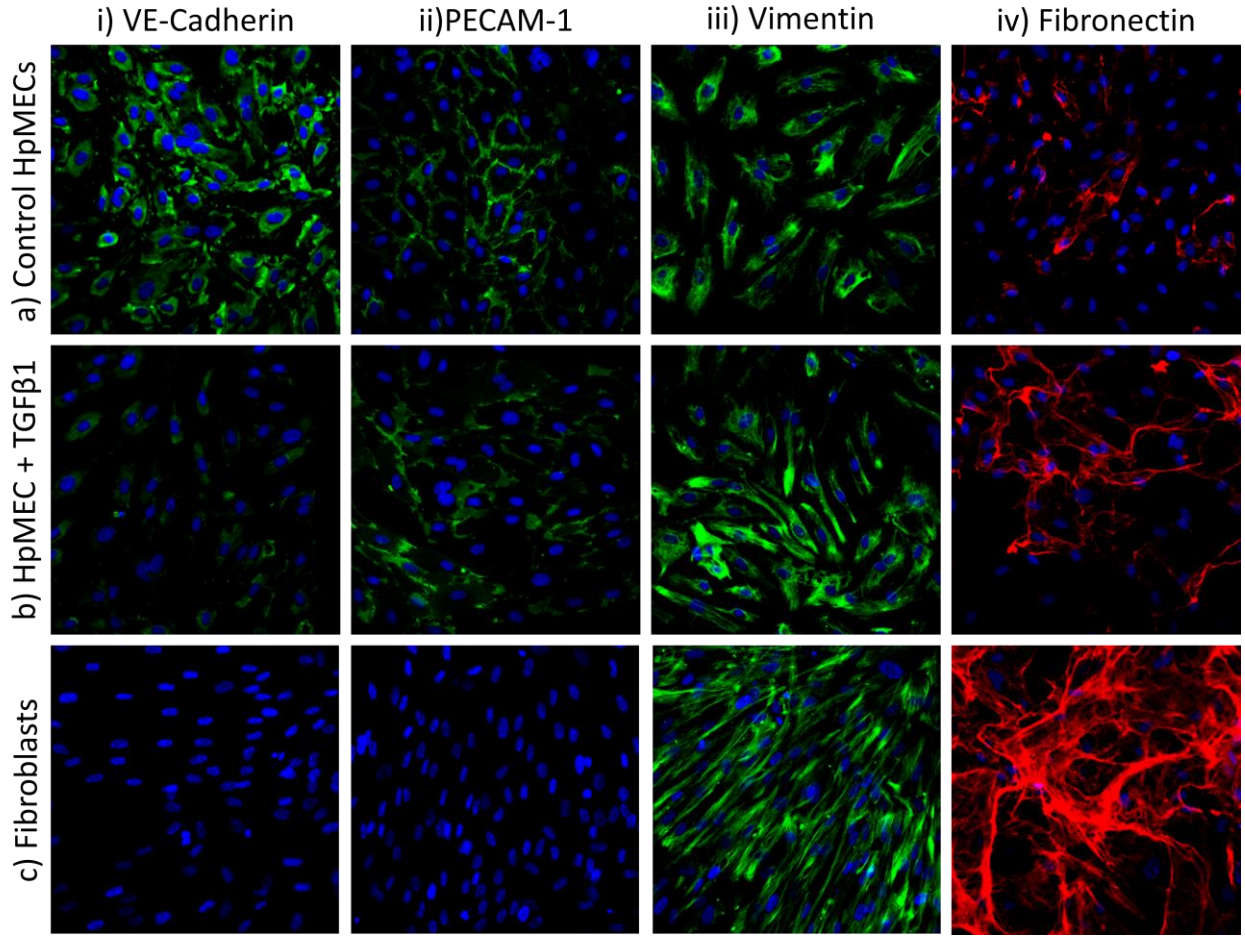


**Figure 6.5:** Confocal microscopy of cells at day 7 post TGFβ1 10ng/ml treatment compared with untreated HLMVECs and fibroblasts. Control HLMVECs stained positively for the endothelial cell surface markers VE-Cadherin (ai) and PECAM-1 (aii) and were also positive for the cytoskeletal protein vimentin (aiii). Minimal fibronectin staining was shown in control HLMVECs (aiv). In response to TGFβ 10ng/ml, HLMVECs down regulated VE-Cadherin (bi) and PECAM-1 (bii). Cells demonstrated change in morphology to spindle cells (biii). TGFβ1 treated cells showed increased fibronectin staining. Fibroblasts stained similarly were negative for VE-Cadherin (ci) and PECAM-1 (cii) but showed bright dense packed spindle cells that were positive for vimentin (ciii) and increased fibronectin deposition (iv).

### *6.4.4 Endothelial cell surface marker expression in response to cigarette smoke extract*

LMVECs treated with 3% CSE for 1 hour and 24 hours were harvested at 7 days, together with untreated cells (controls), and were fixed and stained for the PECAM-1 (endothelial marker) and vimentin, fibronectin and αsma (mesenchymal markers) as above with DAPI nuclear staining. Similar to the previous experiment, untreated control HLMVECs at day 7 were cobblestone like and stained positively for PECAM-1 (Figure 6.6a (i)) and for vimentin (Figure 6.6a (ii)). Cells had very low staining for fibronectin (Figure 6.6a (iii)), but surprisingly were positive for α smooth muscle actin (Figure 6.6a (iv)). In response to 3% CSE for 1 hour, LMVECs appeared to express reduced PECAM-1 (Figure 6.6b (i)) while acknowledging that overall cell number/viability seemed less as suggested by DAPI nuclear stain. Cells became enlarged, spindle shaped and elongated and stained positively for vimentin (Figure 6.6b (ii)) and also demonstrated apparent increased fibronectin staining (Figure 6.6b (iv)). Cells treated with 3% CSE for 24 hours showed very reduced/absent PECAM-1 staining (Figure 6.6c (i)) with reduced cell number/viability indicated by DAPI staining. Remaining cells appeared elongated and stained positively for vimentin (Figure 6.6c (ii)), fibronectin (Figure 6.6c (iii)) and α smooth muscle actin (Figure 6.6c (iv)). Similar to the previous experiment, fibroblasts were negative for PECAM-1 (Figure 6.6d (i)) with high positive staining for vimentin (Figure 6.6d (ii)), fibronectin (Figure 6.6d (iii)) and α smooth muscle actin (Figure 6.6d (iv)).

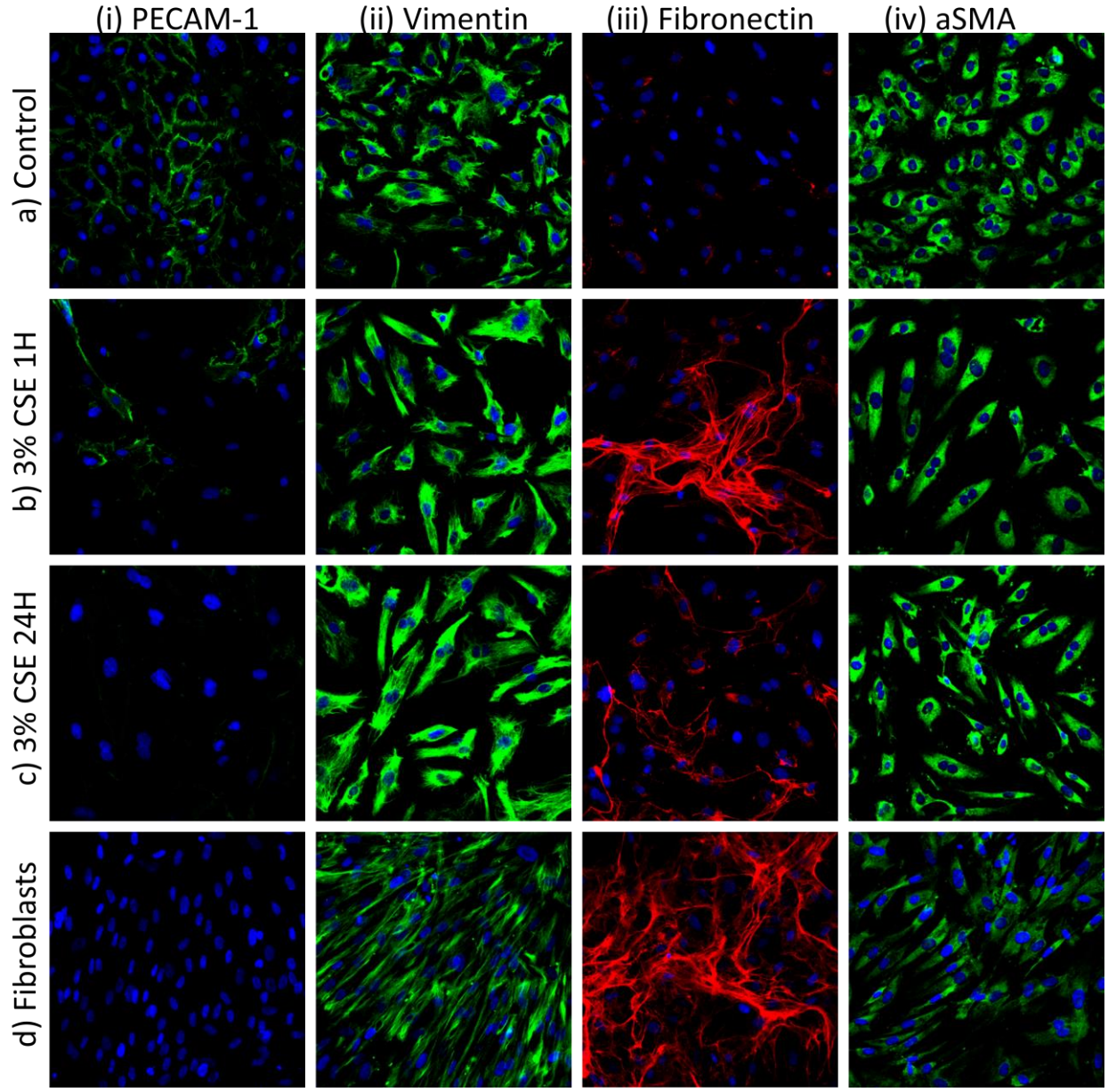


**Figure 6.6:** Confocal microscopy of cells at day 7 post 3% CSE treatment for 1 hour and 24 hours compared with untreated LMVECs and fibroblasts. Control LMVECs stained positively for PECAM-1 (ai) and were also positive for the cytoskeletal protein vimentin (aii). Minimal fibronectin staining was shown in control LMVECs (aiii). The cobblestone outline of control cells was demonstrated via positive α smooth muscle actin staining (aiv). In response to3% CSE at 1 hour and 24 hours, there was marked loss of PECAM-1 (bi), (ci). Cells stained positively for vimentin and became enlarged and elongated (bii), (cii) and similarly showed bright αSMA staining. As in the similar experiment, Fibroblasts were negative for PECAM-1 (di) but showed bright dense packed spindle cells that were positive for vimentin (dii), increased fibronectin deposition (diii) and elongated αSMA positive cells (div).

### *6.4.5 Dual staining for CD31/ fibronectin in LMVECs treated with TGFβ1, CSE and TNFα with untreated dermal fibroblasts as a positive control.*

Following the observation that cells appeared to down regulate endothelial markers with possible upregulation of mesenchymal markers, LMVECs were dual stained for PECAM-1 (CD31) and fibronectin to investigate evidence of co-localisation of markers, as would be expected in transitional cells. PECAM-1 (CD31) a mouse primary antibody was used with FITC (green) mouse secondary antibody. Fibronectin a rabbit antibody was used with a TRITC (red) rabbit secondary antibody. Control cells displayed cell surface staining for PECAM-1 (green) with absent fibronectin staining (red) (Figure 6.7a). Cells treated with TGFβ1 (10ng/ml for 7 days) also demonstrated cells staining for positively for PECAM-1 (green) (Figure 6.7b). However some TGFβ1 treated cells appeared to lack PECAM-1 expression and instead expressed low levels of fibronectin (red) (Figure 6.7b). One cell appeared to express both fibronectin and PECAM-1 which may be evidence of a transitional cell (arrow).

Cells treated with 3% CSE for 1 hour (Figure 6.7c) and 24 hours (Figure 6.7d) at 7 days had reduced cell surface expression of PECAM-1 (green). Cells appeared to express increased fibronectin within the cytoplasm (red). Interestingly the cells treated with CSE appeared more transitional than those treated with TGFβ1 (Figure 6.7b), the archetypal orchestrator of phenotypic switch.

In this experiment, some cells were also treated with TNFα. Cells treated with TNFα alone markedly down regulated PECAM-1 (green) (Figure 6.7e-g). Cells appeared elongated on phase contrast in keeping with reports in the literature [164] [165], but did not increase fibronectin expression or deposition. The down regulation of CD31 was more apparent in the TNFα treated cells than in either those treated with TGFB1 (Figure 6.7b) or CSE (figure 6.7c-d). No transitional cells were evident in this population. Control fibroblasts stained with the same dual staining protocol showed confluent fibronectin staining (red) and absent CD31 (green) (Figure 6.7h).

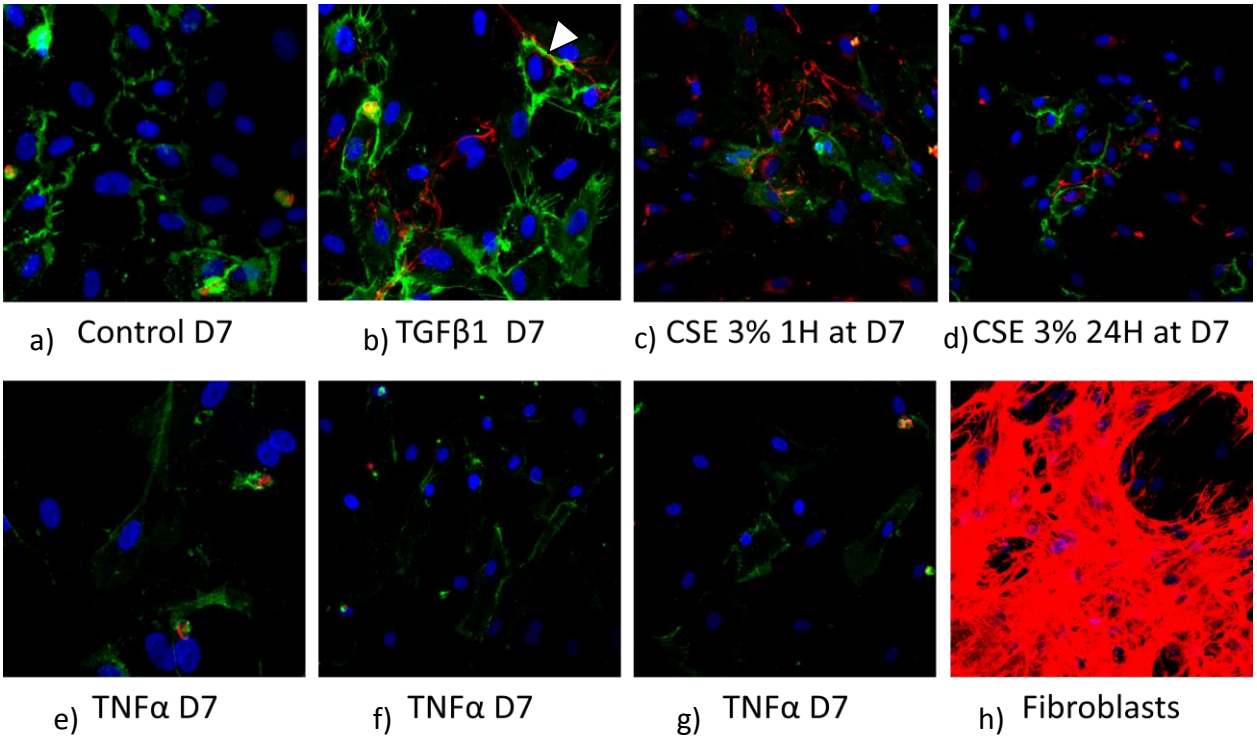


**Figure 6.7:** Dual staining of HLMVECs for PECAM-1/CD31(green, endothelial) and fibronectin (red, mesenchymal) detected via Confocal microscopy at day 7 post TGFβ1 10ng/ml, TNFα 20ng/ml, 3% CSE treatment for 1 hour and 24 hours on day one compared with untreated cells and fibroblasts. Control (untreated cells) stained positively for PECAM-1 but negatively for fibronectin (Figure 7.7a). Cells treated with TGFβ1 10ng/ml showed some cells had absent PECAM-1 staining (green) with low levels of fibronectin staining (red). Some cells appeared to have localisation of CD31 (green) and fibronectin (red) suggesting the possibility of transitional cells (arrow). Cells treated with 3% CSE treatment for 1 hour and 24 hours on day had markedly reduced CD31 staining with increased fibronectin staining. Cells treated with TNFα 20ng/ml showed down regulation of CD31 but with no similar increase in fibronectin. Fibroblasts stained confluently with fibronectin (red) and had absent CD31 (green) staining.

### *6.4.6 Dual staining for CD31/αSMA in LMVECs treated with TGFβ1 and 3% CSE for 1 hour, 24 hours, 48 hours and 72 hours at 7 days compared with untreated cells and dermal fibroblasts.*

Cellular plasticity was further investigated with dual staining via confocal microscopy using another more mature mesenchymal marker αSMA together with CD31. αSMA a rabbit antibody was used with a TRITC (red) rabbit secondary antibody with the same PECAM-1 (CD31) (mouse primary antibody with FITC (green) mouse secondary antibody) as used in the previous experiment.

Control fibroblasts stained with the same dual staining protocol showed elongated cells with strong αSMA (red) and absent CD31 (green) (Figure 6.8a). Untreated LMVECs displayed cell surface staining for PECAM-1 (green) with absent αSMA staining (red) (Figure 6.8b). In this experiment the cells surface staining for CD31 on control cells was less clear than in previous experiments. Cells treated with TGFβ1 (10ng/ml for 7 days) also demonstrated cells staining for positively for PECAM-1 (green) (Figure 6.8c). However some TGFβ1 treated cells appeared to lack PECAM-1 expression while expressing low levels of αSMA (red) (Figure 6.8d). Some cells treated with 3% CSE for 1 hour (Figure 7.8e), 24 hours (Figure 7.8f), 48 hours (Figure 7.8g) and 72 hours (Figure 7.8h) at 7 days had reduced cell surface expression of PECAM-1 (green). The most marked changes were witnessed in the cells treated for 72 hours. Importantly, this was not a universal response with some cells continuing to express their native CD31 in a similar pattern to the untreated cells. There was no clear evidence of cells expressing αSMA in response to CSE.

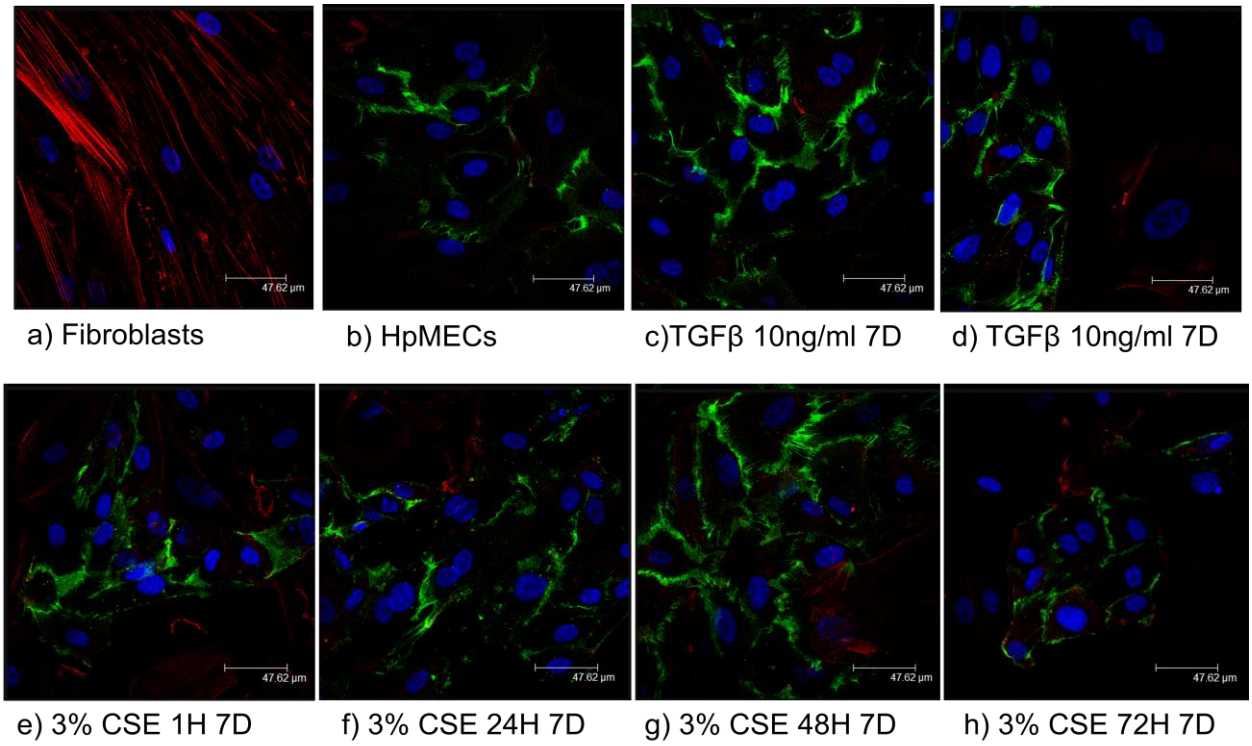


**Figure 6.8:** Dual staining of LMVECs for PECAM-1/CD31(green, endothelial) and αSMA (red, mesenchymal) detected via Confocal microscopy at day 7 post TGFβ1 10ng/ml, 3% CSE treatment for 1 hour, 24 hours, 48 hours and 72 hours compared with untreated cells and fibroblasts. Fibroblasts demonstrated αSMA (red) in sheet like form with absent CD31 (green) staining (Figure 7.8a). Control (untreated cells) stained positively for PECAM-1 but negatively for αSMA (Figure 7.8b). Cells treated with TGFβ1 10ng/ml showed some cells had reduced PECAM-1 staining (Figure 7.8c) with possible low levels of αSMA staining on some cells (Figure 7.8d). Cells treated with 3% CSE treatment for 1 hour (Figure 7.8e), 24 hours (Figure 7.8f), 48 hours (Figure 7.8g) and 72 hours (Figure 7.8h) had reduced CD31 staining. There was no clear evidence of increased αSMA staining in response to CSE

### *6.4.7 Examination of cell surface markers via flow cytometry*

Having identified possible change in cell surface markers, EnMT in response to TGFβ1 and CSE was further investigated via flow cytometry. Cells were treated in triplicate at 70% confluence with TGFβ1 (1ng/ml and 10ng/ml) and CSE 3% for 1 hour and 24 hours as previous. Cells were harvested 7 days post treatment using cell dissociation solution and incubated with the cell surface markers CD31 (endothelial) and CD90 (fibroblast), as used previously in the characterisation experiments (chapter 4). Following incubation, cells were washed and centrifuged at 1000rpm prior to resuspension in PBS and analysed via flow.

All cells stained positively for CD31 and negatively for CD90 (data not shown). However there was a significant reduction in median fluorescence intensity in CD31staining (Figure 6.9) (ANOVA, p=0.028) that was not significant for TGFβ1but significant for CSE at 24 hours (p=0.047). Although the cells were overall positive for the endothelial marker CD31, this data suggests a change in the cellular expression of this marker which may suggest loss of CD31. CD90 was unchanged across all treatments with very low expression, this was however not unsurprising as CD90 is a mature fibroblast marker and such a marked phenotypic switch by 7 days would be unlikely.

Following this experiment, I went on to examine CD31 and CD90 expression at days 11 and 15 to examine whether changes in cell surface expression became more established at later time points (data not presented). However this again showed all cells remained positive for CD31 and negative for CD90 with a reduction in the median fluorescence intensity observed for CD31 but with no change in CD90.

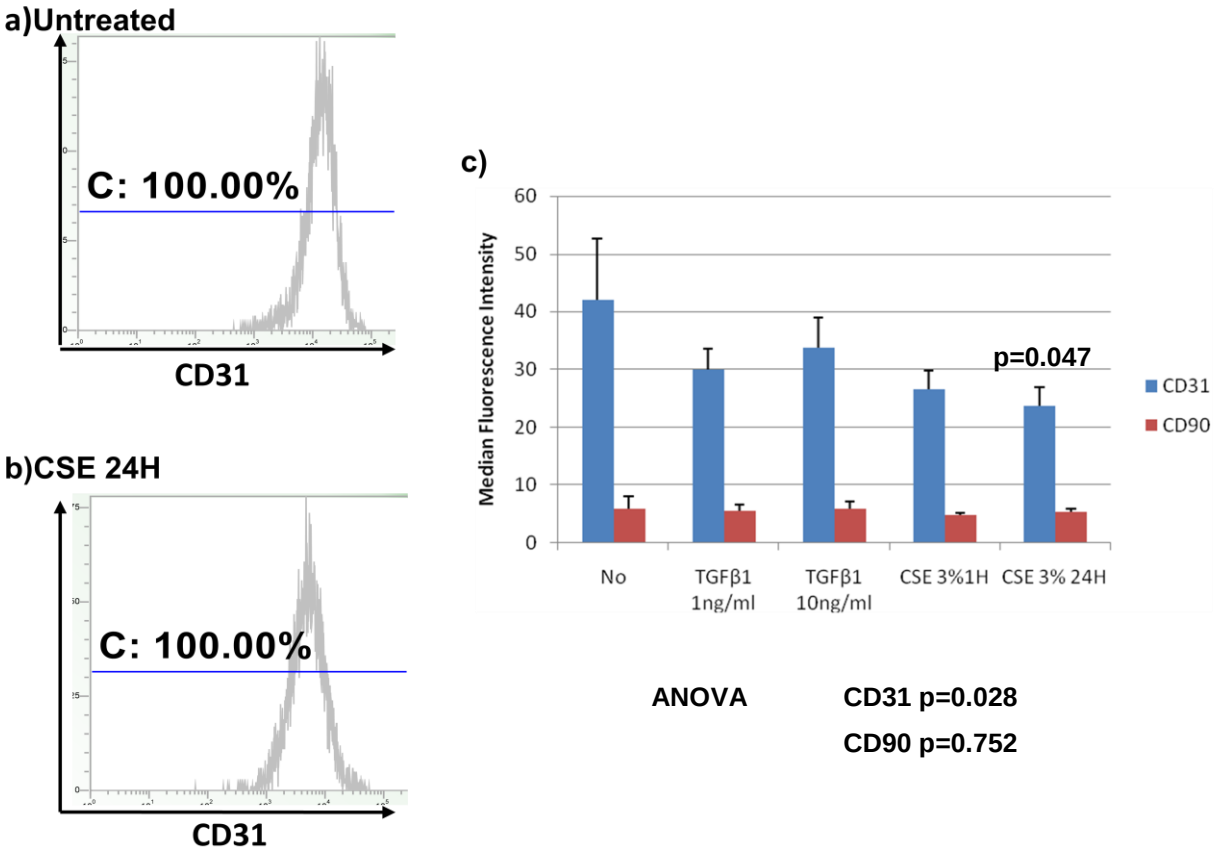


**Figure 6.9:** Examination of cell surface expression in response to TGFβ1 and CSE via flow cytometry. All cells were highly positively for CD31 and negative for CD90 however examination of median fluorescence intensity on the CD31 histograms identified a subtle but significant (p=0.028) leftward shift in the median fluorescence intensity between (6.9a) untreated and (6.9b) CSE treated cells. This CD31 reduction was not significant in response to TGFβ1 but was in response to CSE at 24 hours (p=0.047) (Figure 6.9c).

### *6.4.8 Investigation of change in protein concentration of cell surface markers in response to TGFβ1 via western blotting*

Change in protein expression following treatment with TGFβ1 was thereafter investigated initially in commercial LMVECs (Promocell) but then repeated in emphysema cells and in normal cells.

Cells were treated either with TGFβ1 5ng/ml or TGFβ1 10ng/ml in complete MV2 media. Some cells were also serum starved for 24 hours prior to treatment with 10ng/ml TGFβ1. Control cells had media changed at time zero. Cells were harvested at 7days and lysed in phosphosafe extraction buffer prior to lysing via sonication at 4◦C. Protein concentration of the cell lysates was determined via a BCA protein assay (Figure 6.10).

20ug of protein was loaded for PECAM-1 (CD31), VE-Cadherin, VEGF KDR and αSMA. 5ug protein was loaded for fibronectin and vimentin. Bis Tris 12% gels were ran at 100V and then transferred overnight at 100mAmps onto PVDF. PVDF membranes were blocked in 5% marvel milk. Primary antibodies were thereafter applied and left on a rocker at room temperature for a minimum 90 minutes at room temperature or at 4◦C overnight. Membranes were washed and secondary antibodies applied. Protein bands were detected using chemiluminescence and imaged.

CD31, VEcadherin and VEGF KDR protein expression was unchanged in response to treatment TGFβ1 in LMVECs (Promocell) (Figure 6.11). Fibronectin, Vimentin and αSMA was also unchanged following treatment (Figure 6.11). Serum starvation of cells prior to treatment led to reduced vimentin, asma and fibronectin. β actin was used as a loading control for each membrane and was unchanged across all treatments; a representative blot is also shown in figure 6.11.

This experiment was repeated multiple times in Promocell cells with the same result each time. The experiment was also repeated in cells isolated from patient 15 with normal lungs (Figure 6.12) and in cells isolated from four patients with emphysema (Figure 6.13) and in patient 17 (idiopathic pulmonary arterial hypertension) (Figure 6.14).

| | | | | | | | | | |
|---|---|---|---|---|---|---|---|---|---|
| Read at 490 nm | | | | | | | | | |
| BSA Standards (ug/ml) | | 0 | 25 | 125 | 250 | 500 | 750 | 1000 | 1500 |
| Reading 1 | | 0.099 | 0.134 | 0.283 | 0.419 | 0.672 | 0.854 | 1.172 | 1.49 |
| Reading 2 | | 0.098 | 0.132 | 0.273 | 0.422 | 0.697 | 0.891 | 1.198 | 1.516 |
| Reading 3 | | 0.097 | 0.135 | 0.279 | 0.432 | 0.712 | 0.89 | 1.215 | 1.529 |
| Average Reading | | 0.098 | 0.133667 | 0.278333 | 0.424333 | 0.693667 | 0.878333 | 1.195 | 1.511667 |
| | | 0 | 0.052334 | 0.197 | 0.343 | 0.612334 | 0.797 | 1.113667 | 1.430334 |
| Cell Line | 451/1 | | | | | | | | |
| Length of Treat | 7 days | | | | | | | | |
| Treatment | | control | TGFb1 5 | TGFb1 10 | 10 SF | | | | |
| Reading 1 | | 0.188 | 0.232 | 0.187 | 0.202 | | | | |
| Reading 2 | | 0.197 | 0.241 | 0.187 | 0.209 | | | | |
| Reading 3 | | 0.191 | 0.252 | 0.187 | 0.204 | | | | |
| Average Reading | | 0.192 | 0.241667 | 0.187 | 0.205 | | | | |
| Average - control | | 0.094 | 0.143667 | 0.089 | 0.107 | | | | |
| | | | | | | | | | |
| Protein Concentration mg/ml | | 3.008 | 4.597333 | 2.848 | 3.424 | | | | |
| 60ug = Xul | | 19.946809 | 13.05104 | 21.06742 | 17.52336 | | | | |
| 30ug = Xul | | 9.9734043 | 6.525522 | 10.53371 | 8.761682 | | | | |
| 10ug = Xul | | 3.3244681 | 2.175174 | 3.511236 | 2.920561 | | | | |
| 5ug = Xul | | 1.662234 | 1.087587 | 1.755618 | 1.46028 | | | | |

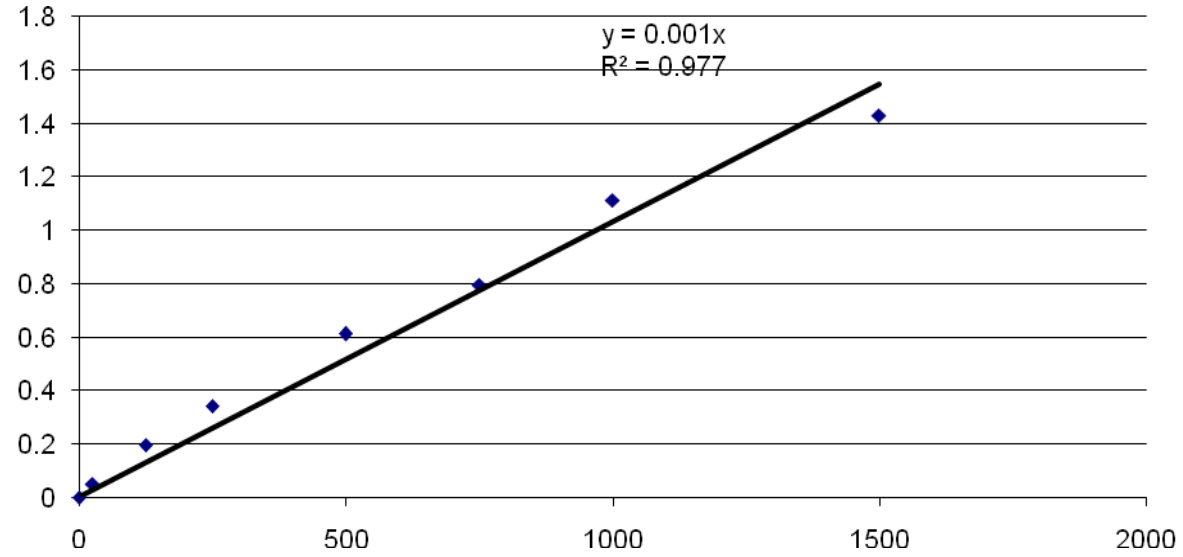


**Figure 6.10:** Cell lysates were placed in phosphosafe extraction buffer and gently sonicated. A BCA protein assay was then ran with standards prepared via serial dilution and plated in triplicate onto an elecsys optical plate. Unknown samples (in this case cells 451.1 control, TGFβ1 5ng/ml, TGFβ1 10ng/ml and Ss TGFβ1 10ng/ml) were also plated in triplicate. The plate was incubated at 37◦C and read at 490nm after 30 minutes incubation. A standard curve was constructed and protein concentration of unknown samples extrapolated from the curve. Protein concentration (mg/ml) was determined and thereafter concentration to plate 20ug or 5ug for each western blot determined.

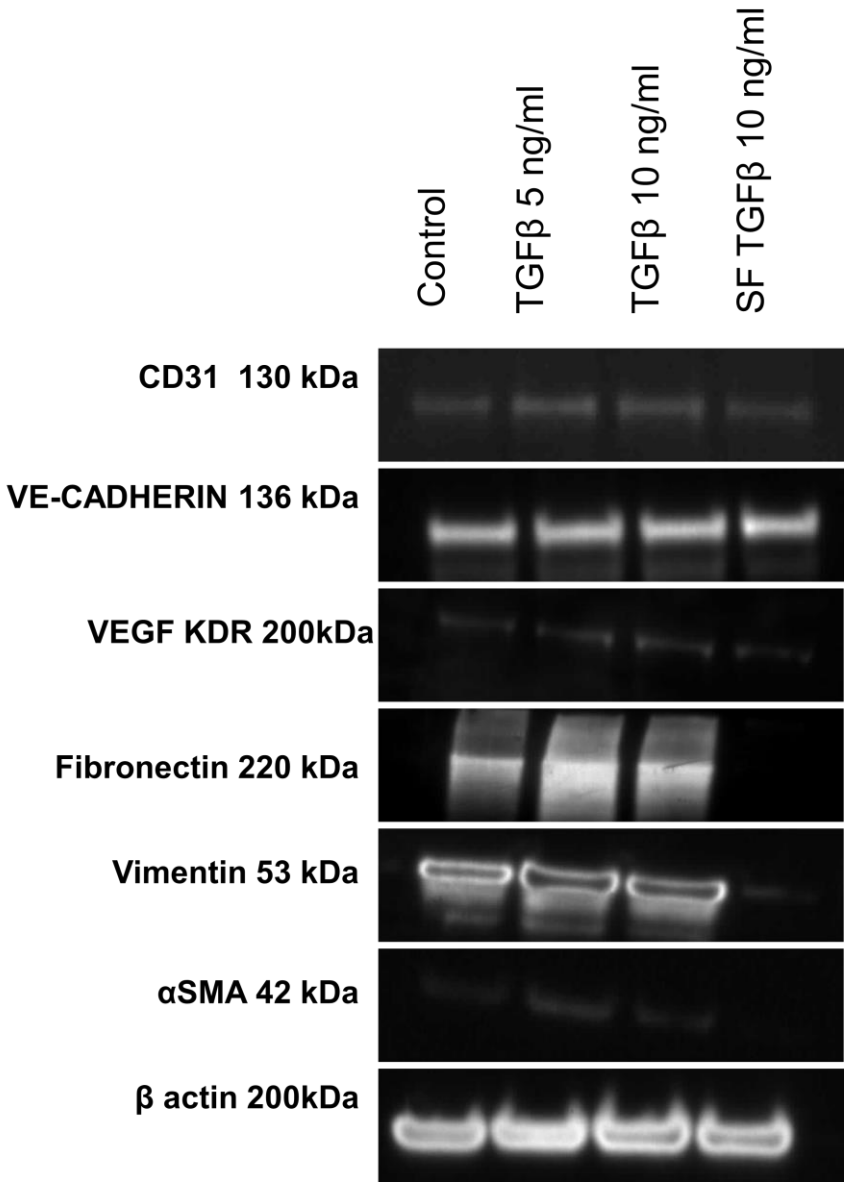


**Figure 6.11:** Normal LMVECs (Promocell) treated with TGFβ1 5ng/ml and 10ng/ml versus control (untreated cells) at 7 days. One sample of cells was also serum starved (Ss) prior to treatment with TGFβ1 10ng/ml. Western blots obtained showed CD31, VEcadherin and VEGF KDR protein expression was unchanged in response to treatment with TGFβ1. There was no change in the mesenchymal markers fibronectin, vimentin and αSMA. Serum starvation of cells prior to treatment led to reduced vimentin, asma and fibronectin, although endothelial markers were unchanged. The cause of this is unclear. βactin was used as a loading control and was unchanged across all treatments.

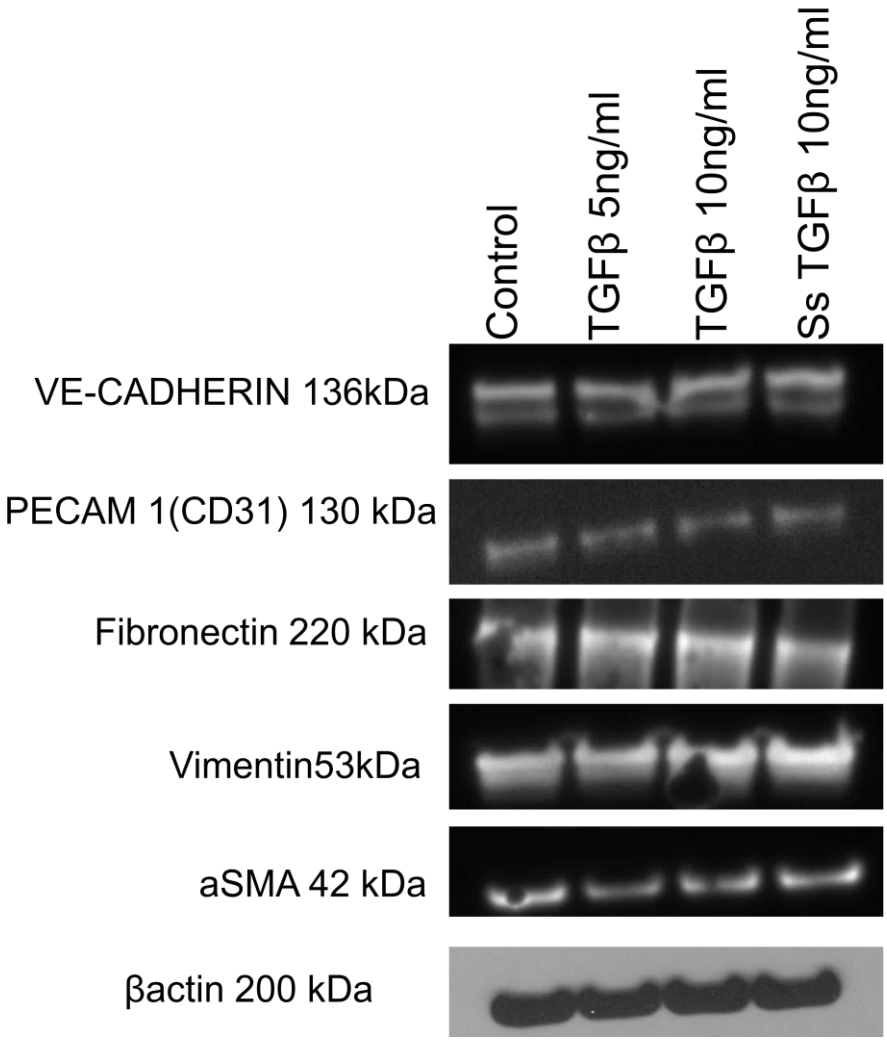


**Figure 6.12:** LMVECs isolated from excess normal tissue at lobectomy (patient 15) treated with TGFβ1 5ng/ml and 10ng/ml versus control (untreated cells) at 7 days. One sample of cells was also serum starved (Ss) prior to treatment with TGFβ1 10ng/ml. Western blots obtained show the endothelial markers CD31, and VE-cadherin protein expression was unchanged in response to treatment with 5ng/ml and 10ng/ml TGFβ1 at 7 days. The mesenchymal markers fibronectin, vimentin and αSMA were also unchanged. βactin acted as a loading control and was unchanged across all treatments.

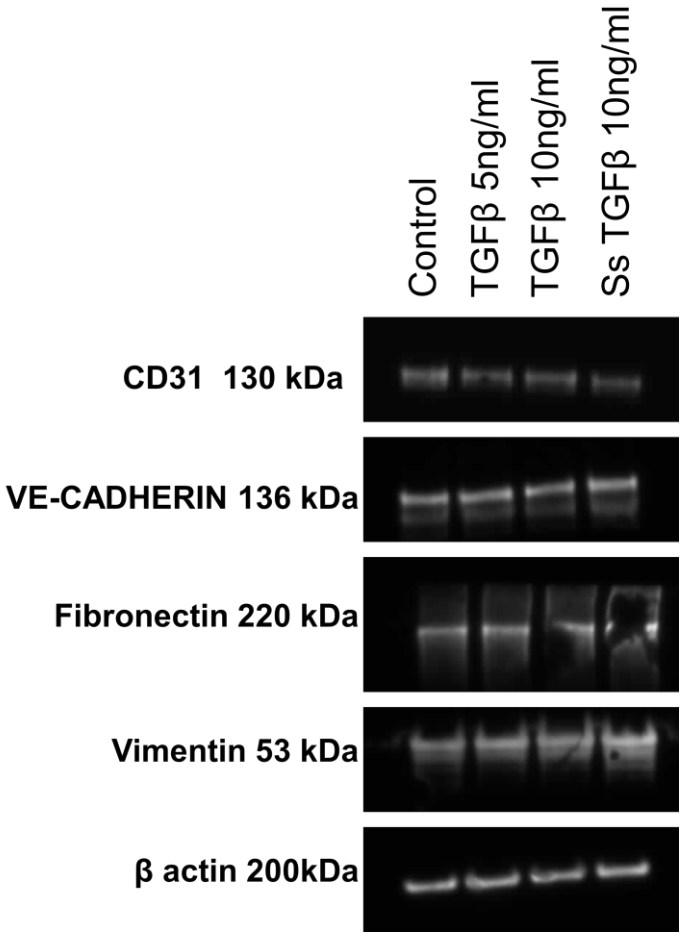


**Figure 6.13:** LMVECs isolated from a patient with emphysema (patient 8) were treated with TGFβ1 5ng/ml and 10ng/ml and compared with untreated (control cells) at 7 days. One sample of cells was also serum starved (Ss) prior to treatment with TGFβ1 10ng/ml. Western blots obtained show that CD31 and VE-cadherin protein expression (endothelial markers) were unchanged in response to treatment with 5ng/ml and 10ng/ml TGFβ1 at 7 days. The mesenchymal markers fibronectin and vimentin were also unchanged. βactin acted as a loading control and was unchanged across all treatments.

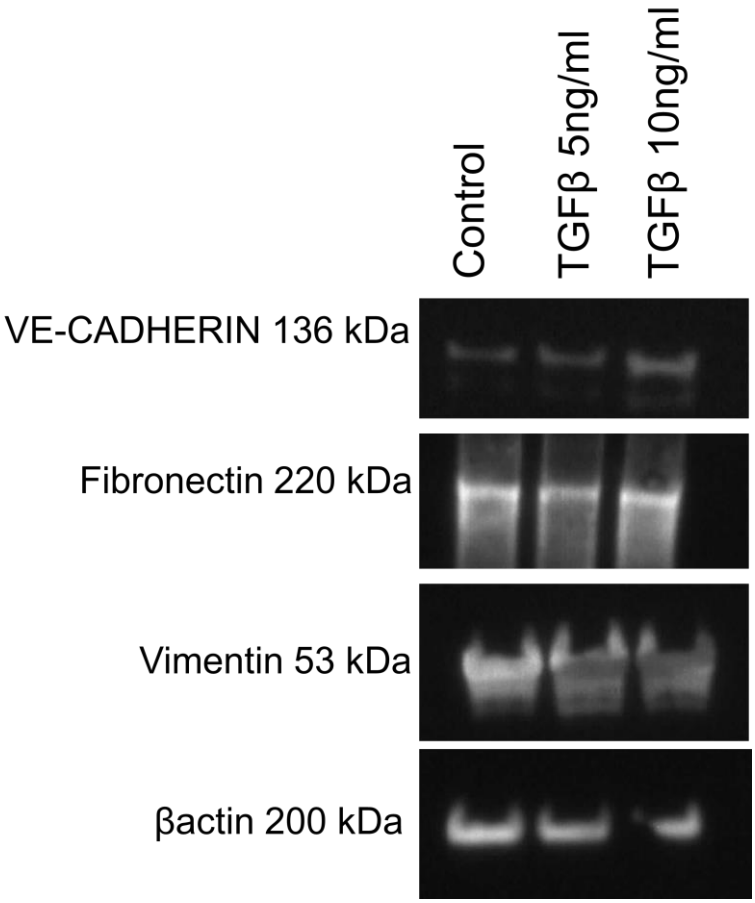


**Figure 7.14:** LMVECs isolated from patient with idiopathic pulmonary arterial hypertension (patient 17) treated with TGFβ1 5ng/ml and 10ng/ml versus control (untreated cells) at 7 days. Limited markers were used in this exploratory experiment. Western blots obtained show the endothelial marker VE-cadherin protein expression was unchanged across the treatments at 7 days. The mesenchymal markers fibronectin and vimentin were also unchanged across treatments. βactin acted as a loading control.

In view of these persistently negative findings, A549 cells were treated similarly to the above experiments with TGFβ1 to investigate whether I could induce epithelial to mesenchymal transition as has been reported extensively by other researchers, including those in my own group. The result shown in Figure 7.15 confirmed a positive control that epithelial cells but not endothelial cells undergo a possible phenotype switch in response to TGFβ1 as evidenced by down regulation of the endothelial marker E-cadherin with associated increased fibronectin and vimentin. β actin was again used as a loading control and was unchanged, further validating these results.

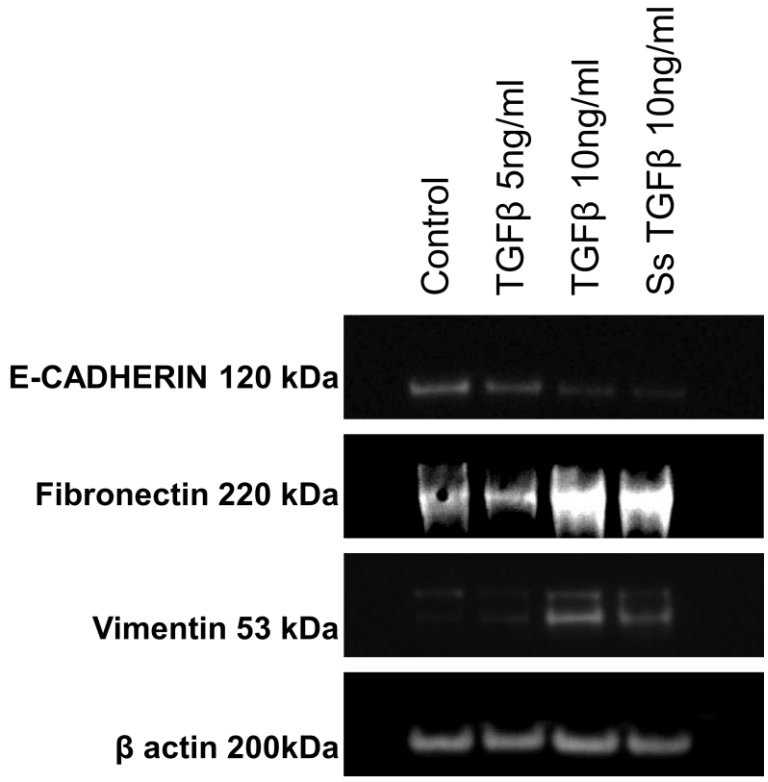


**Figure 6.15:** The epithelial cell line A549 was treated with TGFβ1 5ng/ml and 10ng/ml and compared with control (untreated cells) at 7 days. Some cells were also treated after serum starvation (Ss) for 24 hours prior to treatment. Cellular protein expression was investigated via the epithelial cell marker E-cadherin and the mesenchymal markers fibronectin and vimentin. βactin was used as a loading control.Western blots show loss of the epithelial marker E-cadherin in response to treatment with TGFβ1 10ng/ml but not 5ng/ml. Fibronectin and Vimentin were increased following TGFβ1 10ng/ml compared with untreated cells and those treated with TGFβ1 5ng/ml. Response was similar in the serum starved cells treated with TGFβ1 10ng/ml and those treated with TGFβ1 10ng/ml without serum starvation. A representative blot for β actin is shown. A loading control was checked for each blot and confirmed equal loading further validating these results of loss of epithelial markers with acquisition of mesenchymal markers in response to TGFβ1 10ng/ml.

### *6.4.9 Investigation of change in protein concentration of cell surface markers in response to CSE via western blotting*

In view of the preliminary observations on confocal microscopy which suggested CSE may be a more potent stimulator of phenotypic change in endothelial cells, western blotting was performed on cell lysates prepared from cells treated with 3% CSE. From the viability work, it was decided to investigate EnMT following treatment with 3% CSE for 1 hour and 24 hours at 7 days. Initially experiments used LMVECs (Promocell) (Figure 6.16), but thereafter all work was repeated in cells isolated from patients with emphysema and in cells isolated from normal excess tissue obtained at lobectomy. The endothelial and mesenchymal markers used in the TGFβ1 stimulation experiments were used similarly in these experiments. EnMT was also investigated at earlier time points, with cells treated with 3% CSE for 24, 48 and 72 hours and EnMT investigated thereafter.

LMVECs (Promocell) treated with TGFβ1 10ng/ml for 7 days or 3% CSE for 1 hour or 24 hours with cells harvested 7 days post exposure and compared with untreated cells showed no discernible change in CD31, fibronectin or vimentin (Figure 6.16). LMVECs (Promocell) treated with 3% CSE for 24, 48 and 72 hours showed no loss of CD31 (endothelial marker) and no upregulation of fibronectin, vimentin and aSMA (mesenchymal markers) (Figure 6.17). This experiment was repeated in cells isolated from patients with emphysema (Figure 6.18-6.19), cells isolated from excess normal tissue (Figure 6.20) and using A549 cells (epithelial cell line) (Figure 6.21). There was no evidence of change in protein expression found in support of EnMT or EMT in response to CSE.

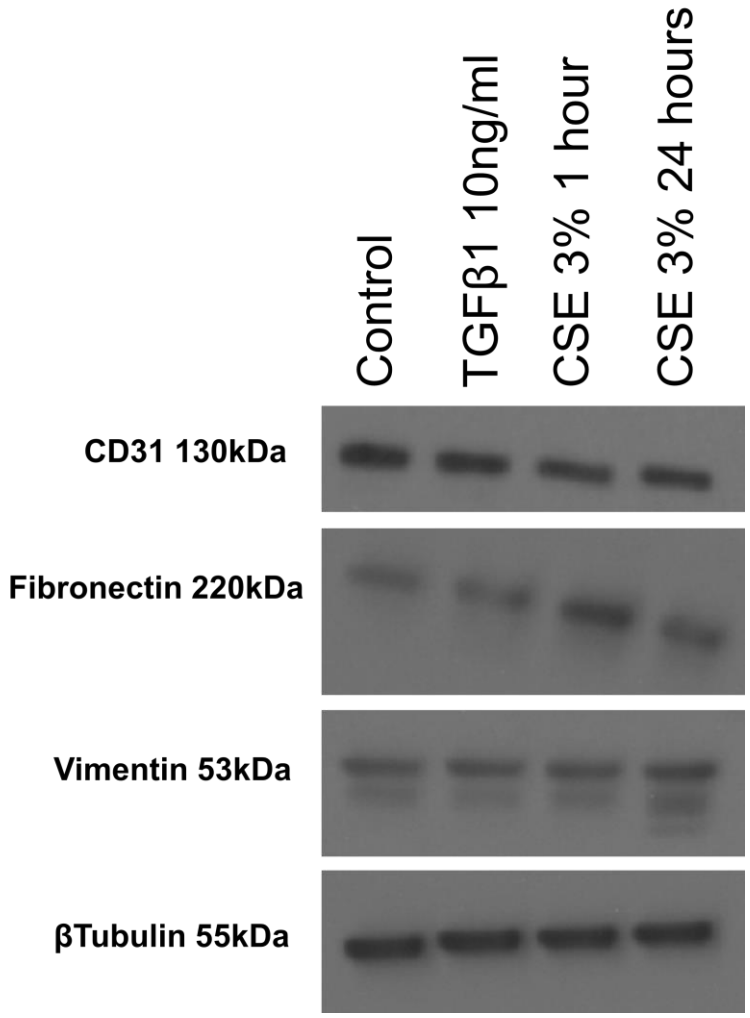


**Figure 6.16:** HLMVECs (Promocell) treated with TGFβ1 10ng/ml for 7 days or 3% CSE for 1 hour or 24 hours with cells harvested at 7 days post exposure and compared with protein expression of untreated cells at 7 days. Limited markers were used in this exploratory experiment. There was no change in CD31 or vimentin or fibronectin in response to TGFβ1, 3% CSE for 1 hour and 24 hours. βtubulin was used as a loading control.

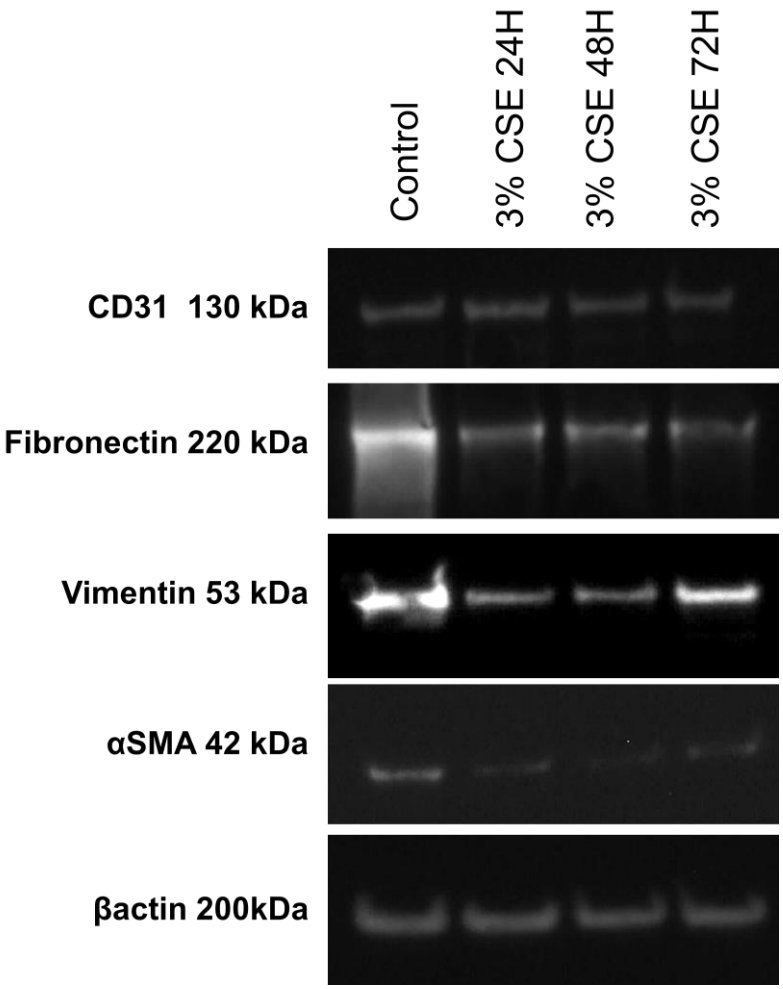


**Figure 6.17:** HLMVECs (Promocell) were treated with 3% CSE for 24, 48 and 72 hours and compared with untreated cells (controls). Protein expression was investigated via western blotting for the endothelial marker CD31 and for the mesenchymal markers fibronectin, vimentin and aSMA. β actin was used as a loading control. Western blots showed no change in CD31 expression on cells treated with 3% CSE across the 3 time points. There was no increase in mesenchymal markers observed in response to CSE, indeed control cells expressed more fibronectin, vimentin and aSMA than treated cells. Loading controls for each blot were confirmed using βactin, a representative blot is shown.

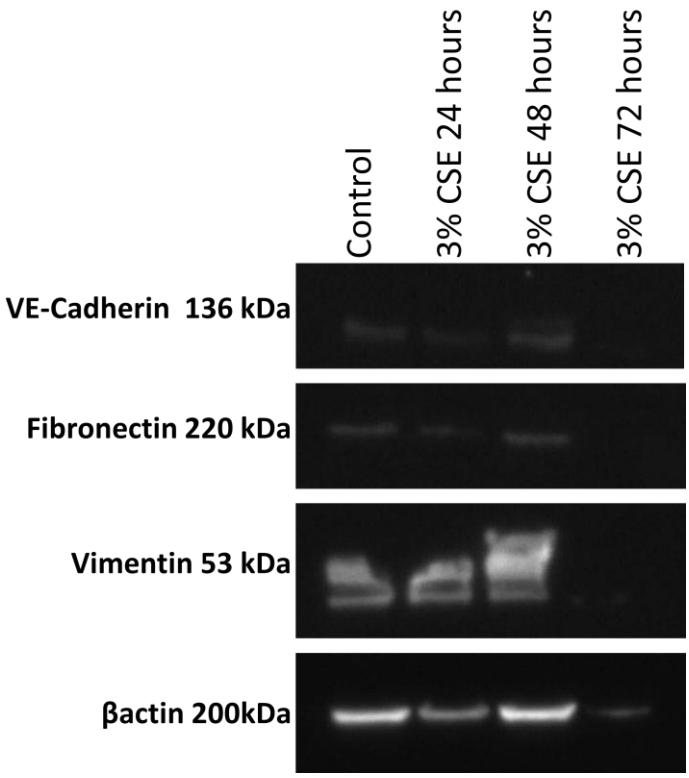


**Figure 6.18:** LMVECs isolated from emphysema lung tissue (patient 8) were treated with 3% CSE for 24, 48 and 72 hours and compared with untreated cells (controls). Protein expression was investigated via western blotting for the endothelial marker VE-cadherin and for the mesenchymal markers fibronectin, and vimentin. There was no change in VE-cadherin or vimentin or fibronectin in response to 3% CSE for 24, 48, 72 hours. βactin was used as a loading control.

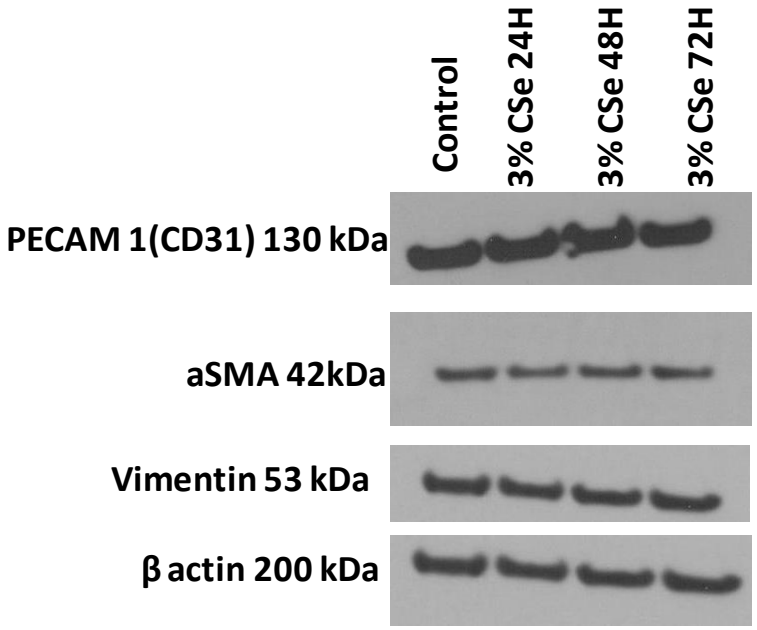


**Figure 6.19:** LMVECs isolated from emphysema lung tissue (patient 4) were treated with 3% CSE for 24, 48 and 72 hours and compared with untreated cells (controls). Protein expression was investigated via western blotting for the endothelial marker CD31 and for the mesenchymal markers vimentin and aSMA. There was no change in PECAM-1, aSMA or vimentin in response to 3% CSE for 24, 48, 72 hours. βactin was used as a loading control.

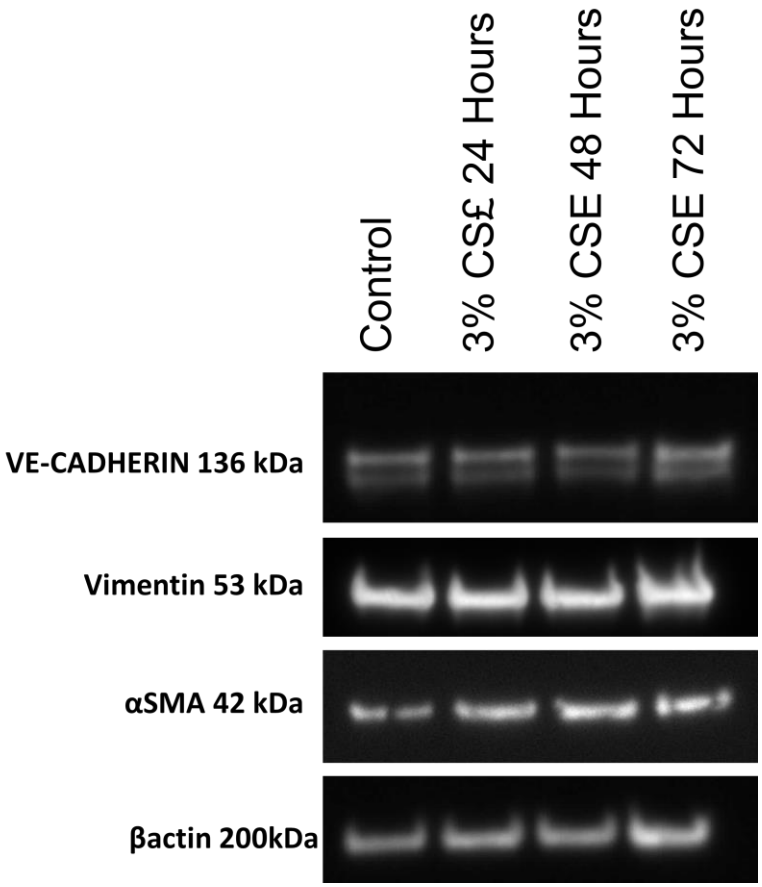


**Figure 6.20:** LMVECs isolated from normal lung tissue (patient 15) were treated with 3% CSE for 24, 48 and 72 hours and compared with untreated cells (controls). Protein expression was investigated via western blotting for the endothelial marker VE-Cadherin and for the mesenchymal markers fibronectin, vimentin and aSMA. There was no change in VE-cadherin or vimentin or aSMA in response to 3% CSE for 24, 48, 72 hours. βactin was used as a loading control.

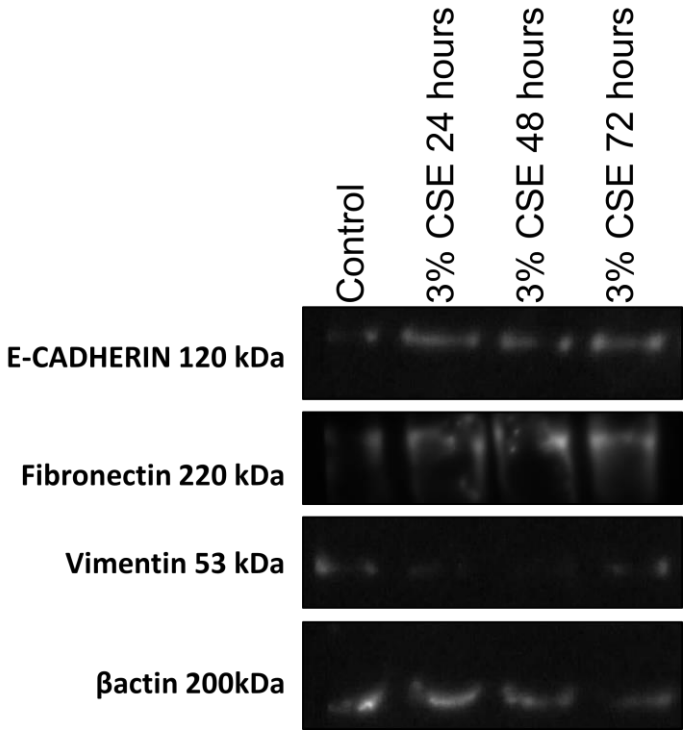


**Figure 6.21:** A549 cells were treated with 3% CSE for 24, 48 and 72 hours and compared with untreated cells (controls). Protein expression was investigated via western blotting for the epithelial marker E-Cadherin and for the mesenchymal markers fibronectin and vimentin. β actin was used as a loading control. Western blots showed no change in E-cadherin expression on cells treated with 3% CSE across the 3 time points. There was no increase in mesenchymal markers observed in response to CSE. Loading controls for each blot were confirmed using βactin, a representative blot is shown.

### *6.4.10 Endothelial cell activation in response to cigarette smoke extract*

Endothelin-1, the potent vasoconstrictor peptide associated with cigarette smoke induced endothelial dysfunction in the systemic circulation, has been reported to be induced by TGFβ1 [160], [166]. Endothelin-1 release from cells treated with TGFβ1 and CSE was therefore investigated via ELISA.

Using a standard commercial ELISA kit, standards (0-100pg/ml) were titrated together with samples of media from endothelial cells treated with TGFβ1 5ng/ml and 10ng/ml and 3% CSE for 24, 48 and 72 hours as in previous experiments. Cells from 2 donors with emphysema (patient 7) and patient 8), from excess normal tissue (patient 15) and from Promocell were used for experiments. A standard curve was constructed from the absorbance at 450nm (Figure 6.22) and then concentration of Endothelin-1 in media from cells treated (n=2 for TGFβ1 experiment, n=3 for CSE experiments) calculated and tabulated (Figure 6.23 & Figure 6.24). Concentration of Endothelin-1 in media from commercial HLMVECs (Promocell) was too high and above the greatest standard concentration used (100pg/ml) and so these results were unable to be included. It is difficult to interpret whether this reflects less ET1 in emphysema cells or whether lower cell viability and thus lower cell density accounted for this observation.

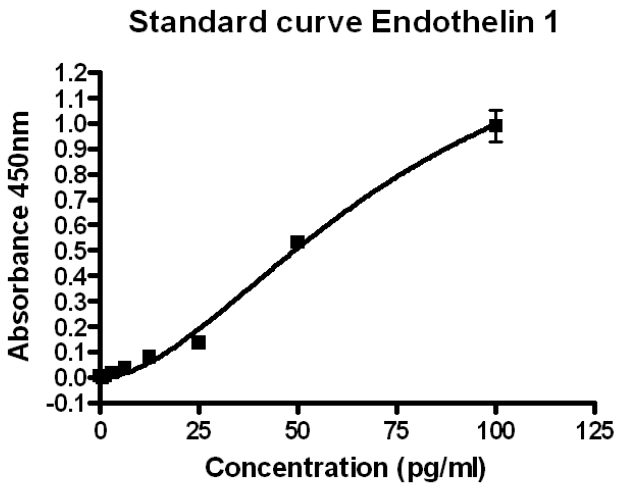


**Figure 6.22:** Standard curve using Endothelin-1 standards incubated with primary antibody and detected via enzyme linked immunoabsorbant assay (ELISA).

Cell supernatants showed a trend towards increase in endothelin-1 in response to treatment with TGFβ1 5ng/ml and 10ng/ml but this did not reach significance (p=0.078).

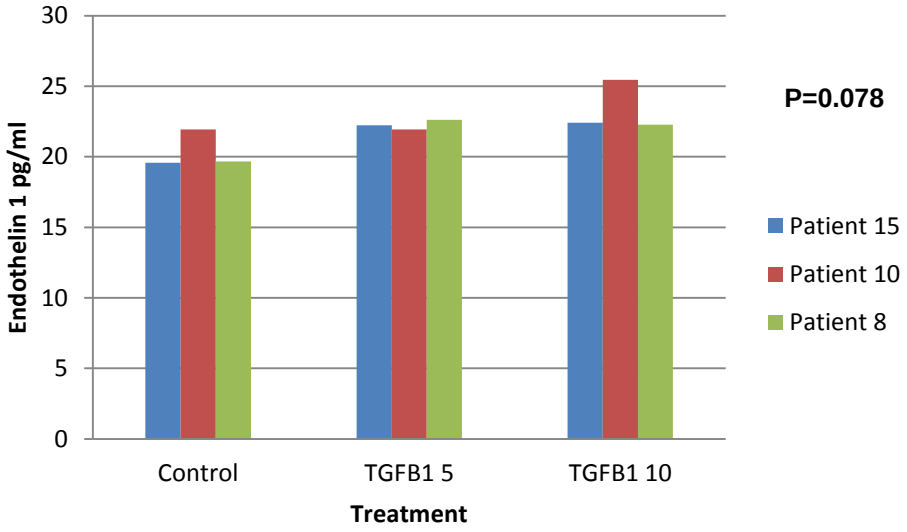


**Figure 6.23:** ELISA of cell supernatants to investigate endothelin-1 release in response to TGFβ1 in cells from normal tissue (patient 15 (451.1)) and from emphysema tissue (patient 7 (295A) and patient 8 (300C). Cell supernatants showed a trend towards increase in endothelin-1 in response to treatment with TGFβ1 5ng/ml and 10ng/ml but this did not reach significance (p=0.078), (all results n=2).

Supernatants from cells treated with CSE did not show such a relationship with normal cells (patient 15) showing essentially unchanged levels of Endothelin-1, while there was a tendency to a reduction in endothelin-1 in (patient 8) but an increase in another (patient 7). All results represent n=3, however due to the conflicting results no statistical analysis was performed and no further conclusions can be drawn from this experiment.

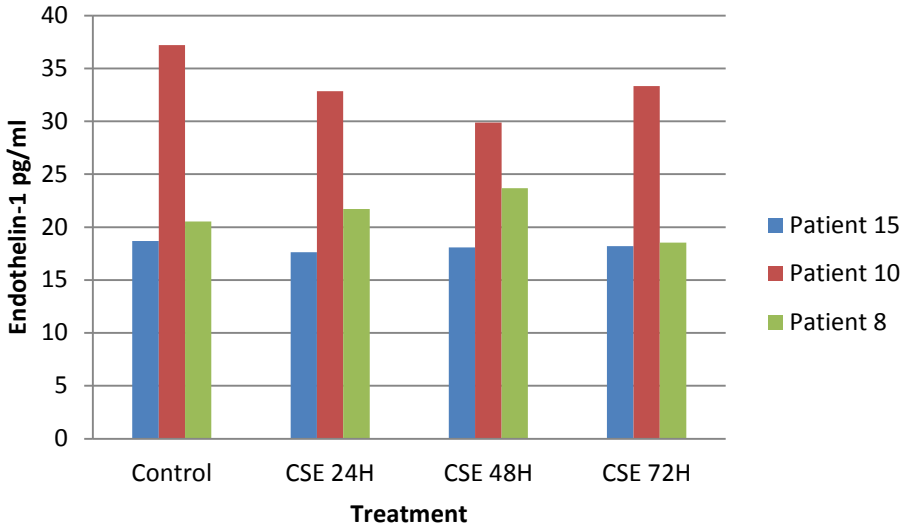


**Figure 6.24:** ELISA of cell supernatants to investigate endothelin-1 release in response to CSE in cells from normal tissue (patient 15) and from emphysema tissue (patient 7 and patient 8). Supernatants from cells treated with CSE showed no clear response, with normal cells (patient 15) showing essentially unchanged levels of Endothelin-1, while there was a tendency to a reduction in endothelin-1 in one emphysema donor (patient 8) but an increase in another (patient 7). All results represent n=3. No further conclusions should be drawn from this experiment unless repeated.

### *6.4.11 In vivo evidence of endothelial plasticity/ phenotype change*

To further investigate the existence of transitional cells and EnMT in the emphysematous lung, I attempted to perform dual staining for CD31 and aSMA via immunohistochemistry on paraffin embedded blocks from which emphysema lung from which cells were isolated. In vivo evidence of EMT has been demonstrated in the post lung transplant airway via dual immunofluorescence [156] by colleagues in our institute and so I employed the same technique in order to investigate EnMT. Unlike airways, the alveolar bed has a very high autofluorescence due to elastin (Figure 6.25). Figure 7.25a shows an arteriole (arrow), venule and surrounding alveolar bed with CD31 detected with a FITC secondary antibody. Figure 6.25b shows the same section with no primary antibody applied i.e. no CD31, but with FITC secondary alone. There is similar bright green staining suggesting autofluorescence. This was further confirmed with no primary or secondary antibody applied with DAPI alone (Figure 6.25c) in which there was clear autofluorescence, rendering the stain uninterpretable. No such difficulties were encountered with αSMA which gave a clear signal (red) with no autofluorescence (Figure 6.26). In view of this, I therefore attempted to quench autofluorescence using pontamine sky blue.

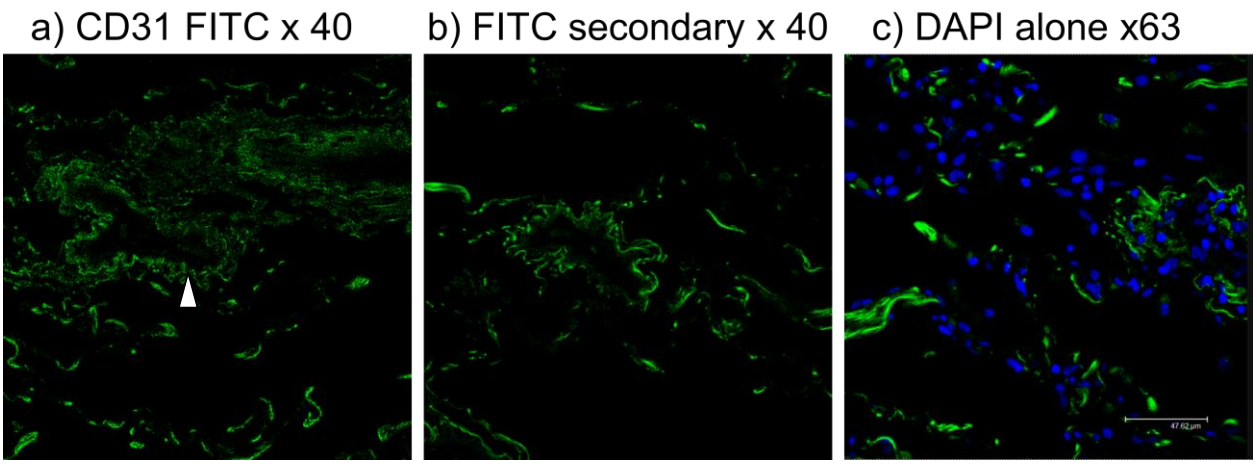


**Figure 6.25:**CD31/αSMA immunohistochemistry on paraffin embedded blocks from emphysema lung tissue visualised via the FITC green channel. CD31 with FITC secondary (a) allowed visualisation of an arteriole (arrow), venule and surrounding alveolar bed. However the same section with FITC secondary alone applied (b) showed similar staining with visualisation of arteriole and supporting alveolar bed suggesting autofluorescence. This was confirmed when no primary or secondary antibody was applied (DAPI alone) (c) in which there was clear autofluorescence, rendering the stain uninterpretable.

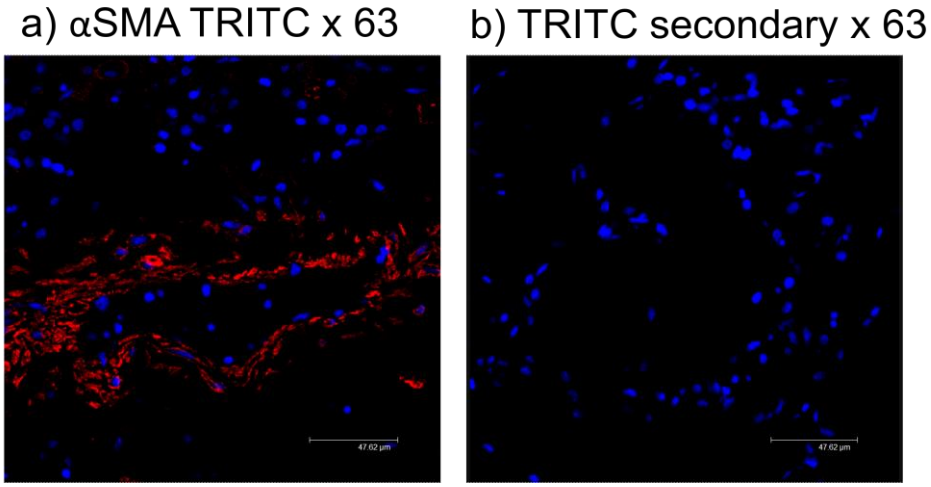


**Figure 6.26:** CD31/αSMA immunohistochemistry on paraffin embedded blocks from emphysema lung tissue detected via the TRITC channel. αSMA with TRITC secondary (a) allowed visualisation of an arteriole and surrounding alveolar bed. The same section with TRITC secondary alone applied (b) showed no background autofluorescence.

Elastin and collagen are abundant in the lung and autofluoresce under ultraviolet light. Elastin contains several fluorophores, one of which is a tricarboxylic amino acid with a pyridinium ring [167] which is similar to a fluorophore found in collagen. Studying the lung microvasculature therefore poses a problem as the internal elastic lamina of arterioles and the elastin associated with the alveolar bed emits a signal which is frequently more intense than any signal detected with the primary antibodies of study. Supporting collagen around vessels and in the alveolar bed further compounds this. Pontamine sky blue has been used to quench autofluorescence in a pre-treatment stage prior to antigen retrieval and immunostaining [168]. I therefore stained multiple sections of lung tissue in order to investigate whether I could achieve a clean CD31 immunofluorescent stain.

HRP CD31 immunostaining requires pre-treatment with boric acid in order to bring out the microvasculature, thus adding further complexity. The results are shown in figure 6.27. Tissue pre-treated with boric acid prior to CD31 staining showed intense fluorescent green staining (a) in alveolar bed and external elastic lamina of vessels, consistent with the previous experiment and well documented autofluorescence. Similarly pre-treatment with boric acid but with only FITC secondary antibody i.e. no CD31, showed high autofluorescence. Pre-treatment of the section with pontamine sky blue followed by FITC secondary antibody alone (c) showed reduced but not complete attenuation of autofluorescence, When tissue was pre-treated with pontamine sky blue and then boric acid as an antigen retrieval agent prior to antibody staining with CD31 followed by FITC secondary, there was very weak staining and no autofluorescence (d). CD31 was only applied for 1 hour at room temperature and so it may be that a more prolonged incubation period i.e. overnight at 4◦C may have increased the signal. This was confirmed by the same finding when incubated without primary antibody (e). However when the section was pre-treated with pontamine sky blue and boric acid and stained for CD31 was viewed on the TRITC (red) channel, there was now intense autofluorescence detected (f). Thus pontamine sky blue fluoresces red, shifting the autofluorescence from green to red and so for such dual staining is unsuitable. Due to such difficulties encountered trying to quench lung autofluorescence, I converted the stain to light microscopy immunocytochemistry.

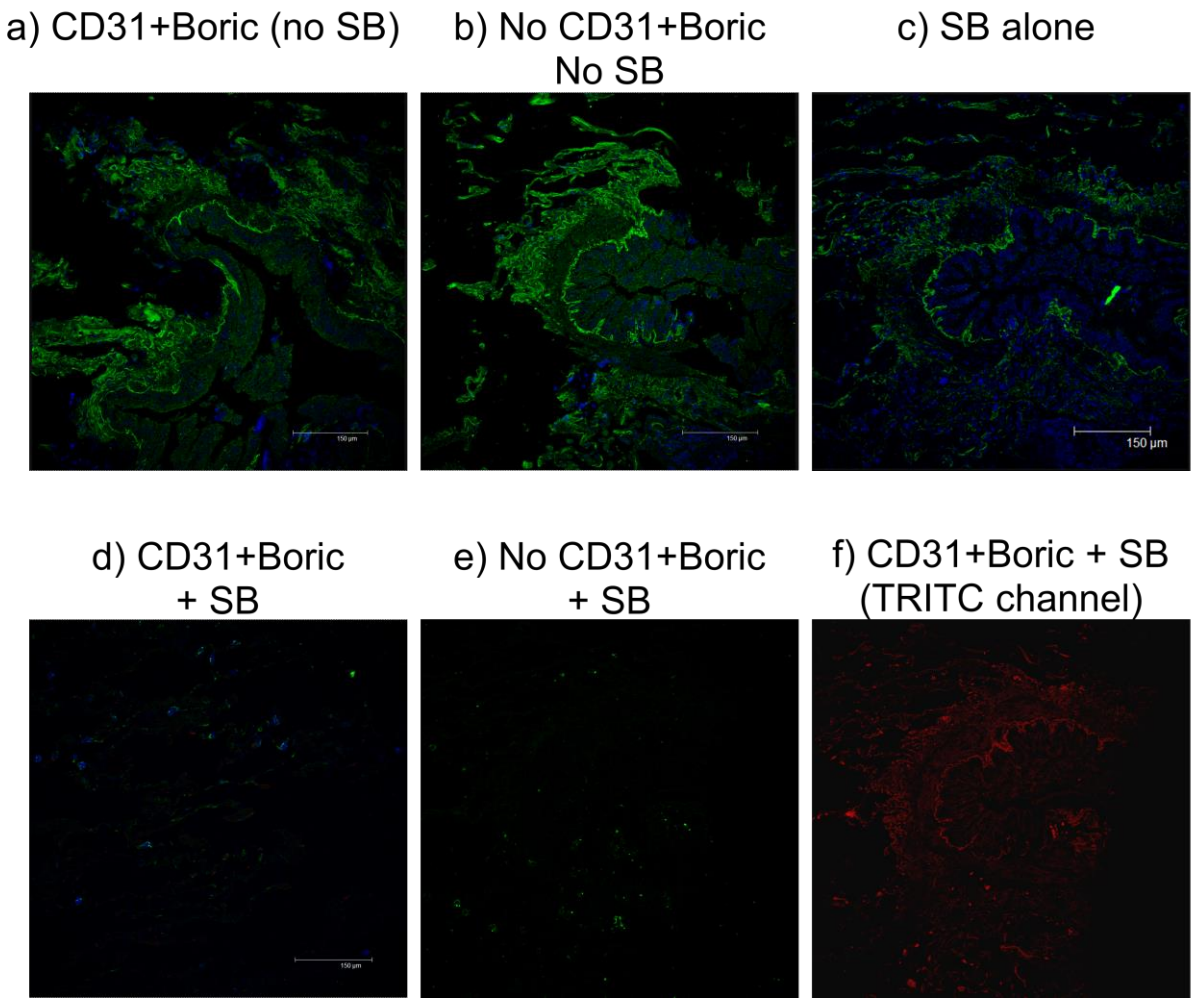


**Figure 6.27:** CD31 immunostaining on paraffin embedded emphysema lung tissue. Tissue pre-treated with boric acid (antigen retrieval agent) with CD31 showed intense fluorescent green staining (a) in alveolar bed and external elastic lamina of vessels. However as before similar pre-treatment but without any primary antibody applied i.e. no CD31 produced similar staining suggesting autofluorescence. Pre-treatment of paraffin embedded tissue with pontamine sky blue but no primary antibody (c) showed reduced but not complete attenuation of autofluorescence, When tissue was pre-treated with pontamine sky blue and then boric acid as an antigen retrieval agent prior to antibody staining with CD31 followed by FITC secondary, there was very weak staining but no autofluorescence (d). CD31 was only applied for 1 hour at room temperature and so it may be that a more prolonged incubation period i.e. overnight at 4◦C may have increased the signal. This was confirmed by the same finding when incubated without primary antibody (e). However when the section was pre-treated with pontamine sky blue and boric acid and stained for CD31 was viewed on the TRITC (red) channel, there was now intense autofluorescence detected (f).

CD34 is an alternative marker of endothelial cells that has been used to investigate the lung microvasculature. CD34 immunocytochemistry did not require antigen retrieval with boric acid and therefore in addition to CD31/αSMA, I also stained tissue for CD34/ αSMA due to concerns over the quality of CD31 on dual staining. CD31 and CD34 were detected via HRP/DAB (brown). 0.5% hydrogen peroxide was used to quench endogenous peroxidise. αSMA was detected via ABC-AP kit with Vector red detection (red/pink). Levamisole was used to quench the endogenous alkaline phosphatise (AP). The CD31 stain was again very weak and difficult to interpret together with αSMA, however CD34 stained the microvasculature well together with αSMA and allowed interpretation. Lung tissue sections were therefore immunostained for CD34/αSMA from normal excess tissue (Figure 6.28) and tissue obtained at transplantation for emphysema (Figure 6.29). Sections were examined to determine the relationship between endothelial cells (CD34 positive cells) and matrix (αSMA positive cells), with evidence of transitional cells (co-localisation of CD34 and αSMA) sought.

Normal excess paraffin embedded lung tissue immunostained for CD34 (brown) an endothelial marker and αSMA (red) a marker of matrix/mesenchymal cells demonstrated differentiation of brown/red immunostaining as shown in figures 6.28a) and b). The vessel at higher power magnification 6.28b) illustrates the flat circumferential endothelial cells (brown) with associated supporting matrix cells (red) in close apposition but with clear distinction of red and brown. Figure 6.28c) shows the alveolar bed of normal lung tissue. The small alveolar capillaries (brown) can be clearly seen. Figure 6.28d), at higher power supports this, with few αSMA positive cells. No dual stained (transitional cells) were identified in sections of normal lung tissue.

Emphysema lung tissue immunostained for CD34 (brown) and αSMA (red) shows the alveolar bed, with well-preserved capillaries (CD34+ brown cells) with a cluster of small vessels (CD34+ brown cells) (Figure 6.29a). Lateral to these vessels is an area of thickened matrix with intense αSMA staining, with absent CD34 staining. Some peripheral fibrotic sprouts also stain positively for αSMA. Two small

muscularised arterioles and the surrounding alveolar bed are captured in figure 6.29b). In this section there is intense αSMA of the vessels, but the CD34+ endothelial monolayer appears diminished. Between the two vessels the alveolar bed is very thin, with loss of supporting structure including capillaries. In this area there is a thickened septum with few very weakly positive CD34 cells but no dual stained cells. Figure 6.29c) shows a thin septum and associated vessels. The capillaries are relatively well preserved although in one part of the septum (arrow) there is low intensity CD34 (brown) staining with associated low intensity (αSMA) red staining, although these stains are not truly co-localised. Figure 6.29d) shows the emphysematous alveolar bed, with marked regional loss of capillaries. In this section there is a septum which appears to have flat cells typical of endothelial cells which stain red/brown (arrows). These could represent transitional or activated endothelial cells.

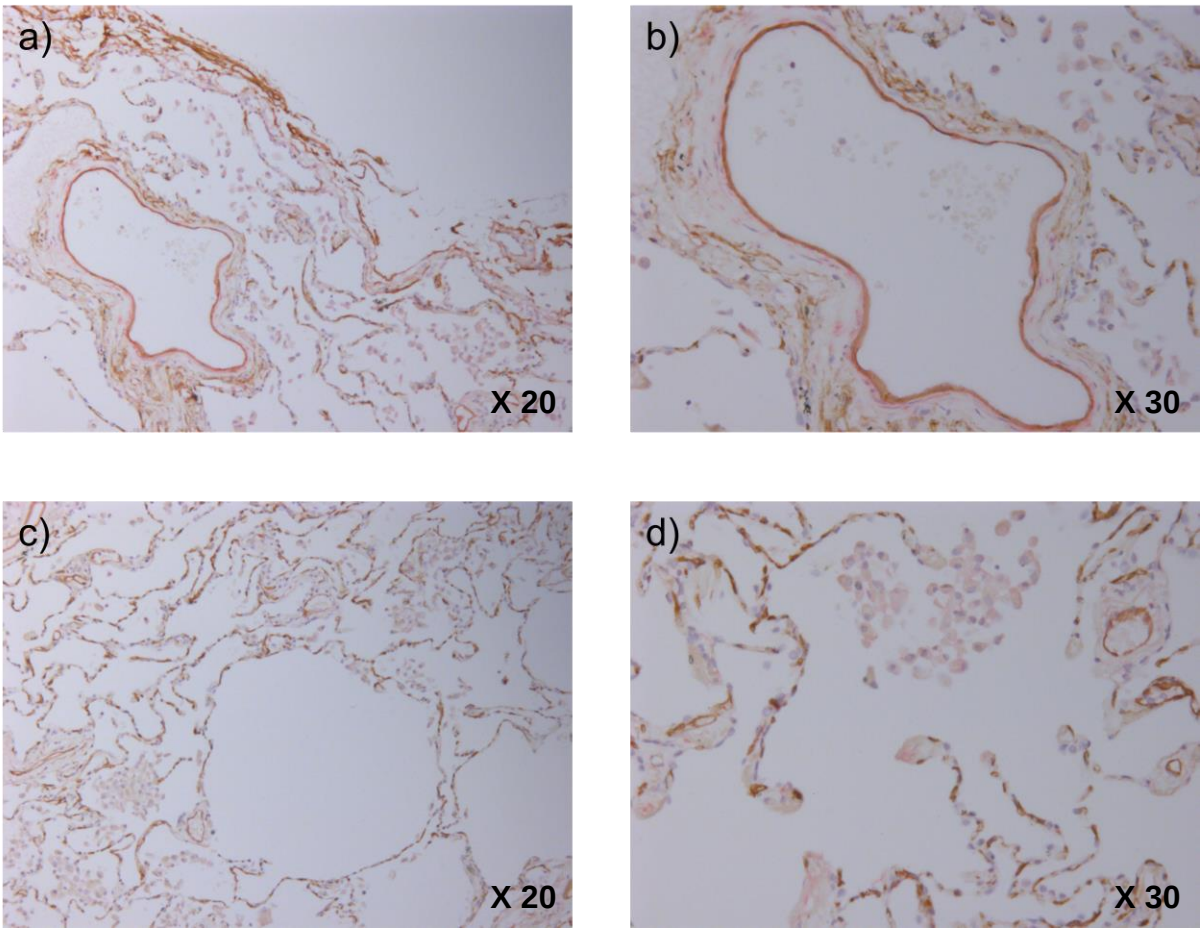


**Figure 7.28: Normal Tissue.** Normal excess paraffin embedded lung tissue immunostained for CD34 (brown) an endothelial marker and αSMA (red) a marker of matrix/mesenchymal cells. Figure a) shows a vessel and surrounding alveolar bed. The vessel at higher power magnification b) illustrates clearly the flat circumferential endothelial cells (brown) with associated supporting matrix cells (red) in close apposition. Importantly there is clear distinction of red and brown. Figure c) shows the alveolar bed of normal lung tissue. The small alveolar capillaries (brown) can be clearly seen with only low levels of αSMA. Figure d), at higher power supports this, with few αSMA positive cells. No dual stained i.e. transitional cells were identified in sections of normal lung tissue.

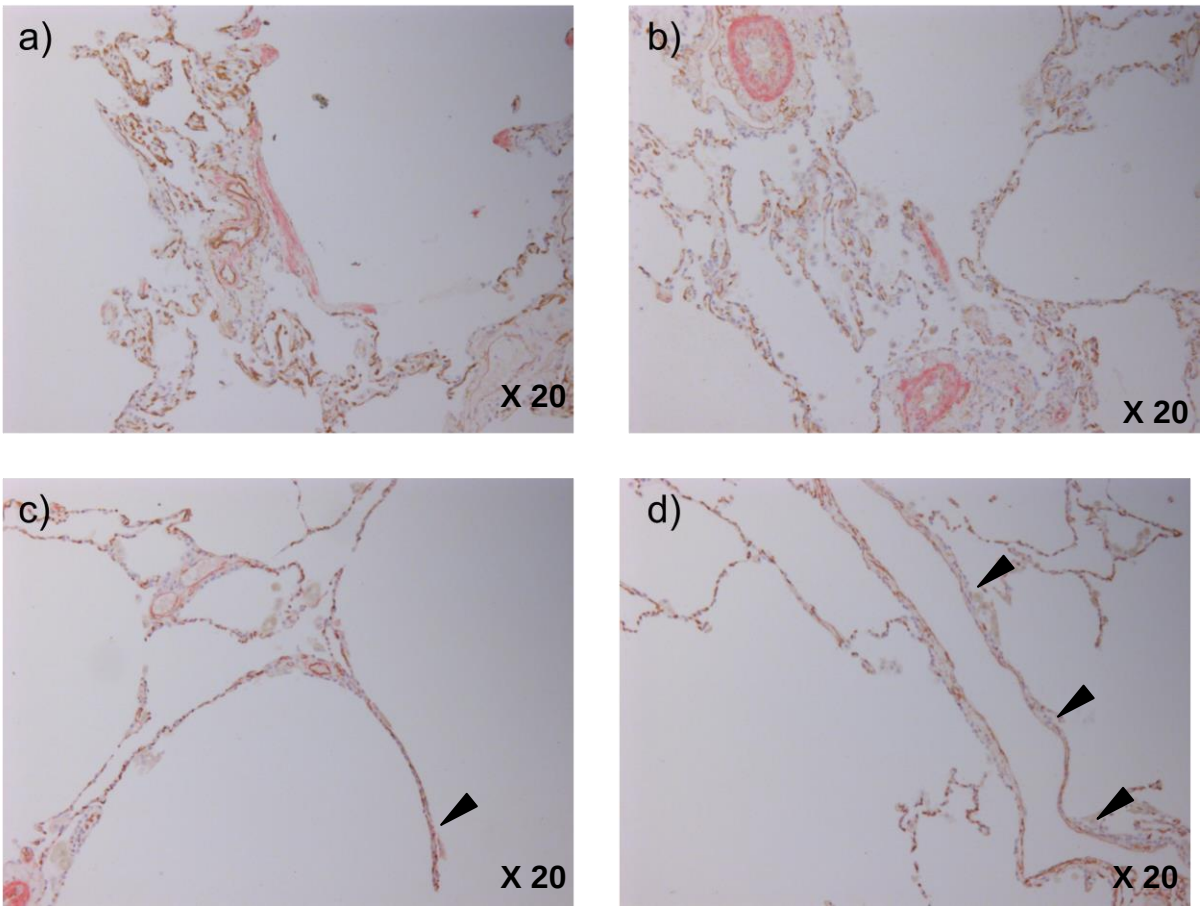


**Figure 7.29: Emphysema Tissue.** Emphysema lung tissue immunostained for CD34 (brown), an endothelial marker, and αSMA (red), a marker of matrix/mesenchymal cells. Figure a) shows the alveolar bed with a cluster of small vessels. The microvasculature is well preserved, with no apparent loss of capillaries. Just lateral to the vessels there is an area of thickened matrix with intense αSMA staining. No cells in this region stain positively for CD34. There are also some peripheral tissue sprouts which stain positively for αSMA. Figure b) shows 2 small muscularised arterioles and alveolar bed. In this section there is intense αSMA of the vessels, but the endothelial monolayer appears reduced. Between the two vessels the alveolar bed is very thin with loss of supporting structure including capillaries with numerous reed-ghosts cells. In this area there is a thickened septum with few very weakly positive CD34 cells but no dual stained cells. Figure c) shows a thin, septum with associated vessels. The capillaries are relatively well preserved although in one part of the septum (arrow) there is low intensity brown staining with low intensity red staining although not truly co-localised to suggest transitional cells. Figure d) shows peripheral lung tissue. Again there is marked regional loss of capillaries. In this section there is a long septum which appears to have flat cells typical of endothelial cells which stain a red/brown (arrows). These may represent transitional or activated endothelial cells and may be evidence of in vivo EnMT.

## *7.5 Discussion*

Endothelial to mesenchymal transition (EnMT) has been reported by other researchers in large vessel endothelial cells, in animal models and in commercial lung microvascular endothelial cells. In this chapter I have attempted to systematically investigate EnMT *ex vivo* and *in vivo*. I have demonstrated morphological changes in cell structure that have been supported by change in cell surface markers on individual cells via confocal microscopy and reduction in endothelial surface expression via flow cytometry. Following these preliminary supportive experiments I investigated dual staining for endothelial and mesenchymal markers on individual cells via confocal microscopy. There was however no evidence of dual staining of cells.

I therefore further investigated EnMT via protein expression on western blotting, examining both the response of cells to TGFβ1 and CSE. These results however did not support a change in protein expression at 7 days, with no loss of endothelial markers or gain of mesenchymal markers. To validate these findings, I repeated these experiments on multiple occasions and in different cells types (both commercial cells, and isolated emphysema cells and normal cells). In the TGFβ1 stimulation experiments, I also treated cells isolated from a patient with idiopathic pulmonary arterial hypertension (IPAH). IPAH is a disease characterised by remodelling of the pulmonary arterioles, with proliferation and a resulting obstructive vasculopathy. Cells isolated from patients with IPAH had a much shorter doubling time and produced a high cell yield at low passage. Thus I hypothesised that EnMT may be most likely to be observed in such cells. Once again there was no change in markers to suggest a phenotype change. After such surprising and disappointing negative results I believed it important to prove that the technique and materials were sound as so treated A549 cells with TGFβ1 via the same protocol and showed that EMT occurred as reported by previous investigators. No such phenotype change occurred however when A549 cells were treated with CSE.

Such results are interesting. Cells clearly show areas of reduced CD31 expression however lack of measurable change on western blotting suggests that a full phenotypic switch has not occurred. Such changes observed may be more in keeping with endothelial activation. Endothelial cells play an important function in maintaining vascular homeostasis and generally exist in a quiescent form, with a monolayer of cells formed by tight adherens junctions and contact inhibition [14]. This provides important anti-coagulant properties for the vessels and assists in laminar blood flow and leucocyte trafficking. When disruption to this monolayer occurs, via mechanical injury, infection or chemical injury such as smoking, endothelial cells become activated in order to respond to this change in environment. This is an energy independent process which does not require protein synthesis[169]. Activation of endothelial cells may be transient but may become prolonged if there is a chronic insult or more potent injury. Activated endothelial cells exhibit many of the qualities that mesenchymal cells display. Activated endothelial cells are reported to lose their tight barrier function, to allow extravasation of fluid and migration of neutrophils into the area of injury. This is archetypically seen in pneumonia, where there is oedema and expansion with inflammation of the alveolus. Activated endothelial cells also act as chemoattractants recruiting leucocytes to the area of injury may display proliferative and secretory actions as they respond to the injury. Decrease in endothelial barrier function has been reported within 1-3 hours of treatment with TGFβ1 and VEGF in vitro with a possibly more rapid activation observed using in vivo models [170], [171]. Cells tend to remain in this activated state until the injury is removed or subsides.

Endothelial cell activation is a normal physiological mechanism important for angiogenesis in both wound repair and has been studied in cancer biology specifically metastasis. VEGF is an important activator of endothelial cells, with stimulation causing increased proliferation and migration with the ability to form small vessel sprouts [50]. Endothelin-1 also promotes proliferation and as shown in this chapter TGFβ1 stimulation increases ET-1 production, however TGFβ1 tends to inhibit cell growth [172]. Activated endothelial cells are also pro-coagulant, which is an important feature which facilitates protection against vascular injury [173]. While

not the focus of this study, it is important not to view endothelial cells in a one dimensional ex vivo model, rather relate their function to the three-dimensional characteristics including flow. Thus endothelial cells must not be considered a passive monolayer of cells, but rather as a complex adapted system which maintains and restores vascular homeostasis. Thus endothelial cells can behave with a more secretory phenotype which could be interpreted as a phenotypic switch, but rather as this data would support, it may simply represent endothelial cell activation.

These observations are further supported by the observations that TNFα causes conformational changes and loss of endothelial cell surface markers, but no change in mesenchymal markers [164]. Mawatari et al were the first to examine the effect of human TNFα on cultured human microvascular endothelial cells from omental tissue removed at surgery [164]. They noted that “cobblestone like endothelial cells transformed into a disordered array of criss-crossed, elongated, spindle shaped cells” when incubated with TNFα and that this was accentuated when co-incubated with TNFα and epidermal growth factor (EGF). Such description appears very close to the effects observed in these studies, and would suggest that what we are witnessing is an activation of endothelial cells in response to TGFβ1, TNFα and CSE rather than a true phenotypic switch.

I initially planned to investigate change in function of the cells following stimulation particularly looking for evidence of change in matrix metalloproteinases and secretion of proteins such as collagen. Due to the largely negative studies of EnMT this work was not pursued, although preliminary studies (work not shown) did not show any change in MMP 2 and MMP 9 via gelatine zymmography. Similarly, western blotting of TCA precipitates for collagen I and collagen III did not show an increase compared to control cells.

Dual staining for the endothelial marker CD34 and the mesenchymal marker aSMA on peripheral lung tissue was also conducted to look for in vivo evidence of EnMT. Normal tissue showed no evidence of endothelial cell injury and there were no dual

stained cells observed. In emphysema tissue there were regions of alveolar endothelial cell loss and other regions in which there was expansion of the alveolar matrix with aSMA deposition. Some of these areas were discrete but many of these alveolar changes were found in close apposition to each other. Reed ghost cells are sclerotic casts of endothelial cells that are a marker of endothelial cell injury. They were commonly observed in the alveolar bed of emphysema tissue. Distal to these sclerotic casts, some of the alveolar bed appeared very thin and almost avascular. In some regions of the thin septa, flattened cells were seen typical of endothelial cells, but these cells were negative for endothelial cells and instead stained positively for aSMA. No dual stained cells were easily identified in emphysema tissue.

In these studies I did not find evidence of EnMT but did note change in cell surface expression and propose that EnMT should not be discounted, but rather questioned and further investigated in order to understand the response of microvascular endothelial cells to injury.

# *Chapter 7: Summary, Discussion and Future work*

## *7.1 Summary*

In this thesis I utilised severely emphysematous lungs obtained at transplantation to investigate the pathogenesis of emphysema. The study was conducted to attempt to challenge the existing models of emphysema and allow close correlation between clinical characteristics, pathological findings and cell biology responses *ex vivo*. This was logistically challenging, technically difficult and demanding work. The potential gains from this model to improve our understanding of the pathophysiology of this complex disease were the impetus and reason for persisting with the construction of a new model and the investigation of the complex stress that is cigarette smoking.

Returning to answer my original aims:

- **I attempted to establish a reliable and reproducible method to isolate and fully characterise microvascular endothelial cells from the excess emphysematous tissue obtained at lung transplantation**

  Large numbers of microvascular endothelial cells were isolated from severely emphysematous explanted lungs with good success (71%). These cells were fully characterised and proven to be of microvascular origin. Cells were stable up to passage 7 and could be cryopreserved and later reanimated for use in future experimental work. The methodology has been published and has been highly accessed.

- **To investigate whether these susceptible endothelial cells undergo apoptosis in response to cigarette smoke, in comparison with untreated cells and rates of apoptosis in cells isolated from normal individuals.**

  Investigation of apoptosis was complex using these precious primary cells. Determining the concentration at which to stress cells in order to induce cell death via apoptosis and the time point at which to harvest cells and examine

them was complex and may have differed between donors as initial results were inconsistent as determined by annexin V staining on flow cytometry. TUNEL staining of individual cells also did not confirm whether apoptosis was observed in response to cigarette smoke. Live cell imaging was therefore employed. This technique identified and reinforced the inherent problems of cellular autofluorescence while using cigarette smoke as an injury. I attempted to control for this with the results suggesting that cells isolated from emphysema lung tissue may undergo apoptosis and earlier and at lower concentration than commercial normal lung microvascular endothelial cells. This would be in keeping with my hypothesis that these cells are more susceptible to injury. However due to autofluorescence such conclusions are not proven and need further investigation using methods which do not employ fluorescence as a method of detection of apoptosis.

Further investigation of gene expression of these cells in response to cigarette smoking showed that cells from commercially available normal donors showed upregulation/ no change in VEGFr2 in response to cigarette smoke extract. Microvascular endothelial cells isolated from emphysema tissue in contrast showed a down regulation in VEGFr2 in response to cigarette smoking. VEGFr2 is the main receptor for human VEGF1 and is important for maintaining cell structure, function and defence. Thus a downregulation in VEGFr2 in response to cigarette smoking appears to be a maladaptive response to injury in these susceptible cells.

Unfortunately the controls used in these experiments were commercially available cells and not cells isolated from excess normal tissue as planned. This was due to the time constraints of isolating and purifying large numbers of endothelial cells with sufficient donor numbers to allow repeat experiments to provide meaningful data. Thus the focus was on isolating the microvascular endothelial cells from emphysema lung tissue and not from excess normal tissue as this was novel and unique exploratory work. Each experiment however had

an internal control of being compared with untreated cells i.e. control and more than 1 normal donor was used for the experiments in normal cells.

- **To investigate characteristics of cells which are resistant to apoptosis.**

The characteristic of cells resistant to apoptosis was unfortunately not investigated and as such is beyond the scope of this thesis. The properties of the cells which remain and are resistant to the insult of cigarette smoking should be the focus of further work to identify any protective mechanisms which they exhibit that could be exploited as a protective mechanism for therapeutic benefit.

- **To investigate endothelial plasticity in response to cigarette smoking, examining cell activation and phenotype via change in cellular expression and matrix production in response to cigarette smoke extract.**

Microvascular endothelial cells isolated from explanted severely emphysematous lung tissue were used to investigate endothelial plasticity in response to cigarette smoking. Cells showed morphological changes and changes in cellular expression via confocal microscopy with elongation of cells, loss of contact inhibition, down regulation of endothelial markers. Upregulation of mesenchymal markers was less clear. There was however no change in protein expression of endothelial markers or mesenchymal markers on western blotting. This raises the possibility that endothelial cells are activated in response to cigarette smoke extract, with change in cell morphology and expression, but without transcriptional change i.e. not a true phenotypic switch rather exhibiting cellular plasticity. The same results were observed with both commercial normal cells and the cells isolated from emphysema lung tissue. Preliminary studies confirmed that there was no change in matrix metalloproteinase production in response to CSE, however further work is required to examine change in function i.e. do activated endothelial cells exhibit a secretory function with attempts to lay down new matrix and assist with alveolar repair?

## *7.2 Implications of this study*

This study is to my knowledge the first study into the pathogenesis of emphysema using microvascular endothelial cells isolated from patients with severe emphysema who donated their explanted lung for research. This *ex vivo* model which allows study of the microvascular hypothesis of COPD is unique as it is not only a human model using primary lung cells, the cells were isolated from individuals who had very severe disease, enough to warrant transplantation. Thus biological mechanisms can be studied in response to the injurious stimulus, in this case cigarette smoke, which is believed to have precipitated the disease in cells that have been proven to be susceptible to the injury and which have taken part in the pathophysiology of the disease. Although cell isolation was initially labour intensive, large numbers of cells were obtained that showed stability of phenotype up to passage 7 and could be cryopreserved for use in future experiments. This study therefore challenges the current models used in lung science. While some researchers might argue that proof of concept work must first be investigated in animal models or in stable cell lines or in normal cells, this study would argue and put forward that the information and results gained from studying these diseased cells is more relevant and closer to the *in vivo* response and is more likely to be translational.

This thesis highlights two important mechanisms that may be relevant in emphysema, namely apoptosis and activation of endothelial cells in response to cigarette smoke.

I attempted to systematically investigate apoptosis in this study however due to autofluorescence of cells in response to CSE no clear conclusions can be drawn. With attempts to control for autofluorescence (on live cell imaging) there was an apparent apoptosis of cells that occurred earlier and at lower dose of cigarette smoke extract in these cells isolated from individuals with severe emphysema.

However such preliminary findings need to be investigated further using methods to detect apoptosis that do not employ fluorescence.

Endothelial cells appear to become activated in response to cigarette smoke. Endothelial activation is described more often in acute lung injury models and to my knowledge has not been reported in emphysema. In this thesis I have not demonstrated a true endothelial to mesenchymal transition, but propose that I have demonstrated a degree of cellular plasticity, which remain of endothelial pedigree, but change shape and expression and may change function, although due to time constraints such studies of function were investigated briefly but not fully enough to be reported in this study.

## *7.3 Limitations of this study*

One limitation of this study is the use of severe end stage emphysematous lung tissue to examine the pathogenesis of early emphysema and it could be suggested that using normal tissue from smokers may be a better model. However I propose that very diseased cells are unlikely to survive the isolation process thus the isolated cells are likely to represent susceptible LMVECs from the disease in question. I chose this model over the use of LMVECs isolated from cancer resection specimens or excess normal tissue obtained at surgery for other purposes as only 1 in 5 individuals who smoke develop COPD so studying the disease in cells isolated from individuals who had developed the disease had potential advantages. Furthermore each cell model has limitations including the use of cancer resection specimens (the surrounding tissue removed may have altered expression of VEGF) or excess normal tissue from lungs deemed unsuitable for transplantation (brain death causes a massive inflammatory response thus limiting the use of cells isolated from this model). I propose that this model is relevant to studying the pathogenesis of COPD as even within severely damaged emphysematous lungs there is ongoing evidence of repair and active inflammation and that within severely damaged lung there are some areas of near normality but acknowledge its limitations.

This study was ambitious and novel, requiring a lot of preliminary work in order to achieve the model in which the cellular responses to cigarette smoke, namely apoptosis and endothelial to mesenchymal transition, could be studied. Thus one of the inherent weaknesses of this study is the small number of repeats and small numbers of donors studied. Additionally, as discussed before, many of the experiments using "normal control" cells from healthy lung tissue use commercially available cells rather than cells isolated in the same manner from excess tissue obtained at lobectomy as planned. This was an unavoidable compromise of this thesis as I had to focus efforts on experimental work using primary cells rather than concentrating efforts on tissue banking sufficient cells in order to conduct multiple repeats on "normal cells". I am however unable to determine the effect of the cell isolation on the results as I have not been able to study similarly isolated cells from normal lungs. While this is a limitation of this study, it should be acknowledged and emphasised that the novelty of this study is the investigation of responses of vulnerable cells from diseased individuals to the stimulus which caused the disease i.e. the response of microvascular endothelial cells from patients with emphysema to injury with cigarette smoke extract. Thus although interesting and an important comparator to study normal cells, the information gained in this study from the response of the diseased cells alone compared to untreated affords important information which must not be disregarded or underestimated. The results obtained from the commercially available normal cells should now be supported with repeat studies in cells isolated from excess normal tissue using the same methodology as described in this thesis.

Similarly the number of samples tested for each experiment (n=) is relatively small throughout this thesis and reflects the precious nature of the microvascular endothelial cells isolated and also the difficulties in dealing with primary cells which can have slowed growth kinetics, which may in part reflect the underlying pathology. Thus it was not always possible to conduct each experiment in triplicate or more. Although this is conventional methodology, repeating the experiment in triplicate only demonstrates the ability to pipette exactly and treat/injure cells in a consistent manner, thus as long as results are in agreement, duplicate rather than triplicate

experiments are acceptable. What is actually required but seldom reported is stressing different cell populations i.e. different donors at the same time with the same injury/stress. In reality however, the ability to have all primary cells at the same level of confluence and same passage ready to treat on the same day is almost impossible. Therefore one has to accept the limitations of work with primary cells and accept that the information gained from such experiments, although not as stringent as using a stable cell line population, is more insightful and meaningful as the cells reflect the in vivo situation more accurately.

One of the major limitations of this study is the use of cigarette smoking as an injury. Cigarette smoke extract itself is a rather rudimentary stimulus. It differs markedly in a number of ways from the true injury that occurs in vivo. Firstly cigarette smoking tends to be a chronic injurious stimulus rather than the acute injury that is reported in this thesis. This in itself makes it a challenging subject to research. Cigarette smoke extract is in the liquid phase as opposed to the gaseous phase that is cigarette smoking. This is a standard model that has been used for over 30 years and was the most standard and controlled way in which I could study cigarette smoking injury. The live cell imaging on cells was the closest I was able to achieve in terms of studying injury over time, although this was essentially still an acute injury. It is unsurprising that apoptosis was difficult to detect and measure as clearly if microvascular endothelial cells underwent apoptosis in significant numbers in response to cigarette smoke, this would cause a chemical pneumonitis and not emphysema. Similarly for cells to undergo measurable endothelial to mesenchymal transition acutely in response to cigarette smoke would cause large amounts of mesenchyme deposition with gross organ dysfunction. This is an inherent problem in the study of chronic disease and surrogate models such as this and acute injury must be utilized with results extrapolated.

Another limitation is the variability between emphysema donors and their cellular responses. All patients who donated their lung for research had by definition very severe emphysema and fulfilled the criteria for transplantation. However despite having severe airflow limitation and of similar functional class, the macroscopic

appearance of their lung tissue at times was quite heterogeneous and similarly the number of cells isolated and their responses in vivo differed. This is an inherent limitation of studying patients in the real world and although may lead to greater spread of results, this limitation is offset by the valuable results that such studies bring. Thus one must look for signals from such experiments and accept variability amongst results.

Finally the disease COPD itself provides problems and limitations for researchers. Emphysema is one part of the disease COPD. Various phenotypes found between patients with some patients exhibiting severe airflow obstruction with dynamic hyperinflation, while others have predominant bronchitic features with goblet cell hypertrophy and mucus hypersecretion. Yet another group of patients have features of bronchiectasis, with chronic distal airway enlargement, scarring, impaired innate defences with colonization with pathogens which further damage lung anatomy and in turn affect physiology. The patients in this study all had severe COPD with emphysema as characterized by hyperinflation, gas trapping and reduced diffusing capacity on pulmonary function testing. How this study relates to patients with COPD with predominant small airways disease is uncertain and also to patients with extensive smoking history yet milder COPD. Thus this study also highlights the problem with COPD classification and may suggest the need for further subclassification in research and clinical trials.

## *7.4 Future directions*

This model must now be continued to be used for the investigation of microvascular mechanisms in emphysema. Indeed the cell isolation technique may be able to be refined and improved as newer techniques and equipment become available. This may allow cells at even lower passage to be used in experimental work with cells reflecting even more closely the environment from which they were isolated.

For the apoptosis arm of the study, apoptosis should be further investigated using techniques which do not employ the use of fluorescence. If such studies confirm apoptosis in response to CSE, the characteristic of cells resistant to apoptosis should then be investigated as this may identify protective mechanisms which they exhibit that could be exploited as a protective mechanism for therapeutic benefit.

Endothelial activation in emphysema must also be further investigated with a focus on change in function of the endothelial cells, focusing on secretion of matrix proteins and production of matrix metalloproteinases which are thought to play an important role in the pathogenesis of COPD and emphysema.

Finally, ex vivo lung perfusion of explanted lungs could be used to incorporate a smoking model, whereby the same equipment used to recondition the lungs which the transplant recipient receives could be used to model smoking injury to the severely damaged emphysematous lung. This study would be worthwhile as this thesis has highlighted that active attempts at repair are ongoing even in the most severely damaged emphysematous lungs and that some areas of near normality are also witnessed. This would therefore allow three dimensional study with appreciation for dynamic volume stress and shear stress changes associated with blood flow and would have the additional benefit that the cigarette smoke injury would be in the gaseous phase and so again would be a close mimic of the *in vivo* situation.

## *References:*


[1] M. Britton, “The burden of COPD in the U.K.: results from the Confronting COPD survey.,” *Respir. Med.*, vol. 97 Suppl C, pp. S71–9, Mar. 2003.

[2] A. D. Lopez, K. Shibuya, C. Rao, C. D. Mathers, A. L. Hansell, L. S. Held, V. Schmid, and S. Buist, “Chronic obstructive pulmonary disease: current burden and future projections.,” *Eur. Respir. J.*, vol. 27, no. 2, pp. 397–412, Feb. 2006.

[3] “Global Initiative for Chronic Obstructive Lung Disease (GOLD),” 2015.

[4] J. Vestbo, A. Agusti, E. F. M. Wouters, P. Bakke, P. M. A. Calverley, B. Celli, H. Coxson, C. Crim, L. D. Edwards, N. Locantore, D. A. Lomas, W. MacNee, B. Miller, S. I. Rennard, E. K. Silverman, J. C. Yates, and R. Tal-Singer, “Should we view chronic obstructive pulmonary disease differently after ECLIPSE? A clinical perspective from the study team.,” *Am. J. Respir. Crit. Care Med.*, vol. 189, no. 9, pp. 1022–30, May 2014.

[5] J. Vestbo, L. D. Edwards, P. D. Scanlon, J. C. Yates, A. Agusti, P. Bakke, P. M. A. Calverley, B. Celli, H. O. Coxson, C. Crim, D. A. Lomas, W. MacNee, B. E. Miller, E. K. Silverman, R. Tal-Singer, E. Wouters, and S. I. Rennard, “Changes in forced expiratory volume in 1 second over time in COPD.,” *N. Engl. J. Med.*, vol. 365, no. 13, pp. 1184–92, Sep. 2011.

[6] P. Boschetto, M. Miniati, D. Miotto, F. Braccioni, E. De Rosa, I. Bononi, A. Papi, M. Saetta, L. M. Fabbri, and C. E. Mapp, “Predominant emphysema phenotype in chronic obstructive pulmonary.,” *Eur. Respir. J. Off. J. Eur. Soc. Clin. Respir. Physiol.*, vol. 21, no. 3, pp. 450–4, Mar. 2003.

[7] P. Boschetto, S. Quintavalle, E. Zeni, S. Leprotti, A. Potena, L. Ballerin, A. Papi, G. Palladini, M. Luisetti, L. Annovazzi, P. Iadarola, E. De Rosa, L. M. Fabbri, and C. E. Mapp, “Association between markers of emphysema and more severe chronic obstructive pulmonary disease.,” *Thorax*, vol. 61, no. 12, pp. 1037–42, Dec. 2006.

[8] A. Løkke, P. Lange, H. Scharling, P. Fabricius, and J. Vestbo, “Developing COPD: a 25 year follow up study of the general population.,” *Thorax*, vol. 61, no. 11, pp. 935–9, Nov. 2006.

[9] C. Fletcher and R. Peto, “The natural history of chronic airflow obstruction.,” *Br. Med. J.*, vol. 1, no. 6077, pp. 1645–8, Jun. 1977.

[10] J. C. Hogg, “Why does airway inflammation persist after the smoking stops?,” *Thorax*, vol. 61, no. 2, pp. 96–7, Feb. 2006.

[11] S. R. Rutgers, D. S. Postma, N. H. ten Hacken, H. F. Kauffman, T. W. van Der Mark, G. H. Koëter, and W. Timens, “Ongoing airway inflammation in patients with COPD who do not currently smoke.,” *Thorax*, vol. 55, no. 1, pp. 12–8, Jan. 2000.

[12] J. C. Hogg, F. Chu, S. Utokaparch, R. Woods, W. M. Elliott, L. Buzatu, R. M. Cherniack, R. M. Rogers, F. C. Sciurba, H. O. Coxson, and P. D. Paré, “The nature of small-airway obstruction in chronic obstructive pulmonary disease.,” *N. Engl. J. Med.*, vol. 350, no. 26, pp. 2645–53, Jun. 2004.

[13] N. A. Haslett C; Chilvers E.R; Hunter, J.A.A; Boon, *Davidson’s Principles and Practice of Medicine*, 18th Editi. Churchill Livingstone, 1999.

[14] C. E. Patterson and M. A. Matthay, *Perspectives on Lung Endothelial Barrier Function*, vol. 35. Elsevier, 2005.

[15] “The definition of emphysema. Report of a National Heart, Lung, and Blood Institute, Division of Lung Diseases workshop.,” *Am. Rev. Respir. Dis.*, vol. 132, no. 1, pp. 182–5, Jul. 1985.

[16] J. C. Hogg, P. T. Macklem, and W. M. Thurlbeck, “Site and nature of airway obstruction in chronic obstructive lung disease.,” *N. Engl. J. Med.*, vol. 278, no. 25, pp. 1355–60, Jun. 1968.

[17] NICE, “Management of chronic obstructive pulmonary disease in adults in primary and secondary care,” CG101, 2010.

[18] A. Barua, P. Vaughan, R. Wotton, and B. Naidu, “Do endobronchial valves improve outcomes in patients with emphysema?,” *Interact. Cardiovasc. Thorac. Surg.*, vol. 15, no. 6, pp. 1072–6, Dec. 2012.

[19] M. Takahashi, J. Fukuoka, N. Nitta, R. Takazakura, Y. Nagatani, Y. Murakami, H. Otani, and K. Murata, “Imaging of pulmonary emphysema: a pictorial review.,” *Int. J. Chron. Obstruct. Pulmon. Dis.*, vol. 3, no. 2, pp. 193–204, Jan. 2008.

[20] E. J. Stern and M. S. Frank, “CT of the lung in patients with pulmonary emphysema: diagnosis, quantification, and correlation with pathologic and physiologic findings.,” *AJR. Am. J. Roentgenol.*, vol. 162, no. 4, pp. 791–8, Apr. 1994.

[21] W. M. Thurlbeck and N. L. Müller, “Emphysema: definition, imaging, and quantification.,” *AJR. Am. J. Roentgenol.*, vol. 163, no. 5, pp. 1017–25, Nov. 1994.

[22] S. F. van Eeden and J. C. Hogg, “Chronic obstructive pulmonary disease: do regional differences in tissue inflammation matter?,” *Respiration.*, vol. 81, no. 5, pp. 359–61, Jan. 2011.

[23] J. E. McDonough, R. Yuan, M. Suzuki, N. Seyednejad, W. M. Elliott, P. G. Sanchez, A. C. Wright, W. B. Gefter, L. Litzky, H. O. Coxson, P. D. Paré, D. D. Sin, R. A. Pierce, J. C. Woods, A. M. McWilliams, J. R. Mayo, S. C. Lam, J. D. Cooper, and J. C. Hogg, “Small-airway obstruction and emphysema in chronic obstructive pulmonary disease.,” *N. Engl. J. Med.*, vol. 365, no. 17, pp. 1567–75, Oct. 2011.

[24] G. L. Snider, “Clinical relevance summary: Collagen vs elastin in pathogenesis of emphysema; cellular origin of elastases; bronchiolitis vs emphysema as a cause of airflow obstruction.,” *Chest*, vol. 117, no. 5 Suppl 1, p. 244S–6S, May 2000.

[25] D. G. Morris and D. Sheppard, “Pulmonary emphysema: when more is less.,” *Physiology (Bethesda).*, vol. 21, pp. 396–403, Dec. 2006.

[26] L. Taraseviciene-Stewart and N. F. Voelkel, “Molecular pathogenesis of emphysema.,” *J. Clin. Invest.*, vol. 118, no. 2, pp. 394–402, Feb. 2008.

[27] A. Dirksen, J. H. Dijkman, F. Madsen, B. Stoel, D. C. Hutchison, C. S. Ulrik, L. T. Skovgaard, A. Kok-Jensen, A. Rudolphus, N. Seersholm, H. A. Vrooman, J. H. Reiber, N. C. Hansen, T. Heckscher, K. Viskum, and J. Stolk, “A randomized clinical trial of alpha(1)-antitrypsin augmentation therapy.,” *Am. J. Respir. Crit. Care Med.*, vol. 160, no. 5 Pt 1, pp. 1468–72, Nov. 1999.

[28] A. A. LIEBOW, “Pulmonary emphysema with special reference to vascular changes.,” *Am. Rev. Respir. Dis.*, vol. 80, no. 1, Part 2, pp. 67–93, Jul. 1959.

[29] P. M. Henson, R. W. Vandivier, and I. S. Douglas, “Cell death, remodeling, and repair in chronic obstructive pulmonary disease?,” *Proc. Am. Thorac. Soc.*, vol. 3, no. 8, pp. 713–7, Nov. 2006.

[30] R. M. Tuder, T. Yoshida, I. Fijalkowka, S. Biswal, and I. Petrache, “Role of lung maintenance program in the heterogeneity of lung destruction in emphysema.,” *Proc. Am. Thorac. Soc.*, vol. 3, no. 8, pp. 673–9, Nov. 2006.

[31] S. I. Rennard, S. Togo, and O. Holz, “Cigarette smoke inhibits alveolar repair: a mechanism for the development of emphysema.,” *Proc. Am. Thorac. Soc.*, vol. 3, no. 8, pp. 703–8, Nov. 2006.

[32] D. E. Newby, A. L. McLeod, N. G. Uren, L. Flint, C. A. Ludlam, D. J. Webb, K. A. Fox, and N. A. Boon, “Impaired coronary tissue plasminogen activator release is associated with coronary atherosclerosis and cigarette smoking: direct link between endothelial dysfunction and atherothrombosis.,” *Circulation*, vol. 103, no. 15, pp. 1936–41, Apr. 2001.

[33] J. D. Maclay, D. A. McAllister, N. L. Mills, F. P. Paterson, C. A. Ludlam, E. M. Drost, D. E. Newby, and W. Macnee, “Vascular dysfunction in chronic obstructive pulmonary disease.,” *Am. J. Respir. Crit. Care Med.*, vol. 180, no. 6, pp. 513–20, Sep. 2009.

[34] T. Münzel, C. Sinning, F. Post, A. Warnholtz, and E. Schulz, “Pathophysiology, diagnosis and prognostic implications of endothelial dysfunction.,” *Ann. Med.*, vol. 40, no. 3, pp. 180–96, Jan. 2008.

[35] R. M. Tuder, T. Yoshida, W. Arap, R. Pasqualini, and I. Petrache, “State of the art. Cellular and molecular mechanisms of alveolar destruction in emphysema: an evolutionary perspective.,” *Proc. Am. Thorac. Soc.*, vol. 3, no. 6, pp. 503–10, Aug. 2006.

[36] N. F. Voelkel, J. Gomez-Arroyo, and S. Mizuno, “COPD/emphysema: The vascular story.,” *Pulm. Circ.*, vol. 1, no. 3, pp. 320–6, Jul. 2011.

[37] P. Carmeliet, “Angiogenesis in life, disease and medicine.,” *Nature*, vol. 438, no. 7070, pp. 932–6, Dec. 2005.

[38] A. Hislop, “Developmental biology of the pulmonary circulation.,” *Paediatr. Respir. Rev.*, vol. 6, no. 1, pp. 35–43, Mar. 2005.

[39] A. A. Hislop, “Airway and blood vessel interaction during lung development.,” *J. Anat.*, vol. 201, no. 4, pp. 325–34, Oct. 2002.

[40] B. Thébaud and S. H. Abman, “Bronchopulmonary dysplasia: where have all the vessels gone? Roles of angiogenic growth factors in chronic lung disease.,” *Am. J. Respir. Crit. Care Med.*, vol. 175, no. 10, pp. 978–85, May 2007.

[41] E. Baraldi and M. Filippone, “Chronic lung disease after premature birth.,” *N. Engl. J. Med.*, vol. 357, no. 19, pp. 1946–55, Nov. 2007.

[42] S. H. Abman, “Bronchopulmonary dysplasia: ‘a vascular hypothesis’.,” *Am. J. Respir. Crit. Care Med.*, vol. 164, no. 10 Pt 1, pp. 1755–6, Nov. 2001.

[43] M. Jakkula, T. D. Le Cras, S. Gebb, K. P. Hirth, R. M. Tuder, N. F. Voelkel, and S. H. Abman, “Inhibition of angiogenesis decreases alveolarization in the developing rat lung.,” *Am. J. Physiol. Lung Cell. Mol. Physiol.*, vol. 279, no. 3, pp. L600–7, Sep. 2000.

[44] E. Dejana, M. Corada, and M. G. Lampugnani, “Endothelial cell-to-cell junctions.,” *FASEB J.*, vol. 9, no. 10, pp. 910–8, Jul. 1995.

[45] G. Bazzoni, “Endothelial tight junctions: permeable barriers of the vessel wall.,” *Thromb. Haemost.*, vol. 95, no. 1, pp. 36–42, Jan. 2006.

[46] E. Dejana and D. Vestweber, “The role of VE-cadherin in vascular morphogenesis and permeability control.,” *Prog. Mol. Biol. Transl. Sci.*, vol. 116, pp. 119–44, Jan. 2013.

[47] P. L. Hordijk, E. Anthony, F. P. Mul, R. Rientsma, L. C. Oomen, and D. Roos, “Vascular-endothelial-cadherin modulates endothelial monolayer permeability.,” *J. Cell Sci.*, vol. 112 ( Pt 1, pp. 1915–23, Jun. 1999.

[48] P. J. Newman, “The biology of PECAM-1.,” *J. Clin. Invest.*, vol. 99, no. 1, pp. 3–8, Jan. 1997.

[49] Y. Ishii, C. A. Partridge, P. J. Del Vecchio, and A. B. Malik, “Tumor necrosis factor-alpha-mediated decrease in glutathione increases the sensitivity of pulmonary vascular endothelial cells to H2O2.,” *J. Clin. Invest.*, vol. 89, no. 3, pp. 794–802, Mar. 1992.

[50] N. F. Voelkel, R. W. Vandivier, and R. M. Tuder, “Vascular endothelial growth factor in the lung.,” *Am. J. Physiol. Lung Cell. Mol. Physiol.*, vol. 290, no. 2, pp. L209–21, Feb. 2006.

[51] P. Carmeliet, V. Ferreira, G. Breier, S. Pollefeyt, L. Kieckens, M. Gertsenstein, M. Fahrig, A. Vandenhoeck, K. Harpal, C. Eberhardt, C. Declercq, J. Pawling, L. Moons, D. Collen, W. Risau, and A. Nagy, “Abnormal blood vessel development and lethality in embryos lacking a single VEGF allele.,” *Nature*, vol. 380, no. 6573, pp. 435–9, Apr. 1996.

[52] R. M. Tuder, M. Chacon, L. Alger, J. Wang, L. Taraseviciene-Stewart, Y. Kasahara, C. D. Cool, A. E. Bishop, M. Geraci, G. L. Semenza, M. Yacoub, J. M. Polak, and N. F. Voelkel, “Expression of angiogenesis-related molecules in plexiform lesions in severe pulmonary hypertension: evidence for a process of disordered angiogenesis.,” *J. Pathol.*, vol. 195, no. 3, pp. 367–74, Oct. 2001.

[53] D. R. Thickett, L. Armstrong, S. J. Christie, and A. B. Millar, “Vascular endothelial growth factor may contribute to increased vascular permeability in acute respiratory distress syndrome.,” *Am. J. Respir. Crit. Care Med.*, vol. 164, no. 9, pp. 1601–5, Nov. 2001.

[54] Y. Kasahara, R. M. Tuder, C. D. Cool, D. A. Lynch, S. C. Flores, and N. F. Voelkel, “Endothelial cell death and decreased expression of vascular endothelial growth factor and vascular endothelial growth factor receptor 2 in emphysema.,” *Am. J. Respir. Crit. Care Med.*, vol. 163, no. 3 Pt 1, pp. 737–44, Mar. 2001.

[55] N. Rovina, A. Papapetropoulos, A. Kollintza, M. Michailidou, D. C. M. Simoes, C. Roussos, and C. Gratziou, “Vascular endothelial growth factor: an angiogenic factor reflecting airway inflammation in healthy smokers and in patients with bronchitis type of chronic obstructive pulmonary disease?,” *Respir. Res.*, vol. 8, p. 53, Jan. 2007.

[56] H. Kanazawa, K. Asai, K. Hirata, and J. Yoshikawa, “Possible effects of vascular endothelial growth factor in the pathogenesis of chronic obstructive pulmonary disease.,” *Am. J. Med.*, vol. 114, no. 5, pp. 354–8, Apr. 2003.

[57] H. Kanazawa, “Role of vascular endothelial growth factor in the pathogenesis of chronic obstructive pulmonary disease.,” *Med. Sci. Monit.*, vol. 13, no. 11, pp. RA189–195, Nov. 2007.

[58] L. E. Huang and H. F. Bunn, “Hypoxia-inducible factor and its biomedical relevance.,” *J. Biol. Chem.*, vol. 278, no. 22, pp. 19575–8, May 2003.

[59] I. K. Demedts, T. Demoor, K. R. Bracke, G. F. Joos, and G. G. Brusselle, “Role of apoptosis in the pathogenesis of COPD and pulmonary emphysema.,” *Respir. Res.*, vol. 7, p. 53, Jan. 2006.

[60] J. F. Kerr, A. H. Wyllie, and A. R. Currie, “Apoptosis: a basic biological phenomenon with wide-ranging implications in tissue kinetics.,” *Br. J. Cancer*, vol. 26, no. 4, pp. 239–57, Aug. 1972.

[61] S. Elmore, “Apoptosis: a review of programmed cell death.,” *Toxicol. Pathol.*, vol. 35, no. 4, pp. 495–516, Jan. 2007.

[62] J. A. Trapani and M. J. Smyth, “Functional significance of the perforin/granzyme cell death pathway.,” *Nat. Rev. Immunol.*, vol. 2, no. 10, pp. 735–47, Oct. 2002.

[63] Y. Kasahara, R. M. Tuder, L. Taraseviciene-Stewart, T. D. Le Cras, S. Abman, P. K. Hirth, J. Waltenberger, and N. F. Voelkel, “Inhibition of VEGF receptors causes lung cell apoptosis and emphysema.,” *J. Clin. Invest.*, vol. 106, no. 11, pp. 1311–9, Dec. 2000.

[64] K. Imai, B. A. Mercer, L. L. Schulman, J. R. Sonett, and J. M. D’Armiento, “Correlation of lung surface area to apoptosis and proliferation in human emphysema.,” *Eur. Respir. J. Off. J. Eur. Soc. Clin. Respir. Physiol.*, vol. 25, no. 2, pp. 250–8, Feb. 2005.

[65] F. Calabrese, C. Giacometti, B. Beghe, F. Rea, M. Loy, R. Zuin, G. Marulli, S. Baraldo, M. Saetta, and M. Valente, “Marked alveolar apoptosis/proliferation imbalance in end-stage emphysema.,” *Respir. Res.*, vol. 6, p. 14, Jan. 2005.

[66] K. Aoshiba, N. Yokohori, and A. Nagai, “Alveolar wall apoptosis causes lung destruction and emphysematous changes.,” *Am. J. Respir. Cell Mol. Biol.*, vol. 28, no. 5, pp. 555–62, May 2003.

[67] N. Yokohori, K. Aoshiba, and A. Nagai, “Increased levels of cell death and proliferation in alveolar wall cells in patients with pulmonary emphysema.,” *Chest*, vol. 125, no. 2, pp. 626–32, Feb. 2004.

[68] N. Yasuda, K. Gotoh, S. Minatoguchi, K. Asano, K. Nishigaki, M. Nomura, A. Ohno, M. Watanabe, H. Sano, H. Kumada, T. Sawa, and H. Fujiwara, “An increase of soluble Fas, an inhibitor of apoptosis, associated with progression of COPD.,” *Respir. Med.*, vol. 92, no. 8, pp. 993–9, Aug. 1998.

[69] I. Petrache, I. Fijalkowska, T. R. Medler, J. Skirball, P. Cruz, L. Zhen, H. I. Petrache, T. R. Flotte, and R. M. Tuder, “alpha-1 antitrypsin inhibits caspase-3 activity, preventing lung endothelial cell apoptosis.,” *Am. J. Pathol.*, vol. 169, no. 4, pp. 1155–66, Oct. 2006.

[70] I. Petrache, I. Fijalkowska, L. Zhen, T. R. Medler, E. Brown, P. Cruz, K.-H. Choe, L. Taraseviciene-Stewart, R. Scerbavicius, L. Shapiro, B. Zhang, S. Song, D. Hicklin, N. F. Voelkel, T. Flotte, and R. M. Tuder, “A novel antiapoptotic role for alpha1-antitrypsin in the prevention of pulmonary emphysema.,” *Am. J. Respir. Crit. Care Med.*, vol. 173, no. 11, pp. 1222–8, Jun. 2006.

[71] R. M. Tuder, L. Zhen, C. Y. Cho, L. Taraseviciene-Stewart, Y. Kasahara, D. Salvemini, N. F. Voelkel, and S. C. Flores, “Oxidative stress and apoptosis interact and cause emphysema due to vascular endothelial growth factor receptor blockade.,” *Am. J. Respir. Cell Mol. Biol.*, vol. 29, no. 1, pp. 88–97, Jul. 2003.

[72] S. I. Rennard, “Cigarette smoke in research.,” *Am. J. Respir. Cell Mol. Biol.*, vol. 31, no. 5, pp. 479–80, Nov. 2004.

[73] T. Rangasamy, C. Y. Cho, R. K. Thimmulappa, L. Zhen, S. S. Srisuma, T. W. Kensler, M. Yamamoto, I. Petrache, R. M. Tuder, and S. Biswal, “Genetic ablation of Nrf2 enhances susceptibility to cigarette smoke-induced emphysema in mice.,” *J. Clin. Invest.*, vol. 114, no. 9, pp. 1248–59, Nov. 2004.

[74] H. Kanazawa and J. Yoshikawa, “Elevated oxidative stress and reciprocal reduction of vascular endothelial growth factor levels with severity of COPD.,” *Chest*, vol. 128, no. 5, pp. 3191–7, Nov. 2005.

[75] L. HAYFLICK and P. S. MOORHEAD, “The serial cultivation of human diploid cell strains.,” *Exp. Cell Res.*, vol. 25, pp. 585–621, Dec. 1961.

[76] J. Campisi, “Aging, cellular senescence, and cancer.,” *Annu. Rev. Physiol.*, vol. 75, pp. 685–705, Jan. 2013.

[77] S. Teramoto, “Age-related changes in lung structure and function in the senescence-accelerated mouse (SAM): SAM-P/1 as a new model of senile hyperinflation of lung.,” *Am. J. Respir. Crit. Care Med.*, vol. 156, no. 4 Pt 1, p. 1361, Oct. 1997.

[78] K. Ito and P. J. Barnes, “COPD as a disease of accelerated lung aging(a).,” *Rev. Port. Pneumol.*, vol. 15, no. 4, pp. 743–746, Jan. .

[79] T. Tsuji, K. Aoshiba, and A. Nagai, “Alveolar cell senescence in patients with pulmonary emphysema.,” *Am. J. Respir. Crit. Care Med.*, vol. 174, no. 8, pp. 886–93, Oct. 2006.

[80] T. Tsuji, K. Aoshiba, and A. Nagai, “Alveolar cell senescence exacerbates pulmonary inflammation in patients with chronic obstructive pulmonary disease.,” *Respiration.*, vol. 80, no. 1, pp. 59–70, Jan. 2010.

[81] K. Koli, M. Myllärniemi, J. Keski-Oja, and V. L. Kinnula, “Transforming growth factor-beta activation in the lung: focus on fibrosis and reactive oxygen species.,” *Antioxid. Redox Signal.*, vol. 10, no. 2, pp. 333–42, Feb. 2008.

[82] J. Gauldie, M. Kolb, K. Ask, G. Martin, P. Bonniaud, and D. Warburton, “Smad3 signaling involved in pulmonary fibrosis and emphysema.,” *Proc. Am. Thorac. Soc.*, vol. 3, no. 8, pp. 696–702, Nov. 2006.

[83] A. Shifren and R. P. Mecham, “The stumbling block in lung repair of emphysema: elastic fiber assembly.,” *Proc. Am. Thorac. Soc.*, vol. 3, no. 5, pp. 428–33, Jul. 2006.

[84] G. Vlahovic, M. L. Russell, R. R. Mercer, and J. D. Crapo, “Cellular and connective tissue changes in alveolar septal walls in emphysema.,” *Am. J. Respir. Crit. Care Med.*, vol. 160, no. 6, pp. 2086–92, Dec. 1999.

[85] J. V Gosselink, S. Hayashi, W. M. Elliott, L. Xing, B. Chan, L. Yang, C. Wright, D. Sin, P. D. Paré, J. A. Pierce, R. A. Pierce, A. Patterson, J. Cooper, and J. C. Hogg, “Differential expression of tissue repair genes in the pathogenesis of chronic obstructive pulmonary disease.,” *Am. J. Respir. Crit. Care Med.*, vol. 181, no. 12, pp. 1329–35, Jun. 2010.

[86] A. Spira, J. Beane, V. Pinto-Plata, A. Kadar, G. Liu, V. Shah, B. Celli, and J. S. Brody, “Gene expression profiling of human lung tissue from smokers with severe emphysema.,” *Am. J. Respir. Cell Mol. Biol.*, vol. 31, no. 6, pp. 601–10, Dec. 2004.

[87] S. Kononov, K. Brewer, H. Sakai, F. S. Cavalcante, C. R. Sabayanagam, E. P. Ingenito, and B. Suki, “Roles of mechanical forces and collagen failure in the development of elastase-induced emphysema.,” *Am. J. Respir. Crit. Care Med.*, vol. 164, no. 10 Pt 1, pp. 1920–6, Nov. 2001.

[88] S. Ito, E. P. Ingenito, K. K. Brewer, L. D. Black, H. Parameswaran, K. R. Lutchen, and B. Suki, “Mechanics, nonlinearity, and failure strength of lung tissue in a mouse model of emphysema: possible role of collagen remodeling.,” *J. Appl. Physiol.*, vol. 98, no. 2, pp. 503–11, Feb. 2005.

[89] E. Arciniegas, A. B. Sutton, T. D. Allen, and A. M. Schor, “Transforming growth factor beta 1 promotes the differentiation of endothelial cells into smooth muscle-like cells in vitro.,” *J. Cell Sci.*, vol. 103 ( Pt 2, pp. 521–9, Oct. 1992.

[90] M. G. Frid, V. A. Kale, and K. R. Stenmark, “Mature vascular endothelium can give rise to smooth muscle cells via endothelial-mesenchymal transdifferentiation: in vitro analysis.,” *Circ. Res.*, vol. 90, no. 11, pp. 1189–96, Jun. 2002.

[91] E. M. Zeisberg, O. Tarnavski, M. Zeisberg, A. L. Dorfman, J. R. McMullen, E. Gustafsson, A. Chandraker, X. Yuan, W. T. Pu, A. B. Roberts, E. G. Neilson, M. H. Sayegh, S. Izumo, and R. Kalluri, “Endothelial-to-mesenchymal transition contributes to cardiac fibrosis.,” *Nat. Med.*, vol. 13, no. 8, pp. 952–61, Aug. 2007.

[92] V. Bassaneze, A. A. Miyakawa, and J. E. Krieger, “A quantitative chemiluminescent method for studying replicative and stress-induced premature senescence in cell cultures.,” *Anal. Biochem.*, vol. 372, no. 2, pp. 198–203, Jan. 2008.

[93] E. O’Riordan, N. Mendelev, S. Patschan, D. Patschan, J. Eskander, L. Cohen-Gould, P. Chander, and M. S. Goligorsky, “Chronic NOS inhibition actuates endothelial-mesenchymal transformation.,” *Am. J. Physiol. Heart Circ. Physiol.*, vol. 292, no. 1, pp. H285–94, Jan. 2007.

[94] S. Vyas-Read, P. W. Shaul, I. S. Yuhanna, and B. C. Willis, “Nitric oxide attenuates epithelial-mesenchymal transition in alveolar epithelial cells.,” *Am. J. Physiol. Lung Cell. Mol. Physiol.*, vol. 293, no. 1, pp. L212–21, Jul. 2007.

[95] L. Rosanò, F. Spinella, V. Di Castro, M. R. Nicotra, S. Dedhar, A. G. de Herreros, P. G. Natali, and A. Bagnato, “Endothelin-1 promotes epithelial-to-mesenchymal transition in human ovarian cancer cells.,” *Cancer Res.*, vol. 65, no. 24, pp. 11649–57, Dec. 2005.

[96] A. Sterner-Kock, I. S. Thorey, K. Koli, F. Wempe, J. Otte, T. Bangsow, K. Kuhlmeier, T. Kirchner, S. Jin, J. Keski-Oja, and H. von Melchner, “Disruption of the gene encoding the latent transforming growth factor-beta binding protein 4 (LTBP-4) causes abnormal lung development, cardiomyopathy, and colorectal cancer.,” *Genes Dev.*, vol. 16, no. 17, pp. 2264–73, Sep. 2002.

[97] D. G. Morris, X. Huang, N. Kaminski, Y. Wang, S. D. Shapiro, G. Dolganov, A. Glick, and D. Sheppard, “Loss of integrin alpha(v)beta6-mediated TGF-beta activation causes Mmp12-dependent emphysema.,” *Nature*, vol. 422, no. 6928, pp. 169–73, Mar. 2003.

[98] K. J. Greenlee, Z. Werb, and F. Kheradmand, “Matrix metalloproteinases in lung: multiple, multifarious, and multifaceted.,” *Physiol. Rev.*, vol. 87, no. 1, pp. 69–98, Jan. 2007.

[99] P. Bonniaud, M. Kolb, T. Galt, J. Robertson, C. Robbins, M. Stampfli, C. Lavery, P. J. Margetts, A. B. Roberts, and J. Gauldie, “Smad3 null mice develop airspace enlargement and are resistant to TGF-beta-mediated pulmonary fibrosis.,” *J. Immunol.*, vol. 173, no. 3, pp. 2099–108, Aug. 2004.

[100] A. R. Pons, J. Sauleda, A. Noguera, J. Pons, B. Barceló, A. Fuster, and A. G. N. Agustí, “Decreased macrophage release of TGF-beta and TIMP-1 in chronic obstructive pulmonary disease.,” *Eur. Respir. J. Off. J. Eur. Soc. Clin. Respir. Physiol.*, vol. 26, no. 1, pp. 60–6, Jul. 2005.

[101] A. Zandvoort, D. S. Postma, M. R. Jonker, J. A. Noordhoek, J. T. W. M. Vos, Y. M. van der Geld, and W. Timens, “Altered expression of the Smad signalling pathway: implications for COPD pathogenesis.,” *Eur. Respir. J. Off. J. Eur. Soc. Clin. Respir. Physiol.*, vol. 28, no. 3, pp. 533–41, Sep. 2006.

[102] H. Takizawa, M. Tanaka, K. Takami, T. Ohtoshi, K. Ito, M. Satoh, Y. Okada, F. Yamasawa, K. Nakahara, and A. Umeda, “Increased expression of transforming growth factor-beta1 in small airway epithelium from tobacco smokers and patients with chronic obstructive pulmonary disease (COPD).,” *Am. J. Respir. Crit. Care Med.*, vol. 163, no. 6, pp. 1476–83, May 2001.

[103] R. D. Hautamaki, D. K. Kobayashi, R. M. Senior, and S. D. Shapiro, “Requirement for macrophage elastase for cigarette smoke-induced emphysema in mice.,” *Science*, vol. 277, no. 5334, pp. 2002–4, Sep. 1997.

[104] R. F. Foronjy, Y. Okada, R. Cole, and J. D’Armiento, “Progressive adult-onset emphysema in transgenic mice expressing human MMP-1 in the lung.,” *Am. J. Physiol. Lung Cell. Mol. Physiol.*, vol. 284, no. 5, pp. L727–37, May 2003.

[105] R. M. Senior, “Mechanisms of COPD: conference summary.,” *Chest*, vol. 117, no. 5 Suppl 1, p. 320S–3S, May 2000.

[106] S. Baraldo, E. Bazzan, M. E. Zanin, G. Turato, S. Garbisa, P. Maestrelli, A. Papi, M. Miniati, L. M. Fabbri, R. Zuin, and M. Saetta, “Matrix metalloproteinase-2 protein in lung periphery is related to COPD progression.,” *Chest*, vol. 132, no. 6, pp. 1733–40, Dec. 2007.

[107] S.-H. Lee, S. Goswami, A. Grudo, L.-Z. Song, V. Bandi, S. Goodnight-White, L. Green, J. Hacken-Bitar, J. Huh, F. Bakaeen, H. O. Coxson, S. Cogswell, C. Storness-Bliss, D. B. Corry, and F. Kheradmand, “Antielastin autoimmunity in tobacco smoking-induced emphysema.,” *Nat. Med.*, vol. 13, no. 5, pp. 567–9, May 2007.

[108] S. Sakao, L. Taraseviciene-Stewart, K. Wood, C. D. Cool, and N. F. Voelkel, “Apoptosis of pulmonary microvascular endothelial cells stimulates vascular smooth muscle cell growth.,” *Am. J. Physiol. Lung Cell. Mol. Physiol.*, vol. 291, no. 3, pp. L362–8, Sep. 2006.

[109] S. Sakao, L. Taraseviciene-Stewart, C. D. Cool, Y. Tada, Y. Kasahara, K. Kurosu, N. Tanabe, Y. Takiguchi, K. Tatsumi, T. Kuriyama, and N. F. Voelkel, “VEGF-R blockade causes endothelial cell apoptosis, expansion of surviving CD34+ precursor cells and transdifferentiation to smooth muscle-like and neuronal-like cells.,” *FASEB J.*, vol. 21, no. 13, pp. 3640–52, Nov. 2007.

[110] S. P. Nana-Sinkam, J. D. Lee, S. Sotto-Santiago, R. S. Stearman, R. L. Keith, Q. Choudhury, C. Cool, J. Parr, M. D. Moore, T. M. Bull, N. F. Voelkel, and M. W. Geraci, “Prostacyclin prevents pulmonary endothelial cell apoptosis induced by cigarette smoke.,” *Am. J. Respir. Crit. Care Med.*, vol. 175, no. 7, pp. 676–85, Apr. 2007.

[111] H. Carp and A. Janoff, “Possible mechanisms of emphysema in smokers. In vitro suppression of serum elastase-inhibitory capacity by fresh cigarette smoke and its prevention by antioxidants.,” *Am. Rev. Respir. Dis.*, vol. 118, no. 3, pp. 617–21, Sep. 1978.

[112] J.-H. Lee, D.-S. Lee, E.-K. Kim, K.-H. Choe, Y.-M. Oh, T.-S. Shim, S.-E. Kim, Y.-S. Lee, and S.-D. Lee, “Simvastatin inhibits cigarette smoking-induced emphysema and pulmonary hypertension in rat lungs.,” *Am. J. Respir. Crit. Care Med.*, vol. 172, no. 8, pp. 987–93, Oct. 2005.

[113] R. A. Pauwels, A. S. Buist, P. M. Calverley, C. R. Jenkins, and S. S. Hurd, “Global strategy for the diagnosis, management, and prevention of chronic obstructive pulmonary disease. NHLBI/WHO Global Initiative for Chronic Obstructive Lung Disease (GOLD) Workshop summary.,” *Am. J. Respir. Crit. Care Med.*, vol. 163, no. 5, pp. 1256–76, Apr. 2001.

[114] L. M. Fabbri and S. S. Hurd, “Global Strategy for the Diagnosis, Management and Prevention of COPD: 2003 update,” *Eur. Respir. J.*, vol. 22, no. 1, pp. 1–1, Jul. 2003.

[115] S. D. Shapiro, “Vascular atrophy and VEGFR-2 signaling: old theories of pulmonary emphysema meet new data.,” *J. Clin. Invest.*, vol. 106, no. 11, pp. 1309–10, Dec. 2000.

[116] W. MacNee and R. M. Tuder, “New paradigms in the pathogenesis of chronic obstructive pulmonary disease I.,” *Proc. Am. Thorac. Soc.*, vol. 6, no. 6, pp. 527–31, Sep. 2009.

[117] P. J. Barnes, “The cytokine network in chronic obstructive pulmonary disease.,” *Am. J. Respir. Cell Mol. Biol.*, vol. 41, no. 6, pp. 631–8, Dec. 2009.

[118] E. A. Jaffe, R. L. Nachman, C. G. Becker, and C. R. Minick, “Culture of human endothelial cells derived from umbilical veins. Identification by morphologic and immunologic criteria.,” *J. Clin. Invest.*, vol. 52, no. 11, pp. 2745–56, Nov. 1973.

[119] J. King, T. Hamil, J. Creighton, S. Wu, P. Bhat, F. McDonald, and T. Stevens, “Structural and functional characteristics of lung macro- and microvascular endothelial cell phenotypes.,” *Microvasc. Res.*, vol. 67, no. 2, pp. 139–51, Mar. 2004.

[120] J. Shen, R. G. Ham, and S. Karmiol, “Expression of adhesion molecules in cultured human pulmonary microvascular endothelial cells.,” *Microvasc. Res.*, vol. 50, no. 3, pp. 360–72, Nov. 1995.

[121] P. W. Hewett and J. C. Murray, “Human lung microvessel endothelial cells: isolation, culture, and characterization.,” *Microvasc. Res.*, vol. 46, no. 1, pp. 89–102, Jul. 1993.

[122] D. J. Giard, S. A. Aaronson, G. J. Todaro, P. Arnstein, J. H. Kersey, H. Dosik, and W. P. Parks, “In vitro cultivation of human tumors: establishment of cell lines derived from a series of solid tumors.,” *J. Natl. Cancer Inst.*, vol. 51, no. 5, pp. 1417–23, Nov. 1973.

[123] H. L. Winton, H. Wan, M. B. Cannell, D. C. Gruenert, P. J. Thompson, D. R. Garrod, G. A. Stewart, and C. Robinson, “Cell lines of pulmonary and non-pulmonary origin as tools to study the effects of house dust mite proteinases on the regulation of epithelial permeability.,” *Clin. Exp. Allergy*, vol. 28, no. 10, pp. 1273–85, Oct. 1998.

[124] H. Wan, H. L. Winton, C. Soeller, G. A. Stewart, P. J. Thompson, D. C. Gruenert, M. B. Cannell, D. R. Garrod, and C. Robinson, “Tight junction properties of the immortalized human bronchial epithelial cell lines Calu-3 and 16HBE14o-.,” *Eur. Respir. J. Off. J. Eur. Soc. Clin. Respir. Physiol.*, vol. 15, no. 6, pp. 1058–68, Jun. 2000.

[125] M. Skelin, M. Rupnik, and A. Cencic, “Pancreatic beta cell lines and their applications in diabetes mellitus research.,” *ALTEX*, vol. 27, no. 2, pp. 105–13, Jan. 2010.

[126] N. T. Georgopoulos, L. A. Kirkwood, C. L. Varley, N. J. Maclaine, N. Aziz, and J. Southgate, “Immortalisation of normal human urothelial cells compromises differentiation capacity.,” *Eur. Urol.*, vol. 60, no. 1, pp. 141–9, Jul. 2011.

[127] N. Chung-Welch, D. Shepro, B. Dunham, and H. B. Hechtman, “Prostacyclin and prostaglandin E2 secretions by bovine pulmonary microvessel endothelial cells are altered by changes in culture conditions.,” *J. Cell. Physiol.*, vol. 135, no. 2, pp. 224–34, May 1988.

[128] B. Meyrick, R. Hoover, M. R. Jones, L. C. Berry, and K. L. Brigham, “In vitro effects of endotoxin on bovine and sheep lung microvascular and pulmonary artery endothelial cells.,” *J. Cell. Physiol.*, vol. 138, no. 1, pp. 165–74, Jan. 1989.

[129] J. N. Lou, N. Mili, C. Decrind, Y. Donati, S. Kossodo, A. Spiliopoulos, B. Ricou, P. M. Suter, D. R. Morel, P. Morel, and G. E. Grau, “An improved method for isolation of microvascular endothelial cells from normal and inflamed human lung.,” *In Vitro Cell. Dev. Biol. Anim.*, vol. 34, no. 7, pp. 529–36.

[130] J. Folkman, C. C. Haudenschild, and B. R. Zetter, “Long-term culture of capillary endothelial cells.,” *Proc. Natl. Acad. Sci. U. S. A.*, vol. 76, no. 10, pp. 5217–21, Oct. 1979.

[131] P. W. Hewett and J. C. Murray, “Human microvessel endothelial cells: isolation, culture and characterization.,” *In Vitro Cell. Dev. Biol. Anim.*, vol. 29A, no. 11, pp. 823–30, Nov. 1993.

[132] C. J. Jackson, P. K. Garbett, B. Nissen, and L. Schrieber, “Binding of human endothelium to Ulex europaeus I-coated Dynabeads: application to the isolation of microvascular endothelium.,” *J. Cell Sci.*, vol. 96 ( Pt 2), pp. 257–62, Jun. 1990.

[133] C. E. Gargett, K. Bucak, and P. A. Rogers, “Isolation, characterization and long-term culture of human myometrial microvascular endothelial cells.,” *Hum. Reprod.*, vol. 15, no. 2, pp. 293–301, Feb. 2000.

[134] M. Subramaniam, J. A. Koedam, and D. D. Wagner, “Divergent fates of P- and E-selectins after their expression on the plasma membrane.,” *Mol. Biol. Cell*, vol. 4, no. 8, pp. 791–801, Aug. 1993.

[135] C. Garlanda and E. Dejana, “Heterogeneity of endothelial cells. Specific markers.,” *Arterioscler. Thromb. Vasc. Biol.*, vol. 17, no. 7, pp. 1193–202, Jul. 1997.

[136] M. Mutin, F. Dignat-George, and J. Sampol, “Immunologic phenotype of cultured endothelial cells: quantitative analysis of cell surface molecules.,” *Tissue Antigens*, vol. 50, no. 5, pp. 449–58, Nov. 1997.

[137] J. M. Brown and L. D. Attardi, “The role of apoptosis in cancer development and treatment response.,” *Nat. Rev. Cancer*, vol. 5, no. 3, pp. 231–7, Mar. 2005.

[138] M. C. Morissette, J. Parent, and J. Milot, “Alveolar epithelial and endothelial cell apoptosis in emphysema: what we know and what we need to know.,” *Int. J. Chron. Obstruct. Pulmon. Dis.*, vol. 4, pp. 19–31, Jan. 2009.

[139] R. Tuder, K. Wood, L. Taraseviciene, S. Flores, and N. Voekel, “Cigarette smoke extract decreases the expression of vascular endothelial growth factor by cultured cells and triggers apoptosis of pulmonary endothelial cells,” *Chest*, vol. 117, no. 5 Suppl 1, p. 241S–2S, May 2000.

[140] K. Aoshiba, J. Tamaoki, and A. Nagai, “Acute cigarette smoke exposure induces apoptosis of alveolar macrophages.,” *Am. J. Physiol. Lung Cell. Mol. Physiol.*, vol. 281, no. 6, pp. L1392–401, Dec. 2001.

[141] S. Carnevali, S. Petruzzelli, B. Longoni, R. Vanacore, R. Barale, M. Cipollini, F. Scatena, P. Paggiaro, A. Celi, and C. Giuntini, “Cigarette smoke extract induces oxidative stress and apoptosis in human lung fibroblasts.,” *Am. J. Physiol. Lung Cell. Mol. Physiol.*, vol. 284, no. 6, pp. L955–63, Jun. 2003.

[142] Y. Hoshino, T. Mio, S. Nagai, H. Miki, I. Ito, and T. Izumi, “Cytotoxic effects of cigarette smoke extract on an alveolar type II cell-derived cell line.,” *Am. J. Physiol. Lung Cell. Mol. Physiol.*, vol. 281, no. 2, pp. L509–16, Aug. 2001.

[143] S.-E. Michaud, C. Ménard, L.-G. Guy, G. Gennaro, and A. Rivard, “Inhibition of hypoxia-induced angiogenesis by cigarette smoke exposure: impairment of the HIF-1alpha/VEGF pathway.,” *FASEB J.*, vol. 17, no. 9, pp. 1150–2, Jun. 2003.

[144] R. Aldonyte, T. E. Hutchinson, E. T. Hutchinson, B. Jin, M. Brantly, E. Block, J. Patel, and J. Zhang, “Endothelial alpha-1-antitrypsin attenuates cigarette smoke induced apoptosis in vitro.,” *COPD*, vol. 5, no. 3, pp. 153–62, Jun. 2008.

[145] J. S. Edmiston, J. W. Flora, M. J. Scian, G. Li, G. S. J. B. Rana, T. B. Langston, T. K. Sengupta, and W. J. McKinney, “Cigarette smoke extract induced protein phosphorylation changes in human microvascular endothelial cells in vitro.,” *Anal. Bioanal. Chem.*, vol. 394, no. 6, pp. 1609–20, Jul. 2009.

[146] D. Thorne, J. Kilford, R. Payne, J. Adamson, K. Scott, A. Dalrymple, C. Meredith, and D. Dillon, “Characterisation of a Vitrocell® VC 10 in vitro smoke exposure system using dose tools and biological analysis.,” *Chem. Cent. J.*, vol. 7, no. 1, p. 146, Jan. 2013.

[147] Y. Kitaguchi, L. Taraseviciene-Stewart, M. Hanaoka, R. Natarajan, D. Kraskauskas, and N. F. Voelkel, “Acrolein induces endoplasmic reticulum stress and causes airspace enlargement.,” *PLoS One*, vol. 7, no. 5, p. e38038, Jan. 2012.

[148] R. S. Y. Wong, “Apoptosis in cancer: from pathogenesis to treatment.,” *J. Exp. Clin. Cancer Res.*, vol. 30, p. 87, Jan. 2011.

[149] G. Koopman, C. P. Reutelingsperger, G. A. Kuijten, R. M. Keehnen, S. T. Pals, and M. H. van Oers, “Annexin V for flow cytometric detection of phosphatidylserine expression on B cells undergoing apoptosis.,” *Blood*, vol. 84, no. 5, pp. 1415–20, Sep. 1994.

[150] S. H. MacKenzie and A. C. Clark, “Death by caspase dimerization.,” *Adv. Exp. Med. Biol.*, vol. 747, pp. 55–73, Jan. 2012.

[151] K. Kyrylkova, S. Kyryachenko, M. Leid, and C. Kioussi, “Detection of apoptosis by TUNEL assay.,” *Methods Mol. Biol.*, vol. 887, pp. 41–7, Jan. 2012.

[152] H. Cen, F. Mao, I. Aronchik, R. J. Fuentes, and G. L. Firestone, “DEVD-NucView488: a novel class of enzyme substrates for real-time detection of caspase-3 activity in live cells.,” *FASEB J.*, vol. 22, no. 7, pp. 2243–52, Jul. 2008.

[153] F. Labat-Moleur, C. Guillermet, P. Lorimier, C. Robert, S. Lantuejoul, E. Brambilla, and A. Negoescu, “TUNEL apoptotic cell detection in tissue sections: critical evaluation and improvement.,” *J. Histochem. Cytochem.*, vol. 46, no. 3, pp. 327–34, Mar. 1998.

[154] T. Nolan, R. E. Hands, and S. A. Bustin, “Quantification of mRNA using real-time RT-PCR.,” *Nat. Protoc.*, vol. 1, no. 3, pp. 1559–82, Jan. 2006.

[155] G. Houge, B. Robaye, T. S. Eikhom, J. Golstein, G. Mellgren, B. T. Gjertsen, M. Lanotte, and S. O. Døskeland, “Fine mapping of 28S rRNA sites specifically cleaved in cells undergoing apoptosis.,” *Mol. Cell. Biol.*, vol. 15, no. 4, pp. 2051–62, Apr. 1995.

[156] L. A. Borthwick, S. M. Parker, K. A. Brougham, G. E. Johnson, M. R. Gorowiec, C. Ward, J. L. Lordan, P. A. Corris, J. A. Kirby, and A. J. Fisher, “Epithelial to mesenchymal transition (EMT) and airway remodelling after human lung transplantation.,” *Thorax*, vol. 64, no. 9, pp. 770–7, Sep. 2009.

[157] R. Kalluri and E. G. Neilson, “Epithelial-mesenchymal transition and its implications for fibrosis.,” *J. Clin. Invest.*, vol. 112, no. 12, pp. 1776–84, Dec. 2003.

[158] T. A. Wynn, “Cellular and molecular mechanisms of fibrosis.,” *J. Pathol.*, vol. 214, no. 2, pp. 199–210, Jan. 2008.

[159] B. Hinz, S. H. Phan, V. J. Thannickal, A. Galli, M.-L. Bochaton-Piallat, and G. Gabbiani, “The Myofibroblast: One Function, Multiple Origins,” *Am. J. Pathol.*, vol. 170, no. 6, pp. 1807–1816, Apr. 2007.

[160] S. D. Lee, D. S. Lee, Y. G. Chun, S. H. Paik, W. S. Kim, D. S. Kim, W. D. Kim, R. M. Tuder, and N. F. Voelkel, “Transforming growth factor-beta1 induces endothelin-1 in a bovine pulmonary artery endothelial cell line and rat lungs via cAMP.,” *Pulm. Pharmacol. Ther.*, vol. 13, no. 6, pp. 257–65, Jan. 2000.

[161] P. Zhu, L. Huang, X. Ge, F. Yan, R. Wu, and Q. Ao, “Transdifferentiation of pulmonary arteriolar endothelial cells into smooth muscle-like cells regulated by myocardin involved in hypoxia-induced pulmonary vascular remodelling.,” *Int. J. Exp. Pathol.*, vol. 87, no. 6, pp. 463–74, Dec. 2006.

[162] M. Königshoff, N. Kneidinger, and O. Eickelberg, “TGF-beta signaling in COPD: deciphering genetic and cellular susceptibilities for future therapeutic regimen.,” *Swiss Med. Wkly.*, vol. 139, no. 39–40, pp. 554–63, Oct. 2009.

[163] A. Sánchez, A. M. Alvarez, M. Benito, and I. Fabregat, “Apoptosis induced by transforming growth factor-beta in fetal hepatocyte primary cultures: involvement of reactive oxygen intermediates.,” *J. Biol. Chem.*, vol. 271, no. 13, pp. 7416–22, Mar. 1996.

[164] M. Mawatari, K. Kohno, H. Mizoguchi, T. Matsuda, K. Asoh, J. Van Damme, H. G. Welgus, and M. Kuwano, “Effects of tumor necrosis factor and epidermal growth factor on cell morphology, cell surface receptors, and the production of tissue inhibitor of metalloproteinases and IL-6 in human microvascular endothelial cells.,” *J. Immunol.*, vol. 143, no. 5, pp. 1619–27, Sep. 1989.

[165] K. Kohno, R. Hamanaka, T. Abe, Y. Nomura, A. Morimoto, H. Izumi, K. Shimizu, M. Ono, and M. Kuwano, “Morphological change and destabilization of beta-actin mRNA by tumor necrosis factor in human microvascular endothelial cells.,” *Exp. Cell Res.*, vol. 208, no. 2, pp. 498–503, Oct. 1993.

[166] C. Castañares, M. Redondo-Horcajo, N. Magan-Marchal, S. Lamas, and F. Rodriguez-Pascual, “Transforming growth factor-beta receptor requirements for the induction of the endothelin-1 gene.,” *Exp. Biol. Med. (Maywood).*, vol. 231, no. 6, pp. 700–3, Jun. 2006.

[167] Z. Deyl, K. Macek, M. Adam, and O. Vancíková, “Studies on the chemical nature of elastin fluorescence.,” *Biochim. Biophys. Acta*, vol. 625, no. 2, pp. 248–54, Oct. 1980.

[168] T. Cowen, A. J. Haven, and G. Burnstock, “Pontamine sky blue: a counterstain for background autofluorescence in fluorescence and immunofluorescence histochemistry.,” *Histochemistry*, vol. 82, no. 3, pp. 205–8, Jan. 1985.

[169] C. E. Patterson and D. Stamenović, *Perspectives on Lung Endothelial Barrier Function*, vol. 35. Elsevier, 2005.

[170] N. Kurimoto, Y.-S. Nan, Z.-Y. Chen, G.-G. Feng, T. Komatsu, N. Kandatsu, J. Ko, N. Kawai, and N. Ishikawa, “Effects of specific signal transduction inhibitors on increased permeability across rat endothelial monolayers induced by neuropeptide Y or VEGF.,” *Am. J. Physiol. Heart Circ. Physiol.*, vol. 287, no. 1, pp. H100–6, Jul. 2004.

[171] I. V Hurst V, P. L. Goldberg, F. L. Minnear, R. L. Heimark, and P. A. Vincent, “Rearrangement of adherens junctions by transforming growth factor-beta1: role of contraction.,” *Am. J. Physiol.*, vol. 276, no. 4 Pt 1, pp. L582–95, Apr. 1999.

[172] K. Takehara, E. C. LeRoy, and G. R. Grotendorst, “TGF-beta inhibition of endothelial cell proliferation: alteration of EGF binding and EGF-induced growth-regulatory (competence) gene expression.,” *Cell*, vol. 49, no. 3, pp. 415–22, May 1987.

[173] D. B. Cines, E. S. Pollak, C. A. Buck, J. Loscalzo, G. A. Zimmerman, R. P. McEver, J. S. Pober, T. M. Wick, B. A. Konkle, B. S. Schwartz, E. S. Barnathan, K. R. McCrae, B. A. Hug, A. M. Schmidt, and D. M. Stern, “Endothelial cells in physiology and in the pathophysiology of vascular disorders.,” *Blood*, vol. 91, no. 10, pp. 3527–61, May 1998.